Doctoral theses at NTNU, 2021:382

Bjørn T. Svendsen

Numerical and experimental studies for damage detection and structural health monitoring of steel bridges

Doctoral thesis

NTNU
Norwegian University of Science and Technology
Thesis for the Degree of
Philosophiae Doctor
Faculty of Engineering
Department of Structural Engineering

NTNU
Norwegian University of
Science and Technology

Bjørn T. Svendsen

Numerical and experimental studies for damage detection and structural health monitoring of steel bridges

Thesis for the Degree of Philosophiae Doctor

Trondheim, December 2021

Norwegian University of Science and Technology
Faculty of Engineering
Department of Structural Engineering

NTNU
Norwegian University of
Science and Technology

NTNU
Norwegian University of Science and Technology

Thesis for the Degree of Philosophiae Doctor

Faculty of Engineering
Department of Structural Engineering

ISBN 978-82-326-6327-9 (printed ver.)
ISBN 978-82-326-5895-4 (electronic ver.)
ISSN 1503-8181 (printed ver.)
ISSN 2703-8084 (online ver.)

Doctoral theses at NTNU, 2021:382

Printed by NTNU Grafisk senter

Preface

This thesis is submitted in partial fulfilment of the requirements for the degree of Philosophiae Doctor at the Norwegian University of Science and Technology (NTNU). The work has been carried out at the Department of Structural Engineering, Faculty of Engineering. Professor Anders Rønnquist and Professor Ole Øiseth have supervised the work. The thesis consists of a collection of four papers, referred to as Parts 1-4. Parts 1 and 2 are published in international peer-reviewed journals, and Parts 3 and 4 are submitted for publication. A synopsis binds the individual parts together.

Bjørn Thomas Svendsen

Trondheim, Norway
September 13, 2021

Publications

Included publications

The following papers are included in this thesis:

I. Svendsen, B. T., Frøseth, G. T., and Rønnquist, A. (2020). *Damage detection applied to a full-scale steel bridge using temporal moments*. Shock and Vibration, 1-16. https://doi.org/10.1155/2020/3083752.

II. Svendsen, B. T., Petersen, Ø. W., Frøseth, G. T., and Rønnquist, A. (2021). *Improved finite element model updating of a full-scale steel bridge using sensitivity analysis*. Structure and Infrastructure Engineering, 1-17. https://doi.org/10.1080/15732479.2021.1944227.

III. Svendsen, B. T., Øiseth, O., Frøseth, G. T., and Rønnquist, A. (2021). *A hybrid structural health monitoring approach for damage detection in steel bridges under simulated environmental conditions using numerical and experimental data*. Submitted for journal publication.

IV. Svendsen, B. T., Frøseth, G. T., Øiseth, O., and Rønnquist, A. (2021). *A data-based structural health monitoring approach for damage detection in steel bridges using experimental data*. Journal of Civil Structural Health Monitoring, 1-15. https://doi.org/10.1007/s13349-021-00530-8.

Declaration of authorship

The first author has been responsible for the numerical and experimental work, implementation of the theory, analyses, and the preparation of all the manuscripts. The co-authors have contributed with valuable suggestions, discussions, and reviews of the scientific content to improve the research quality.

Other scientific contributions

The following papers are published in conference proceedings during the work of this thesis:

- Svendsen, B. T., Frøseth, G. T., and Rønnquist, A. (2018). *Inspection of steel bridges by modal hammer from bridge deck only*. In Maintenance, Safety, Risk, Management and Life-Cycle Performance of Bridges, 2865-2872. https://doi.org/10.1201/9781315189390-389.

- Svendsen, B. T., Frøseth, G. T., and Rønnquist, A. (2018). *Damage detection of steel bridge by numerical simulations and measurements*. In Life-Cycle Analysis and Assessment in Civil Engineering, 72.

Abstract

There is a vast number of existing bridges in infrastructure that are approaching or have exceeded their original design lives. A large part of these bridges are steel and composite steel-concrete bridges. The primary damage mechanism in these bridges is fatigue, which can lead to component failure that is critical for the structural integrity. Structural health monitoring systems can provide information regarding the state of the bridge condition, with the aim of increasing the economic and life-safety benefits through damage detection. The primary motive of structural health monitoring is to design a system that minimizes false positive indications of damage for economic and reliability concerns and false negative indications of damage for life-safety issues. For infrastructure owners, structural health monitoring systems can result in enhanced decision support and structural diagnosis of the structure.

This thesis considers damage detection and structural health monitoring through numerical and experimental studies of a full-scale steel bridge. An essential part of this research is the establishment of an experimental benchmark study to obtain response measurement data under different structural state conditions with imposed damage. The thesis consists of four papers, referred to as parts. In the first part, the damage detection possibilities for improved bridge inspection are determined. Damage detection of existing structural damage is assessed through analysis of response measurements obtained from a systematic experimental study using a modal hammer. In the second part, a strategy to effectively establish a validated numerical finite element model using model updating is developed and implemented. A validated finite element model can be utilized to perform numerical simulations for damage detection and structural health monitoring purposes.

The research then follows logically into using the validated finite element model in the third part. More specifically, a novel hybrid structural health monitoring framework for damage detection is proposed by integrating numerical models, experimental data, and machine learning. A challenge in structural health monitoring is that almost all statistical decision making must be done in an unsupervised learning mode. This part aims at providing an important contribution towards solving this challenge. Finally, a data-based structural health monitoring approach for damage detection in bridges using only experimental data is presented in the fourth paper. Damage detection of local and global structural damage using an unsupervised learning algorithm by novelty detection is performed. Furthermore, the detectability of different damage types within the established dataset is evaluated by considering the average performance of four supervised learning algorithms.

In this thesis, current approaches for damage detection and structural health monitoring of bridges have been implemented, evaluated, and further developed through numerical and experimental studies. The results presented demonstrate that damage detection of bridges can be performed using structural health monitoring

approaches and practices. In conclusion, this thesis provides valuable contributions to the field of structural health monitoring regarding its application to bridges.

Keywords: Structural health monitoring, damage detection, machine learning, finite element model updating, operational modal analysis, bridge, experimental benchmark study.

Acknowledgements

First, I would like to acknowledge my main supervisor, Professor Anders Rønnquist, for excellent supervision in terms of encouragement, support and sharing knowledge. Particularly, our countless discussions have been invaluable. I truly could not have asked for better guidance. I would also like to acknowledge my co-supervisor, Professor Ole Øiseth, for providing insightful and highly appreciated feedback on the scientific work.

A dedicated acknowledgement is made to Gunnstein Frøseth for all the good talks, scientific cooperation and support during the experimental studies. Øyvind Wiig Petersen also deserves acknowledgement for the scientific cooperation and valuable discussions. I would also like to thank all the colleagues in the Structural Dynamics group for making an outstanding and enjoyable working environment. My good friend and colleague, Stefano Derosa, is worthy of sincere thanks for all the support during my experimental work and funny conversations.

My first office mate, Arne Ilseng, deserves special thanks for all the moral support during office times and our sophisticated (and not-so-sophisticated) conversations. An acknowledgement also goes to my second office mate, Anno Christian Dederichs, for providing great company in the office in the last part of my PhD and for proofreading this thesis.

I would also like to thank Bernd Schmid, Terje Petersen and Steinar Seehuus from the lab for all the help related to the experimental work at the bridge. Furthermore, special thanks go to Ole Gabrielsen in DNV for the support and encouragement prior to and during the PhD period.

I would also like to make a dedicated acknowledgement to my family. My mum, dad and sister have always provided endless support, for which I am very grateful. Finally, the last acknowledgement goes to the most special person in my life, Mona, and our two amazing girls, Hedda and Nora. Your encouragement and dedication during this period mean everything to me. You are simply incredible, and I love you to the moon and back.

Contents

Chapter 1

1 Synopsis

1.1 Introduction

Ageing and deterioration of infrastructure is a major concern worldwide. Bridges are complex structures that provide critical links in the infrastructure. Table 1.1 summarizes the total number of highway and railway bridges in service in the United States and Europe. Many of these bridges, which were built after 1945 with a design life of 50–100 years, are approaching or have exceeded their original design lives. Furthermore, these bridges experience increasing demands from operational and environmental conditions, for which they were originally not designed. Considering the requirements for more efficient transportation systems due to the increase in traffic loads, speed and intensity, many bridges are being used despite ageing and the associated damage accumulation. Replacing bridges, which are associated with considerable investment costs and undesirable traffic interruptions, is not feasible due to the large number of existing bridges in the infrastructure. Although many uncertainties related to ageing and the associated damage accumulation are present in these bridges, lifetime extension is the preferred option to ensure continuous operation.

Table 1.1: Bridges in the United States and Europe.

	Number of bridges		
Location	Highway	Railway	References
United States	> 600 000	> 100 000	[1], [2]
Europe[1]	-	> 300 000	[3]–[5]
Norway	16 971	2 370	[6], [7]

[1] More than 1234 km of highway bridges longer than 100 m (a significantly higher number is expected when smaller bridges are included).

A large part of the existing highway and railway bridges presented in Table 1.1 are steel and composite steel-concrete bridges. Based on an overview and extensive investigation of the common damage types experienced by such bridges, it is found that most damages are caused by fatigue and most frequently occur in or below the bridge deck [8]. Concerning structural integrity, several of these damage types can be critical with respect to operational and strong environmental loading. Consequently, many case studies have been performed on service life estimation and fatigue reliability analysis of structural components in the bridge deck of steel and composite steel-concrete bridges [9]–[16]. If not detected at an early stage, such damage can develop and lead to component failure and, ultimately, system failure.

There are extensive requirements for inspections of existing bridges. Inspections are performed to ensure the safe operation of bridges and are typically specified in regular intervals to establish maintenance needs. Requirements of minor inspections every year, major inspections every fifth or sixth year, and special inspections when needed, are common practice. However, many bridges are in remote locations and have low accessibility, requiring operational downtime or temporary installation of access platforms to be able to perform a full inspection. Furthermore, there is often limited information about existing damage. Fatigue damage can be difficult to detect due to low visibility, and critical structural damage can be difficult to establish until the structure is subjected to operational or strong environmental loading. Therefore, significant challenges are associated with the inspections of such bridges in terms of finding critical structural damage.

Maintenance of bridges is mainly performed in a time-based mode based on information obtained from inspections. However, periodic inspections do not provide complete up-to-date information about the current state of the bridge condition. Moving towards a condition-based maintenance philosophy where a sensing system on the structure monitors the system response and notifies if structural damage is detected would be cost-effective. However, condition-based maintenance is only helpful if such a monitoring system provides sufficient warning for corrective actions to be made before damage evolves to failure. Being able to detect structural damage at the earliest possible time and monitor the health of bridges is becoming increasingly important.

Structural health monitoring (SHM) systems can provide information regarding the state of the bridge condition. As such, SHM systems can monitor the condition and integrity of bridges, which allow for (1) prioritization of inspections and planning for maintenance works, (2) rapid evaluation of structural integrity after extreme events in operational and environmental conditions, (3) the identification of changes in the structural condition over time, (4) validation of the bridge design and numerical models for future analysis and (5) lifetime extension opportunities. However, and most importantly, the primary purpose of SHM systems is to detect structural damage.

Table 1.2 summarizes two of the largest and, perhaps, most complex projects in the world concerning the application of advanced bridge SHM systems. For the SHM systems of these bridges, sensors are included to measure environmental actions, bridge actions and bridge responses. Two important observations are made from Table 1.2: first, only a part of each SHM system includes measurements of the bridge responses, which is essential for damage detection purposes; and second, although many sensors are included and integrated into each SHM system, the bridges are still considered sparsely instrumented. Consequently, there are limited possibilities to detect structural damage, particularly local structural damage. This aspect signifies an important challenge with SHM systems and the structural damage detection possibilities.

Table 1.2: Projects with advanced structural health monitoring systems.

Bridge	Location	Type	Length (m)	Longest span (m)	Sensors[1]
The Queensferry Crossing [17]	United Kingdom	Cable-stayed	2700	650	1972 (1106)
The Stonecutters [18]	Hong Kong	Cable-stayed	1596	1018	1505 (1010)

[1] In parentheses: the number of sensors of the total measuring the bridge responses.

In the context of SHM, numerous methods and applications of damage detection exist, of which most applications are based on numerical studies or laboratory studies performed in a controlled environment [19], [20]. Furthermore, there are several important benchmark studies of test structures relevant for bridges [21], [22]. However, there are few studies where experimental tests have been performed of bridges progressing from an undamaged (reference) state to known damage states. Table 1.3 summarizes the experimental studies that have been reported in the literature where relevant structural damage is imposed on bridges. From this table, it is seen that a majority of the studies are related to concrete bridges. Additionally, only highway bridges are considered. It should also be noted that most of the studies contain limited data for machine learning applications. One notable exception is, however, the Z24 bridge study.

In general, the few experimental studies on real bridges provide limited opportunities in terms of validating existing and developing new techniques for damage detection and structural health monitoring. Furthermore, variability in the operational and environmental conditions affects the structural response and can mask changes caused by structural damage [32]. To further develop the possibilities of employing SHM systems on bridges, research should be focused on tests of real structures in their operating and environmental conditions, rather than numerical or laboratory studies of representative structures [4], [33]–[37].

In summary, three important observations are made. First, there are many existing bridges in infrastructure, and significant challenges exist with respect to inspecting and maintaining these bridges. Second, although advanced SHM systems are installed on bridges, these bridges are in many cases still considered sparsely instrumented, which limits the damage detection possibilities. Last, considering the vast amount of technical literature that is published on damage detection and structural health monitoring of bridges, exceptionally few studies have been reported in the literature where relevant structural damage is imposed on bridges. Consequently, two major research needs are identified. First, there is a need for SHM systems on bridges that can detect relevant local and global structural damage, taking into consideration variability in the operational and environmental conditions. Second, there is a need for research that is focused on tests of full-scale bridges rather than numerical or laboratory studies of representative structures. Particularly, studies where SHM approaches are tested experimentally on bridges are needed.

Table 1.3: Experimental studies of bridges for damage detection purposes.

Bridge	Location	Traffic	Type	Length (m)[1]	Reference(s)
I-40	United States	Highway	Composite steel-concrete plate girder	129.5	[23]
Z24	United States	Highway	Prestressed concrete	63.4	[24], [25]
Dogna	Italy	Highway	Reinforced concrete	16.0	[26]
Deutsche Bank	Luxembourg	Highway	Prestressed concrete	59.0	[27]
Avenue JFK	Luxembourg	Highway	Prestressed concrete	29.0	[27]
S101	Austria	Highway	Prestressed concrete	56.0	[28]
I-40 westbound	United States	Highway	Composite steel-concrete plate girder	52.1	[29]
-	Japan	Highway	Steel truss bridge	65.5	[30]
Old ADA	Japan	Highway	Steel truss bridge	59.2	[31]

[1] Length of the bridge considered in the testing.

SHM systems can provide information regarding the state of the bridge condition, with the aim of increasing the economic and life-safety benefits through damage identification. The primary motive of SHM is to design a system that minimizes false positive (FP) indications of damage for economic and reliability concerns and false negative (FN) indications of damage for life-safety issues. For infrastructure owners, structural health monitoring systems can result in enhanced decision support and structural diagnosis of the structure.

1.2 Structural health monitoring

1.2.1 SHM approaches

Structural health monitoring (SHM) is referred to as the process of implementing an automated and online strategy for damage detection in a structure [38], [39]. SHM has traditionally been performed using two main approaches: model-based and data-based [40]. However, a hybrid approach to SHM, which takes principles from both the model-based and data-based approaches into consideration, has emerged in the recent years [41]. Common for all the approaches is that they provide some form of decision support or structural diagnosis of the structure under consideration. The main approaches to SHM are summarized in Figure 1.1.

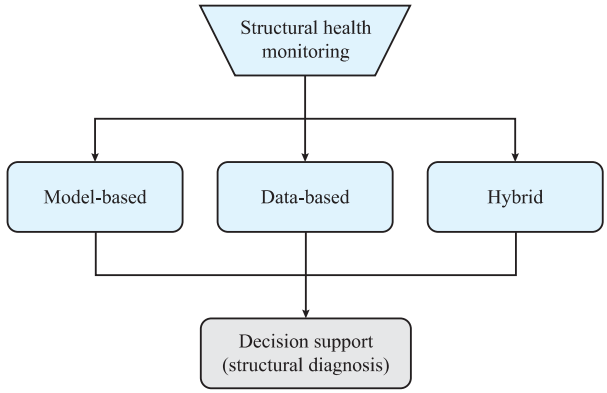

Figure 1.1: SHM approaches.

The model-based approach, shown in Figure 1.2, consists of two stages and involves the calibration of numerical finite element (FE) models. In the first stage, an initial FE model is calibrated based on data from the undamaged condition to obtain a validated FE model or reference model. In the second stage, the reference model is calibrated based on data from the damaged condition (assuming that the operational and environmental conditions have been eliminated). Damage detection is then performed based on the resulting change in the updated parameters. As such, the model-based approach is also considered an inverse approach.

Applications of the model-based approach by considering relevant structural damage in bridges have been reported [42]–[47]. However, in the context of SHM, the model-based approach is considered impractical for large and complex structures such as bridges due to several disadvantages and limited possibilities to detect local structural damage. Particularly, parameterizing the numerical model for the parameters to be associated with damage is challenging.

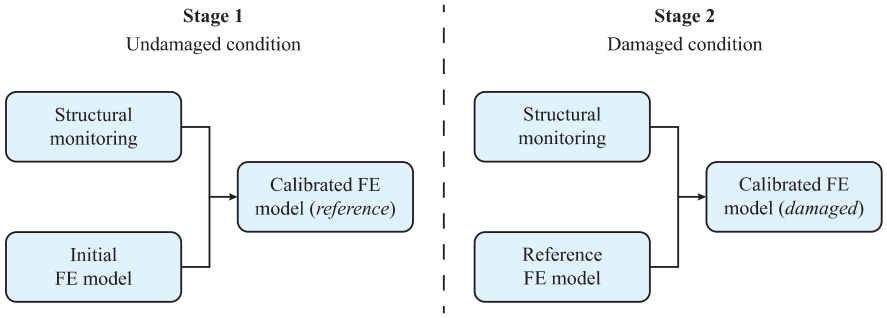

Figure 1.2: The model-based SHM approach.

The data-based approach is based on the statistical pattern recognition (SPR) paradigm, which is also referred to as the SHM *process* [48]. The data-based approach, shown in a simplified version in Figure 1.3, builds a statistical model based only on experimental data and generally relies on machine learning algorithms. Damage detection is performed by analyzing the damage-sensitive features using unsupervised or supervised learning, referred to as statistical model development. In the context of SHM, unsupervised learning refers to the situation where data are available only from the undamaged condition of the structure, whereas supervised learning refers to the situation where data are available from both undamaged and damaged conditions. Unsupervised learning is often required for bridges in operation since data from both the undamaged and damaged conditions are rarely available. For a complete description of the SHM process, it is referred to [48].

Figure 1.3: The data-based SHM approach (simplified version).

There are several applications of statistical model development in the data-based approach using numerical models or test structures, which are relevant to bridges [49]–[54]. However, there are few examples of applications to real bridges where relevant structural damage has been considered [55]–[57]. Furthermore, these examples consider relevant structural damage mostly applicable to concrete bridges. There are mainly two challenges with this approach. First, unsupervised learning is often required due to the lack of data from damaged conditions. Second, data normalization, which is referred to as the process of separating changes caused by operational and environmental conditions from changes caused by structural damage [58], must be considered. Despite these challenges, the data-based approach is the preferred SHM approach for the application to bridges.

The hybrid SHM approach takes principles from the model-based and data-based approaches into consideration. Although there are different ways to utilize this approach, a common understanding is that numerical model(s), experimental data, and machine learning are integrated in some way. A general configuration of the hybrid SHM approach is shown in Figure 1.4. Two studies have been reported in the literature in which this approach is considered: one study applied to a test structure [59], and one applied to a real bridge [60]. Although this approach has received little attention in the literature, it can be used to overcome the limitations and challenges experienced in the traditional SHM approaches.

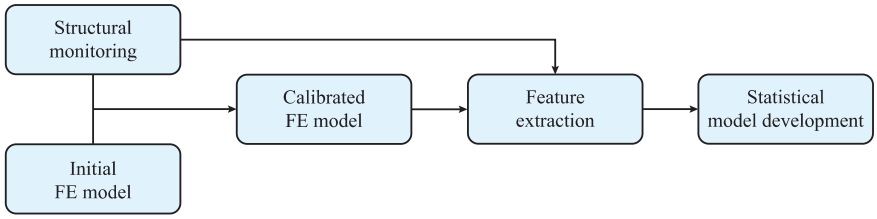

Figure 1.4: The hybrid SHM approach.

Data normalization should be considered irrespective of the SHM approach chosen. There are mainly two approaches to separate changes caused by operational and environmental conditions from changes caused by damage [33]. In the first approach, structural response measurements and direct measurements of parameters related to the operational and environmental conditions are made. The damage-sensitive features extracted from the structural response measurements in the undamaged condition can then be parameterized as a function of the measured operational and environmental conditions. In the second approach, only structural response measurements are used to assess the influence of the operational and environmental variability on the damage-sensitive features. From the application of machine learning algorithms, the underlying relationship between the features and the variables of the operational and environmental conditions can implicitly be modelled.

As such, data normalization can be considered in several parts of the SHM process. However, this possibility is limited in the model-based approach to only apply to the part involving structural monitoring. Furthermore, the possibility of performing decision support or structural diagnosis in terms of statistical models can only be done in the data-based and hybrid approaches. Consequently, the data-based and hybrid approaches are considered in this thesis due to the many advantages and few limitations compared to the model-based approach.

1.2.2 Levels of damage detection in SHM

Decision support or structural diagnosis involves determining the damage state of the structure, which is performed according to the hierarchical structure of damage identification [39], [61]:

- Level I (*existence*).
- Level II (*location*).
- Level III (*type*).
- Level IV (*extent*).
- Level V (*prediction*).

Increased knowledge of the damage state is represented in the given order of the levels. The vertical structure of the hierarchy implies that each level (generally) requires that information from the lower levels is available.

In the model-based approach, level I, II and IV damage detection can be performed. Here, it is assumed that the type of damage, or classification, cannot be determined based on the parameters of the numerical model to be associated with damage. It is simply assumed that the damage produces a local change in the considered parameters which provides no information regarding the type of damage. In the data-based approach, unsupervised learning is often required, which allows for level I, and, to a certain extent, level II damage detection. Although supervised learning provides the opportunities for level I-V damage detection, data from all realistic damage situations are generally not available for large operating structures such as bridges. Therefore, supervised learning is not considered feasible in the data-based approach. The hybrid approach can consider both unsupervised and supervised learning. Furthermore, statistical models can, in theory, when coupled with numerical models and applied in supervised learning, be used for level I-V damage detection. Consequently, the hybrid approach has the potential to provide a significant impact on the future development of SHM.

According to the hierarchical structure of damage identification, level III damage detection requires level II. In other words, classifying or determining the type of damage requires knowledge of the damage location. There is, however, no clear distinction between level III and the degree of level II damage detection provided in the literature. Consequently, a brief discussion of this subject is included in the following.

In supervised learning, the appropriate class labels can encode damage information, such as the location and type. However, the degree of level II damage detection depends on the chosen analysis approach. To utilize supervised learning for location purposes, the damage state conditions must be quantized. In other words, in terms of the location, the structure should be divided into labelled substructures. In this case, the machine learning algorithm can perform localization within a substructure, and the degree of localization depends on the number of labelled substructures. Furthermore, the machine learning algorithm can be trained to yield the probability of a class membership. The following analysis approaches in supervised learning can be considered:

- Consider an analysis approach in which the target variable is a matrix, $\mathbf{y} \in \mathbb{N}^{n \times q}$, where n denotes the samples, and q denotes the substructures. The localization is performed in the labelled substructures, and the degree of localization depends on the chosen resolution of the structure. This situation pertains to supervised learning with increased possibilities of realizing level II damage detection.
- Consider an analysis approach in which the target variable is a vector consisting of discrete class labels, $\mathbf{y} \in \mathbb{N}^{n \times 1}$. The localization is performed in the labelled substructure, which, in this case, is the entire structure represented by the scalar discrete class label in the target variable. This situation pertains to supervised learning with limited possibilities of realizing level II damage detection.

This thesis is mainly concerned with implementing the latter analysis approach in supervised learning, which limits the possibility of performing level II damage detection. It should also be noted that, within supervised learning, other level II damage detection approaches can be implemented by considering feature selection to determine the statistical significance of the features, or dimension reduction techniques to reduce features that are of minor or no relevance. Such alternatives can be used to realize level II damage detection; however, some uncertainties related to these alternatives exist depending on the type and number of features used.

The aim of statistical model development is to reduce classification errors, which fall into two categories: Type I and Type II errors. Type I errors, or false positive indications of damage, provide indications of damage in the structure when no damage is present. Type II errors, or false negative indications of damage, provide no indications of damage in the structure when damage is present. As such, the primary motive of SHM is to design a system that minimizes FP indications of damage for economic and reliability concerns and FN indications of damage for life-safety issues.

As a final note, statistical model development allows the implementation of two types of SHM [40]: protective and predictive monitoring. Protective monitoring refers to the situation where damage-sensitive features are used to identify upcoming failure before catastrophic failure occurs, whereas predictive monitoring refers to the situation where trends in damage-sensitive features are identified to predict the critical damage level. The latter is needed to develop cost-effective planning of maintenance, which is an important motive for asset owners.

1.2.3 The fundamental axioms of SHM

Based on the research performed within SHM over the last 30 years, fundamental axioms or general principles have been formed. These SHM axioms are summarized in the following [62], [63]:

- **Axiom I.** All materials have inherent flaws or defects.

  Imperfections or defects are inherent in all materials. Defects lead to damage, and damage ultimately leads to failure. Structures can be designed to be tolerant to damage at some point during the operational lifetime, provided that monitoring systems are introduced to ensure safe operation.

- **Axiom II.** The damage assessment requires a comparison between two system states.

  In both the model-based and data-based SHM approaches, data representing the undamaged condition, or baseline, is needed. Furthermore, to perform damage detection beyond level I and II, the data must be expanded to contain information corresponding to various damage conditions. Baseline data must always be present to compare between two system states to assess damage.

- **Axiom III.** Identifying the existence and location of damage can be done in an unsupervised learning mode, but identifying the type of damage present and the damage severity can generally only be done in a supervised learning mode.

  Unsupervised learning refers to the situation where data are available from the undamaged condition of the structure, whereas supervised learning refers to the situation where data are available from both undamaged and damaged conditions. Novelty detection is the main class of algorithms applied in unsupervised learning. Furthermore, classification and regression analysis are associated with discrete and continuous classification, respectively, and are categories of supervised learning.

- **Axiom IVa**. Sensors cannot measure damage. Feature extraction through signal processing and statistical classification are necessary to convert sensor data into damage information.

  Sensors cannot directly measure damage; they merely measure the response of the structure to the operational and environmental conditions. This can be understood by considering the equation $\mathbf{x} = \mathbf{f}(D)$, where the (multidimensional) vector $\mathbf{x}$ measures some quantity of interest and $\mathbf{f}(D)$ is a function of the damage state of the structure, D. The challenge in SHM is that $\mathbf{f}(D)$ must be learned from the data obtained from the sensors since this function is generally not known from basic physics.

- **Axiom IVb.** Without intelligent feature extraction, the more sensitive a measurement is to damage, the more sensitive it is to changing operational and environmental conditions.

  Features derived from measured data depend on the operational and environmental variables in addition to the damage. Feature extraction should ideally result in features that depend only on the damage and have reduced or eliminated sensitivity to other factors.

- **Axiom V.** The length and time scales associated with damage initiation and evolution dictate the required properties of the SHM sensing system.

  The design parameters of the SHM system hardware depend on (1) the length scale associated with the damage, i.e., somewhere between a defect and a failure, and (2) the time scale associated with the damage, which can be a short time scale caused by sudden discrete events or a long time scale through a gradual accumulation of damage. Quantifying the length and time scales prior to installing the SHM systems allows for an efficient design.

- **Axiom VI.** There is a trade-off between the sensitivity to damage of an algorithm and its noise rejection capability.

  The level of noise in the data should be reduced as much as possible to increase the likelihood of successful damage detection.

- **Axiom VII.** The size of damage that can be detected from changes in system dynamics is inversely proportional to the frequency range of excitation.

  By considering the relationship $\lambda = v/f$, where λ, v and f denote the wavelength, wave phase velocity and frequency, respectively, it is clear that the wavelength will decrease as the frequency increases when a constant velocity is considered. This, in turn, implies that the damage sensitivity will increase. Hence, the sensitivity to damage increases with increasing frequency. Global low-frequency modes of structures such as bridges have long wavelengths that are insensitive to local damage. Local damage is more likely to be detected in high frequencies.

- **Axiom VIII.** Damage increases the complexity of a structure.

  The complexity of the structure increases in cases where damage causes a structure that originally exhibits linear behavior to exhibit nonlinear behavior. A change in the complexity is assessed through structural response measurements. Furthermore, a change in the complexity, or information content, can be evaluated in terms of complex quantitative measures such as the entropy as defined in information theory. Almost all features in SHM assess changes in the complexity of a structure resulting from damage.

1.2.4 Challenges in SHM

In addition to the research issues stated in the fundamental axioms, the following challenges in SHM are defined in various literature:

- Structural damage is typically a local phenomenon and may not significantly influence the global response of the structure. As a result of Axiom VII, this challenge is inevitably relevant in SHM applications of bridges.

- Instrumenting large structures, such as bridges, with many sensors still represent a sparsely instrumented system. This was exemplified in Section 1.1. Furthermore, SHM systems involving many sensors provide challenges with respect to maintenance, reliability, redundancy, and data management. Additionally, there is no accepted methodology for the sensor design in SHM systems since individual considerations must be made for all structures.

- Variability in the operational and environmental conditions affects the structural response and can mask changes caused by damage. A fundamental challenge in SHM is the process of separating changes caused by operational and environmental conditions from changes caused by damage. Considering data normalization is important for the successful deployment of a robust SHM system.

- A fundamental challenge in SHM is that almost all statistical decision making must be done in an unsupervised learning mode. Unsupervised learning is often required for bridges in operation since data from both the undamaged and damaged conditions are rarely available.

- There are no criteria for selecting machine learning or deep learning algorithms in SHM applications. There is a large variety of different algorithms and network architectures to choose from. Furthermore, setting classification boundaries in the decision-making process is challenging. There is a trade-off between acceptable levels of FP and FN indications of damage.

- It is desirable to optimize the cost-benefit of SHM systems in the operational evaluation or design process [64]. However, quantifying the cost of SHM is difficult. Furthermore, there is no general accepted procedure to demonstrate the rate of return on investment in SHM systems.

- There is a need for recommended practices, certification, regulations, and standardization in SHM. Codes and standards for SHM have been developed [65]. However, further development with respect to requirements in SHM of large structures is needed.

- There is a need for validation of SHM approaches, procedures, techniques and algorithms on real bridge structures. This aspect also includes the application of statistical model development. Experimental benchmark studies that are representative of real bridge structures are essential in this regard.

1.3 PhD thesis

1.3.1 General

The research needs stated in Section 1.1, along with the fundamental axioms and challenges defined in SHM in Section 1.2 form the basis of the research objective in this PhD thesis.

1.3.2 Objective

The research objective in this thesis is to implement, evaluate and further develop current approaches for damage detection and SHM on steel bridges through numerical and experimental studies.

1.3.3 Scope of work

To accomplish the research objective in this thesis, the following scope of work is defined:

- **Determine the damage detection possibilities for improved bridge inspection by simple existing experimental methods**
  Inspection is the preferred non-destructive evaluation method of existing bridges in service. To improve the quality and process of current bridge inspections, a part of the scope of work is to assess the damage detection possibilities by introducing a methodology that performs analysis of response measurements obtained from a systematic experimental study of a full-scale bridge using a modal hammer.

- **Establish data from an extensive experimental benchmark study of a full-scale bridge under different structural state conditions**
  There are currently no available data of steel bridges that provide dynamic response measurements (acceleration and strain) under different structural state conditions with multiple relevant damage scenarios. An important part of the scope of work is therefore to establish data from a full-scale bridge for use in damage detection and SHM applications.

- **Establish a validated numerical FE model**
  To perform numerical simulations for damage detection and SHM purposes, it is imperative to have an accurate numerical FE model with realistic parameter values. Therefore, a vital part of the scope of work is to develop and implement a strategy to effectively establish a validated numerical FE model using FE model updating.

- **Develop a hybrid SHM framework for damage detection in bridges using numerical and experimental data**
  To further advance the field of SHM for the application to bridges, an approach that can overcome the limitations of the model-based and data-based SHM approaches is needed. Consequently, an essential part of the scope of work is to develop a hybrid SHM framework for damage detection by integrating numerical models, experimental data, and machine learning.

- **Implement and evaluate a data-based SHM approach for damage detection in bridges using only experimental data**
  Currently, there are no studies in the literature where statistical model development is performed based on experimental studies of steel bridges. A key part of the scope of work is therefore to implement and evaluate a data-based SHM approach using both unsupervised and supervised machine learning algorithms for damage detection based only on experimental data.

1.3.4 Assumptions and limitations

The Hell Bridge Test Arena is used as a case study in the research. To further clarify the framework of the scope of work defined in this thesis, the following assumptions and limitations are included:

Assumptions

- The bridge is assumed to be highly representative of the existing bridges still in service, despite the minor modifications made when establishing the bridge as a damage detection test structure, i.e., taking the bridge out of service and moving it to new foundations on land.
- Only vibration-based assessments to damage detection and SHM are considered. The underlying assumption for the vibration-based assessment is that (1) damage will somehow change the stiffness, mass or energy dissipation characteristics of the structural system, and (2) damage can provide changes to the boundary conditions or connections of the structural system. In both cases, the damage affects the structural dynamic response characteristics.

Limitations

- The model-based SHM approach is not considered due to the limitations identified with this approach, although a numerical FE model is utilized in large parts of this research.
- There exists a vast number of algorithms for supervised and unsupervised machine learning. This research does not focus on developing new algorithms but merely relies on existing algorithms that are well documented in the literature.
- This thesis is not concerned with topics related to quantifying the cost of SHM or the Value of Information (VoI).

1.4 Experimental benchmark study

1.4.1 General

The Hell Bridge Test Arena, shown in Figure 1.5, is a full-scale steel riveted truss bridge located in Norway. The bridge was built in 1902 and was in operation as a train bridge until it was taken out of service and moved to foundations on land in 2016. Despite its long service time, the bridge is highly representative of the many bridges still in service. The bridge has a main span of 35 m and width of 4.5 m. The structural system of the bridge is composed of two bridge walls, the bridge deck and the lateral bracing.

All cross sections, connections and details were originally made using steel plates connected by rivets. The bridge cross section is formed as a U-section with no upper lateral bracing to provide stiffening of the bridge. Moreover, the bridge deck is made of longitudinal stringers connected to transverse girders. The lateral bracing, located below the bridge deck, provides a stiffening of the bridge in the lateral direction to mainly withstand wind loads.

An extensive experimental benchmark study was performed in 2020 during the summer and fall. The objective of the experimental benchmark study was to establish dynamic response measurement data of the bridge under different structural state conditions for damage detection and SHM applications. As such, the scope of work was divided into two parts. In the first part, relevant local and global structural damage was introduced and prepared. In the second part, the structural monitoring system was installed, and test measurements in the undamaged and damaged state conditions of the bridge were carried out. The experimental benchmark study was conducted over approximately three months, excluding planning and data preprocessing.

Figure 1.5: The Hell Bridge Test Arena (HBTA).

1.4.2 Part 1 – Damage introduction

Relevant structural damage was introduced and prepared in the first part of the experimental benchmark study. The selection of damage types was based on three conditions: the frequent occurrence of the damage types according to the literature; the severity of the damage types with respect to the structural integrity; and the applicability and relevance to the bridge under consideration. An overview of common fatigue damage cases for steel and composite steel-concrete bridges is summarized in Figure 1.6. Based on this overview and the abovementioned conditions, four different damage types were considered: stringer-to-floor-beam connections; stringer cross beams; lateral bracing connections; and connections between floor beams and main load-carrying members. These damage types are highlighted in Figure 1.6. All the damage types are related to fatigue occurring in or below the bridge deck.

Altogether eight damage states were considered by introducing each damage type with varying degrees of severity. To represent different degrees of severity, each damage type was introduced at one or more locations in the bridge. Table 1.4 summarizes the structural state conditions. Additionally, the undamaged state of the bridge was represented by the baseline condition. Figure 1.7 shows an overview of the bridge and the damage state conditions introduced to the bridge deck and lateral bracing. For each damage state, damage was introduced, measurements were performed, and the damage was then repaired. In this way, measurements were obtained before and after introducing damage to the bridge.

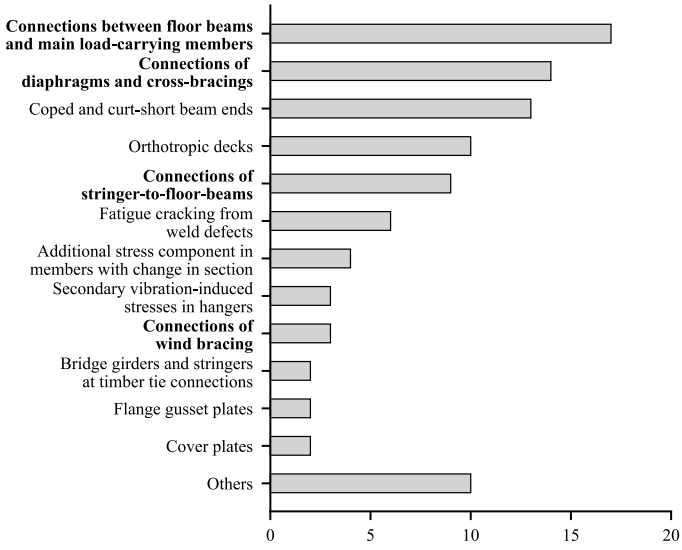

Figure 1.6: Overview of fatigue damage cases for steel and composite steel-concrete bridges [8]. The damage types considered in the experimental benchmark study are highlighted.

Table 1.4: Overview and description of the structural state conditions.

Label	State condition	Categorization[1]	Type	Description
UDS	Undamaged	-	Baseline condition	-
DS1	Damaged	Local	Stringer-to-floor-beam connection	Single connection damaged
DS2	Damaged	Local	Stringer-to-floor-beam connection	Multiple connections damaged
DS3	Damaged	Local	Stringer cross beam	Main part of single cross beam removed
DS4	Damaged	Local	Stringer cross beam	Main parts of multiple cross beams removed
DS5	Damaged	Global	Lateral bracing connection	Single connection damaged
DS6	Damaged	Global	Lateral bracing connection	Single connection damaged
DS7	Damaged	Global	Lateral bracing connection	Multiple connections damaged
DS8	Damaged	Global	Connection between the floor beam and main load-carrying member	Single connection damaged

[1] Local: damage to the secondary steel. Global: damage to the primary steel.

Each damage type and the corresponding damage state conditions were prepared by replacing existing rivets with bolts. Furthermore, each damage state condition was imposed by temporarily removing all bolts. As such, each damage state considered highly progressed damage, representing large cracks or loose connections that open and close under dynamic loading, typically caused by traffic or large environmental loads. These damage states correspond to fully developed cracks resulting from fatigue, leading to a total loss of functionality. It should be noted that this damage progression leads to a redistribution of forces in the structure. This situation would be demanding on the structure over time but is not

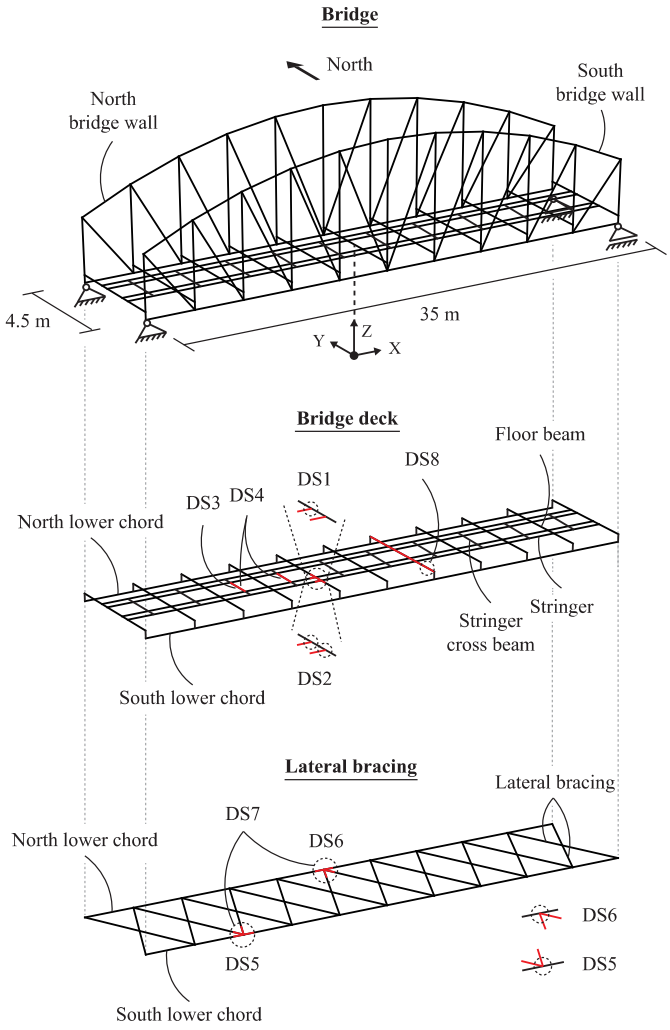

Figure 1.7: Damage introduced to the bridge deck and lateral bracing.

considered critical to the immediate structural integrity due to the structural redundancy of the bridge.

Of the four damage types considered in the experimental benchmark study, two damage types were of major importance with respect to the structural integrity of the bridge considering operational loading (traffic): the stringer-to-floor-beam connections; and the connection between the floor beam and main load-carrying member. Furthermore, the stringer cross beams and lateral bracing connections damage types were of minor importance with respect to the structural integrity and operational loading. These damage types ensure the stability of the bridge against lateral and torsional loads mainly during environmental loading. Figure 1.8 shows the damage types imposed on the bridge before and after damage.

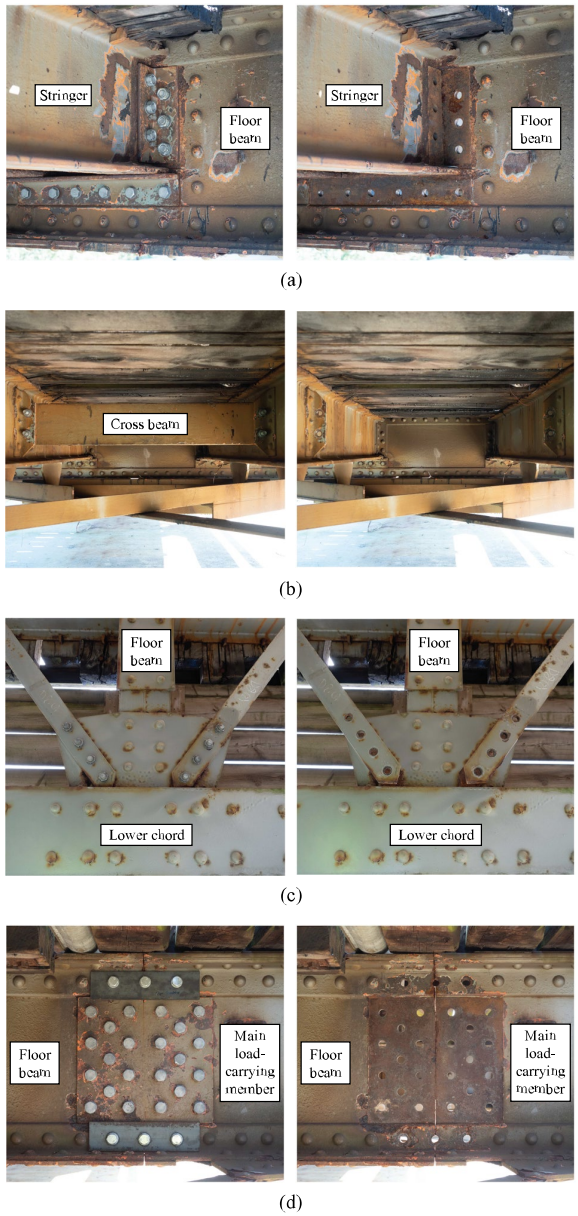

Figure 1.8: The damage types imposed on the bridge (before and after damage). (a) Stringer-to-floor beam connection. (b) Stringer cross beam. (c) Lateral bracing connection. (d) Connection between the floor beam and main load-carrying member.

1.4.3 Part 2 – Experimental setup and test measurements

Installation of the structural monitoring system and test measurements were performed in the second part of the experimental benchmark study. An instrumentation system from National Instruments was used to acquire data from 58 accelerometers and 15 strain gages. Figure 1.9 and Figure 1.10 show overviews of the acceleration and strain sensors, respectively. The environmental conditions (weather) were logged manually.

The acceleration sensors consisted of two groups. Sensor group 1 consisted of 40 single-axis accelerometers to measure the local response of the bridge deck in the vertical direction (global z-direction), whereas sensor group 2 consisted of 18 tri-axial accelerometers to measure the global response of the bridge in both lateral and vertical directions (global y and z-directions). Additionally, one accelerometer was allocated to measure the input force of the load excitation source.

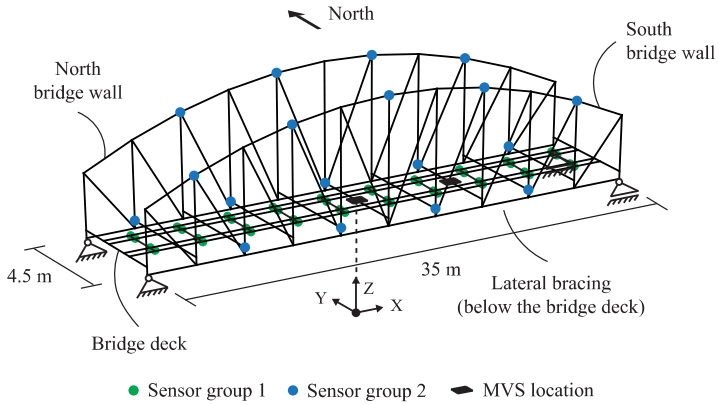

Figure 1.9: Overview of the acceleration sensors and the modal vibration shaker (MVS) locations.

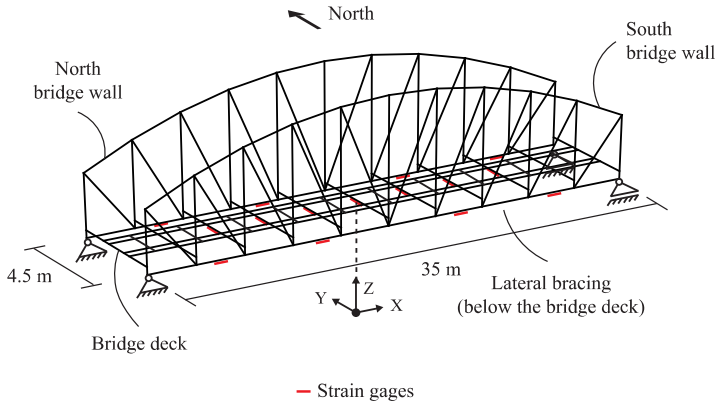

Figure 1.10: Overview of the strain sensors.

Altogether 15 quarter bridge strain gages with a nominal resistance of 120 ohms and 6 mm grid length were used for the strain measurements. The strain gages were located on the primary steel components, i.e., the floor beams and lower chords, to measure the maximum strain from axial forces and bending about the strong and weak axes.

The instrumentation system consisted of three individual data acquisition (DAQ) units, shown in Figure 1.11. Data were sampled at 400 Hz. Preprocessing of the data was performed in two steps after all the measurement data had been collected. In the first step, interpolation of signals and subsequent data merging was performed to obtain synchronous data. The interpolation was based on a common time vector obtained from the global positioning system (GPS) signals of each DAQ unit. In the second step, general data processing was performed by adding sensor sensitivities, detrending, low-pass filtering and resampling.

The bridge was excited in the vertical (global z) and lateral (global y) directions using a modal vibration shaker (APS 420) as a load excitation source. Figure 1.12 shows the modal vibration shaker in the vertical and horizontal configurations. The modal vibration shaker was used in two positions: at bridge midspan and approximately at one-third of the bridge span, shown in Figure 1.9. Furthermore, the modal vibration shaker was operated in sine sweep and noise modes. Specifications of the sine sweep and noise modes are provided in Table 1.5 and Table 1.6, respectively.

In sine mode, the sine sweep counted one when reaching the target (end) frequency. Hence, with the number of sweeps equal to two, a full sweep of the defined frequency range was performed once. The sweep speed, which determined the rate of frequency change, was constant at 1 Oct/min. With a sweep rate of 1 Oct/min, the frequency doubles every minute. It took approximately 10 min to perform one full sweep of the defined frequency range. The modal vibration shaker provided a maximum of 900 N (theoretically) in sine sweep mode. In noise mode, random white noise was generated within the defined frequency spectrum. The length of each run in the noise mode was 15 min (900 sec). The modal vibration shaker provided a varying force in the range of approximately 180-210 N for the noise mode settings summarized in Table 1.6.

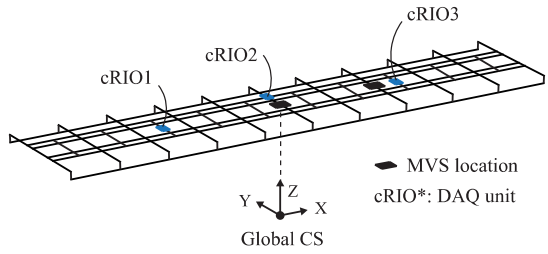

Figure 1.11: Overview of the instrumentation system DAQ units on the bridge deck.

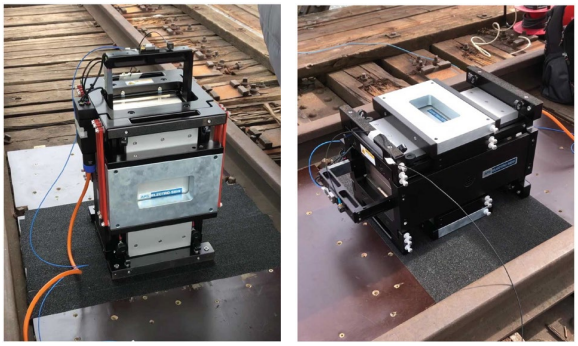

(a) (b)

Figure 1.12: The modal vibration shaker. (a) Vertical position. (b) Horizontal position.

Table 1.5: Sine sweep mode specifications.

Specification	Value
Minimum frequency (Hz)	2
Maximum frequency (Hz)	55
Start frequency (Hz)	2
Start direction	Up
Sweep type[1]	Log
Sweep speed	1
Limit type	Sweep count
Number of sweeps	2

[1] The sweep speed is provided in Oct/min.

Table 1.6: Noise mode specifications.

Specification	Value
Minimum frequency (Hz)	1
Maximum frequency (Hz)	100
Mode	Random
Limit type	Time
Time limit (sec)	900

Altogether, two measurement test setups were performed. In each measurement test setup, all the damage state conditions were introduced with the modal vibration shaker at one of the specified locations. The modal vibration shaker was used in both sine sweep and noise modes at the bridge midspan, while it was only used in sine sweep mode at the approximate one-third bridge span. Different environmental conditions were experienced in each measurement test setup.

1.5 Summary

1.5.1 General

The works in this thesis have been published in international peer-reviewed journals (Parts 1 and 2) or are submitted for publication in international peer-reviewed journals (Parts 3 and 4). The four papers are summarized below.

1.5.2 Part 1

Svendsen, B. T., Frøseth, G. T., and Rønnquist, A. (2020). *Damage detection applied to a full-scale steel bridge using temporal moments*. Shock and Vibration, 1-16. https://doi.org/10.1155/2020/3083752.

The first paper presents a methodology for detecting damage in the joint connections of existing steel bridges to improve the quality of bridge inspections. The paper highlights two important issues: first, there are several challenges with visual bridge inspections, which is the preferred non-destructive evaluation (NDE) method of existing bridges; and second, the most common damage types in existing highway and railway steel bridges are caused by fatigue and most frequently occur in or below the bridge deck. The proposed methodology, which combines the use of temporal moments from response measurements with an appropriate instrumentation setup, addresses these issues. Temporal moments are statistical parameters that characterize transient dynamic signals. The theory of temporal moments is presented, and a description of the experimental study performed on the bridge is provided. The experimental study considers a systematic monitoring procedure where transient acceleration response measurements are obtained using a modal hammer. The temporal moments obtained from each joint are established in feature vectors, which are subsequently assessed using a damage indicator matrix. The damage indicator matrix provides a statistical comparison of all joints based on the measure of correlation. From the results presented, two existing and known damages below the bridge deck are identified and localized. Damage *identification* is performed by comparing statistical parameters based on temporal moments to a baseline, and damage *localization* is performed by utilizing the instrumentation setup. The study also includes a sensitivity analysis by investigating the effects of sampling frequency on the damage identification, which shows that a high sampling frequency is required. The main limitation identified in the study is the need for an adequate number of joint connections or similar structural components to obtain a baseline. In cases where the baseline is adequate, it is concluded that the methodology, which is easy to implement and requires limited technical equipment, can contribute to improving the identification of critical damage during a scheduled bridge inspection.

1.5.3 Part 2

Svendsen, B. T., Petersen, Ø. W., Frøseth, G. T., and Rønnquist, A. (2021). *Improved finite element model updating of a full-scale steel bridge using sensitivity analysis*. Structure and Infrastructure Engineering, 1-17. https://doi.org/10.1080/15732479.2021.1944227.

The second paper investigates the effects of using a sensitivity analysis for improved model updating. The aim of the paper is twofold: first, develop a procedure to obtain an optimal solution from model updating; and second, apply the procedure to obtain a calibrated numerical FE model of the bridge. The sensitivity-based model updating framework, including the implementation of the local parameter bounds in the optimization algorithm, is presented. There are several choices required to be made in model updating with respect to (1) ratios of overdetermined systems, which is related to the parameterization of the numerical model and the number of measured outputs available from the experimental study, and (2) the constraints to enforce on the parameters. These choices largely affect the improvement of the modal parameters and the parameter values of the calibrated model. Therefore, a procedure is developed to consider these choices in a structured approach. Through a sensitivity analysis, the proposed procedure is applied to the numerical model of the bridge, which is established and parameterized by considering general uncertainties and several model simplifications. The sensitivity analysis results in several solutions with improved modal properties but with a large variability in the parameter values. These effects demonstrate the importance of the sensitivity analysis. However, an optimal solution from the sensitivity analysis is obtained, and from this solution an improvement in the modal parameters of the bridge is achieved with highly reliable parameter values. The average absolute frequency error is decreased from 5.22% to 3.84%, and the MAC numbers are improved from 0.72 to 0.75 considering all modes, including the control modes. The main challenge in the work presented lies in the model parameterization, which accounts for modelling inaccuracies, including the model simplifications introduced to reduce the complexity of the model, and uncertainties in the bridge structural properties. Nevertheless, the calibrated numerical model obtained is beneficial for performing a large number of numerical simulations and is developed for the hybrid SHM framework proposed in the third paper.

1.5.4 Part 3

Svendsen, B. T., Øiseth, O., Frøseth, G. T., and Rønnquist, A. (2021). *A hybrid structural health monitoring approach for damage detection in steel bridges under simulated environmental conditions using numerical and experimental data*. Submitted for journal publication.

In the third paper, a novel hybrid SHM framework for damage detection in bridges is presented. A grand challenge in SHM is that almost all statistical decision making must be done in an unsupervised learning mode. This paper aims at providing an important contribution towards solving this challenge. The concept of the hybrid SHM framework is presented. The framework combines the use of a numerical FE model to generate data from different structural state conditions under varying environmental conditions with machine learning algorithms, which allows for supervised learning to be applied. From the resulting machine learning model, experimental test data is applied to provide decision support or diagnose the structure. The extensive experimental benchmark study of the bridge is presented, and the experimental test data are obtained by performing output-only system identification using the covariance-driven stochastic subspace identification (cov-SSI) method. The two most important damage types with respect to the immediate structural integrity of the bridge are considered in the study. Numerical simulations are performed by using the calibrated numerical model developed in the second paper. Importantly, the numerical simulations include variability in the environmental conditions. It is demonstrated that relevant structural damage can be established from the hybrid SHM framework by separately evaluating different cases considering natural frequencies, mode shapes and mode shape derivatives. Other important results include the establishment of all the damage types (including the undamaged state), and the performance of level I (existence), level II (location) and level III (type) damage detection. However, several uncertainties are found to be associated with different parts of the hybrid SHM process. Particularly, uncertainties related to (1) the representation of the numerical model and simulations, (2) the estimation of the modal parameters from the output-only system identification, (3) the performance of the machine learning algorithm and (4) the statistical representation of the experimental data, are highlighted. Reducing the uncertainties can further improve the damage detection and enable improved classification results. Despite the identified uncertainties, the work presented in the paper demonstrates that the hybrid SHM framework is successfully performed for damage detection. The study also shows the importance of a dense sensor network for performing level II (location) damage detection.

1.5.5 Part 4

Svendsen, B. T., Frøseth, G. T., Øiseth, O., and Rønnquist, A. (2021). *A data-based structural health monitoring approach for damage detection in steel bridges using experimental data*. Journal of Civil Structural Health Monitoring, 1-15. https://doi.org/10.1007/s13349-021-00530-8.

In the fourth paper, a data-based SHM approach for damage detection in bridges using only experimental data is presented. The aim of the paper is to detect local and global structural damage using an unsupervised learning algorithm by novelty detection. Furthermore, an important part of the study is to evaluate the detectability of the different damage types within the established dataset by considering the average performance of four supervised learning algorithms. Similar to the third paper, the experimental study is described, including the damage introduced to the bridge and the operational and environmental conditions experienced during the measurements. The main difference from the previous study is that all the damage state conditions are now considered. Furthermore, more data are used, which allows for a quality assessment of the SHM system in terms of receiver operating characteristics (ROC) curves. Autoregressive (AR) parameters are used as damage-sensitive features, and the important process of selecting the appropriate AR model order is detailed. The results obtained from the statistical model development using both supervised and unsupervised learning algorithms are presented. An important finding from the statistical model development in unsupervised learning is that the Mahalanobis squared distance (MSD) algorithm performs well with respect to minimizing both false positive and false negative indications of damage. Importantly, it performs almost equally as well as the best supervised learning algorithms. The importance of a dense sensor network on the classification results in unsupervised learning is also shown. From the statistical model development in supervised learning, the two most important damage types with respect to the immediate structural integrity of the bridge are best detected. Although these results have limited practical significance since data from both the damaged and undamaged conditions are rarely available for bridges in operation, the results provide invaluable information in the design of SHM systems. A limitation in this study is the lack of data normalization assessment; a larger variability in the operational and environmental conditions than experienced during the measurements is needed for the baseline data that represent the undamaged condition. Nevertheless, the study provides several important contributions to the field of SHM regarding its application to bridges.

1.6 Concluding remarks

Based on the results obtained from the research presented in this thesis, the following concluding remarks are made:

- **Damage detection possibilities for improved bridge inspection by simple existing experimental methods.**
  The damage detection possibilities were investigated by introducing a methodology for damage detection on existing bridges for improved bridge inspection. The main limitation concerning the damage detection possibilities of the methodology presented is the need for an adequate number of similar structural components to obtain a baseline for comparison. Additionally, the baseline can be affected in cases where many damages are present in the structural system. Despite this limitation, the methodology is easy to implement, both in a practical and technical manner, and limited technical equipment is needed. Furthermore, temporal moments are found to be excellent features for transient dynamic signals. Most importantly, damage in structural components such as joint connections can be established in an actual bridge.

  Although there are several advantages with the work presented in this part of the research, it is important to highlight that the methodology does not provide solutions to many of the current challenges experienced in traditional bridge inspection; it merely improves the possibilities for detecting local damage of certain structural components. Furthermore, the methodology cannot fully replace existing methods, such as visual assessments, and therefore adds additional manual work to current bridge inspections. Although the methodology is demonstrated to work as a damage detection approach, the main conclusions from this part of the research are that (1) more reliable and advanced approaches for data interpretation to enhance the damage detection, preferably in an SHM context, are needed, and (2) effort should be made in developing automated and reliable SHM systems that can detect both local and global damage.

- **Experimental benchmark study of a full-scale bridge under different structural state conditions.**
  An extensive experimental benchmark study of the Hell Bridge Test Arena was performed to obtain data under different structural state conditions. There are several observations that can be viewed as limitations of the experimental study. First, only fully developed damage is considered, representing loose connections and large cracks that open and close under dynamic loading. Consequently, lower degrees of damage have not been considered. Second, the statistical representation of the experimental data is somewhat limited. Additional measurements and tests are needed to obtain a better statistical representation of the data from each damage state condition, including the baseline condition. This limitation is caused by constraints on time and resources allocated to the experimental study. Third, low variability in the operational and environmental conditions experienced during the experimental

study limits the possibility of performing data normalization. Last, the signal-to-noise (SNR) ratio of the strain data is low. Exciting the bridge in its resonance frequencies by using the modal vibration shaker does not provide significant excitation for the strain measurements. Higher force excitation than provided by the modal vibration shaker is needed to increase the SNR of the strain measurements.

Regardless of the limitations, a database of valuable response measurement data is established. The quality of the acceleration data is excellent, and the strain data are useful. Furthermore, local and global response measurements are obtained from a dense instrumentation setup under different structural state conditions and environmental conditions. All operational and environmental conditions were logged. Additionally, the damage types chosen, including their locations, represent (1) the most common and frequently reported damage types in the literature and (2) the most severe but relevant damage types for this type of bridge. In conclusion, a unique dataset that contains high-quality and valuable structural response measurement data of a full-scale bridge under different structural conditions for use in damage detection and SHM applications have successfully been established.

- **Validation of a numerical FE model.**
  A procedure to obtain an optimal solution from model updating was developed, and the procedure was applied to achieve a validated numerical FE model of the bridge. In general, developing a validated FE model is challenging: the work is time consuming; many assumptions must be made in the modelling and model parameterization; all relevant uncertainties must be accounted for; and small errors can have a significant effect on the analysis results. The main limitation of the developed procedure is the need for an adequate number of modes established from the system identification to be included in the model updating. Additionally, many analyses may be required to find the optimal solution with respect to improved modal properties combined with reasonable parameter values. The main limitation of the validated FE model is the limited improvement obtained in the modal properties. Further improvement in the modal properties would require a different parameterization and an increased complexity of the FE model. However, this is a consequence of the trade-off between a validated detailed FE model in good agreement with measurements and a validated FE model being computationally efficient for numerical simulations.

  There are major advantages of the work presented in this part of the research. The developed procedure can effectively establish an optimal solution in the model updating, resulting in a validated FE model. The procedure can be applied to similar case studies irrespective of the structure under consideration and the corresponding parameterization to be made. Furthermore, a validated FE model of the bridge is established with highly reliable parameter values by applying the procedure. It is concluded that the work performed in this part of the research has been successful in terms of

obtaining a validated FE model to perform numerical simulations for damage detection and SHM purposes.

- **A hybrid SHM framework for damage detection in bridges using numerical and experimental data.**
  A hybrid SHM framework for damage detection was developed by integrating numerical models, experimental data, and machine learning. The main limitation of this work is related to the identified uncertainties of the hybrid SHM framework. Particularly, the uncertainties related to the representation of the FE model and numerical simulations have the most significant effect on the classification results. In the context of SHM, it is instrumental to reduce false positive indications of damage for economic and reliability concerns and false negative indications of damage for life-safety issues. Further development of the hybrid SHM framework is still needed to achieve this.

  Despite the uncertainties, three major advantages with the hybrid SHM framework regarding its application to bridges are obtained. First, a supervised learning approach can be applied. Second, level I, II and III damage detection of relevant structural damage can be performed based only on numerical simulations of a calibrated FE model. Last, and most importantly, the framework is applicable to any bridge structure in which relevant structural damage can be simulated and experimental data obtained. In conclusion, the hybrid SHM framework can overcome the limitations of the model-based and data-based SHM approaches. Although further research is needed, the work in developing and evaluating the hybrid SHM framework represents a significant contribution towards establishing SHM systems that can be applied to existing bridges and can as such further advance the field of SHM for the application to bridges.

- **A data-based SHM approach for damage detection in bridges using only experimental data.**
  A data-based SHM approach was implemented and evaluated using both unsupervised and supervised machine learning algorithms for damage detection based only on experimental data. There are several limitations associated with this work. First, a dense sensor network is applied. A sensitivity analysis is carried out with a reduced number of sensors in different locations of the bridge deck to investigate the effect of a dense sensor network on the classification results. However, the sensitivity analysis is limited in extent with respect to *optimization* of the number and location of sensors on the structure. Second, only level I damage detection is considered in unsupervised learning, i.e., level II damage detection is not attempted. Third, an assessment of the variability in the operational and environmental conditions through data normalization is not included due to a generally low variability in the environmental conditions experienced during the experimental study. Last, the analysis approach used provides a high dimension of the feature space, which limits the number of features that can be included per sensor channel.

Nevertheless, two major advantages of this part of the research are highlighted. First, relevant structural damage can be found and well classified in an unsupervised learning approach from simulated ambient vibration. Furthermore, the unsupervised learning algorithm performs almost as well as the supervised learning algorithms within the established dataset. Second, an evaluation of the damage types that best can be detected is performed by utilizing the supervised learning algorithms. This evaluation is valuable for the design of SHM systems with respect to the instrumentation setup and sensor placement. From the work performed in this part of the research, a data-based approach based on an extensive experimental study has been successfully implemented and evaluated. Although a dense sensor network is utilized, the data-based approach is considered feasible for detecting relevant structural damage using statistical model development. In conclusion, the study provides valuable contributions to the field of SHM regarding its application to bridges.

Through the scope of work defined, current approaches for damage detection and SHM are implemented, evaluated, and further developed through numerical and experimental studies. As such, the objective of the research in this thesis is accomplished.

1.7 Suggestions for further work

Based on the results obtained and conclusions made from the research presented in this thesis, the following suggestions for future work are made:

Experimental benchmark study

- Extend the experimental benchmark study to include (1) the application of lower degrees of damage and (2) additional measurements and tests to obtain a better statistical representation of the data from each damage state condition. The research performed in this thesis has focused on imposing damage considered highly progressed, representing loose connections and large cracks that open and close under dynamic loading. Consequently, all the bolts for each damage type and in each damage state condition have been removed during testing. Future research should investigate if lower degrees of damage can be detected by (*i*) only removing a subset of bolts in the connections and (*ii*) leaving bolts untightened in the connections.
- Extend the experimental benchmark study with additional test measurements to investigate and map the effects of environmental conditions on modal parameters (such as natural frequencies, mode shapes and damping) of steel bridges for the typical European and Scandinavian climate. The long-term effects of environmental conditions with respect to temperature and humidity are of particular interest for damage detection and SHM purposes. The studies currently found in the literature are primarily based on concrete bridges. Data with variability in the operational and environmental conditions allow for studies on data normalization.

The hybrid SHM approach

- Optimize and increase the efficiency of generating training data from the numerical model in the hybrid SHM framework using surrogate modelling. Particularly, the use of surrogate modelling could be introduced by generating training data that takes variability in the operational and environmental conditions into consideration through key parameters of the numerical model for each damage state and location. A resulting outcome could lead to a significantly larger dataset for training.
- Implement an Artificial Neural Network (ANN) configuration for enhanced level II damage detection in the hybrid SHM framework. The appropriate class labels in supervised learning can encode damage information, such as the type and location. However, the degree of level II damage detection depends on the analysis approach chosen. Supervised learning with limited possibilities of performing level II damage detection has been employed in the presented research. To use supervised learning for location purposes, the damage state conditions must be quantized. This means that, for location, the structure should be divided into labelled substructures. In such a case, the machine learning algorithm can perform localization within a substructure, and the degree of localization depends on the number of labelled substructures. Furthermore, the machine learning algorithm can be trained to give the probability of a class membership.

- Extend and further develop the hybrid SHM framework by (1) introducing increased complexity of the numerical model to reduce uncertainties related to the representation of the FE model and numerical simulations and (2) evaluating all damage types imposed in the experimental benchmark study. The damage types considered in the experimental benchmark study have different importance with respect to the traffic loading, environmental loading, and structural integrity. The damage types also have different likelihoods of occurrence. The research presented in this thesis only considered the most important damage types using a simplified numerical model with reduced complexity.

The data-based SHM approach

- Perform a study that optimizes the number and location of sensors on the structure, particularly on the bridge deck. Furthermore, perform sensitivity analyses in a systematic approach to investigate the level II damage detection possibilities in unsupervised learning. The study should be based on the established dataset from the experimental benchmark study, which provides data from a densely instrumented bridge.
- Implement and compare state-of-the-art unsupervised learning algorithms based on the established dataset from the experimental benchmark study. Several studies in the literature present novel unsupervised learning algorithms and comparison of algorithms. However, these studies are mostly based on numerical models or test structures and not on experimental data of real structures where relevant structural damage is imposed.

Other

- Investigate the effects of relevant structural damage imposed on steel bridges by considering only experimental and operational modal analysis. The research performed in this thesis only considered the natural frequencies and mode shapes of a *selection* of the most relevant global modes. Future research should investigate the effect of structural damage on more or all relevant global and local modes. This research should include the investigation of the bridge modal parameters, such as natural frequencies, mode shapes and damping, and how well the damage types, including the severity of the different damage types, can be established. Furthermore, different system identification methods should be compared based on several excitation methods, such as wind and load generated from the modal vibration shaker (band-limited random white noise and sine sweep). The already established dataset from the experimental benchmark study should be used for this purpose.
- Perform features extraction and feature selection studies based on experimental data. There exist numerous features to be applied in the time, frequency, and time-frequency domain in damage detection and SHM studies. In the research presented in this thesis, only a small subset of features has been considered. An evaluation of features, feature selection methods, and dimension reduction techniques for feature selection on the experimental data would be highly useful for consideration in the current and proposed SHM approaches.

- Address the use of SHM from a cost perspective and quantify the expected cost of the damage detection strategy for different sensor networks (number of sensors). The ROC curves constitute an essential tool for determining the best classifier. However, it is difficult to decide among thresholds based on false positive versus true positive rates. Determining appropriate thresholds based on a criterion of the minimum expected cost of the damage detection strategy can be considered for this purpose and would be valuable to consider in an SHM context based on the research performed in this thesis. Ultimately, such studies can allow for improvements in safety and reduction of bridge management costs.

References

[1] P. Rizzo and A. Enshaeian, “Bridge health monitoring in the United States: A review,” *Struct. Monit. Maint.*, vol. 8, no. 1, pp. 1–50, 2021, doi: 10.12989/smm.2021.8.1.001.

[2] B. Goldman, “The Federal Role in Railroad Bridge Safety,” 2018. [Online]. Available: https://www.everycrsreport.com/reports/IF10995.html

[3] K. Gkoumas *et al.*, *Research and innovation in bridge maintenance, inspection and monitoring - A European perspective based on the Transport Research and Innovation Monitoring and Information System (TRIMIS)*. 2019. doi: 10.2760/719505.

[4] M. Vagnoli, R. Remenyte-Prescott, and J. Andrews, “Railway bridge structural health monitoring and fault detection: State-of-the-art methods and future challenges,” *Struct. Heal. Monit.*, vol. 17, no. 4, pp. 971–1007, 2018, doi: 10.1177/1475921717721137.

[5] I. Olofsson *et al.*, “Assessment of European railway bridges for future traffic demands and longer lives – EC project ‘Sustainable Bridges,’” *Struct. Infrastruct. Eng.*, vol. 1, no. 2, pp. 93–100, 2005, doi: 10.1080/15732470412331289396.

[6] VG, “De forsømte broene,” 2017. https://www.vg.no/spesial/2017/de-forsomte-broene/slik-har-vi-jobbet/

[7] G. T. Frøseth, “Load model of historic traffic for fatigue life estimation of Norwegian railway bridges,” Norwegian University of Science and Technology, 2019.

[8] R. Haghani, M. Al-Emrani, and M. Heshmati, “Fatigue-Prone Details in Steel Bridges,” *Buildings*, vol. 2, no. 4, pp. 456–476, 2012, doi: 10.3390/buildings2040456.

[9] B. Åkesson, “Fatigue Life of Riveted Steel Bridges,” Chalmers University of Technology, Gøteborg, Sweden, 1994.

[10] D. H. Tobias and D. A. Foutch, “Reliability-Based Method for Fatigue Evaluation of Railway Bridges,” *J. Bridg. Eng.*, vol. 2, no. 2, pp. 53–60, May 1997, doi: 10.1061/(ASCE)1084-0702(1997)2:2(53).

[11] J. D. DiBattista, D. E. J. Adamson, and G. L. Kulak, “Evaluation of remaining fatigue life for riveted truss bridges,” *Can. J. Civ. Eng.*, vol. 25, no. 4, pp. 678–691, 1998, doi: 10.1139/l98-011.

[12] T. E. Cousins, J. M. Stallings, D. A. Lower, and T. E. Stafford, “Field evaluation of fatigue cracking in diaphragm-girder connections,” *J. Perform. Constr. Facil.*, vol. 12, no. 1, pp. 25–32, 1998, doi: 10.1061/(ASCE)0887-3828(1998)12:1(25).

[13] C. W. Roeder, G. MacRae, P. Crocker, K. Arima, and S. Wong, “Dynamic Response and Fatigue of Steel Tied-Arch Bridge,” *J. Bridg. Eng.*, vol. 5, no. 1, pp. 14–21, Feb. 2000, doi: 10.1061/(ASCE)1084-0702(2000)5:1(14).

[14] B. M. Imam, T. D. Righiniotis, and M. K. Chryssanthopoulos, “Probabilistic Fatigue Evaluation of Riveted Railway Bridges,” *J. Bridg. Eng.*, vol. 13, no. 3, pp. 237–244, May 2008, doi: 10.1061/(ASCE)1084-0702(2008)13:3(237).

[15] T. Guo and Y. W. Chen, “Field stress/displacement monitoring and fatigue reliability assessment of retrofitted steel bridge details,” *Eng. Fail. Anal.*, vol. 18, no. 1, pp. 354–363, 2011, doi: 10.1016/j.engfailanal.2010.09.014.

[16] T. Guo, D. M. Frangopol, and Y. Chen, “Fatigue reliability assessment of steel bridge details integrating weigh-in-motion data and probabilistic finite element analysis,” *Comput. Struct.*, vol. 112–113, pp. 245–257, 2012, doi: 10.1016/j.compstruc.2012.09.002.

[17] O. Riches, C. Hill, and P. Baralos, “Queensferry Crossing, UK: Durability, maintenance, inspection and monitoring,” *Proc. Inst. Civ. Eng. Bridg. Eng.*, vol. 172, no. 2, pp. 175–188, 2019, doi: 10.1680/jbren.18.00020.

[18] Y. Q. Ni and K. Y. Wong, “Integrating Bridge Structural Health Monitoring and Condition-Based Maintenance Management,” in *4th International Workshop on Civil Structural Health Monitoring*, 2012, pp. 6–8.

[19] S. W. Doebling, C. R. Farrar, M. B. Prime, and D. W. Shevitz, *Damage Identification and Health Monitoring of Structural and Mechanical Systems from Changes in Their Vibration Characteristics: A Literature Review*. Los Alamos National Laboratory report LA-13070-MS, 1996.

[20] H. Sohn *et al.*, *A Review of Structural Health Monitoring Literature: 1996-2001*. Los Alamos National Laboratory report, LA-13976-MS, 2004.

[21] E. A. Johnson, H. F. Lam, L. S. Katafygiotis, and J. L. Beck, “Phase I IASC-ASCE Structural Health Monitoring Benchmark Problem Using Simulated Data,” *J. Eng. Mech.*, vol. 130, no. 1, pp. 3–15, 2004, doi: 10.1061/(asce)0733-9399(2004)130:1(3).

[22] E. Figueiredo, G. Park, J. Figueiras, C. Farrar, and K. Worden, “Structural health monitoring algorithm comparisons using standard data sets,” 2009.

[23] C. R. Farrar *et al.*, “Dynamic characterization and damage detection in the I-40 bridge over the Rio Grande,” 1994.

[24] G. De Roeck, “The state-of-the-art of damage detection by vibration monitoring: The SIMCES experience,” *J. Struct. Control*, vol. 10, no. 2, pp. 127–134, 2003, doi: 10.1002/stc.20.

[25] J. Maeck and G. De Roeck, “Description of Z24 benchmark,” *Mech. Syst. Signal Process.*, vol. 17, no. 1, pp. 127–131, 2003, doi: 10.1006/mssp.2002.1548.

[26] M. Dilena and A. Morassi, “Dynamic testing of a damaged bridge,” *Mech. Syst. Signal Process.*, vol. 25, no. 5, pp. 1485–1507, 2011, doi: 10.1016/j.ymssp.2010.12.017.

[27] S. Maas, A. Zürbes, D. Waldmann, M. Waltering, V. Bungard, and G. De Roeck, “Damage assessment of concrete structures through dynamic testing methods. Part 2: Bridge tests,” *Eng. Struct.*, vol. 34, pp. 483–494, 2012, doi: 10.1016/j.engstruct.2011.09.018.

[28] M. Döhler, F. Hille, L. Mevel, and W. Rücker, “Structural health monitoring with statistical methods during progressive damage test of S101 Bridge,” *Eng. Struct.*, vol. 69, pp. 183–193, 2014, doi: 10.1016/j.engstruct.2014.03.010.

[29] R. V. Farahani and D. Penumadu, “Damage identification of a full-scale five-girder bridge using time-series analysis of vibration data,” *Eng. Struct.*, vol. 115, pp. 129–139, 2016, doi: 10.1016/j.engstruct.2016.02.008.

[30] C. W. Kim, K. C. Chang, S. Kitauchi, and P. J. McGetrick, “A field experiment on a steel Gerber-truss bridge for damage detection utilizing vehicle-induced vibrations,” *Struct. Heal. Monit.*, vol. 15, no. 2, pp. 174–192, 2016, doi: 10.1177/1475921715627506.

[31] C.-W. Kim, F.-L. Zhang, K.-C. Chang, P. J. McGetrick, and Y. Goi, “Ambient and Vehicle-Induced Vibration Data of a Steel Truss Bridge Subject to Artificial Damage,” *J. Bridg. Eng.*, vol. 26, no. 7, pp. 1–9, 2021, doi: 10.1061/(asce)be.1943-5592.0001730.

[32] H. Sohn, “Effects of environmental and operational variability on structural health monitoring,” *Philos. Trans. R. Soc. A Math. Phys. Eng. Sci.*, vol. 365, no. 1851, pp. 539–560, Feb. 2007, doi: 10.1098/rsta.2006.1935.

[33] H. Sohn, “Effects of environmental and operational variability on structural health monitoring,” *Philos. Trans. R. Soc. A Math. Phys. Eng. Sci.*, vol. 365, no. 1851, pp. 539–560, 2007, doi: 10.1098/rsta.2006.1935.

[34] L. Sun, Z. Shang, Y. Xia, S. Bhowmick, and S. Nagarajaiah, “Review of Bridge Structural Health Monitoring Aided by Big Data and Artificial Intelligence: From Condition Assessment to Damage Detection,” *J. Struct. Eng.*, vol. 146, no. 5, p. 04020073, 2020, doi: 10.1061/(asce)st.1943-541x.0002535.

[35] J. J. Moughty and J. R. Casas, “A state of the art review of modal-based damage detection in bridges: Development, challenges, and solutions,” *Appl. Sci.*, vol. 7, no. 5, 2017, doi: 10.3390/app7050510.

[36] Y. An, E. Chatzi, S. H. Sim, S. Laflamme, B. Blachowski, and J. Ou, “Recent progress and future trends on damage identification methods for bridge structures,” *Struct. Control Heal. Monit.*, vol. 26, no. 10, pp. 1–30, 2019, doi: 10.1002/stc.2416.

[37] P. Rizzo and A. Enshaeian, “Challenges in bridge health monitoring: A review,” *Sensors*, vol. 21, no. 13, 2021, doi: 10.3390/s21134336.

[38] C. R. Farrar and K. Worden, “An introduction to structural health monitoring,” *Philos. Trans. R. Soc. A Math. Phys. Eng. Sci.*, vol. 365, no. 1851, pp. 303–315, 2007, doi: 10.1098/rsta.2006.1928.

[39] K. Worden and J. M. Dulieu-Barton, “An Overview of Intelligent Fault Detection in Systems and Structures,” *Struct. Heal. Monit.*, vol. 3, no. 1, pp. 85–98, Mar. 2004, doi: 10.1177/1475921704041866.

[40] C. R. Farrar and K. Worden, *Structural Health Monitoring: A Machine Learning Perspective*. Wiley, 2012.

[41] R. J. Barthorpe, “On Model- and Data-Based Approaches to Structural Health Monitoring,” The University of Sheffield, 2010.

[42] I. Behmanesh and B. Moaveni, “Probabilistic identification of simulated damage on the Dowling Hall footbridge through Bayesian finite element model updating,” *Struct. Control Heal. Monit.*, vol. 22, no. 3, pp. 463–483, Mar. 2015, doi: 10.1002/stc.1684.

[43] E. Reynders, A. Teughels, and G. De Roeck, “Finite element model updating and structural damage identification using OMAX data,” *Mech. Syst. Signal Process.*, vol. 24, no. 5, pp. 1306–1323, 2010, doi: 10.1016/j.ymssp.2010.03.014.

[44] E. Reynders, G. De Roeck, P. G. Bakir, and C. Sauvage, “Damage Identification on the Tilff Bridge by Vibration Monitoring Using Optical Fiber Strain Sensors,” *J. Eng. Mech.*, vol. 133, no. 2, pp. 185–193, Feb. 2007, doi: 10.1061/(ASCE)0733-9399(2007)133:2(185).

[45] A. Teughels and G. De Roeck, “Structural damage identification of the highway bridge Z24 by FE model updating,” *J. Sound Vib.*, vol. 278, no. 3, pp. 589–610, 2004, doi: 10.1016/j.jsv.2003.10.041.

[46] J. Maeck, B. Peeters, and G. De Roeck, “Damage identification on the Z24 bridge using vibration monitoring,” *Smart Mater. Struct.*, vol. 10, no. 3, pp. 512–517, 2001, doi: 10.1088/0964-1726/10/3/313.

[47] O. Huth, G. Feltrin, J. Maeck, N. Kilic, and M. Motavalli, “Damage Identification Using Modal Data: Experiences on a Prestressed Concrete Bridge,” *J. Struct. Eng.*, vol. 131, no. 12, pp. 1898–1910, 2005, doi: 10.1061/(asce)0733-9445(2005)131:12(1898).

[48] C. R. Farrar, S. W. Doebling, and D. A. Nix, “Vibration-based structural damage identification,” *Philos. Trans. R. Soc. A Math. Phys. Eng. Sci.*, vol. 359, no. 1778, pp. 131–149, Jan. 2001, doi: 10.1098/rsta.2000.0717.

[49] A. C. Neves, I. González, J. Leander, and R. Karoumi, “Structural health monitoring of bridges: a model-free ANN-based approach to damage detection,” *J. Civ. Struct. Heal. Monit.*, vol. 7, no. 5, pp. 689–702, 2017, doi: 10.1007/s13349-017-0252-5.

[50] A. C. Neves, I. González, R. Karoumi, and J. Leander, “The influence of frequency content on the performance of artificial neural network–based damage detection systems tested on numerical and experimental bridge data,” *Struct. Heal. Monit.*, Jun. 2020, doi: 10.1177/1475921720924320.

[51] H. Pan, M. Azimi, F. Yan, and Z. Lin, “Time-Frequency-Based Data-Driven Structural Diagnosis and Damage Detection for Cable-Stayed Bridges,” *J. Bridg. Eng.*, vol. 23, no. 6, p. 04018033, Jun. 2018, doi: 10.1061/(ASCE)BE.1943-5592.0001199.

[52] E. Figueiredo, G. Park, C. R. Farrar, K. Worden, and J. Figueiras, “Machine learning algorithms for damage detection under operational and environmental variability,” *Struct. Heal. Monit.*, vol. 10, no. 6, pp. 559–572, 2011, doi: 10.1177/1475921710388971.

[53] A. Santos, E. Figueiredo, M. F. M. Silva, C. S. Sales, and J. C. W. A. Costa, “Machine learning algorithms for damage detection: Kernel-based approaches,” *J. Sound Vib.*, vol. 363, pp. 584–599, 2016, doi: 10.1016/j.jsv.2015.11.008.

[54] F. Magalhães, A. Cunha, and E. Caetano, “Vibration based structural health monitoring of an arch bridge: From automated OMA to damage detection,” *Mech. Syst. Signal Process.*, vol. 28, pp. 212–228, Apr. 2012, doi: 10.1016/j.ymssp.2011.06.011.

[55] E. Reynders, G. Wursten, and G. De Roeck, “Output-only structural health monitoring in changing environmental conditions by means of nonlinear system identification,” *Struct. Heal. Monit.*, vol. 13, no. 1, pp. 82–93, 2014, doi: 10.1177/1475921713502836.

[56] E. Figueiredo and E. Cross, “Linear approaches to modeling nonlinearities in long-term monitoring of bridges,” *J. Civ. Struct. Heal. Monit.*, vol. 3, no. 3, pp. 187–194, 2013, doi: 10.1007/s13349-013-0038-3.

[57] A. Santos, E. Figueiredo, M. Silva, R. Santos, C. Sales, and J. C. W. A. Costa, "Genetic-based EM algorithm to improve the robustness of Gaussian mixture models for damage detection in bridges," *Struct. Control Heal. Monit.*, vol. 24, no. 3, pp. 1–9, 2017, doi: 10.1002/stc.1886.

[58] H. Sohn, K. Worden, and C. R. Farrar, "Statistical damage classification under changing environmental and operational conditions," *J. Intell. Mater. Syst. Struct.*, vol. 13, no. 9, pp. 561–574, 2002, doi: 10.1106/104538902030904.

[59] M. Malekzadeh, G. Atia, and F. N. Catbas, "Performance-based structural health monitoring through an innovative hybrid data interpretation framework," *J. Civ. Struct. Heal. Monit.*, vol. 5, no. 3, pp. 287–305, 2015, doi: 10.1007/s13349-015-0118-7.

[60] E. Figueiredo, I. Moldovan, A. Santos, P. Campos, and J. C. W. A. Costa, "Finite Element–Based Machine-Learning Approach to Detect Damage in Bridges under Operational and Environmental Variations," *J. Bridg. Eng.*, vol. 24, no. 7, p. 04019061, Jul. 2019, doi: 10.1061/(ASCE)BE.1943-5592.0001432.

[61] A. Rytter, "Vibrational Based Inspection of Civil Engineering Structures," University of Aalborg, Denmark, 1993.

[62] K. Worden, C. R. Farrar, G. Manson, and G. Park, "The fundamental axioms of structural health monitoring," *Proc. R. Soc. A Math. Phys. Eng. Sci.*, vol. 463, no. 2082, pp. 1639–1664, 2007, doi: 10.1098/rspa.2007.1834.

[63] C. Farrar, K. Worden, and G. Park, "Complexity: A new axiom for Structural Health Monitoring," *Proc. 5th Eur. Work. - Struct. Heal. Monit. 2010*, pp. 882–888, 2010.

[64] C. Neves, "Structural Health Monitoring of Bridges: Data-based damage detection method using Machine Learning," KTH Royal Institute of Technology, 2020. doi: 10.13140/RG.2.2.33168.02562.

[65] F. Moreu, X. Li, S. Li, and D. Zhang, "Technical specifications of structural health monitoring for highway bridges: New chinese structural health monitoring code," *Front. Built Environ.*, vol. 4, no. March, pp. 1–12, 2018, doi: 10.3389/fbuil.2018.00010.

Part 1

The content of this part is published in:

Svendsen, B. T., Frøseth, G. T., and Rønnquist, A (2020). *Damage detection applied to a full-scale steel bridge using temporal moments*. Shock and Vibration, 2020, 1-16.

https://doi.org/10.1155/2020/3083752

Abstract

The most common damages in existing highway and railway steel bridges are related to fatigue and are, as reported in the literature, found in the structural system of the bridge deck. This paper proposes a methodology for detecting damaged joint connections in existing steel bridges to improve the quality of bridge inspections. The methodology combines the use of temporal moments from response measurements with an appropriate instrumentation setup. Damaged joint connections are identified by comparing statistical parameters based on temporal moments to a baseline, where the baseline data are established from statistical parameters evaluated for all considered joint connections. Localization of damaged joint connections is performed by utilizing the instrumentation setup. The feasibility of the proposed methodology is demonstrated through an experimental study on a full-scale steel riveted truss bridge with two known damages below the bridge deck, where both damages are identified and localized. The proposed methodology can improve the identification of critical structural damage during bridge inspections and is applicable to open-deck steel bridges.

Chapter 2

2 Damage detection applied to a full-scale steel bridge using temporal moments

2.1 Introduction

Deterioration and ageing of infrastructure is a major concern worldwide. Many highway and railway bridges are subject to increasing demands with respect to traffic loads and intensity, even though these structures are approaching or have exceeded their original design life. Considering the requirements for more efficient transportation systems, for which these bridges were not originally designed, many bridges are still in service despite ageing and the associated damage accumulation

Many of the existing bridges built in the first half of the 20th century in Europe and the U.S. are made of steel. The primary damage mechanism in these bridges is fatigue, and the most common types of fatigue damage reported are found in the structural system of the bridge deck [1]. Consequently, several case studies are performed on service life estimation and fatigue reliability analysis of structural components in the bridge deck structural system of steel bridges [2]–[9]. The connections between longitudinal stringers and transverse girders are critical and have been subject to investigation in studies of railway bridges [10]–[16]. These stringer-to-girder connections are not easily accessible and are consequently difficult to inspect. The induced damages involve cracking in various parts of the connections and can, if not detected at an early stage, develop and lead to component failure being critical for the structural integrity.

Inspections are performed to ensure the short-term safe operation of bridges. For railway bridges, visual inspection is the preferred non-destructive testing (NDT) method [17]. Typically, these inspections are specified in regular intervals to establish maintenance needs. There are several challenges related to visual inspections. First, inspections require direct access to critical structural components. Many bridges are in remote locations and have low general accessibility. To perform a full inspection requires either operational downtime or temporary installation of access support or both. Second, the quality of the inspection depends on the experience and knowledge of the inspector. Fatigue damage can be difficult to detect due to low visibility. Critical structural damage can be difficult to establish until the structure is subjected to operational or strong environmental loading. As such, having full access to a bridge for inspection is costly and provides no guarantee of finding damage. Third, periodic inspections do not provide full up-to-date information about the current state of the bridge condition. Structural health monitoring (SHM), defined as the process of implementing an automated and online strategy for damage detection in a structure [18], can provide such information. Although SHM systems can undoubtedly optimize the inspection process, development is still needed to ensure that such systems are affordable and reliable, and that these systems are likely to detect both

local and global damages. With the large number of existing bridges in infrastructure, an enhanced inspection methodology is needed to detect damage during bridge inspections.

Many vibration-based damage detection methods exist, of which most applications are based on numerical studies or laboratory studies performed in a controlled environment [19]–[23]. One method not widely reported in the literature is the use of temporal moments [24]. Temporal moments can be used to characterize shock or transient dynamic signals and are useful in describing the shape of such time histories. Only one study is found that has applied this method for damage detection purposes. Hemez *et al*. [25] applied temporal moments to acceleration response measurements obtained from a complex threaded assembly of metallic and joint components, where one of the objectives was to distinguish a loose assembly test from several tight assembly tests. The load was established as patches of explosives on the external surface of the system. The study concluded that the loose assembly test could be successfully distinguished from other tests through analyses using temporal moments. A similar analysis approach is utilized to detect damage in joint connections of full-scale steel bridges.

In this paper, a new methodology is proposed to detect damage in stringer-to-girder connections from the bridge deck to improve the process and quality of bridge inspections. This methodology consists of combining the use of temporal moments from response measurements with an appropriate instrumentation setup and a systematic monitoring procedure. As such, an experimental study on a full-scale steel bridge is carried out. Instrumentation of the bridge deck is performed, and acceleration response measurements are obtained using a modal hammer. By applying the method of temporal moments to the transient part of the acceleration response, feature vectors containing statistical parameters are established for the stringer-to-girder connections. Damaged connections are identified and localized by 1) investigation of individual statistical parameters and 2) establishing a damage indicator matrix by comparing feature vectors using a correlation analysis. The effect of sampling frequency is also investigated. The feasibility of the proposed methodology is discussed with respect to its applicability to similar bridges in service, in particular as a part of a general inspection plan for damage detection.

2.2 Temporal moments

2.2.1 Temporal moments in continuous time signals

Temporal moments describe how the energy of a signal is distributed over time. These are established by considering the square of the signal amplitudes and provide an alternative to statistically characterizing transient signals [26]. The *i*th-order temporal moment, M_i, about a reference time, t_r, for a continuous system is defined as [24]

$$M_i(t_r) = \int_{-\infty}^{+\infty} (t - t_r)^i \, y^2(t) \, dt \tag{2.1}$$

where, t denotes time and $y(t)$ is the system output, which is typically the response measurement signal. The first five moments are of particular relevance to describe the statistical properties of a transient signal: energy (E), central time (T), mean-square duration (D^2), skewness (S_t^3) and kurtosis (K_t^4). These moments are expressed in terms of basic and central moments. A *basic moment* is defined when the reference time, t_r, is 0. A simplified notation can then be introduced as

$$M_i(0) = M_i \tag{2.2}$$

Furthermore, a *central moment*, $M_i(T)$, is defined about a value T of the reference time when the first-order temporal moment is zero, i.e.,

$$M_1(T) = 0 \tag{2.3}$$

The definitions of the first five moments about T are given in terms of the basic and central moments. The energy, E, is the zero-order moment defined as

$$E = M_0(T) = M_0 \tag{2.4}$$

where $M_0(T)$ is the zero-order temporal moment. This moment is defined as the integral of the signal squared. It is independent of any reference time. Thus, it is referred to as the energy of the signal. The central time, T, is the first normalized central moment, which is defined as

$$T = \frac{M_1}{E} \tag{2.5}$$

where the basic moment, M_1, is established from the first-order temporal moment, $M_1(T)$ using Equations (2.1) and (2.2):

$$M_1(T) = \int_{-\infty}^{+\infty} (t - T) y^2(t)\, dt = 0 \tag{2.6}$$

The normalization with respect to E provides the time where the centroid of the energy is located, i.e. the centroid of the area under the squared signal amplitudes. By considering the distribution of energy over time, this moment represents the point where half of the energy has passed and half is to arrive at the sensor. A similar normalization is provided for the higher moments. The mean-square duration, D^2, is the second normalized central moment defined as

$$D^2 = \frac{M_2(T)}{E} \tag{2.7}$$

where $M_2(T)$ is the second-order temporal moment defined according to Equation (2.1). The mean-square duration describes the dispersion of the energy in the signal about the central time, T. The root-mean-square duration, D, is obtained by taking the square root of the expression in Equation (2.7). Due to the normalization, this expression provides the *time* of the energy dispersion. The most significant part of the energy is expected to be around the central time. The mean-square and root-mean-square (RMS) durations are analogous to the variance and

standard deviation of regular statistical moments, respectively. The central skewness, S_t, is the third normalized central moment defined as

$$S_t^3 = \frac{M_3(T)}{E} \tag{2.8}$$

where $M_3(T)$ is the third-order temporal moment defined according to Equation (2.1). Skewness normalized by the RMS duration provides a non-dimensional measure and is defined as

$$S = \frac{S_t}{D} \tag{2.9}$$

Skewness describes the shape of the signal energy in terms of symmetry. Symmetry about the central time T, or centroid, indicates zero skewness. A transient signal with high amplitudes to the left and a corresponding low-amplitude tail on the right side of the centroid has a positive skewness. Similarly, the opposite provides a negative skewness. The central kurtosis, K_t, is the fourth normalized central moment defined as

$$K_t^4 = \frac{M_4(T)}{E} \tag{2.10}$$

where $M_4(T)$ is the fourth-order temporal moment defined according to Equation (2.1). Like skewness, kurtosis normalized by the RMS duration provides a non-dimensional measure and is defined as

$$K = \frac{K_t}{D} \tag{2.11}$$

Kurtosis describes the tail shape of the signal energy. More precisely, kurtosis provides a measure for the outliers in the signal that are represented in the tails of the area under the squared signal amplitudes. In general, a low value of kurtosis indicates few and less extreme outliers, whereas a high value indicates several and more extreme outliers. Hence, a high value of kurtosis indicates more area in the tails. The root energy amplitude, A_E, is an alternative way to describe the energy and is defined as

$$A_E = \sqrt{\frac{E}{D}} \tag{2.12}$$

This expression is simply the square root of the energy normalized by the RMS duration. Table 2.1 summarizes the central moments in terms of the temporal moments.

Table 2.1: Definition of central and normalized central moments.

Parameter	Moment	Moment order	Definition	Units
E	Energy	0	$E = M_0$	$\left(m / s^2\right)^2 s$
T	Central time	1	$T = \frac{M_1}{E}$	s
D	RMS duration	2	$D = \sqrt{\frac{M_2(T)}{E}}$	s
S_t	Central skewness	3	$S_t = \sqrt[3]{\frac{M_3(T)}{E}}$	s
S	Normalized skewness	3	$S = \frac{S_t}{D}$	-
K_t	Central kurtosis	4	$K_t = \sqrt[4]{\frac{M_4(T)}{E}}$	s
K	Normalized kurtosis	4	$K = \frac{K_t}{D}$	-
A_E	Root energy amplitude	-	$A_E = \sqrt{\frac{E}{D}}$	$\left(m / s^2\right)$

The following two clarifications should be noted. First, a central moment is simply a temporal moment with respect to the reference time T when the first-order temporal moment is zero. All central moments of order 1 through 4 are normalized by the basic moment E, which is the zero-order temporal moment. Consequently, the units become seconds. Additionally, a second normalization by the RMS duration, D, provides an alternative measure of the third- and fourth-order central moments with non-dimensional units. Second, considering the definition provided in Equation (2.1), it is obvious that the integral of the signal squared is the total energy of the signal, or the area of the defined signal squared. The signal squared represents a distribution, which is analogous to a probability density function in regular statistical theory. Hence, the central moments are statistical moments of this distribution, also representing how the energy of the signal is distributed in time.

2.2.2 Temporal moments in discrete time signals

The *i*th-order temporal moment defined by Equation (2.1) about the central time T can be approximated for a discrete signal of finite duration as

$$M_i(T) \approx \frac{1}{2}\sum_{j=0}^{N-2}\left[\Delta t\left(j+0.5\right)-T\right]^i \Delta t\left[y_j^2+y_{j+1}^2\right] \tag{2.13}$$

where Δt is the time increment between two response measurements and the sample index is defined to run from 0 to $N-1$ as commonly used in digital signal processing. Furthermore, the general integral

$$\int_{-\infty}^{+\infty} y^2(t)\,dt \approx \sum_{j=0}^{N-2}\frac{\Delta t}{2}\left(y_j^2+y_{j+1}^2\right) \tag{2.14}$$

is based on the trapezoidal rule. The application of Equation (2.13) numerically provides the basis for establishing the central and normalized central moments. The normalized central moments in terms of the basic moments provide an alternative way of establishing the five temporal moments and can be utilized with Equation (2.13):

$$E = M_0 \tag{2.15}$$

$$T = \frac{M_1}{M_0} \tag{2.16}$$

$$D^2 = \left(\frac{M_2}{M_0}\right)-\left(\frac{M_1}{M_0}\right)^2 \tag{2.17}$$

$$S_t^3 = \left(\frac{M_3}{M_0}\right)-3\left(\frac{M_2M_1}{M_0^2}\right)+2\left(\frac{M_1}{M_0}\right)^3 \tag{2.18}$$

$$K_t^4 = \left(\frac{M_4}{M_0}\right)-4\left(\frac{M_3M_1}{M_0^2}\right)+6\left(\frac{M_2M_1^2}{M_0^3}\right)-3\left(\frac{M_1}{M_0}\right)^4 \tag{2.19}$$

The derivations of these relationships can be established by considering the temporal moments according to Equation (2.1) about the reference time T in combination with Equation (2.2) and the provided definitions of the central moments in Table 2.1.

For the application of temporal moments in this study, the signals analysed are acceleration response measurements or time histories. However, the application is also valid for the transient part of the response obtained using other measures, such as strain, force, displacement or velocity [24]. The implementation of temporal moments numerically is made available [27].

2.2.3 Feature vectors

The central and normalized central moments given in Table 2.1 can be established as statistical parameters of a transient signal. In the following, these parameters are also referred to as features, which are defined as quantities established from response measurements that can be used to indicate damage [26]. All features constitute a feature vector, which is defined as

$$\mathbf{d}_m = \begin{bmatrix} E & T & D & A_E & S_t & S & K_t & K \end{bmatrix} \tag{2.20}$$

where the subscript m denotes the joint number.

2.3 Bridge description and experimental study

2.3.1 Bridge description

The Hell Bridge Test Arena is a full-scale, steel riveted railway truss bridge taken out of service and moved to foundations on land, as shown in Figure 2.1. The bridge is 4.5 m wide and has a total span of 35 m. It serves as a full-scale laboratory for research within SHM, damage detection, bridge inspection and service life estimation. Figure 2.2 shows a simplified 3D model of the main structural steel in the Hell Bridge Test Arena.

Figure 2.1: Hell Bridge Test Arena.

The bridge deck consists of longitudinal stringers connected to transverse girders (floor beams). The stringer-to-girder connections are made using double angle connections that are mechanically fastened with rivets. These are designed as shear connections, transferring the stringer end forces to the girder. Two mechanisms are commonly reported in this type of connection [1]: rotation of the stringer ends associated with bending and overlooked interactions between the bridge deck structural system and the main load carrying structure. These mechanisms are generated by deformation-induced secondary effects causing fatigue cracking [11]. In the following sections, the stringer-to-girder connections are referred to as both joints and joint connections.

There are two known damages in the joint connections in the bridge deck structural system of the Hell Bridge Test Arena. These damages are located on one

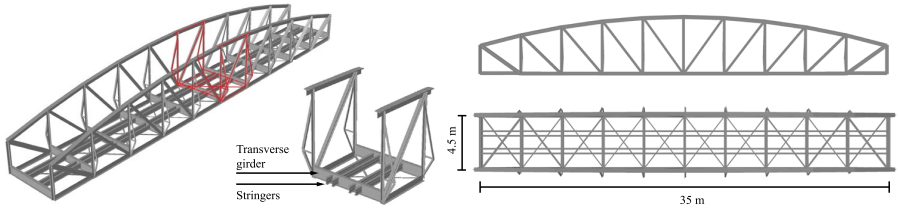

Figure 2.2: Simplified 3D model of the main structural steel in the Hell Bridge Test Arena. (a) 3D perspective view including a detailed bridge section. (b) Vertical wall (top) and plan view of the bridge deck (bottom).

side of the middle of the bridge, which was retrofitted during the initial part of the bridge lifetime. Despite the retrofit, all joint connections have the same loadbearing function. The damages were not found during routine interval inspections while the bridge was operational. These damages were originally discovered during a measurement campaign prior to the bridge being taken out of service, in which strain measurements were performed only on a selection of the joint connections. The damages result in unwanted vertical movement of the respective stringers when the bridge is subjected to operational loads. Consequently, the result is a severe reduction in the loadbearing capacity.

2.3.2 Damage detection strategy

A structure that can function satisfactorily but is no longer operating in an ideal condition is defined as a damaged structure [28]. In the most basic term, damage is defined as a change in the structural system that affects the performance of the structure [18]. Such a change can be in the material properties, geometry, boundary conditions or connections of the structural system. Determining the damage state can be accomplished according to a hierarchical structure, or levels, where increased knowledge of the damage state is represented in the given order of levels. These are defined as 1) existence, 2) localization, 3) type, 4) extent and 5) prediction of damage [28], [29].

Assessing damage requires a comparison between two different states of a system [30]. In this study, all relevant joint connections are investigated to establish damage in the bridge deck. A baseline, representing the normal and undamaged condition, is established from statistical parameters using all joints. Damage is then assessed based on the comparison of the results of individual joints to the baseline. As such, damaged joint connections are *identified* by comparing results to nominally identical connections and *localized* utilizing the instrumentation setup.

2.3.3 Experimental study

An instrumentation setup and systematic monitoring procedure was established in the experimental study. Sensors were placed symmetrically about an impact

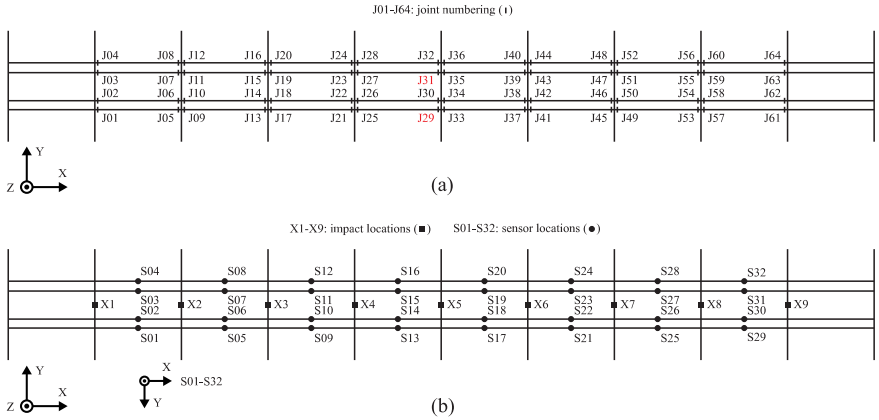

Figure 2.3: Instrumentation setup of the Hell Bridge Test Arena bridge deck (plan view). (a) Joint numbering with known damaged joints highlighted in red. (b) Sensor and impact locations.

location to effectively assess the joint connections. Figure 2.3 shows an overview of the bridge joints subject to investigation and the full bridge deck instrumentation, including all sensor and impact locations.

A symmetric instrumentation setup about the geometric centre of the bridge deck was made using 32 sensor locations, denoted S01–S32, and 9 impact locations, denoted X1–X9. Both sensor and impact locations were accessible from the bridge deck. Altogether, 64 joints, labelled J01–J64, were assessed utilizing the instrumentation setup. This included 8 joints per impact location from X2–X8 and 4 joints per impact location X1 and X9. The known damaged joints in the bridge deck were labelled J29 and J31. The geometric centre of the bridge coincides with impact location X5.

The testing was performed using 16 Dytran 3583BT tri-axial accelerometers and a PCB large-sledge modal impulse hammer (model 086D50). The accelerometers were mounted at the mid-span of the stringers. Data acquisition was performed using a CompactRIO 9036 from National Instruments with 8 input modules (model 9234 C Series Sound and Vibration) at a sampling frequency of 2048 Hz. A minimum of 5 impacts were systematically induced at the predefined impact locations. To obtain a strong transient signal, the testing was performed using a hard-plastic hammer tip (model 084A32), which gave a high-frequency excitation. Measurements were recorded in the z-direction only. The preprocessing of the time series mainly consisted of three steps: first, sensor sensitivity was included; second, the time series were optimized by synchronization using the peak value of each signal and then trimmed to the desired length; and finally, linear trends were removed by detrending the signals. From the preprocessing, each recording resulted in a time series of 1.0 s, where 0.1 s was recorded prior to the impact and 0.9 s was recorded after the impact.

The number of sensors to be applied is not of significant importance. The methodology allows the use of one sensor only as a minimum. Repeated testing by moving the sensors to the predefined sensor locations provides the required

measurements. However, to reduce the number of impacts, a minimum of 8 sensors is recommended. This setup also ensures that the maximum number of joints is analysed using the same input, which increases the accuracy of the results.

By utilizing the symmetry of the instrumentation setup and the systematic monitoring procedure, acceleration response measurements can be established with the fewest number of sensors and impacts. This approach provides information about the transmissibility of the signal in the time domain, where the transmissibility represents the signal from the impact location and through the joint to be assessed.

2.4 Results

2.4.1 General

Acceleration response measurements, together with the average absolute peak acceleration response, provide a basic description of the response from the joints considered. The results from the experimental study are investigated using two approaches: first, the most relevant statistical parameters, i.e. features, are plotted and compared individually for all joints from the acceleration response measurements; second, a damage indicator matrix is established based on the correlation between the feature vectors for each joint analysed.

2.4.2 Basic response description

A comparison of the time histories of the acceleration response measurements for all joints in the middle part of the bridge is shown in Figure 2.4. All joints connected to the same girder specified by the impact location are presented in the vertical columns, where the response is shown for the same impact. All response measurements show the main transient response for one impact occurring in the time interval of 0.09-0.16 s.

From these plots, a general trend in the response measurements of the joints is observed: each response is characterized by a distinct peak followed by an exponential decay in the signal amplitudes. In general, the curves in each plot follow each other fairly well considering the shape of the transient response, including the decay. This finding is expected since most of the joints are in fact assumed to be identical and undamaged. However, exceptions are observed particularly for impact locations X5 and X6. The relevance of these deviations with respect to damage is best evaluated using statistical parameters.

A comparison of all joints for the average absolute peak acceleration response of 5 impacts per impact location is shown in Figure 2.5. A large variation is observed when comparing all joints and the joints within the same impact location. However, the average peak value for J29 deviates from that of the other joints, indicating that this joint behaves differently than the others.

The average absolute peak value can provide a distinction in the results, but it is not an adequate feature for identifying damage. This inadequacy is mainly due to

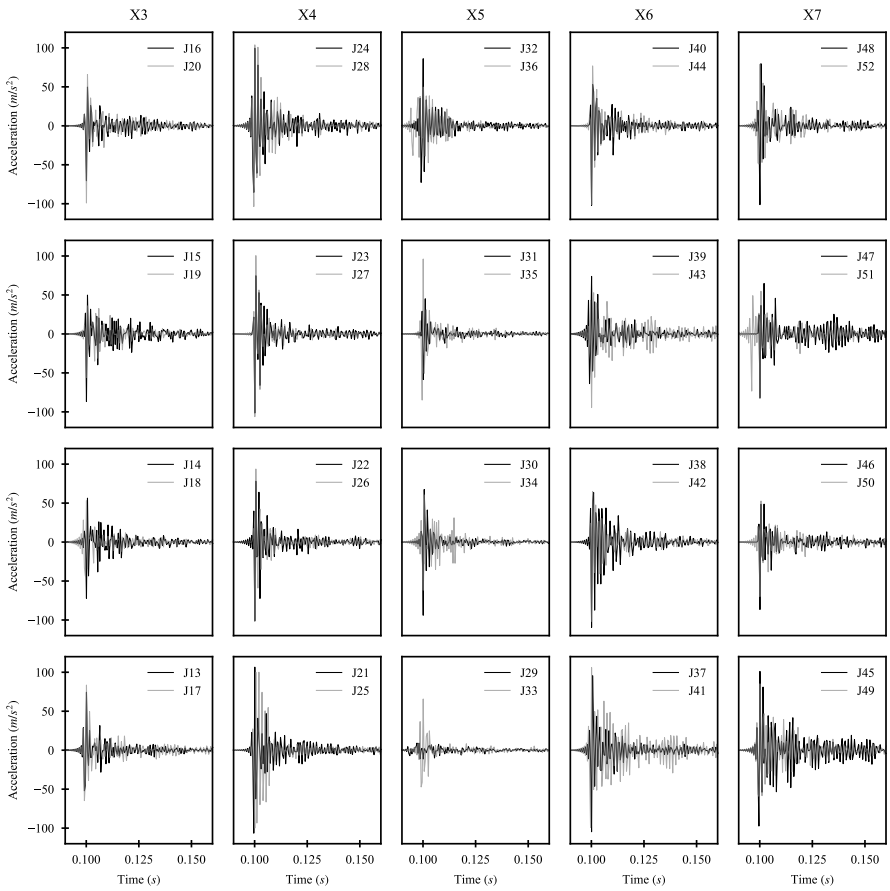

Figure 2.4: Comparison of the acceleration response measurements based on one impact for the joints in the middle part of the bridge.

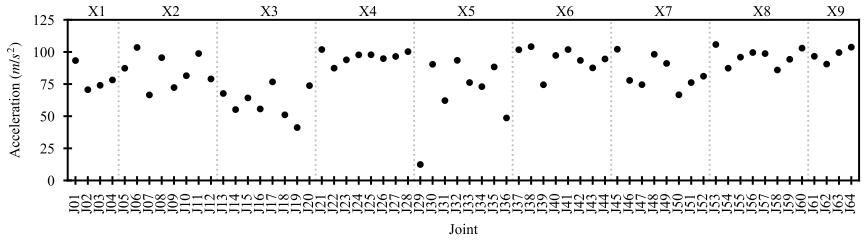

Figure 2.5: Average absolute peak acceleration response.

two reasons. First, this feature is a sensitive measure and is strongly dependent on the sampling frequency, placement of sensors and input force. For transient vibration, sampling at high frequencies can more reliably capture the actual peak acceleration than sampling at low frequencies. Furthermore, small deviations in sensor placements are common when performing field measurements on large

structures. Sensitive features can provide large deviations in results caused by operational and environmental variability and not just from the presence of damage. Second, this feature only provides one measure of a signal that generally contains a vast amount of information

Making observations that may identify damaged joints is challenging due to the general similarity observed in the acceleration response measurements and the large variability in the average absolute peak acceleration values. Hence, establishing statistical parameters of the signals to quantify characteristics of the acceleration response measurements is needed to provide reliable information and increase confidence in results.

2.4.3 Statistical parameters

The results of analysing the main statistical parameters are shown in Figure 2.6 and Figure 2.7 by moment order. Energy (E), central time (T) and RMS duration (D) are presented in Figure 2.6, whereas central skewness (S_t), central kurtosis (K_t) and root energy amplitude (A_E) are presented in Figure 2.7.

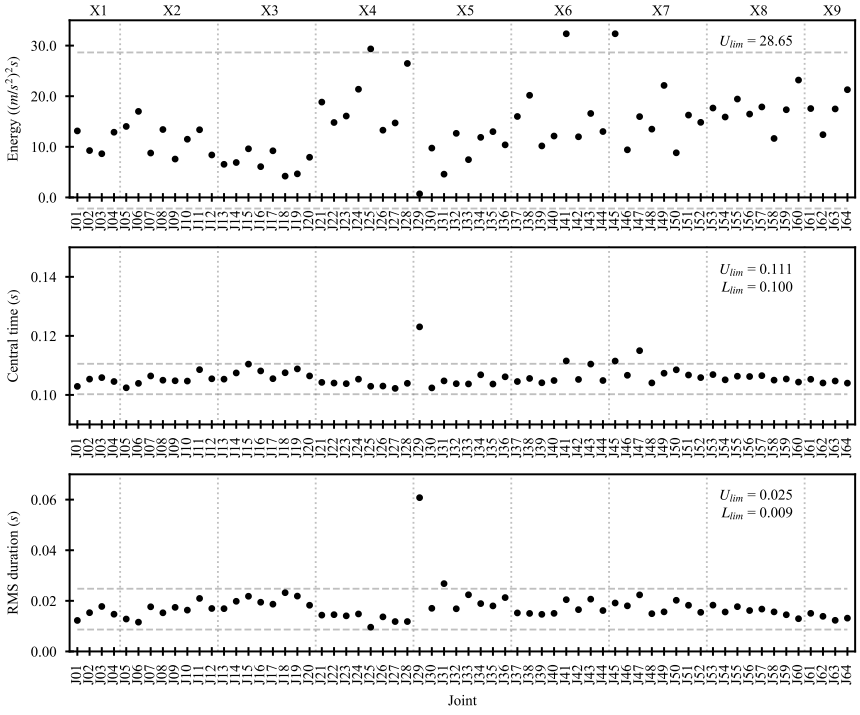

Figure 2.6: Analysis results of the central and first two normalized central moments from the average of 5 impacts.

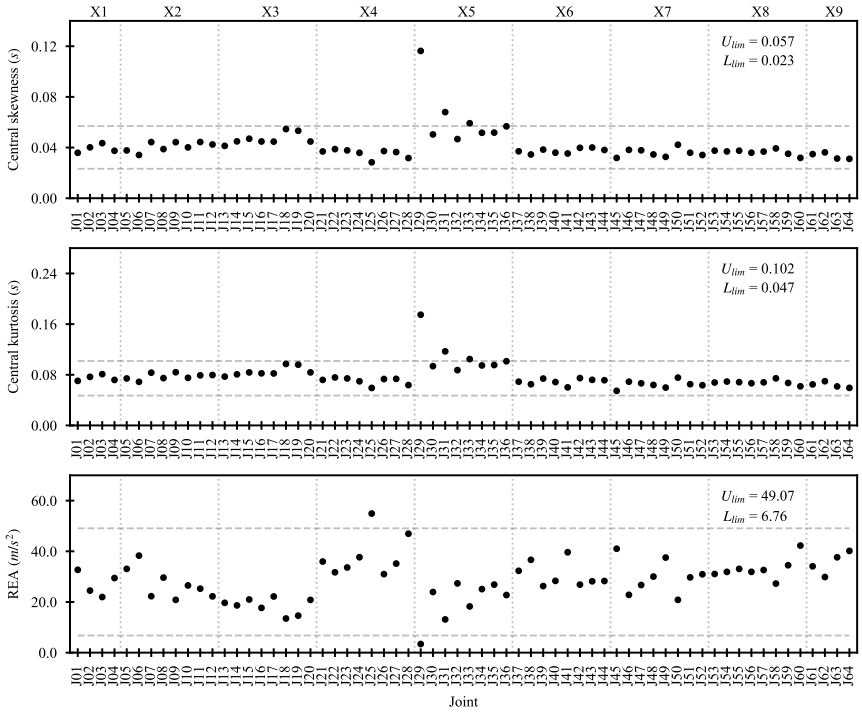

Figure 2.7: Analysis results of the normalized central moments and the root energy amplitude from the average of 5 impacts.

In both figures, each marker in the plots represents the average value obtained from 5 impacts. The short-dashed grey vertical lines separate the impact locations, and all markers within each impact location represent results obtained from the same impacts. The dashed horizontal lines represent the upper and lower outlier limits. To find these limits, the interquartile range (IQR) for each of the data sets with the statistical parameters is established. The IQR is a measure of variability and divides the data considered into quartiles. The IQR is the range between the 75th and 25th percentiles of the data and consequently contains the middle portion or 50%. The outlier limits are defined as 1.5 times the IQR length from the upper and lower percentile, which is considered a common criterion for outliers [31]. Values outside of this range are extreme data values. All plots show both the upper and lower limit, i.e. U_{lim} and L_{lim}, except for the energy. Here, the lower limit is less than zero, representing a negative area or energy not considered realistic.

For the known damaged joint connections, the most obvious results are obtained for J29. For J29, all statistical parameters except for energy are outliers; however, for energy, J29 has the lowest value of all joints. For J31, outliers are observed for RMS duration, central skewness and central kurtosis, but otherwise, the statistical parameters are within the IQR.

For the undamaged joint connections, J41 and J45 are represented with outliers in energy and central time but otherwise have values well within the IQR. Joints J33 and J36 have values very close to or exceeding the outlier limits for central

skewness and central kurtosis. Additionally, high values are observed for RMS duration. J25 has outliers for energy and root energy amplitude. An interesting observation is made for joints J18 and J19. The statistical parameters are observed to be within the IQR. However, the values are close to the outlier limits for all statistical parameters.

Detailed results of all statistical parameters for the abovementioned joints are summarized in Table 2.2. Values exceeding the outlier limits are highlighted. Additionally, the lower and upper limits, arithmetic mean and median values are included in this table.

Table 2.2: Detailed results of the statistical parameters for relevant joint connections.

Joint	E $((m/s^2)^2 s)$	T (s)	D (s)	S_t (s)	K_t (s)	A_E (m/s^2)
J18	4.21	0.108	0.023	0.055	0.097	13.47
J19	4.66	0.109	0.022	0.053	0.096	14.60
J25	**29.35**	0.103	0.010	0.028	0.059	**54.90**
J29	0.71	**0.123**	**0.061**	**0.116**	**0.175**	**3.40**
J31	4.60	0.105	**0.027**	**0.068**	**0.117**	13.11
J33	7.46	0.104	0.022	**0.059**	**0.105**	18.24
J36	10.39	0.106	0.021	**0.057**	**0.101**	22.74
J41	**32.34**	**0.112**	0.021	0.035	0.060	39.63
J45	**32.34**	**0.112**	0.019	0.032	0.055	41.03
Mean	13.94	0.106	0.017	0.042	0.077	28.67
Median	13.21	0.105	0.016	0.038	0.073	28.88
L_{lim}	-	0.100	0.009	0.023	0.047	6.76
U_{lim}	28.65	0.111	0.025	0.057	0.102	49.07

In summary, the analysis results show that the two known damaged joint connections, J29 and J31, can be identified with outliers in all and several of the statistical parameters, respectively, except for energy. Furthermore, joints J25, J33, J36, J41 and J45 have outliers in two of the statistical parameters shown. Finally, J18 and J19 have no outliers; however, these joints have values close to the outlier limits for all statistical parameters.

2.4.4 Damage indicator matrix

The damage indicator matrix provides a comparison of all joints using the statistical parameters. The damage indicator, DI, is related to the correlation coefficient, $\rho_{\mathbf{d}_m\mathbf{d}_n}$, and is defined as

$$DI = 1 - \rho_{\mathbf{d}_m\mathbf{d}_n} = 1 - \frac{\sigma_{\mathbf{d}_m\mathbf{d}_n}}{\sigma_{\mathbf{d}_m}\sigma_{\mathbf{d}_n}} \tag{2.21}$$

Here, $\mathbf{d}_m$ and $\mathbf{d}_n$ are the feature vectors defined according to Equation (2.20) of joints m and n respectively. Correspondingly, $\sigma_{\mathbf{d}_m}$ and $\sigma_{\mathbf{d}_n}$ are the standard deviations of $\mathbf{d}_m$ and $\mathbf{d}_n$, respectively, whereas $\sigma_{\mathbf{d}_m\mathbf{d}_n}$ is the covariance matrix.

The damage indicator provides a non-dimensional measure based on the correlation of the feature vectors. By systematically establishing damage indicators result in the damage indicator matrix; a statistical comparison of all joints based on the measure of correlation.

Correlation describes the degree of linearity, or linear dependence, between two variables or vectors. Thus, the damage indicator provides a measure of similarity in the behaviour of joints. If two variables are independent, the correlation coefficient is 0, whereas it will be in the range between -1 and 1 if one of the variables is partially linearly dependent on the other. The latter depends on the strength of the linear dependence. As such, for the damage indicators, a low value will indicate similar behaviour between joints, whereas higher values will indicate different behaviour. The majority of the joints are undamaged and exhibit similar structural behaviour; thus, these joints have similar statistical parameters. Consequently, the correlation between their respective feature vectors is expected to be close to 1, resulting in a DI value close to 0.

The normalized damage indicator matrix for all joints is shown in Figure 2.8.

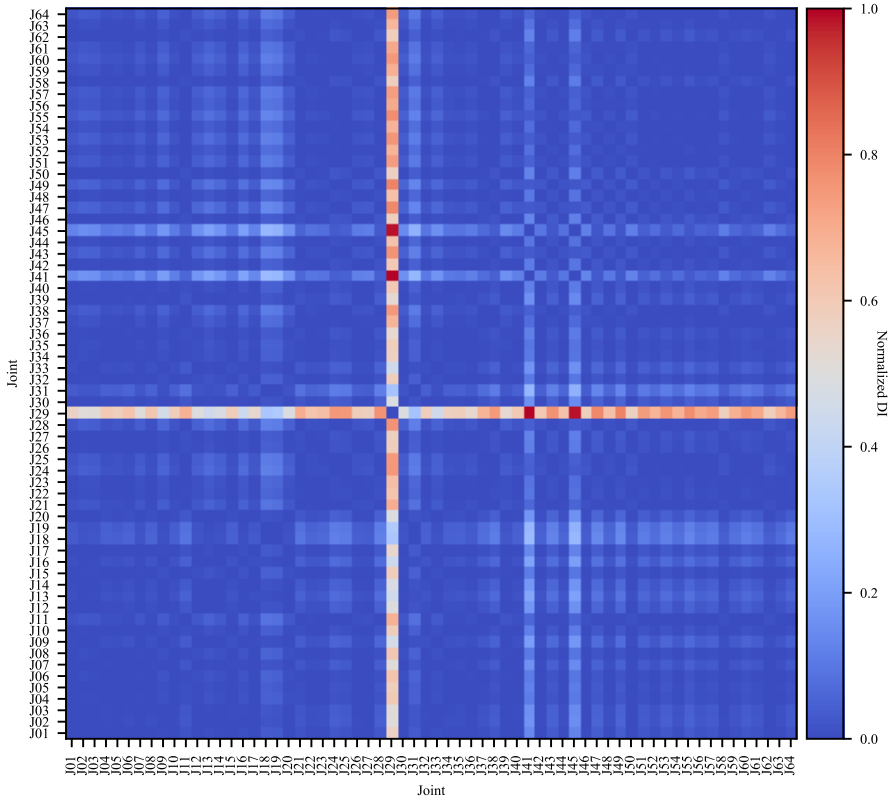

Figure 2.8: Normalized damage indicator matrix.

This figure shows that the damaged joint J29 is clearly indicated. Additionally, weak indications are observed for J31. However, indications of damage are also observed for undamaged joints, particularly J41 and J45 but also J18 and J19. The figure shows that the normalized DI values of J29 to both J41 and J45 are high, and the most obvious reason for this outcome is due to the energy. Energy (E) is simply the area of the signal squared within the defined time of the acceleration response recording. Low energy implies a weak or damped transient vibration. Little or no transmissibility of the signal between the impact location and the sensor is the most obvious cause resulting in low energy. This implies that the signal must travel a longer distance before it is recorded by the sensor, and due to inherent material and structural damping, the signal amplitudes become lower resulting in a loss of energy. This phenomenon in turn provides an indication of structural damage. In contrast, high energy implies strong transient vibration.

For the joints evaluated, there is no obvious explanation for the results of high energy. Hence, a new normalized damage indicator matrix for all joints is established based on feature vectors where the energy is excluded, as shown in Figure 2.9. From this figure, the damaged joint J29 is clearly indicated.

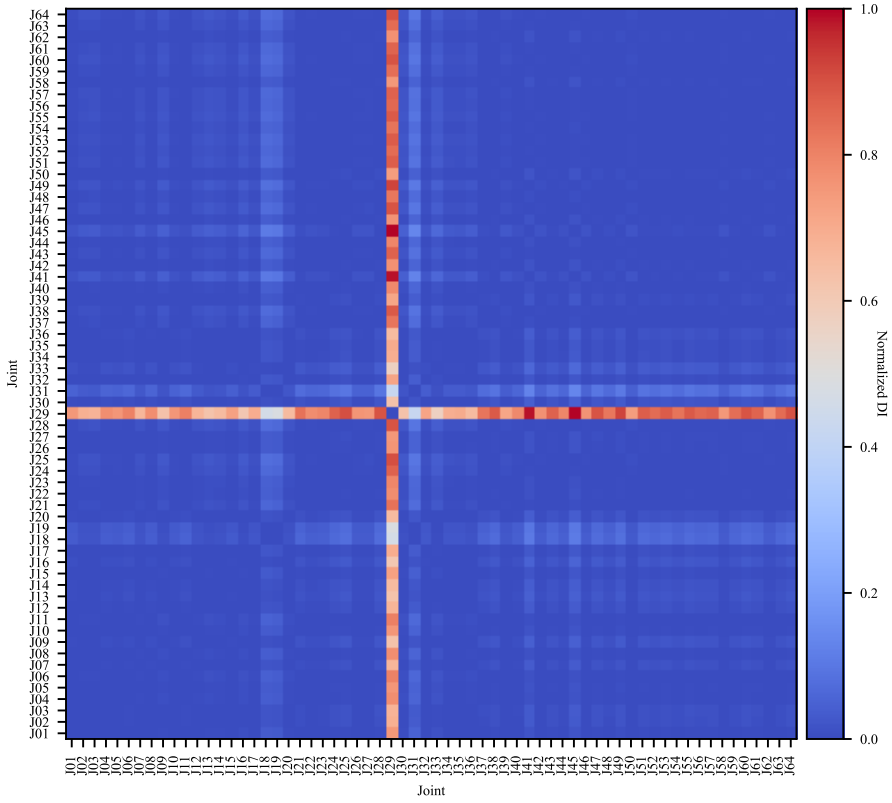

Figure 2.9: Normalized damage indicator matrix. Energy (E) is excluded from the feature vector.

An indication of damage is also observed for the damaged joint J31. Furthermore, false-positive indications, i.e. indication of damage when no damage is present, are seen for joints J18 and J19. The non-normalized mean DI values of these joints are established in Table 2.3. The mean DI value of each joint compared to other joints identifies the joints that, on average, have feature vectors that correlate less with others.

Table 2.3: Non-normalized mean DI values.

Joint	Average DI
J29	0.224
J31	0.020
J18	0.015
J19	0.014

Based on the results obtained, it is observed that 1) most of the joints are well correlated, 2) damage in a joint connection can, but must not necessarily be, well reflected in the correlation between the feature vectors, and 3) the damage indicator is not a measure of the degree of any damage. A discussion of the statistical parameters related to the structural understanding is provided in the following section to conclude on the results obtained.

2.5 Discussions

2.5.1 Importance of statistical parameters on structural damage identification

The known damage in the joint connections of the bridge deck results in unwanted vertical movement and consequently a reduction in the loadbearing capacity of the stringers. Due to damage, the connectivity of the joints is changed by reduced stiffness. This, in turn, is expected to result in a change in the signal transmissibility for the joint considered between the impact location and the sensor. This change caused by damage is mainly expected to reduce the transmissibility of the signal.

As described in the previous section, low energy (E) is caused by low transmissibility of the signal. The root energy amplitude (A_E) normalizes the energy by the RMS duration and is an alternative energy feature. Low values of both energy features are expected to be caused by damaged joint connections. Central time (T) measures the time at which the centroid of the energy is located. In general, the central time is expected to be located shortly after the peak of the signal occurring at 0.1 s. There are two main explanations for obtaining high values of this feature: weak decay of a strong transient signal or generally weak transient signal behaviour. The first is not due to damage. A low local structural damping affects a strong transient signal resulting in low decay. Similarly, any reflection of signals from the surrounding structure affects the transient part of the signal and consequently increases the central time. However, a generally weak transient signal

behaviour is expected to be caused by damage. As such, high values for the central time can occur for both damaged and undamaged joints. RMS duration (D) measures the dispersion of the energy in a signal. Strong transient signals with high transmissibility have low dispersion, whereas weak transient signals with low transmissibility have high dispersion. Hence, RMS duration characterizes the signal well and is consequently a good feature for indicating damage. Central skewness (S_t) describes the shape of the distribution, or the signal itself, in terms of symmetry. Regardless of the presence of damage, all joints considered will have a positive skewness because high amplitudes are located to the left of the central time with a corresponding low-amplitude tail on the right. Damaged joints, characterized by low transmissibility, will obtain a larger skewness than undamaged joints and are expected to be characterized by this feature. The same applies for central kurtosis (K_t), which measures the outliers in the signal energy. A high number of outliers in a signal indicates damage.

The results clearly show that RMS duration, central skewness and central kurtosis best describe the damaged joint connections. Consequently, these are considered the most relevant features. The significance of the energy features in relation to damage is important. However, these features do not clearly describe both damages. Furthermore, the energy feature results in three outliers with high values, which is not well understood. The root energy amplitude provides better results; however, one outlier with a high value is still observed. Central time clearly indicates one damaged joint but shows outliers for undamaged joints.

By excluding energy, the remaining features can be included in the context of observing any trends that can strengthen the indication of damage. This is evident by performing an evaluation using the damage indicator matrix.

2.5.2 Effect of sampling frequency

Sampling at high frequencies instead of low frequencies includes more information in the transient signals. Establishing an appropriate sampling frequency with respect to damage identification is deemed important. Hence, the effect of sampling frequency on the main statistical parameters are investigated and shown in Figure 2.10. In this figure, the average value of all impacts for all joint connections, including J29 and J31, are analysed and compared with the average value of J29 and J31 for different sampling frequencies. Five cases are included. The first case considers the original sampling frequency with no filter applied, whereas the other cases include the original and a systematic reduction in sampling frequency with a filter applied. Data are analysed by resampling the signals after applying an 8th order Bessel antialiasing filter at 80% of the Nyquist frequency. The ability to handle rapid changes in the signal from one value to another, which is characterized in the step response, is optimized with the Bessel filter in contrast to other antialiasing filters [32]. This characteristic is favoured for the analysis of transient vibration in the time domain. However, the Bessel filter reduces the amplitudes in the passband due to the roll-off quality of the filter, which explains the reduction in results for energy and root energy amplitude from a sampling frequency of 2048 Hz with no filter to 2048 Hz with a filter applied.

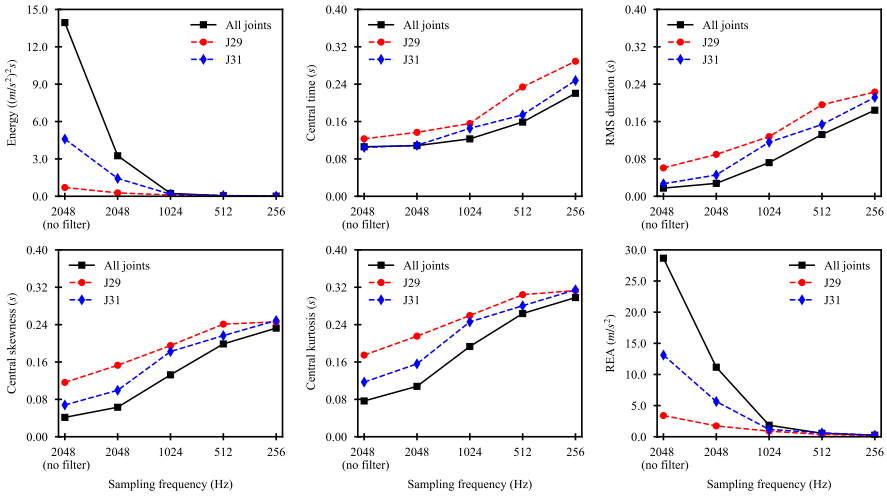

Figure 2.10: Analysis results for different sampling frequencies.

The absolute value of the percentage change in the damaged joints to the value of all joints is summarized in Table 2.4. Figure 2.10 and this table show that lowering the sampling frequency in general decreases the identifiability of known damaged joints from the average of all joints when considering the statistical parameters, except for central time. Information is lost for the resampled signals. This lost information in turn provides a weaker indication of damage. Lower sampling frequencies result in fewer high amplitudes in the signal representations. This is clearly seen when considering the analysis results of the energy features. The central time increases, and the centroid of the signals moves away from 0.1 s. In general, the dispersion of the signals increases with lower sampling frequencies, and the distinction of damaged joint connections appears to be unaffected. However, this is not the case when considering the absolute value of the percentage change for the RMS duration, which shows that the percentage change is lowered with decreasing sampling frequency. For central skewness and central kurtosis, it is apparent that the identification of damage is more difficult with lower sampling frequencies both when considering the analysis results and the absolute value of percentage change.

By considering the parameters most relevant for the identification of damage, it is clearly seen that a reduction in sampling frequency reduces the identifiability of damage, except when considering central time. A higher sampling frequency provides a better representation of the transient signals and includes more information. The values of the statistical parameters strongly depend on the sampling frequency and, as such, can only be used for the purpose of comparison.

The obtained results show that an adequate sampling frequency is needed to identify damage. A minimum sampling frequency of 2048 Hz is recommended for this case. However, it should be noted that using lower sampling frequencies does not exclude the possibility of identifying damage.

Table 2.4: Absolute value of percentage change in the damaged joints to the value of all joints.

Statistical parameter	Joint	Percentage change for different sampling frequencies (%)				
		2048 Hz (no filter)	2048 Hz	1024 Hz	512 Hz	256 Hz
E	J29	95	92	55	35	25
	J31	67	56	30	48	0
T	J29	16	27	27	47	31
	J31	1	1	19	9	13
D	J29	259	221	78	48	21
	J31	59	64	61	17	15
S_t	J29	176	143	47	21	6
	J31	62	57	37	9	7
K_t	J29	127	99	34	15	5
	J31	52	44	27	6	6
A_E	J29	88	84	51	34	18
	J31	54	49	36	13	4

2.5.3 Summary

Experience obtained from the experimental study leads to the following general observations:

- There are two known damaged joint connections, J29 and J31. From the proposed methodology, a clear identification of J29 is established, whereas a weak indication of J31 is observed. Although the methodology identifies both damaged joint connections, the distinction between J31 and the undamaged joint connections J18 and J19 is low, resulting in two false-positive indications of damage.
- When considering the statistical parameters only, the RMS duration, central skewness and central kurtosis are of primary interest. Additionally, root energy amplitude is important due to its significance related to the damage configuration studied.
- The damage indicator matrix provides a statistical comparison of all joints based on the measure of correlation using feature vectors. From the results obtained, three undamaged joint connections obtained high energy. No reasonable explanation of this phenomenon is found. When excluding this statistical parameter from the feature vectors, an improved damage indicator matrix is obtained.
- A high sampling frequency is required. High sampling frequency provides better results and more clear identification of damage due to increased information included in the signals analysed.
- An adequate number of joint connections is needed to obtain a basis for comparison. A high number of identical joints forming the baseline provides a more reliable result. This is clearly observed when comparing results from one impact location to the results of all impact locations.

- The possibility that changes in the statistical parameters are caused by inconsistent input, i.e. excitation, cannot be eliminated. Inconsistent input can be limited to the best extent possible by using the average of multiple impacts. The results obtained in this study show that using 5 impacts per impact location is considered adequate for this purpose.

The proposed methodology establishes damaged joint connections in the bridge deck and is based on the transmissibility of the signal from the impact location to the sensor and through the joint connection to be assessed. All joint connections have the same loadbearing function. The location of any damaged joints, or the distance between any damaged joints, does not affect the indication of damage since the evaluation is based on local response and not on the global response of the structure. Damaged joint connections are *identified* by comparing statistical parameters based on temporal moments to nominally identical connections. The damaged joint connections are *localized* utilizing the instrumentation setup and a systematic monitoring procedure. The baseline is established from the statistical parameters evaluated for all joint connections. The observation made in the first bullet point leads to the conclusion that the methodology can only clearly identify one damaged joint connection. However, from an inspector's perspective, such a result should lead to the further investigation of all four joints with the assumption of damage being present. Further investigation should be to carry out a full visual inspection or consider a long-term SHM system using strain measurements for bridges in operation.

2.6 Conclusion

This paper presented a new methodology for detecting damage in stringer-to-girder connections from the bridge deck of existing steel bridges. The methodology is based on combining the use of temporal moments to establish statistical parameters from response measurements with an appropriate instrumentation setup and a systematic monitoring procedure. An experimental study on a full-scale steel bridge identified and localized two damaged joint connections in the bridge deck by 1) investigating statistical parameters from response measurements and 2) establishing a damage indicator matrix by comparing feature vectors using correlation analysis. The importance of high sampling frequency to obtain the best possible identification of damaged joint connections was shown through a sensitivity analysis. A minimum sampling frequency of 2048 Hz is recommended for similar applications.

The main limitation of the methodology presented herein is the need for an adequate number of joint connections or similar structural components to obtain a baseline for comparison. The baseline for comparison can be affected in cases where many damages are present in the structural system. Nevertheless, the methodology presented in this paper demonstrates that structural damage in joint connections can be effectively established. The proposed methodology is easy to implement, both in a technical and practical manner. Limited technical equipment is needed. Furthermore, this methodology can be applied to components that are difficult to access without the need for temporary installation of access support. As

such, the established methodology can contribute to improving the identification of critical damage during scheduled inspection of existing open-deck highway and railway bridges in service with no, or limited, downtime. Further investigation should be to 1) test the methodology on bridges in service and 2) use the established methodology but consider structural response obtained from vehicles on damage detection for potential automation purposes.

Acknowledgements

The Hell Bridge Test Arena is financially supported by the Norwegian Railway Directorate and Bane NOR.

References

[1] R. Haghani, M. Al-Emrani, and M. Heshmati, "Fatigue-Prone Details in Steel Bridges," *Buildings*, vol. 2, no. 4, pp. 456–476, 2012, doi: 10.3390/buildings2040456.

[2] B. Åkesson, "Fatigue Life of Riveted Steel Bridges," Chalmers University of Technology, Gøteborg, Sweden, 1994.

[3] D. H. Tobias and D. A. Foutch, "Reliability-Based Method for Fatigue Evaluation of Railway Bridges," *J. Bridg. Eng.*, vol. 2, no. 2, pp. 53–60, May 1997, doi: 10.1061/(ASCE)1084-0702(1997)2:2(53).

[4] J. D. DiBattista, D. E. J. Adamson, and G. L. Kulak, "Evaluation of remaining fatigue life for riveted truss bridges," *Can. J. Civ. Eng.*, vol. 25, no. 4, pp. 678–691, 1998, doi: 10.1139/l98-011.

[5] T. E. Cousins, J. M. Stallings, D. A. Lower, and T. E. Stafford, "Field evaluation of fatigue cracking in diaphragm-girder connections," *J. Perform. Constr. Facil.*, vol. 12, no. 1, pp. 25–32, 1998, doi: 10.1061/(ASCE)0887-3828(1998)12:1(25).

[6] C. W. Roeder, G. MacRae, P. Crocker, K. Arima, and S. Wong, "Dynamic Response and Fatigue of Steel Tied-Arch Bridge," *J. Bridg. Eng.*, vol. 5, no. 1, pp. 14–21, Feb. 2000, doi: 10.1061/(ASCE)1084-0702(2000)5:1(14).

[7] B. M. Imam, T. D. Righiniotis, and M. K. Chryssanthopoulos, "Probabilistic Fatigue Evaluation of Riveted Railway Bridges," *J. Bridg. Eng.*, vol. 13, no. 3, pp. 237–244, May 2008, doi: 10.1061/(ASCE)1084-0702(2008)13:3(237).

[8] T. Guo and Y. W. Chen, "Field stress/displacement monitoring and fatigue reliability assessment of retrofitted steel bridge details," *Eng. Fail. Anal.*, vol. 18, no. 1, pp. 354–363, 2011, doi: 10.1016/j.engfailanal.2010.09.014.

[9] T. Guo, D. M. Frangopol, and Y. Chen, “Fatigue reliability assessment of steel bridge details integrating weigh-in-motion data and probabilistic finite element analysis,” *Comput. Struct.*, vol. 112–113, pp. 245–257, 2012, doi: 10.1016/j.compstruc.2012.09.002.

[10] M. Al-Emrani, “Fatigue Performance of Stringer-to-Floor-Beam Connections in Riveted Railway Bridges,” *J. Bridg. Eng.*, vol. 10, no. 2, pp. 179–185, 2005, doi: 10.1061/(asce)1084-0702(2005)10:2(179).

[11] M. Al-Emrani, B. Åkesson, and R. Kliger, “Overlooked Secondary Effects in Open-Deck Truss Bridges,” *Struct. Eng. Int.*, vol. 14, no. 4, pp. 307–312, Nov. 2004, doi: 10.2749/101686604777963612.

[12] M. Al-Emrani and R. Kliger, “FE analysis of stringer-to-floor-beam connections in riveted railway bridges,” *J. Constr. Steel Res.*, vol. 59, no. 7, pp. 803–818, 2003, doi: 10.1016/S0143-974X(02)00114-1.

[13] B. M. Imam, M. K. Chryssanthopoulos, and D. M. Frangopol, “Fatigue system reliability analysis of riveted railway bridge connections,” *Struct. Infrastruct. Eng.*, vol. 8, no. 10, pp. 967–984, 2012, doi: 10.1080/15732479.2011.574817.

[14] T. D. Righiniotis, B. M. Imam, and M. K. Chryssanthopoulos, “Fatigue analysis of riveted railway bridge connections using the theory of critical distances,” *Eng. Struct.*, vol. 30, no. 10, pp. 2707–2715, 2008, doi: 10.1016/j.engstruct.2008.03.005.

[15] B. M. Imam, T. D. Righiniotis, and M. K. Chryssanthopoulos, “Numerical modelling of riveted railway bridge connections for fatigue evaluation,” *Eng. Struct.*, vol. 29, no. 11, pp. 3071–3081, 2007, doi: 10.1016/j.engstruct.2007.02.011.

[16] B. Imam, T. D. Righiniotis, M. K. Chryssanthopoułos, and B. Bell, “Analytical fatigue assessment of riveted rail bridges,” *Proc. Inst. Civ. Eng. Bridg. Eng.*, vol. 159, no. 3, pp. 105–116, 2006, doi: 10.1680/bren.2006.159.3.105.

[17] I. Olofsson *et al.*, “Assessment of European railway bridges for future traffic demands and longer lives – EC project ‘Sustainable Bridges,’” *Struct. Infrastruct. Eng.*, vol. 1, no. 2, pp. 93–100, 2005, doi: 10.1080/15732470412331289396.

[18] C. R. Farrar and K. Worden, “An introduction to structural health monitoring,” *Philos. Trans. R. Soc. A Math. Phys. Eng. Sci.*, vol. 365, no. 1851, pp. 303–315, 2007, doi: 10.1098/rsta.2006.1928.

[19] S. W. Doebling, C. R. Farrar, M. B. Prime, and D. W. Shevitz, *Damage Identification and Health Monitoring of Structural and Mechanical Systems from Changes in Their Vibration Characteristics: A Literature Review*. Los Alamos National Laboratory report LA-13070-MS, 1996.

[20] H. Sohn *et al.*, *A Review of Structural Health Monitoring Literature: 1996-2001*. Los Alamos National Laboratory report, LA-13976-MS, 2004.

[21] H. R. Ahmadi, F. Daneshjoo, and N. Khaji, "New damage indices and algorithm based on square time-frequency distribution for damage detection in concrete piers of railroad bridges," *Struct. Control Heal. Monit.*, vol. 22, no. 1, pp. 91–106, Jan. 2015, doi: 10.1002/stc.1662.

[22] H. R. Ahmadi and D. Anvari, "New damage index based on least squares distance for damage diagnosis in steel girder of bridge's deck," *Struct. Control Heal. Monit.*, vol. 25, no. 10, pp. 1–22, 2018, doi: 10.1002/stc.2232.

[23] M. Bayat, H. R. Ahmadi, and N. Mahdavi, "Application of power spectral density function for damage diagnosis of bridge piers," *Struct. Eng. Mech.*, vol. 71, no. 1, pp. 57–63, 2019, doi: 10.12989/sem.2019.71.1.057.

[24] D. O. Smallwood, "Characterization and simulation of transient vibrations using band limited temporal moments," *Shock Vib.*, vol. 1, no. 6, pp. 507–527, 1994, doi: 10.3233/SAV-1994-1602.

[25] F. M. Hemez and S. W. Doebling, "From shock response spectrum to temporal moments and vice-versa," Los Alamos National Laboratory report, LA-UR-02-6790, 2002.

[26] C. R. Farrar and K. Worden, *Structural Health Monitoring: A Machine Learning Perspective*. Wiley, 2012.

[27] B. T. Svendsen, "Implementation of temporal moments in Python." 2020. doi: 10.5281/zenodo.3609158.

[28] K. Worden and J. M. Dulieu-Barton, "An Overview of Intelligent Fault Detection in Systems and Structures," *Struct. Heal. Monit.*, vol. 3, no. 1, pp. 85–98, Mar. 2004, doi: 10.1177/1475921704041866.

[29] A. Rytter, "Vibrational Based Inspection of Civil Engineering Structures," University of Aalborg, Denmark, 1993.

[30] K. Worden, C. R. Farrar, G. Manson, and G. Park, "The fundamental axioms of structural health monitoring," *Proc. R. Soc. A Math. Phys. Eng. Sci.*, vol. 463, no. 2082, pp. 1639–1664, 2007, doi: 10.1098/rspa.2007.1834.

[31] E. Kreyszig, *Advanced Engineering Mathematics*, 9th ed. John Wiley & Sons, Inc., 2006.

[32] S. Smith, *Digital Signal Processing: A Practical Guide for Engineers and Scientists*. Newness, 2002.

Part 2

The content of this part is published in:

Svendsen, B. T., Petersen, Ø. W., Frøseth, G. T., and Rønnquist, A. (2021). *Improved finite element model updating of a full-scale steel bridge using sensitivity analysis*. Structure and Infrastructure Engineering, 1-17.

https://doi.org/10.1080/15732479.2021.1944227

Abstract

There are many uncertainties related to existing bridges that are approaching or have exceeded their original design life. Lifetime extension analysis of bridges should be based on validated numerical models that can be effectively established. This paper presents a new procedure to obtain an optimal solution from sensitivity-based model updating with respect to an improvement in the modal properties, such as the natural frequencies and mode shapes, based on realistic parameter values. The procedure combines variations in the ratios of overdetermined systems with different definitions of local parameter bounds in a structured approach using a sensitivity analysis. The feasibility of the procedure is demonstrated in an experimental case study. Model updating is performed on a full-scale steel bridge using the natural frequencies and modal assurance criterion (MAC) numbers, where the numerical model is established by considering general uncertainties and model simplifications to reduce the model complexity. From the optimal solution for the case study considered, an improvement in modal parameters is obtained with highly reliable parameter values. The proposed procedure can be applied to similar case studies, irrespective of the structure under consideration and the corresponding parameterization to be made, to effectively obtain a validated numerical model.

Keywords: Finite element model updating; sensitivity method; parameter bounds; experimental study; steel bridge; lifetime extension; structural health monitoring.

Chapter 3

3 Improved finite element model updating of a full-scale steel bridge using sensitivity analysis

3.1 Introduction

There are increasing demands on existing infrastructure with respect to traffic loads and intensity. Many highway and railway bridges are still in use despite that they are approaching or have exceeded their original design life. Although many uncertainties related to ageing, deterioration and damage accumulation are present in these bridges, lifetime extension is the preferred option to ensure continuous operation. Considering the requirements for precise numerical models in lifetime extension analyses of bridges, analyses should be carried out using validated models that adequately represent the current state given inherent uncertainties present in these structures.

Structural health monitoring (SHM) systems can provide updated information regarding the current state of a bridge condition. SHM, defined as the process of implementing an automated and online strategy for damage detection in a structure [1], can be utilized for lifetime extension purposes. There are two main approaches in SHM: model-based and data-based [2], [3]. The model-based approach is an inverse problem, where a numerical model of the structure is established, and the relation to changes in the measured data from the structure to changes in the numerical model are investigated. The data-based approach relies on the use of machine learning for the identification of damage and ideally requires training data for all considered structural states, healthy and damaged, which can be challenging for bridges in service. However, the effective use of a numerical model can be made in a hybrid approach, which takes principles from both the model-based and data-based approaches into consideration by integrating a numerical model, experimental data and machine learning. In the SHM approaches where a numerical model is utilized, a validated numerical model is inevitable.

Finite element (FE) model updating is the process of calibrating the parameters of a numerical FE model based on vibration test data, where the aim of model updating is to reduce the discrepancy between the numerical model and available measurement data [4]. Model updating is essential for obtaining a validated numerical model. A validated numerical model can reduce model uncertainty in a reliability framework to improve the estimation of the remaining service life, where model uncertainty is quantified by the stress ratio between the structure (actual stress) and the numerical model (estimated stress). Furthermore, a validated numerical model can increase the accuracy of predictions in analysis related to the (1) structural response to the type of loads other than that used in the vibration test, (2) structural system behaviour in a different frequency range or in degrees of freedom (DOFs) different from those used in the model updating process and, (3) effects of structural modifications and structural damage [5]. For the latter, several

case studies are performed with respect to SHM and damage detection based on model updating [6]–[12]. Comprehensive reviews of model updating techniques and relevant methods are available in the literature [5], [13]–[16]. With the increasing establishment of SHM systems on bridge structures and the considerable improvement in numerical models that can be obtained from model updating, applications on several case studies are reported in the literature. These studies include applications on highway and railway bridges [17]–[24], footbridges [25], [26], cable-stay bridges [27]–[33], suspension and floating bridges [34]–[37], and relevant test structures [38]–[40].

Of the many model updating applications on bridges, several different approaches can be found. Sensitivity-based model updating considering parameterized models is a preferred method for full-scale bridges [37]. Model updating can provide large improvements in the modal properties such as the natural frequencies and mode shapes. However, it is still a requirement that the modelling errors are minimized and that the improvements are based on reasonable parameter values to consider the model validated. In sensitivity-based model updating, an overdetermined system should be considered, allowing for a unique solution to be obtained [5]. Depending on (1) the overdetermined system and (2) the constraints enforced on the parameters of the numerical model, large variations in parameter values can render improved modal properties, irrespective of the type of model parameterization. Constraining the parameters is necessary when dealing with large models. Furthermore, the overdetermined system depends on the model parameterization and available modes from the system identification. Therefore, several choices can be made for how overdetermined the system should be and the size of the constraints to enforce on the parameters, or how these should be combined in the model updating. These choices require careful consideration and a structured approach in the model updating process. There are no studies in the literature where this problem has been addressed or fully considered in model updating of bridges.

Model updating should be performed by considering a detailed numerical model, to a level different from a conventional numerical model, to adequately represent the geometric and structural form [41], [42]. However, there is a trade-off between a validated detailed numerical model in good agreement with measurements and a validated numerical model being computationally efficient for numerical simulations. For many engineering considerations, it is desirable to effectively obtain a validated numerical model that can be considered for several analysis purposes where the complexity of the model is left to a minimum but is still in acceptable agreement with measurements. Overall, the goal of model updating is to obtain improved modal properties based on reasonable and realistic parameter values. With the increased demand for validated models in lifetime extension analysis and a large number of ageing bridges, a procedure irrespective of the model parameterization is needed to effectively establish validated models based on model updating.

This paper investigates the effects of using a sensitivity analysis for improved model updating. A new procedure based on a structured approach is proposed to obtain an optimal solution from sensitivity-based model updating with respect to an

improvement in the modal properties combined with reasonable parameter values. The procedure is demonstrated on a full-scale steel bridge, a case study representative of many bridges still in service. The paper is organized in three parts. In the first part, the theory of the model updating framework is presented, including the theory of local parameter bounds to be included in the optimization algorithm. The implementation of the theoretical framework using ABAQUS and Python is made available [43]. The second part of the paper presents the experimental case study and outlines the proposed procedure. A numerical model is established and parameterized considering general uncertainties and model simplifications, where the model simplifications are introduced to reduce complexity. The effects from a sensitivity analysis are investigated by considering different ratios of overdetermined systems combined with two definitions of local parameter bounds. The results based on the optimal solution from the sensitivity analysis are presented. The final part presents a discussion of the proposed procedure. Based on the presented work, general recommendations are made with respect to the applicability to similar bridges in service.

3.2 Finite element model updating theory

3.2.1 General theoretical framework

The sensitivity method is used for performing the model updating. The main theoretical framework implemented is presented in the following section according to [5], with a similar notation. It is assumed that q measured outputs are available and the model is considered to be parameterized in p parameters. In general, the number of output measurements should be larger than the number of parameters in the model, i.e., $q > p$, yielding an overdetermined system with a unique solution. In this study, an overdetermined system is considered using both the identified measured natural frequencies and the modal assurance criterion (MAC) numbers as the objective for the calibration of parameters in the numerical model. The model updating is performed by perturbation analysis.

The sensitivity method is based on a linearization of the difference between the measured and analytically predicted outputs:

$$\boldsymbol{\varepsilon}_z = \mathbf{z}_m - \mathbf{z}(\boldsymbol{\theta}) \tag{3.1}$$

where $\mathbf{z}_m$ is the measured output and $\mathbf{z}(\boldsymbol{\theta})$ is the analytically predicted output as a function of the vector of parameters, $\boldsymbol{\theta}$. By reformulating the analytically predicted output, this becomes

$$\boldsymbol{\varepsilon}_z \approx \left(\mathbf{z}_m - (\mathbf{z}(\boldsymbol{\theta}_i) + \mathbf{G}_{i|\boldsymbol{\theta}=\boldsymbol{\theta}_i} \Delta\boldsymbol{\theta}_i) = \mathbf{z}_m - \mathbf{z}(\boldsymbol{\theta}_i) - \mathbf{G}_{i|\boldsymbol{\theta}=\boldsymbol{\theta}_i} \Delta\boldsymbol{\theta}_i \right) \tag{3.2}$$

The final form of the system equation is given as

$$\boldsymbol{\varepsilon}_z \approx \mathbf{r}_i - \mathbf{G}_{i|\boldsymbol{\theta}=\boldsymbol{\theta}_i} \Delta\boldsymbol{\theta}_i \tag{3.3}$$

where $\mathbf{r}_i = \mathbf{z}_m - \mathbf{z}(\boldsymbol{\theta}_i)$ is the residual, $\mathbf{G}_{i|\boldsymbol{\theta}=\boldsymbol{\theta}_i}$ is the sensitivity matrix and $\Delta\boldsymbol{\theta}_i$ is the parameter increment vector. The index i denotes the point of linearization

occurring at each iteration. The linear system, described in Equation (3.3), is established for q measured outputs (representing the rows) and p parameters (representing the columns) and is scaled:

$$\begin{bmatrix} \frac{\varepsilon_1}{z_{0,1}} \\ \vdots \\ \frac{\varepsilon_q}{z_{0,q}} \end{bmatrix} = \begin{bmatrix} \frac{r_1}{z_{0,1}} \\ \vdots \\ \frac{r_q}{z_{0,q}} \end{bmatrix} - \begin{bmatrix} \frac{\partial z_1}{\partial \theta_1}\frac{\theta_{0,1}}{z_{0,1}} & \cdots & \frac{\partial z_1}{\partial \theta_p}\frac{\theta_{0,p}}{z_{0,1}} \\ \vdots & \ddots & \vdots \\ \frac{\partial z_q}{\partial \theta_1}\frac{\theta_{0,1}}{z_{0,q}} & \cdots & \frac{\partial z_q}{\partial \theta_p}\frac{\theta_{0,p}}{z_{0,q}} \end{bmatrix} \begin{bmatrix} \frac{\Delta\theta_1}{\theta_{0,1}} \\ \vdots \\ \frac{\Delta\theta_p}{\theta_{0,p}} \end{bmatrix} \tag{3.4}$$

The frequencies are represented in the upper half of the sensitivity matrix, whereas the MAC numbers are represented in the lower half. The subscript zero denotes the scaling factors; i.e., θ_0 is the initial parameter value, and z_0 is the initial output value. The initial output value is taken as the analytically predicted value for the frequencies obtained from the initial numerical model and is 1 for the MAC numbers. The advantage of scaling is particularly to avoid large numerical values in the sensitivity matrix, which reduces potential ill-conditioning or matrix singularity. The terms in the sensitivity matrix can be established using an analytical approach or using numerical approximations by the perturbation procedure. For the latter,

$$\begin{aligned} \partial z_q &= z_{i,q}^{pert} - z_{i,q} \\ \partial \theta_p &= \theta_{i,p}^{pert} - \theta_{i,p} \end{aligned} \tag{3.5}$$

where the perturbed value is indicated with a superscript. The goal is to minimize the objective function, defined as

$$J(\Delta\boldsymbol{\theta}_i) = \boldsymbol{\varepsilon}_z^T \mathbf{W}_\varepsilon \boldsymbol{\varepsilon}_z \tag{3.6}$$

where $\mathbf{W}_\varepsilon$ is the symmetric weighting matrix. The weighting matrix is established as a diagonal and normalized matrix taking into consideration both natural frequencies and MAC numbers. In evaluating the minimization, the objective function is reformulated as a weighted sum of the normalized residual squared:

$$J\left(\Delta\boldsymbol{\theta}_i\right)^* = \sum_{j=1}^{q} \left[\mathbf{W}_\varepsilon\right]_{j,j} \left(\frac{z_{m,j} - z_{i,j}}{z_{0,j}} \right)^2 \tag{3.7}$$

For the overdetermined system, the objective function defined in Equation (3.6) is minimized with respect to $\Delta\boldsymbol{\theta}_i$ at each iteration to give an improved parameter estimate of $\Delta\boldsymbol{\theta}_i$. The model is then updated to give

$$\boldsymbol{\theta}_{i+1} = \boldsymbol{\theta}_i + \Delta\boldsymbol{\theta}_i \tag{3.8}$$

Significant changes in parameters can occur during the minimization, particularly during the first iteration steps. Hence, the parameters are constrained by establishing bounds in the minimization problem to obtain a model improvement with reasonable changes in the defined parameters.

3.2.2 Local parameter bounds

The parameters are constrained by implementing lower and upper bounds in the minimization problem, i.e.,

$$\boldsymbol{\theta}_{\min} \leq \boldsymbol{\theta}_{i+1} \leq \boldsymbol{\theta}_{\max} \tag{3.9}$$

Introducing Equation (3.8) and rearranging, the bounds at iteration, i, become

$$\boldsymbol{\theta}_{i,\min} \leq \boldsymbol{\theta}_i + \Delta\boldsymbol{\theta}_i \leq \boldsymbol{\theta}_{i,\max} \tag{3.10}$$

$$\boldsymbol{\theta}_{i,\min} - \boldsymbol{\theta}_i \leq \Delta\boldsymbol{\theta}_i \leq \boldsymbol{\theta}_{i,\max} - \boldsymbol{\theta}_i \tag{3.11}$$

Considering the sensitivity matrix, the bounds must be scaled accordingly. The final scaled lower and upper bounds to be used in the minimization become:

$$\begin{aligned} \Delta\boldsymbol{\theta}_{i,\min} &= \frac{\boldsymbol{\theta}_{i,\min} - \boldsymbol{\theta}_i}{\boldsymbol{\theta}_0} \\ \Delta\boldsymbol{\theta}_{i,\max} &= \frac{\boldsymbol{\theta}_{i,\max} - \boldsymbol{\theta}_i}{\boldsymbol{\theta}_0} \end{aligned} \tag{3.12}$$

The objective function can be minimized by solving the linear least squares problem with the defined bounds on the parameters. The bounds defined in Equation (3.12) are established as lower and upper allowable limits on the parameters per iteration and are referred to as local bounds.

3.2.3 Global parameter bounds

Global bounds are considered as the final lower and upper allowable limits for the parameters. The global bounds ensure that the parameters always attain values that are within a reasonable range from an engineering point of view. Ideally, these limits are never exceeded during the iterations in the model updating process. The local bounds mainly ensure that the parameter step is not too large in each iteration. These limits are established as a percentage of the given parameter value in the current iteration. The lower and upper local bounds have the same percentwise change for each iteration step. Local bounds "move" together with the updated parameter values within the global bounds. Figure 3.1 shows the relation between the local and global bounds.

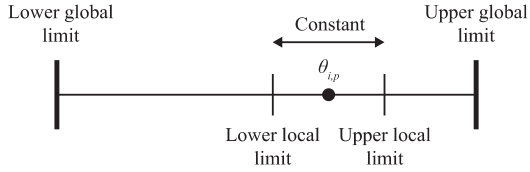

Figure 3.1: Relation between the local and global bounds.

3.2.4 Optimization

The optimization problem to be solved is, on a general form,

$$\min_{\mathbf{x}} \frac{1}{2}\left\|\mathbf{A}\mathbf{x}-\mathbf{b}\right\|_2^2, \quad lb \le \mathbf{x} \le ub \tag{3.13}$$

where $\mathbf{A}$ is the design matrix, $\mathbf{b}$ is the target vector and $\mathbf{x}$ is the vector of parameters to be optimized subject to the lower and upper bounds, lb and ub, respectively. The subscript 2 denotes the Euclidean norm. By introducing Equation (3.3) into Equation (3.6), utilizing that the weighting matrix is diagonal and thus symmetric, the objective function can be written as

$$J\left(\Delta\boldsymbol{\theta}\right) = \left\|-\mathbf{W}^{1/2}\mathbf{G}_i\Delta\boldsymbol{\theta}_i + \mathbf{W}^{1/2}\mathbf{r}_i\right\|_2^2 \tag{3.14}$$

with $\mathbf{A} = -\mathbf{W}^{1/2}\mathbf{G}_i$, $\mathbf{x} = \Delta\boldsymbol{\theta}_i$ and $\mathbf{b} = -\mathbf{W}^{1/2}\mathbf{r}_i$. Note that $\mathbf{A}$ is a q-by-p matrix and $\mathbf{b}$ is a vector of q elements. The subscript ε from the weighting matrix is removed for brevity. The bounds defined in Equation (3.12) are used directly as lower and upper bounds. Equation (3.14) is solved using the *scipy.optimize.lsq_linear* function in Python [44]. The optimization problem defined in Equation (3.14) is convex. Hence, the found minimum of the bounded linear least squares problem is expected to be global. However, the final solution of the model updating can depend on the initial parameter values and the parameter bounds. Consequently, the model updating can converge to a local minimum and there is as such no guarantee of convergence to a global minimum.

Constraining parameters can be useful when dealing with complex models parametrized in a fair number of parameters, although at the cost of finding an optimal theoretical solution. Constraining parameters are mainly introduced to avoid large and non-realistic parameter changes. The constraints can provide some numerical stability since the unconstrained iterative optimization based on first-order gradients sometimes can take too large steps, possibly stepping out of the area of interest. A similar effect can be obtained by applying a small amount of regularization to the objective function defined in Equation (3.6), see [5].

3.2.5 Mode identification

A mode match index (MMI) is introduced to ensure the identification of correct modes during model updating [14]:

$$MMI = \left(1-\gamma\right)MAC_{m,n} - \gamma\frac{\left|f_m - f_n\right|}{f_m} \tag{3.15}$$

where γ is a value between 0 and 1 that provides the weighting to be considered between the MAC numbers and natural frequencies, f. The subscripts m and n are denoted for the measured and numerical modes, respectively. Furthermore, the MAC number is defined as [45], [46]

$$MAC_{m,n} = \frac{\left|\boldsymbol{\Phi}_m^T \boldsymbol{\Phi}_n\right|^2}{\left(\boldsymbol{\Phi}_m^T \boldsymbol{\Phi}_m\right)\left(\boldsymbol{\Phi}_n^T \boldsymbol{\Phi}_n\right)} \tag{3.16}$$

where $\boldsymbol{\Phi}_m$ and $\boldsymbol{\Phi}_n$ are the measured and numerical mode shape vectors, respectively, and the superscript T denotes the transpose. The MMI is also utilized as an indicator to measure the overall performance of the model updating results.

The order of modes changes during the model updating, particularly for systems with closely spaced modes. Hence, an equal weighting obtained by setting $\gamma = 0.5$ is considered effective for the MMI.

3.2.6 Implementation of the theoretical framework

The theoretical framework is implemented using Python version 3.7.2, including SciPy version 1.3.2 [44], in combination with ABAQUS [47]. The implementation is validated through a numerical case study and is made available [43].

3.3 Experimental case study

3.3.1 Bridge description

The Hell Bridge Test Arena, shown in Figure 3.2, is an open-deck steel riveted truss bridge with a main span of 35 m and width of 4.5 m. The bridge was formerly in operation as a train bridge for more than 100 years before it was taken out of service and moved to concrete foundations on land. The bridge serves as a full-scale laboratory for research and development for damage detection and SHM [48].

All cross sections, connections and details of the bridge were originally made using steel plates connected by rivets. The bridge has no upper lateral bracing, i.e., no lateral stiffening connected to the top girder of the bridge walls. Hence, the bridge cross section is formed as a U-section. The lateral bracing system is located below the bridge deck and provides a stiffening of the bridge in the lateral direction. The bridge deck structural system is made of longitudinal stringers connected to transverse girders with double angle connections.

Figure 3.2: Hell Bridge Test Arena.

3.3.2 Experimental study and system identification

Figure 3.3 shows an overview of the bridge, including the sensor locations used in the experimental study. The results obtained from ambient vibrations considering wind only are used. Data from 18 triaxial accelerometers were sampled at 400 Hz. The data were detrended, then low-pass filtered using an 8th order Butterworth filter with a cut-off frequency at 40 Hz and resampled to 100 Hz before it was used for analysis. A 30 min long time series was selected as the basis for performing the system identification. The wind was in the range of 5-8 m/s with wind gusts up to 12 m/s during the measurement period.

System identification was performed using the frequency domain decomposition (FDD) method [49]. A Welch average was used for estimating the power spectral density. The first three singular values of the acceleration response spectrum and the modes identified are shown in Figure 3.4. All peaks in the acceleration response spectrum are evaluated, but only modes corresponding with the initial numerical model are used for FE model updating purposes. Altogether, 21 modes are established: 13 global modes and 8 semi-global modes. The global modes are related to modes in the lateral, vertical, torsional and longitudinal directions, whereas the semi-global modes are related to modes including mainly the bridge walls and to some extent the bridge deck. Modes 1-4 and 13-21 are global, whereas modes 5-12 are semi-global. No local modes identified are considered. The identified natural frequencies are given in Table 3.6.

Closely spaced modes are observed in the system, specifically related to the higher vertical and torsional modes. However, the modes established in the system identification are generally considered well separated.

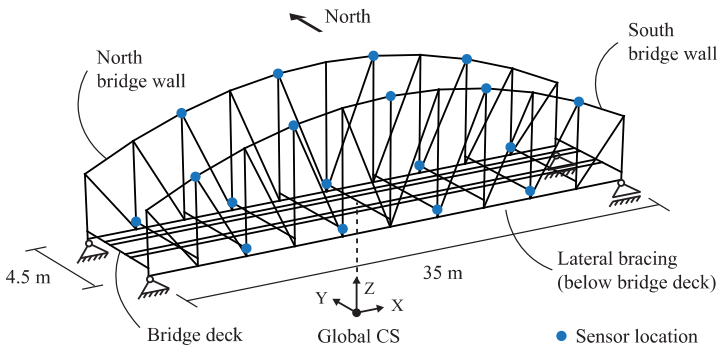

Figure 3.3: Overview of the bridge, including the sensor locations.

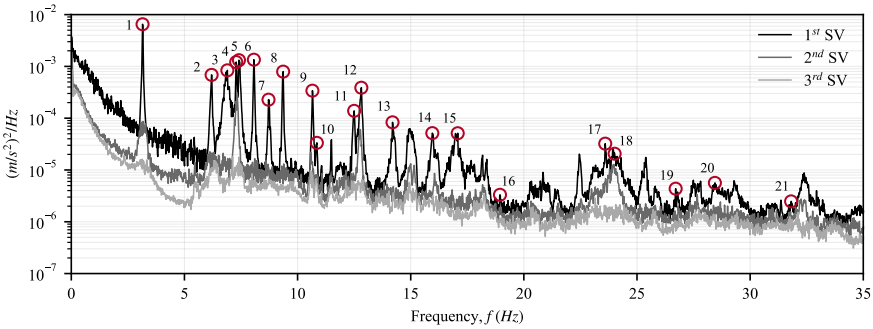

Figure 3.4: The first three singular values of the acceleration response spectrum. The identified modes are highlighted and numbered.

3.3.3 Model updating procedure

In model updating considering experimental case studies, there are several choices that can be made for how overdetermined the system is and the size of the constraints to enforce on the parameters. These choices depend on how the model is parameterized and the number of outputs available. Such considerations affect the results in the model updating and should be included in a sensitivity analysis. The following procedure is established as a structured approach to obtain an improved model updating:

1. Model parameterization and definition of global parameter bounds. A numerical model is established, and model parameterization is performed by considering general uncertainties and model simplifications.
2. Definitions of local parameter bounds. Two definitions of local parameter bounds are defined: rigid and semi-rigid. These definitions represent the different sizes of the constraints to enforce on the parameters.
3. Considerations of the overdetermined system ratios. The overdetermined system ratios are based on the model parameterization and available outputs from the system identification.
4. Establishing underlying assumptions. The underlying assumptions are needed as common criteria for the analysis cases defined in the sensitivity analysis. These assumptions include considerations of the model quality assessment, the weighting of updating modes, the maximum number of iterations to perform and other assumptions.

From bullet points 2 – 4, the effects of the sensitivity analysis can be investigated based on a given model parameterization. The overdetermined system ratio is defined as

$$r_{os} = \frac{q}{p}, \quad r_{os} > 1.0 \tag{3.17}$$

where q is the number of measured outputs and p is the number of parameters. Furthermore, the requirement for the overdetermined system is that $r_{os} > 1.0$. A

low overdetermined system ratio implies updating on a small number of modes, whereas a high overdetermined system ratio implies updating on a large number of modes for the system considered.

Model quality assessment is an important consideration for the underlying assumptions. Determining the model quality requires the use of control modes, i.e., modes that are not used to update the parameters [4]. The quality of the underlying model is thus indicated by the correlation between the results obtained for the control modes of the updated model and the measurements.

The model updating procedure is included to depend on both the natural frequencies and MAC numbers as the modal properties of the structural system. It should be noted that performing model updating on large structures, often rendering complex models with high parameterization, using natural frequencies only, can result in a significant improvement in natural frequencies but no improvement or even a decrease in the MAC numbers. Including both natural frequencies and MAC numbers in the model updating is advantageous for several reasons: it can preferably improve but most importantly avoid a decrease in MAC numbers; it ensures stability in the model updating procedure through improved mode identification; and it ensures more representative parameter values in the final updated model.

3.4 Finite element model and updating parameters

3.4.1 Finite element model

The numerical model is established using the FE software ABAQUS [47]. The main structure of the bridge is included in the model, which consists of four major parts: two vertical walls, including wall diagonals and wall stiffeners, the bridge deck and the lateral bracing system. Secondary steel and non-structural items are represented as lumped point masses on the bridge deck to ensure proper mass distribution. Specifications provided by technical drawings and site inspections are used as the basis for constructing the model. Figure 3.5 shows the numerical model.

A beam element model representation is established using two-node Timoshenko linear beam elements (B31) for the main structure and two-node connector elements (CONN3D2) for connections between beam elements of the main bridge parts. Three different connection types are utilized with different DOFs activated. The connection types account for local geometry and particularly joint details such as gusset plate design. The bridge is modelled as simply supported with pinned boundary conditions on one end (global translational x, y and z-direction constrained) and rolled boundary conditions on the other end (global translational x-direction partly constrained by spring elements and global translational y and z-direction constrained). The model is divided into 3035 elements, with a total of 8906 nodes and 15590 DOFs. Altogether, the model is established using a straightforward modelling procedure with several simplifications included based on engineering judgement.

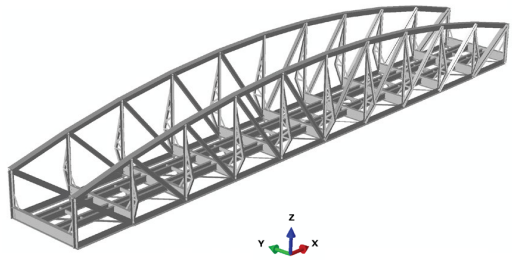

Figure 3.5: Numerical model.

3.4.2 Updating parameters

The updating parameters are based on the understanding of the local and global structural behaviour of the bridge. Parameters are chosen to mainly account for (1) modelling inaccuracies, including model simplifications, such as general uncertainties related to modelling and differences in the geometry of the model compared to the real structure, and (2) uncertainties in the bridge structural properties. The parameters represent regions of the structure where modelling inaccuracies and general uncertainties might cause discrepancies in the predictions. In this study, four different parameter types are chosen: density, stiffness, mass and spring stiffness. The parameter types are related to the material properties of the bridge, mass of non-structural items and boundary conditions.

The numerical model is parameterized in a total of 10 parameters. Table 3.1 summarizes the parameters used in the model updating, together with the global upper and lower parameter bounds. Engineering judgement is required to set the bounds, particularly for complex cases where large uncertainties are inherent in the parameters. Two parameters related to the density are included. The density of steel, ρ_{steel}, is introduced to account for any uncertainty in the mass of the structure. This parameter is valid for all the main steel, and consequently, the global and semi-global modes of the bridge are sensitive to this parameter. The lower part of the wall verticals is originally designed with complex plate geometry but is simplified in the numerical model using dummy beam elements with increased stiffness. The density of the lower part of the wall verticals, ρ_{wvl}, is included to account for the underestimation of the mass and is as such expected to increase. This parameter mainly influences the global modes of the structure.

Six stiffness parameters are included in the parameterization. The stiffness of the lateral bracing, E_{lb}, is included mainly to account for the simplifications introduced in the numerical model, i.e., continuous beam element modelling. The stiffness of the bridge deck, E_{bd}, is included to account for both the uncertainties and model simplifications. A reasonable engineering simplification is to exclude the substructure on the bridge deck from the model, i.e., the rails and wooden sleepers. This substructure is connected to the bridge deck structural system by steel hooks between the sleepers and the top flange of the longitudinal stringers. The substructure represents some additional stiffness to the bridge deck, which is initially not considered. This stiffness is highly difficult to estimate due to the large

Table 3.1: Parameters used in the model updating, including global lower and upper bounds.

Parameter	Type	Location	Reference value, $\boldsymbol{\theta}_0$	Global lower bound, $\boldsymbol{\theta}_{\min}$	Global upper bound, $\boldsymbol{\theta}_{\max}$	Unit
ρ_{steel}	Density	Main steel structure	7850	7065	8635	kg/m^3
ρ_{wvl}	Density	Wall verticals, lower	7850	6280	15700	kg/m^3
E_{lb}	Stiffness	Lateral bracing	2.10E+11	1.68E+11	2.52E+11	N/m^2
E_{bd}	Stiffness	Bridge deck	2.10E+11	1.47E+11	2.73E+11	N/m^2
E_{wg}	Stiffness	Wall girders, top and bottom	2.10E+11	1.68E+11	2.52E+11	N/m^2
E_{wd}	Stiffness	Wall diagonals	2.10E+11	1.68E+11	2.52E+11	N/m^2
E_{wvu}	Stiffness	Wall verticals, upper	2.10E+11	1.68E+11	2.52E+11	N/m^2
E_{wvl}	Stiffness	Wall verticals, lower	1.05E+12	2.10E+11	2.10E+12	N/m^2
m_{bd}	Mass	Substructure, bridge deck	18500	9250	37000	kg
k_x	Spring stiffness	End Support BC	1.00E+06	1.00E+05	1.00E+08	N/m

variability observed in the remaining functionality of the connections within the substructure and the connections of the substructure to the bridge deck.

The profiles constituting the truss beams of the bridge are made of riveted plates. For the top and bottom wall girders particularly, the profiles are tapered in parts of the beam lengths and especially towards the joints for strengthening purposes. The profiles are represented as equivalent beam element profiles in the numerical model, and any uncertainty with this representation is taken into account

by the stiffness of the top and bottom wall girders, E_{wg}. The stiffness of the wall diagonals, E_{wd}, is included in the model due to the uncertainty of the joint flexibility in the upper and lower parts of the diagonals. Diagonals are connected to the wall joints using gusset plate details. The rotational out-of-plane stiffness of these diagonals are released in both ends in the numerical model to account for these details. Although this is considered a common engineering simplification, the true joint stiffness is represented somewhere in the middle of a full release and no release.

The stiffness of the upper and lower wall verticals, i.e., E_{wvu} and E_{wvl}, respectively, represent uncertainties related to model simplifications. The upper wall verticals are well represented in the model; however, the lower wall verticals are represented by dummy beam elements with estimated stiffness since secondary steel is excluded. Since these two parts of the wall verticals are connected, the relatively high uncertainty in the lower part may affect the upper part. Consequently, either an increase or decrease in parameter values is expected to occur for both. All stiffness parameters are sensitive to both the global and semi-global modes of the structure. Figure 3.6 shows the parameterization of the numerical model with respect to the density and stiffness parameters.

The mass of the bridge deck substructure, m_{bd}, is introduced to account for the mass estimation error. This parameter is mostly sensitive to the global modes. Furthermore, there is a high degree of general uncertainty related to the spring stiffness, k_x, representing the roller boundary conditions. No information is available on how much functionality remains in the boundary conditions with respect to friction. Hence, it is important to include this parameter, although it has the least influence on the modes of all parameters included. Figure 3.7 shows the parameterization of the numerical model with respect to the spring stiffness parameter. The sensitivity of all the updating parameters on the natural frequencies and MAC numbers is shown in Figure 3.9.

In addition to the abovementioned, additional uncertainties inherent in the model parameterization of the chosen parameter types are considered. First, all secondary steel and structural details are excluded or represented as mass in the numerical model. Second, all joints in the bridge are riveted. However, the flexibility of these joints is prone to high uncertainty based on operational wear during the bridge service life. An imprecision in the rivet connections and a deviation in the intended behaviour of individual rivets caused by damage result in unwanted joint flexibility and the possibility of nonlinear behaviour during loading. Third, unwanted joint behaviour and damage in the structural details of the bridge, particularly in the bridge deck, is likely caused by fatigue damage, which is common in these types of bridges [50]. Fourth, effective beam lengths comprise uncertainty. Last, the material properties of steel that is more than 100 years old comprise uncertainty. Notably, there is a systematic error due to the difference between the measurements and the numerical model caused by meshing. Altogether, these uncertainties are also taken into consideration through the model parameterization. Several of the uncertainties mentioned are difficult to quantify and thus represent in a numerical model, resulting in the need for introducing model simplifications.

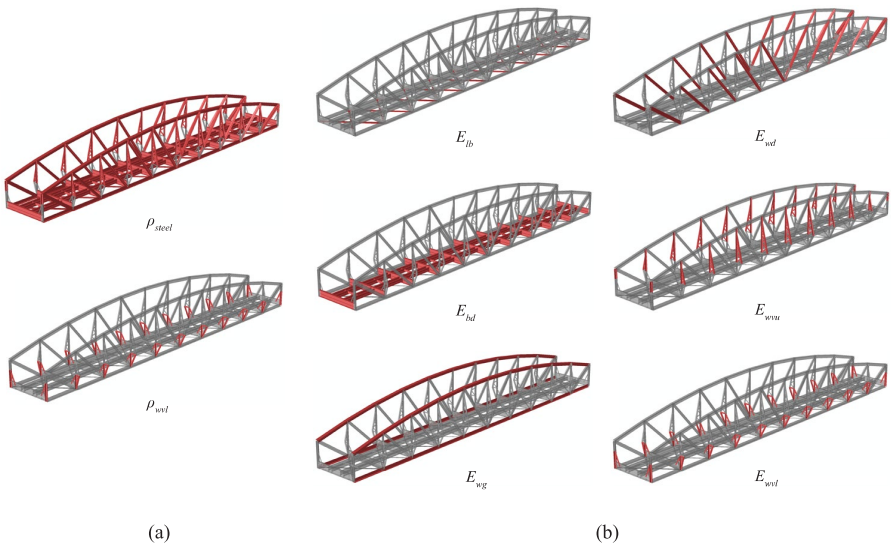

Figure 3.6: Parameterization of the numerical model considering the material properties. The specific parameterized area is highlighted in red. (a) Density parameters. (b) Stiffness parameters.

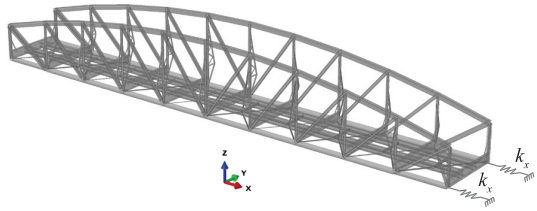

Figure 3.7: Parameterization of the numerical model considering the spring stiffness parameter.

3.5 Sensitivity analysis

3.5.1 Basis for evaluation

Table 3.2 shows the average values of the frequency error, MAC and MMI considering the different number of modes before model updating. Table 3.2 shows that for all 21 modes, the average frequency error is 5.22 % with an average MAC and MMI of 0.72 and 0.33, respectively. It is also observed that the average values of the frequency error, MAC and MMI are better for 10 and 12 modes than the average values when more modes are considered. This observation clearly indicates that the lower modes of the initial numerical model compare better with the measured modes from the system identification than the higher modes.

Table 3.2: Average values of the frequency error, MAC and MMI before model updating.

Modes	Δf_{error}	MAC	MMI
10	4.22 %	0.86	0.41
12	4.85 %	0.83	0.39
14	5.24 %	0.77	0.36
15	5.45 %	0.77	0.36
16	5.39 %	0.77	0.36
17	5.11 %	0.78	0.36
All	5.22 %	0.72	0.33

3.5.2 Underlying assumptions for the sensitivity analysis

The sensitivity analysis is performed by considering different sets of definitions for the local parameter bounds and ratios of overdetermined systems. Two definitions for the parameter bounds are considered: rigid (R) and semi-rigid (SR). The semi-rigid definition provides less constraints on the parameters than the rigid definition. However, both definitions ensure that overly large steps are avoided in each iteration. The scaled local lower and upper parameter bounds for the rigid and semi-rigid definitions, together with the scaled global bounds, are summarized in Table 3.3.

Table 3.3: Scaled local parameter bounds for the rigid and semi-rigid definitions.

				Rigid (R)		Semi-rigid (SR)	
Para-meter	Reference value	Global lower bound (scaled)[1]	Global upper bound (scaled)[1]	Local lower allowable change[2]	Local upper allowable change[2]	Local lower allowable change[2]	Local upper allowable change[2]
p	$\boldsymbol{\theta}_0$	$\boldsymbol{\theta}_{\min,scaled}$	$\boldsymbol{\theta}_{\max,scaled}$	$\Delta\boldsymbol{\theta}_{i,\min,scaled}$	$\Delta\boldsymbol{\theta}_{i,\max,scaled}$	$\Delta\boldsymbol{\theta}_{i,\min,scaled}$	$\Delta\boldsymbol{\theta}_{i,\max,scaled}$
ρ_{steel}	7850	0.90	1.10	-3 %	3 %	-3 %	3 %
ρ_{wvl}	7850	0.80	2.00	-10 %	10 %	-15 %	15 %
E_{lh}	2.10E+11	0.80	1.20	-5 %	5 %	-10 %	10 %
E_{hd}	2.10E+11	0.70	1.30	-5 %	5 %	-10 %	10 %
E_{wg}	2.10E+11	0.80	1.20	-5 %	5 %	-10 %	10 %
E_{wd}	2.10E+11	0.80	1.20	-5 %	5 %	-10 %	10 %
E_{wvu}	2.10E+11	0.80	1.20	-3.5 %	3.5 %	-5 %	5 %
E_{wvl}	1.05E+12	0.20	2.00	-10 %	10 %	-15 %	15 %
m_{bd}	18500	0.50	2.00	-15 %	15 %	-25 %	25 %
k_x	1.00E+06	0.10	100.00	-50 %	400 %	-50 %	900 %

[1] Scale factor of the specific parameter reference value.

[2] Allowable change of the specific parameter value in the current iteration, unless a global bound is reached.

Altogether, 12 analysis cases are included by considering six different ratios and two definitions of the parameter bounds. A set of underlying assumptions are included as a basis. First, both natural frequencies and MAC numbers are used consistently in the model updating. Second, model updating is performed by considering model quality assessment. Two considerations are made when choosing control modes: modes 11 and 12 are chosen for general model quality assessment, whereas higher end modes are chosen as additional indicators of model performance with respect to the structural response outside of the measurement frequency range. Hence, for all cases, the model updating is performed by including the lowest modes and excluding the control modes from the updating algorithm. The largest number of updating modes is 17, leaving a minimum of 4 control modes. Third, the weighting, $\mathbf{W}_{\varepsilon}$, is set equal for all considered cases. All modes are considered equally important and consequently given equal weighting. Natural frequencies are prioritized and weighted 2/3 per mode, whereas MAC numbers are weighted 1/3 per mode. Fourth, a maximum of 8 iterations are used in each case. If a global bound is exceeded, then the parameter value is set equal to the limit of this bound before the minimization is carried out. To avoid model updating with parameters exceeding their global bounds, the analysis is terminated if the global bound of a parameter is exceeded two consecutive times. Last, to improve mode identification both during the perturbation analysis and during the iterations, local numerical modes are filtered out before performing the mode matching. A total of 250 modes are extracted in each numerical analysis. Combining the filtering of the local numerical modes with the MMI in the model updating process is effective, particularly for numerical model representations resulting in many local modes.

3.5.3 Results

The results obtained from the sensitivity analysis are summarized in Table 3.4 and Table 3.5 for the rigid and semi-rigid definitions, respectively. Average values of the frequency error, MAC and MMI in addition to the change in the objective function, $J(\Delta\theta)^*$, and the number of iterations used are shown for the 12 cases considered. The results obtained are based on iterations in the updating algorithm until a fair stabilization of the objective function is reached.

Table 3.4: Results from the sensitivity analysis for the rigid parameter bounds definition.

Modes	Ratio r_{os}	Δf_{error} (%)		MAC		MMI		Change in J*	No. of iterations
		Updating modes	All modes	Updating modes	All modes	Updating modes	All modes		
10	2.0	4.38 %	5.21 %	0.89	0.74	0.42	0.34	-23.5 %	3
12	2.4	4.27 %	4.25 %	0.88	0.76	0.42	0.36	-49.9 %	6
14	2.8	5.59 %	4.82 %	0.81	0.73	0.38	0.34	-36.7 %	3
15	3.0	5.34 %	5.63 %	0.84	0.77	0.39	0.36	-50.4 %	7
16	3.2	4.66 %	5.21 %	0.81	0.74	0.38	0.35	-37.4 %	8
17	3.4	4.51 %	4.46 %	0.80	0.74	0.38	0.35	-15.3 %	3

Table 3.5: Results from the sensitivity analysis for the semi-rigid parameter bounds definition.

Modes	Ratio r_{os}	Δf_{error} (%)		MAC		MMI		Change in J*	No. of iterations
		Updating modes	All modes	Updating modes	All modes	Updating modes	All modes		
10	2.0	3.76 %	4.24 %	0.91	0.74	0.44	0.35	-43.7 %	7
12	2.4	3.60 %	3.85 %	0.86	0.72	0.41	0.34	-45.6 %	7
14	2.8	4.81 %	5.12 %	0.82	0.71	0.39	0.33	-38.3 %	5
15	3.0	4.76 %	4.07 %	0.83	0.75	0.39	0.35	-51.5 %	3
16	3.2	3.89 %	3.84 %	0.80	0.75	0.38	0.35	-30.8 %	6
17	3.4	3.88 %	3.99 %	0.82	0.75	0.39	0.35	-42.8 %	7

From Table 3.4 and Table 3.5, it is clearly seen that the choice of definition for the parameter bounds affects the results. An evaluation of the results is performed by considering both the decrease in the objective function and the overall results in the modal properties, i.e., the average frequency error, MAC and MMI. The decrease in the objective function is based on the updating modes only. Hence, to fully assess the model quality, the evaluation of the results is mainly based on the overall modal properties considering all modes, which takes into consideration both the updating modes and the control modes.

Two general observations are made. First, analysis cases using a semi-rigid definition generally provide better results for the modal properties than cases using a rigid definition. By considering all modes, the average frequency errors obtained for analysis cases using the semi-rigid definition are all lower than for cases using the rigid definition, except when considering the case $r_{os} = 2.8$. Furthermore, there is little variation in the average MAC and MMI considering all modes for the 12 cases considered, ranging from 0.71 to 0.77 for MAC and 0.33 to 0.36 for MMI. Second, a large variability in the results can be obtained considering a specific overdetermined system ratio but using different parameter bounds definitions. This is particularly observed in the case $r_{os} = 3.2$, where the results obtained for the MAC and MMI are similar, considering all modes for the rigid and semi-rigid definitions. However, a large difference in the results is obtained considering the average frequency error. For this analysis case, using the rigid definition provides practically no improvement in the average frequency error, whereas using the semi-rigid definition provides the best improvement of all 12 cases considered, compared to the initial numerical model.

For the cases $r_{os} = 2.0$, $r_{os} = 3.0$, $r_{os} = 3.2$ and $r_{os} = 3.4$, the best results are obtained using the semi-rigid definition when considering the overall results in the modal properties. Similarly, for the cases $r_{os} = 2.4$ and $r_{os} = 2.8$, the best results are obtained using the rigid definition. Furthermore, a majority of the overdetermined system ratios obtain a larger decrease in the objective function for the semi-rigid definition compared to the corresponding rigid definition. For the cases rendering the best results, the significance of the overdetermined system ratio is seemingly small considering the improvement in the modal properties of the

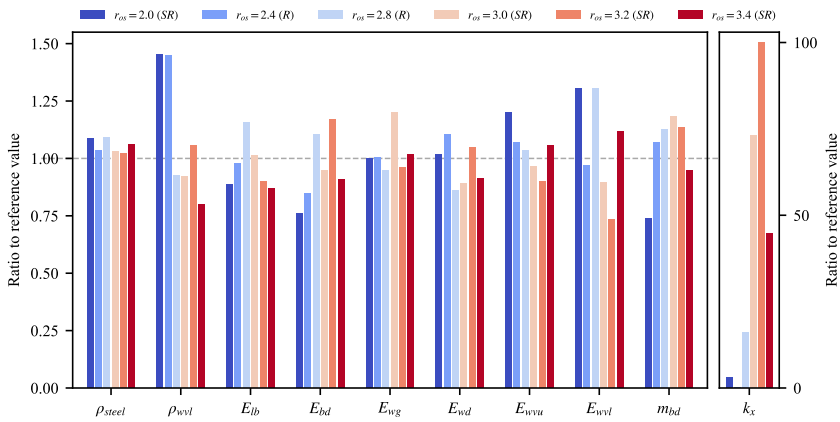

Figure 3.8: Ratio of parameter values.

updated models. As such, improved results by evaluating the modal properties only can be obtained with variations in the overdetermined system ratio and different parameter bound definitions. However, the change in parameter values for the updated models is of importance. Many of the parameters affect the system in a similar way, and several combinations of parameters can solve the optimization problem. Hence, the choice of final system overdetermined ratio to use should be based on the improvement in the overall modal parameters combined with how the parameter values are changed in the model updating.

The ratio of the parameter values obtained for the analysis cases with the best results are shown in Figure 3.8. From this figure, Table 3.4 and Table 3.5, it is observed that a large variability in updated parameter values can be obtained despite fairly similar results in the modal properties. Parameters that are expected to obtain small changes are the density of steel, ρ_{steel}, and the stiffness of the wall girders and wall diagonals, i.e., E_{wg} and E_{wd}, respectively. All cases obtain reasonable results with respect to these parameters. The density of the lower wall verticals, ρ_{wvl}, and mass of the bridge deck, m_{bd}, can both increase or decrease and can cancel each other out in the optimization. However, a large reduction in both parameters is unlikely, which excludes the case $r_{os} = 3.4(SR)$. The bridge deck stiffness, E_{bd}, can be used as a control parameter. Based on prior discussions, an increase in this updated parameter value is expected. Two cases obtain an increase in the bridge deck stiffness: $r_{os} = 3.2(SR)$ and $r_{os} = 2.8(R)$. For the latter, the other parameter values obtained are also acceptable; however, the overall results in the modal properties are not satisfactory. The remaining cases, i.e., $r_{os} = 2.0(SR)$, $r_{os} = 2.4(R)$ and $r_{os} = 3.0(SR)$, all result in a decrease in the bridge deck stiffness. Furthermore, less realistic values for the other parameters are obtained for these cases than for the case $r_{os} = 3.2(SR)$.

From the sensitivity analysis, the analysis case $r_{os} = 3.2(SR)$ clearly provides the most reasonable parameter values. Moreover, this case also renders the best results of the modal properties, particularly considering the natural frequencies that were weighted higher than the MAC numbers in the model updating. It is,

however, observed that this case has the smallest decrease in the objective function of all cases for the semi-rigid definition, and it has less decrease in the objective function than the corresponding analysis case for the rigid definition. This discrepancy is due to two low MAC values from modes 4 and 6 that penalize the objective function result. However, it has little effect on the average MAC result and is thus not reflected in the results presented in Table 3.5. A further evaluation of the results for this case is provided in the following section.

3.6 Model updating results

3.6.1 Parameter sensitivities and weighting

For the analysis case $r_{os} = 3.2(SR)$, 16 modes are used, resulting in a total of 32 outputs. The remaining 5 modes are used as control modes for the assessment of the model quality. Two small changes in the parameter bounds have been implemented for the analysis case compared to Table 3.3. The stiffness of the lateral bracing, E_{lb}, is decreased from 10 % to 5 %, and the upper bound of the spring stiffness is decreased from 900 % to 400 %. These changes have minor effects on the results.

Normalized sensitivity plots of the natural frequencies and MAC numbers with respect to the updating parameters are shown in Figure 3.9. The normalized sensitivity plots illustrate how the parameters influence the natural frequencies and MAC numbers of the modes used in the model updating. The sensitivity plots change for each iteration in the model updating process. In Figure 3.9, the sensitivity plots for the initial model are shown. It is observed that all parameters

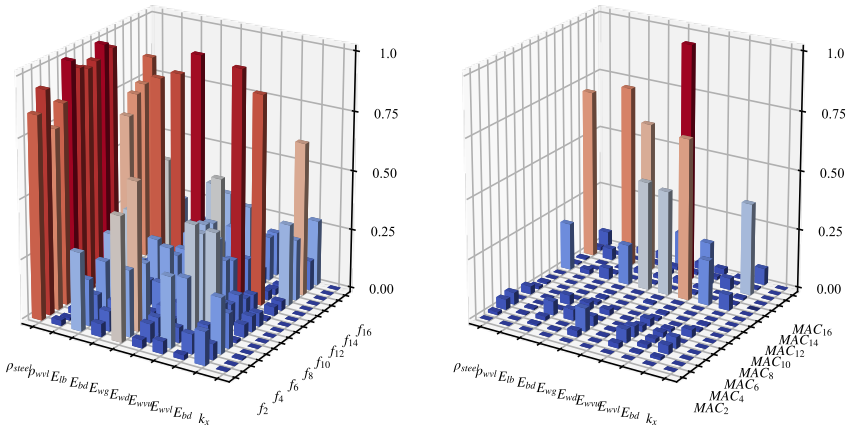

Figure 3.9: Normalized sensitivity plots of the frequencies (left) and MAC numbers (right) for the updating modes. The plots are normalized with respect to the frequencies and MAC individually.

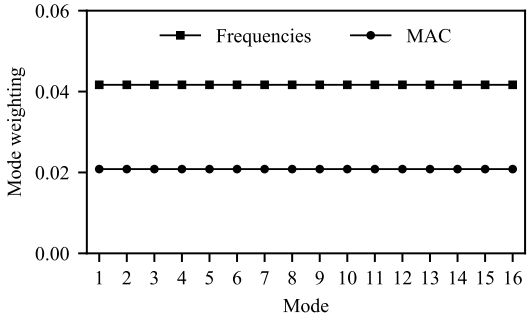

Figure 3.10: Weighting of the modes in the model updating.

influence both the natural frequencies and MAC numbers, except for k_x, which is shown to have a minor influence. Although this parameter has little influence in the initial part of the model updating, all parameters are included in the model updating process.

The weighting implemented for the updating modes is shown in Figure 3.10. The weighting is given as 0.04167 and 0.02083 for the natural frequencies and MAC numbers per mode, respectively, and sum to 1 by considering the outputs of all modes.

3.6.2 Model updating results

Altogether, six iterations in the analysis are performed. The final value of the objective function decreased from 0.0302 to 0.0209, resulting in a decrease of 30.8 %. The average absolute frequency errors for the initial and updated models are shown in Figure 3.11. The dashed horizontal lines represent the average absolute frequency error considering all modes for the initial and updated model, which is decreased from 5.22 % to 3.84 %. By considering the updating modes only, a decrease in the average absolute frequency error from 5.38 % to 3.89 % is obtained, whereas a decrease from 4.67 % to 3.69 % is obtained by considering the control modes only.

Figure 3.12 shows the MAC numbers between the measured and numerical modes for the initial and updated models. In general, the average MAC increased from 0.72 to 0.75 for all modes, whereas it increased from 0.77 to 0.80 and from 0.54 to 0.58 for the updating modes and control modes, respectively. An improvement in the MAC numbers is particularly seen for higher modes, i.e., from modes 11 to 21.

The MMI is used to assess the overall performance of the modal properties in the model updating. An identical match in the natural frequency and MAC between the numerical model and the measurements results in the maximum MMI value of 0.5. The MMIs for the initial and updated models are shown in Figure 3.13. The dashed horizontal lines represent the average MMI considering all modes for the initial and updated model, which is increased from 0.33 to 0.35. By considering the updating modes and control modes separately, an increase in the MMI from 0.36 to 0.38 and from 0.25 to 0.27 is obtained, respectively. It should be noted that the

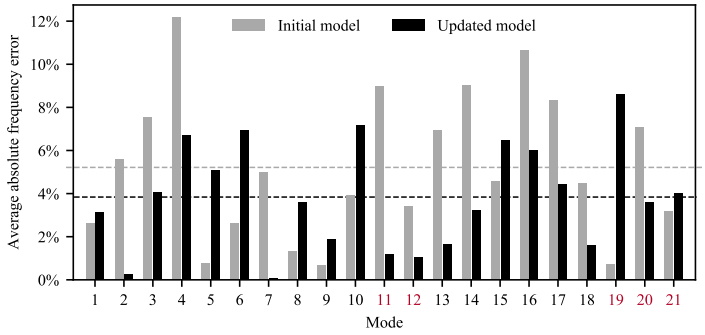

Figure 3.11: Average absolute frequency error for the initial and updated model. Control modes are highlighted in red.

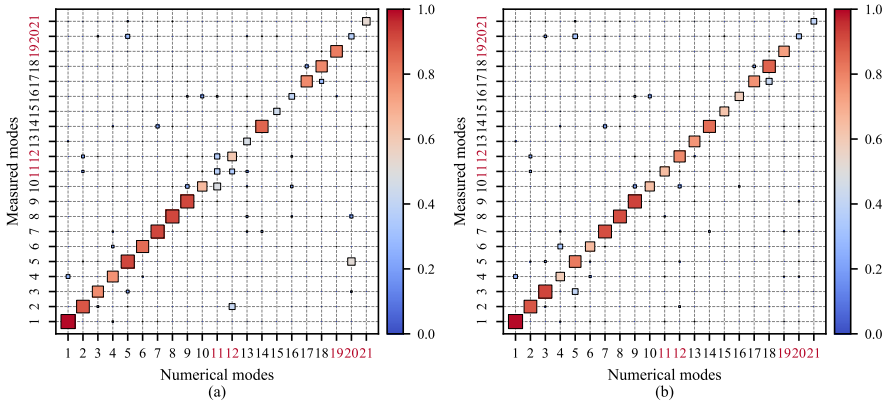

Figure 3.12: MAC numbers between the measured and numerical modes with control modes highlighted in red. (a) Initial model. (b) Updated model.

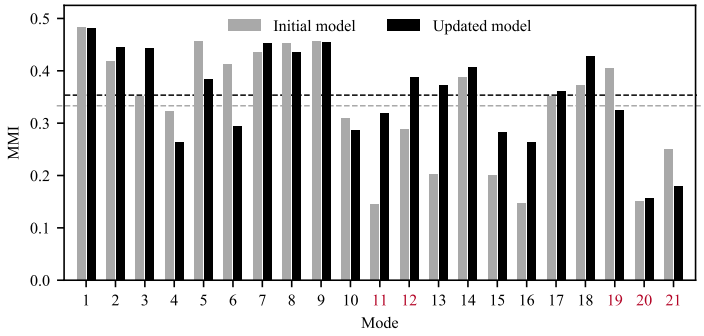

Figure 3.13: MMI for the initial and updated model. Control modes are highlighted in red.

MMI is generally higher for the lower modes, indicating a larger difficulty in obtaining a good correspondence between measurements and numerical models for the higher modes.

Detailed results for the natural frequencies, MAC numbers and MMI before and after the model updating are summarized in Table 3.6. In summary, the results show that good improvement is obtained from the model updating when considering all modes. The best improvement is obtained when considering the reduction in the average absolute frequency error, as expected. A fair improvement is obtained in the MAC numbers, which in general are less sensitive than the natural frequencies.

Table 3.6: Natural frequencies, MAC and MMI for the initial and updated model.

	Frequency, f (Hz)					MAC			MMI	
Mode	Mea-sured	Initial	Error	Up-dated	Error	Initial	Up-dated	Change	Initial	Up-dated
1	3.15	3.23	2.63 %	3.25	3.13 %	0.99	0.99	0.00	0.48	0.48
2	6.20	6.55	5.60 %	6.22	0.25 %	0.89	0.89	0.00	0.42	0.45
3	6.90	6.38	-7.55 %	6.62	-4.04 %	0.78	0.93	0.15	0.35	0.44
4	7.29	8.17	12.17 %	7.78	6.68 %	0.77	0.60	-0.17	0.32	0.26
5	7.41	7.35	-0.76 %	7.03	-5.09 %	0.92	0.82	-0.10	0.46	0.38
6	8.07	7.86	-2.60 %	7.51	-6.92 %	0.85	0.66	-0.19	0.41	0.29
7	8.72	9.15	4.98 %	8.71	-0.08 %	0.92	0.91	-0.01	0.44	0.45
8	9.36	9.49	1.33 %	9.03	-3.60 %	0.92	0.91	-0.01	0.45	0.44
9	10.66	10.73	0.67 %	10.45	-1.90 %	0.92	0.93	0.01	0.46	0.45
10	10.85	10.43	-3.91 %	10.08	-7.15 %	0.66	0.65	-0.01	0.31	0.29
11	12.50	13.62	8.99 %	12.35	-1.20 %	0.38	0.65	0.27	0.15	0.32
12	12.82	13.25	3.39 %	12.69	-1.02 %	0.61	0.79	0.17	0.29	0.39
13	14.20	15.18	6.93 %	14.43	1.63 %	0.47	0.76	0.29	0.20	0.37
14	15.96	17.39	9.02 %	16.47	3.22 %	0.86	0.85	-0.02	0.39	0.41
15	17.08	16.30	-4.55 %	15.97	-6.46 %	0.45	0.63	0.18	0.20	0.28
16	18.95	20.96	10.66 %	20.08	6.01 %	0.40	0.59	0.19	0.15	0.26
17	23.60	25.56	8.34 %	24.64	4.42 %	0.79	0.77	-0.02	0.35	0.36
18	24.01	25.08	4.47 %	24.40	1.60 %	0.79	0.87	0.08	0.37	0.43
19	26.71	26.89	0.70 %	29.01	8.60 %	0.82	0.74	-0.08	0.40	0.33
20	28.44	30.46	7.09 %	29.47	3.62 %	0.37	0.35	-0.02	0.15	0.16
21	31.81	32.83	3.18 %	33.09	4.01 %	0.53	0.40	-0.13	0.25	0.18

An improvement in both the average absolute frequency error and MAC is obtained for the control modes, which indicates good model quality. By considering the overall assessment of the modal properties shown by the MMI, altogether 16 modes improve or exhibit no or a negligible decrease (i.e., less than or equal to 0.02 decrease). The best improvement is obtained for the higher modes; for modes 11 to 21, improvement is obtained in all modes, except for modes 19 and 21. Less improvement is obtained in the lower modes, i.e., modes 1 to 10, where 3 modes improve and 4 modes demonstrate no or a negligible decrease. Although all

modes are considered equally important in this study, obtaining improvement in the higher modes is a good result considering the overall assessment.

The results of the updated parameter values, including the change from the initial parameter values, are summarized in Table 3.7. For the density parameters, a modest change in the parameter values is obtained. The density of the steel, ρ_{steel}, highly influences all modes, and an increase of 2.3 % is obtained. This is a reasonable change, considering the material property itself but also considering all details of the structure such as the rivets and plates not being included in the numerical model. The density of the lower part of the wall verticals, ρ_{wvl}, increased 5.8 %. This increase is highly relevant since this part of the structure consists of steel plates but is simplified in the numerical model using dummy beam elements.

Table 3.7: Parameter values from the initial and updated model, including change.

Parameter	Reference value	Updated value	Change	Percentage change
ρ_{steel}	7850	8032	182	2.3 %
ρ_{wvl}	7850	8305	455	5.8 %
E_{lb}	2.10E+11	1.89E+11	-2.14E+10	-10.2 %
E_{bd}	2.10E+11	2.46E+11	3.57E+10	17.0 %
E_{wg}	2.10E+11	2.02E+11	-8.20E+09	-3.9 %
E_{wd}	2.10E+11	2.20E+11	9.87E+09	4.7 %
E_{wvu}	2.10E+11	1.89E+11	-2.14E+10	-10.2 %
E_{wvl}	1.05E+12	7.72E+11	-2.78E+11	-26.5 %
m_{bd}	18500	20963	2463	13.3 %
k_x	1.00E+06	1.00E+08	9.90E+07	9900.0 %

For the stiffness parameters, reasonable changes in the parameter values are obtained. The stiffness of the lateral bracing, E_{lb}, decreased by 10.2 %. This reduction can be attributed to the continuous beam element modelling made; the pin connections in all bracing cross points are excluded in the numerical model. An increase in the bridge deck stiffness, E_{bd}, of 17.0 % is obtained. This increase is as expected due to the engineering simplification made of excluding the substructure of rails and wooden sleepers on the bridge deck, adding stiffness that initially is not taken into consideration. The wall girder stiffness, E_{wg}, obtained a decrease of 3.9 %, well within reasonable changes. This change is attributed to simplifications from representing the model with equivalent beam element profiles. The stiffness of the wall diagonals, E_{wd}, obtained an increase of 4.7 %. This increase in stiffness is reasonable considering that the rotational out-of-plane stiffness of all diagonals are released in both ends in the numerical model by accounting for the gusset plate details.

The largest changes in stiffness values are obtained for the lower and upper vertical wall stiffeners, with a decrease of 10.2 % for the upper part, E_{wvu}, and a decrease of 26.5 % for the lower part, E_{wvl}. The stiffness parameter for the lower part has the largest uncertainty of all stiffness parameters, and the initial

assumptions based on estimation were clearly too stiff. However, the change is within the defined global limit. Furthermore, this change clearly also affects the stiffness of the upper part, and it is thus reasonable to reduce the stiffness of the upper part when a reduction in the lower part is obtained.

The mass of the bridge deck substructure is increased by 13.3 %, well within the limits defined. Uncertainty is inherent in the estimation of this mass, especially related to the density of the wooden sleepers and the total mass of structural details such as the rivets, bolts and steel hooks. The largest change is observed for the spring stiffness parameter, k_x, which reaches its upper global limit. There are two main explanations for this change: first, there is a high uncertainty in this parameter; and second, this is the parameter with the least influence on the natural frequencies and MAC numbers, and consequently, large changes are required to influence the modal properties. The global limits could be extended; however, it is unlikely that the boundary conditions that were originally designed as rollers with little or no friction in the longitudinal direction completely lost their function. As such, this parameter change is accepted, but caution should be taken in accepting this as the definite result.

In summary, a fair improvement in the modal properties is obtained from model updating. The improvement is obtained based on the development of parameter values that are highly realistic and generally accepted. A further improvement can as such only be obtained with a different parameterization of the model.

3.7 Discussion

From the sensitivity analysis, the following general observations are made:

- Semi-rigid local bounds on the parameters are preferred over rigid local bounds. Less constraints on the parameters, however, within reasonable values, allow for larger parameter adjustments in each iteration. This is more likely to ensure convergence towards an optimal solution rather than a suboptimal solution, although the solution may be based on a local minimum of the objective function. Moreover, including both local and global parameter bounds increases the control of the parameters in the updating process.
- Using a low overdetermined ratio, by updating on a few modes, improved the modal properties of all modes on average; however, it did not provide the best improvement in the modal parameters or reasonable parameter values. Using a high overdetermined system ratio yielded reasonable parameter values and the best improvement in the modal properties considering all modes on average, particularly for the higher modes of the structure.
- By considering the proposed procedure in a structured approach, allowing for an extensive number of analysis cases to be evaluated, the optimal solution for the model updating with respect to an improvement in modal properties is established with high confidence. Further improvement in modal properties would require a different model parameterization.

- A large variability in the parameter values can be obtained when considering different combinations of overdetermined system ratios and rigidity of parameter bounds, leading to adequate results in terms of improved modal properties. These effects clearly demonstrate that care should be taken in allowing the model updating algorithm to decide upon the final parameter values without any predefined expectation or knowledge of what the final updated parameter values should be. These effects also demonstrate the importance of the sensitivity analysis for improved model updating results.

Many uncertainties are present for bridges that are approaching or have exceeded their initial design life. The numerical model is established using a straightforward modelling procedure with several simplifications included based on engineering judgement. As a result, there is a certain expectation on the outcome of the parameter values from the model updating, which strongly depends on the model parameterization. For the considered case study, the validated model is intended for hybrid SHM using machine learning for detecting relevant damages of existing steel bridges that are approaching or have exceeded their original design life. As such, the reduced complexity of the validated model is beneficial for the large number of numerical simulations to be performed.

In general, the goal is to obtain an updated model with the best possible improvement in the modal properties combined with the most reasonable and realistic parameter values. Improved modal properties and realistic parameter values depend on the overdetermined system ratio and rigidity of the local parameter bounds. From the sensitivity analysis, cases with a high overdetermined system ratio combined with a semi-rigid parameter bounds definition provided the best results. Although a high overdetermined system ratio was found to provide the best results in this case study, it does not necessarily need to be valid for other case studies. The overdetermined system ratio strongly depends on the number of parameters for the model considered and the number of modes that are available from the system identification. As such, a generalization of the overdetermined system ratio to use cannot be made since this is highly system specific. Nevertheless, it is recommended to start with a high overdetermined system ratio in the model updating process, as this can ensure a good improvement in modal properties combined with acceptable parameter values, in addition to obtaining an updated model that is likely to be improved over a wide frequency range. For parameter bounds, a semi-rigid definition is generally preferred over a rigid definition. Establishing parameter bounds definitions depends on the type of parameters and the uncertainty associated with these, the number of parameters and model parameterization. Furthermore, setting parameter bounds requires engineering judgement to a large extent.

As such, for structures with similar applications as presented in this study, where higher modes are relevant and a wide frequency range in the modal properties are of interest for future applications, it is recommended to include a structured approach using a sensitivity analysis by combining the assessment of high overdetermined system ratios with a corresponding general semi-rigid

definition for parameter bounds in model updating. Furthermore, it is advised to include a verification of the final numerical model using other results such as strain, if such data are available, for increased model validation purposes.

3.8 Conclusion

This paper presented a procedure to obtain an optimal solution from sensitivity-based model updating with respect to an improvement in the modal properties, such as the natural frequencies and mode shapes, combined with realistic parameter values. The procedure consists of performing a sensitivity analysis, which considers variations in the overdetermined system ratios combined with local parameter bounds definitions, in a structured approach.

An experimental study and system identification of a full-scale steel bridge identified 21 modes to be used in the model updating process. The numerical model was parameterized in a total of 10 parameters taking into consideration general uncertainties and model simplifications to obtain a model with reduced complexity. Sensitivity-based model updating was performed based on the natural frequencies and MAC numbers, and the effects from the sensitivity analysis were investigated. The effects showed that considering a high overdetermined system ratio with a corresponding general semi-rigid definition for parameter bounds provides an optimal solution for the model updating with respect to the improvement in modal properties based on realistic and acceptable parameters. From the optimal solution, the average absolute frequency error decreased from 5.22 % to 3.84 %, and the MAC numbers improved from 0.72 to 0.75 considering all modes, including the control modes. By considering the uncertainties inherent in the structure and the subsequent establishment of the numerical model with model simplifications, the results obtained are in acceptable agreement with the measurements.

The main limitation of the procedure presented is the need for an adequate number of modes established from the system identification to be included in the model updating. Depending on the case study considered, many analysis cases may be required to find the optimal solution with respect to improved modal properties combined with reasonable parameters. Nevertheless, the procedure presented in this paper demonstrates that an optimal solution can be effectively established. The procedure can be applied to similar case studies, irrespective of the structure under consideration and the corresponding parameterization to be made. Furthermore, the procedure is applicable to case studies for model updating in a wide frequency range where the numerical model is parameterized in a fair number of parameters and an adequate number of modes are available from the system identification. Through the experimental case study, it is demonstrated that for an existing bridge with considerable uncertainties, a numerical model with several simplifications can be established, and a subsequent validated model with acceptable improvement from the model updating can be achieved.

Acknowledgements

The Hell Bridge Test Arena is financially supported by Bane NOR and the Norwegian Railway Directorate.

References

[1] C. R. Farrar and K. Worden, "An introduction to structural health monitoring," *Philos. Trans. R. Soc. A Math. Phys. Eng. Sci.*, vol. 365, no. 1851, pp. 303–315, 2007, doi: 10.1098/rsta.2006.1928.

[2] C. R. Farrar and K. Worden, *Structural Health Monitoring: A Machine Learning Perspective*. Wiley, 2012.

[3] R. J. Barthorpe, "On Model- and Data-Based Approaches to Structural Health Monitoring," The University of Sheffield, 2010.

[4] M. I. Friswell and J. E. Mottershead, *Finite Element Model Updating in Structural Dynamics*, vol. 38. Dordrecht: Springer Netherlands, 1995. doi: 10.1007/978-94-015-8508-8.

[5] J. E. Mottershead, M. Link, and M. I. Friswell, "The sensitivity method in finite element model updating: A tutorial," *Mech. Syst. Signal Process.*, vol. 25, no. 7, pp. 2275–2296, Oct. 2011, doi: 10.1016/j.ymssp.2010.10.012.

[6] A. Teughels and G. De Roeck, "Structural damage identification of the highway bridge Z24 by FE model updating," *J. Sound Vib.*, vol. 278, no. 3, pp. 589–610, 2004, doi: 10.1016/j.jsv.2003.10.041.

[7] A. Teughels and G. De Roeck, "Damage detection and parameter identification by finite element model updating," *Arch. Comput. Methods Eng.*, vol. 12, no. 2, pp. 123–164, 2005, doi: 10.1007/BF03044517.

[8] S. W. Doebling, C. R. Farrar, and M. B. Prime, "A summary review of vibration-based damage identification methods," *Shock Vib. Dig.*, vol. 30, no. 2, pp. 91–105, 1998, doi: 10.1177/058310249803000201.

[9] H. Sohn *et al.*, *A Review of Structural Health Monitoring Literature: 1996-2001*. Los Alamos National Laboratory report, LA-13976-MS, 2004.

[10] N. F. Alkayem, M. Cao, Y. Zhang, M. Bayat, and Z. Su, "Structural damage detection using finite element model updating with evolutionary algorithms: a survey," *Neural Comput. Appl.*, vol. 30, no. 2, pp. 389–411, 2018, doi: 10.1007/s00521-017-3284-1.

[11] P. G. Bakir, E. Reynders, and G. De Roeck, "Sensitivity-based finite element model updating using constrained optimization with a trust region algorithm," *J. Sound Vib.*, vol. 305, no. 1–2, pp. 211–225, 2007, doi: 10.1016/j.jsv.2007.03.044.

[12] E. Reynders, G. De Roeck, P. G. Bakir, and C. Sauvage, "Damage Identification on the Tilff Bridge by Vibration Monitoring Using Optical Fiber Strain Sensors," *J. Eng. Mech.*, vol. 133, no. 2, pp. 185–193, Feb. 2007, doi: 10.1061/(ASCE)0733-9399(2007)133:2(185).

[13] J. E. Mottershead and M. I. Friswell, "Model updating in structural dynamics: A survey," *J. Sound Vib.*, vol. 167, no. 2, pp. 347–375, 1993, doi: 10.1006/jsvi.1993.1340.

[14] E. Simoen, G. De Roeck, and G. Lombaert, "Dealing with uncertainty in model updating for damage assessment: A review," *Mech. Syst. Signal Process.*, vol. 56, pp. 123–149, 2015, doi: 10.1016/j.ymssp.2014.11.001.

[15] S. Sehgal and H. Kumar, "Structural Dynamic Model Updating Techniques: A State of the Art Review," *Arch. Comput. Methods Eng.*, vol. 23, no. 3, pp. 515–533, 2016, doi: 10.1007/s11831-015-9150-3.

[16] M. Link, "Updating of analytical models – review of numerical procedures and application aspects," 1999.

[17] L. Deng and C. S. Cai, "Bridge model updating using response surface method and genetic algorithm," *J. Bridg. Eng.*, vol. 15, no. 5, pp. 553–564, 2010, doi: 10.1061/(ASCE)BE.1943-5592.0000092.

[18] M. Sanayei, J. E. Phelps, J. D. Sipple, E. S. Bell, and B. R. Brenner, "Instrumentation, nondestructive testing, and finite-element model updating for bridge evaluation using strain measurements," *J. Bridg. Eng.*, vol. 17, no. 1, pp. 130–138, 2012, doi: 10.1061/(ASCE)BE.1943-5592.0000228.

[19] H. Schlune, M. Plos, and K. Gylltoft, "Improved bridge evaluation through finite element model updating using static and dynamic measurements," *Eng. Struct.*, vol. 31, no. 7, pp. 1477–1485, 2009, doi: 10.1016/j.engstruct.2009.02.011.

[20] B. Jaishi and W. X. Ren, "Structural Finite Element Model Updating Using Ambient Vibration Test Results," *J. Struct. Eng.*, vol. 131, no. 4, pp. 617–628, Apr. 2005, doi: 10.1061/(ASCE)0733-9445(2005)131:4(617).

[21] T. Zordan, B. Briseghella, and T. Liu, "Finite element model updating of a tied-arch bridge using Douglas-Reid method and Rosenbrock optimization algorithm," *J. Traffic Transp. Eng. (English Ed.*, vol. 1, no. 4, pp. 280–292, 2014, doi: 10.1016/S2095-7564(15)30273-7.

[22] D. Ribeiro, R. Calçada, R. Delgado, M. Brehm, and V. Zabel, "Finite element model updating of a bowstring-arch railway bridge based on experimental modal parameters," *Eng. Struct.*, vol. 40, pp. 413–435, 2012, doi: 10.1016/j.engstruct.2012.03.013.

[23] G. T. Frøseth, A. Rönnquist, and O. Øiseth, “Operational Modal Analysis and Model Updating of Riveted Steel Bridge,” in *Dynamics of Civil Structures, Volume 2*, P. Shamim and J. Caicedo, Eds. Springer International Publishing, 2016, pp. 229–235. doi: 10.1007/978-3-319-29751-4_23.

[24] D. Feng and M. Q. Feng, “Model Updating of Railway Bridge Using in Situ Dynamic Displacement Measurement under Trainloads,” *J. Bridg. Eng.*, vol. 20, no. 12, pp. 1–12, 2015, doi: 10.1061/(ASCE)BE.1943-5592.0000765.

[25] A. Pavic, M. J. Hartley, and P. Waldron, “Updating of the analytical models of two footbridges based on modal testing of full-scale structures,” in *Proceedings of the 23rd International Conference on Noise and Vibration Engineering, ISMA*, 1998, no. May, pp. 401–408.

[26] J. Naranjo-Pérez, J. F. Jiménez-Alonso, A. Pavic, and A. Sáez, “Finite-element-model updating of civil engineering structures using a hybrid UKF-HS algorithm,” *Struct. Infrastruct. Eng.*, vol. 0, no. 0, pp. 1–18, 2020, doi: 10.1080/15732479.2020.1760317.

[27] B. Asgari, S. A. Osman, and A. Adnan, “Sensitivity analysis of the influence of structural parameters on dynamic behaviour of highly redundant cable-stayed bridges,” *Adv. Civ. Eng.*, vol. 2013, 2013, doi: 10.1155/2013/426932.

[28] B. A. Zárate and J. M. Caicedo, “Finite element model updating: Multiple alternatives,” *Eng. Struct.*, vol. 30, no. 12, pp. 3724–3730, 2008, doi: 10.1016/j.engstruct.2008.06.012.

[29] Q. W. Zhang, T. Y. P. Chang, and C. C. Chang, “Finite-Element Model Updating for the Kap Shui Mun Cable-Stayed Bridge,” *J. Bridg. Eng.*, vol. 6, no. 4, pp. 285–293, Aug. 2001, doi: 10.1061/(ASCE)1084-0702(2001)6:4(285).

[30] Y. Ding and A. Li, “Finite element model updating for the Runyang Cable-stayed Bridge tower using ambient vibration test results,” *Adv. Struct. Eng.*, vol. 11, no. 3, pp. 323–335, 2008, doi: 10.1260/136943308785082599.

[31] F. Benedettini and C. Gentile, “Operational modal testing and FE model tuning of a cable-stayed bridge,” *Eng. Struct.*, vol. 33, no. 6, pp. 2063–2073, 2011, doi: 10.1016/j.engstruct.2011.02.046.

[32] R. Zhong, Z. Zong, J. Niu, Q. Liu, and P. Zheng, “A multiscale finite element model validation method of composite cable-stayed bridge based on Probability Box theory,” *J. Sound Vib.*, vol. 370, pp. 111–131, 2016, doi: 10.1016/j.jsv.2016.01.055.

[33] Q. Zhu, Y. L. Xu, and X. Xiao, "Multiscale modeling and model updating of a cable-stayed bridge. I: Modeling and influence line analysis," *J. Bridg. Eng.*, vol. 20, no. 10, pp. 1–10, 2015, doi: 10.1061/(ASCE)BE.1943-5592.0000722.

[34] Ø. W. Petersen and O. Øiseth, "Finite element model updating of a long span suspension bridge," *Geotech. Geol. Earthq. Eng.*, vol. 47, pp. 335–344, 2019, doi: 10.1007/978-3-319-78187-7_25.

[35] R. N. Merce, G. N. Doz, J. L. V. de Brito, J. H. G. Macdonald, and M. I. Friswell, "Finite Element Model Updating of a Suspension Bridge Using ANSYS Software," 2007.

[36] A. L. Hong, F. Ubertini, and R. Betti, "Wind analysis of a suspension bridge: Identification and finite-element model simulation," *J. Struct. Eng.*, vol. 137, no. 1, pp. 133–142, 2011, doi: 10.1061/(ASCE)ST.1943-541X.0000279.

[37] Ø. W. Petersen and O. Øiseth, "Sensitivity-based finite element model updating of a pontoon bridge," *Eng. Struct.*, vol. 150, pp. 573–584, 2017, doi: 10.1016/j.engstruct.2017.07.025.

[38] J. L. Zapico, M. P. González, M. I. Friswell, C. A. Taylor, and A. J. Crewe, "Finite element model updating of a small scale bridge," *J. Sound Vib.*, vol. 268, no. 5, pp. 993–1012, 2003, doi: 10.1016/S0022-460X(03)00409-7.

[39] Q. W. Zhang, C. C. Chang, and T. Y. P. Chang, "Finite element model updating for structures with parametric constraints," *Earthq. Eng. Struct. Dyn.*, vol. 29, no. 7, pp. 927–944, 2000, doi: 10.1002/1096-9845(200007)29:7<927::AID-EQE955>3.0.CO;2-4.

[40] M. Sanayei, A. Khaloo, M. Gul, and F. N. Catbas, "Automated finite element model updating of a scale bridge model using measured static and modal test data," *Eng. Struct.*, vol. 102, pp. 66–79, 2015, doi: 10.1016/j.engstruct.2015.07.029.

[41] J. M. W. Brownjohn and P. Q. Xia, "Dynamic Assessment of Curved Cable-Stayed Bridge by Model Updating," *J. Struct. Eng.*, vol. 126, no. 2, pp. 252–260, Feb. 2000, doi: 10.1061/(ASCE)0733-9445(2000)126:2(252).

[42] J. M. W. Brownjohn, P. Q. Xia, H. Hao, and Y. Xia, "Civil structure condition assessment by FE model updating: Methodology and case studies," *Finite Elem. Anal. Des.*, vol. 37, no. 10, pp. 761–775, 2001, doi: 10.1016/S0168-874X(00)00071-8.

[43] B. T. Svendsen, "FE model updating in Python." 2020. doi: http://doi.org/10.5281/zenodo.4243875.

[44] P. Virtanen *et al.*, “SciPy 1.0: fundamental algorithms for scientific computing in Python,” *Nat. Methods*, vol. 17, no. 3, pp. 261–272, 2020, doi: 10.1038/s41592-019-0686-2.

[45] R. J. Allemang and D. L. Brown, “A correlation coefficient for modal vector analysis,” in *Proceedings of the 1st International Modal Analysis Conference & Exhibit*, 1982, pp. 110–116.

[46] R. J. Allemang, “The modal assurance criterion - Twenty years of use and abuse,” *Sound Vib.*, vol. 37, no. 8, pp. 14–21, 2003.

[47] Dassault Systémes Simulia Corp., “Abaqus/CAE 6.14 - Documentation.” Dassault Systémes Simulia Corp., Providence, RI, USA, 2014. [Online]. Available: https://www.3ds.com/

[48] B. T. Svendsen, G. T. Frøseth, and A. Rönnquist, “Damage Detection Applied to a Full-Scale Steel Bridge Using Temporal Moments,” *Shock Vib.*, vol. 2020, pp. 1–16, Feb. 2020, doi: 10.1155/2020/3083752.

[49] R. Brincker, L. Zhang, and P. Andersen, “Modal identification of output-only systems using frequency domain decomposition,” *Smart Mater. Struct.*, vol. 10, no. 3, pp. 441–445, 2001, doi: 10.1088/0964-1726/10/3/303.

[50] R. Haghani, M. Al-Emrani, and M. Heshmati, “Fatigue-Prone Details in Steel Bridges,” *Buildings*, vol. 2, no. 4, pp. 456–476, 2012, doi: 10.3390/buildings2040456.

Part 3

The content of this part is submitted to an international peer-reviewed journal:

Svendsen, B. T., Øiseth, O., Frøseth, G. T., and Rønnquist, A. (2021). *A hybrid structural health monitoring approach for damage detection in steel bridges under simulated environmental conditions using numerical and experimental data*.

Abstract

This paper presents a novel hybrid structural health monitoring (SHM) framework for damage detection in bridges using numerical and experimental data. The framework is based on the hybrid SHM approach and combines the use of a calibrated numerical finite element (FE) model to generate data from different structural state conditions under varying environmental conditions with a machine learning algorithm in a supervised learning approach. An extensive experimental benchmark study is performed to obtain data from a local and global sensor setup on a real bridge under different structural state conditions, where structural damage is imposed based on a comprehensive investigation of common types of steel bridge damage reported in the literature. The experimental data are subsequently tested on the machine learning model. It is demonstrated that relevant structural damage can be established based on the hybrid SHM framework by separately evaluating different cases considering natural frequencies, mode shapes and mode shape derivatives. Consequently, the work presented in this study represents a significant contribution toward establishing SHM systems that can be applied to existing steel bridges. The proposed framework is applicable to any bridge structure in which relevant structural damage can be simulated and experimental data obtained.

Keywords: Structural health monitoring (SHM), hybrid approach, damage detection, machine learning, support vector machine (SVM), finite element (FE) model, statistical model development, experimental study, bridge, system identification, stochastic subspace identification (SSI), modal parameters, fatigue.

Chapter 4

4 A hybrid structural health monitoring approach for damage detection in steel bridges under simulated environmental conditions using numerical and experimental data

4.1 Introduction

The aim of structural health monitoring (SHM) systems is to identify damage at an early stage to avoid the failure of structural components or systems. For bridges, SHM systems can be used to increase life-safety benefits through continuous monitoring and economic benefits through improved inspection efficiency and minimized unplanned downtime. The many bridges in need of lifetime extension comprise a major concern worldwide, while demands on operational conditions such as traffic loads, speed and intensity are increasing. For steel and composite bridges, the most common damage types are related to fatigue occurring in or below the bridge deck [1]. Furthermore, variability in the operational and environmental conditions affects the structural response and can mask changes caused by damage [2]. With the large number of existing steel and composite bridges in the infrastructure, there is a need for SHM systems that can detect both local and global structural damage while taking the variability in the operational and environmental conditions into consideration. To further develop the possibilities of employing SHM systems for such bridges, research should be focused on tests of real structures in their operating and environmental conditions rather than numerical or laboratory studies of representative structures [2]–[5].

SHM, defined as the process of implementing an automated and online strategy for damage detection in structures [6], has traditionally been performed using two main approaches: model-based and data-based [7], [8]. In the model-based approach, a numerical finite element (FE) model is established, and model updating is performed in two stages. In the first stage, an initial numerical model is updated based on data from the undamaged condition to obtain a validated numerical model or reference model. In the second stage, the reference model is updated based on data from the damaged condition. Damage detection can then be performed based on the change in the updating parameters. Although, according to the hierarchical structure of damage states [9], [10], the model-based approach allows for level I (existence), level II (location) and level IV (extent) damage detection, there are several disadvantages with this approach. First, a numerical model must be developed, parameterized and validated. Parameterizing the numerical model can be challenging, particularly for the selection of the parameters associated with damage. Second, there are inherent uncertainties in the application of numerical models for damage detection due to modeling inaccuracies, including model simplifications and uncertainties in the structural properties. Third,

variability in operational and environmental conditions affecting the structural response may mask the changes caused by damage, inducing uncertainty in the model updating process. Last, the model updating process depends on the measured outputs including, but not limited to, the modal properties. The sensitivities of the damage detection results to the number of measured outputs and the accuracy and weighting of these outputs in the model updating are limitations. Applications of the model-based approach have been reported by considering relevant structural damage in concrete bridges [11]–[15]. Furthermore, Behmanesh and Moaveni successfully applied the model-based approach using simulated damage in a composite steel-concrete footbridge [16]. From these applications, large damage resulting in a significant global effect on the structures has been considered. However, due to the many disadvantages and limited possibilities for detecting local structural damage, the model-based approach is considered impractical in the context of SHM for large and complex structures such as bridges.

In the data-based approach, however, a statistical model based only on experimental data is established using machine learning algorithms. Damage detection can be performed by analyzing the distribution of damage-sensitive features using unsupervised or supervised learning, referred to as statistical model development [17]. In the context of SHM, unsupervised learning refers to the situation where data are available only from the undamaged condition of the structure, while supervised learning refers to the situation where data are available from both undamaged and damaged conditions. Although there are no requirements for developing and validating a numerical model in the data-based approach, there are two main challenges that remain, both of which are related to the lack of data. First, unsupervised learning is often required. This challenge is evidenced by the lack of data from the damaged conditions, which are rarely available for bridges. Second, data normalization, referred to as the process of separating changes caused by operational and environmental conditions from changes caused by structural damage [18], must be considered. This challenge is evidenced either by the lack of baseline data from the undamaged condition, which requires response measurement data where all operational and environmental variations are included, or by the lack of direct measurement data from the parameters related to the operational and environmental conditions. There are several applications of the data-based approach that use numerical models or test structures that are relevant to bridges and where variability in the operational and environmental conditions are considered [19]–[22]. Moreover, applications have been applied to the Z24 prestressed concrete bridge by considering relevant structural damage [23]–[25]; however, these are currently the only examples of applications to real bridges. From the applications of the data-based approach, it is evident that unsupervised learning algorithms are primarily applied, allowing for level I (existence) and, to some extent, level II (location) damage detection. Furthermore, the performance of unsupervised learning algorithms strongly depends on the amount and variability of the data. These observations can be viewed as limitations of the data-based approach. Consequently, to further develop the field of SHM for application to bridges, a framework that can overcome these limitations is needed.

The hybrid SHM approach, which takes principles from the model-based and data-based approaches into consideration, can be used to overcome such limitations. There are different ways to utilize this approach; however, a common understanding is that numerical model(s), experimental data, and machine learning are integrated in some way. There are few studies in the literature that have considered this approach. Malekzadeh et al. [26] proposed a hybrid approach using supervised learning, but the experimental study was carried out using a bridge structure in the laboratory, where variability in the operational and environmental conditions was not included. On the other hand, Figueiredo et al. [27] presented a hybrid approach for damage detection in bridges by considering the variability in the operational and environmental conditions. This approach consisted of using a numerical model to enrich the monitoring data from the undamaged condition to improve damage detection using an unsupervised learning algorithm. This study was based on data from the Z24 bridge. In general, most practical applications of the SHM approaches are based on concrete bridges, particularly on the Z24 benchmark study. Consequently, in the literature, there is a need for studies in which SHM approaches are tested experimentally on steel bridges.

This paper presents a novel hybrid SHM framework for damage detection in bridges. The framework is based on the hybrid SHM approach and combines the use of a numerical model to generate data from different structural state conditions under varying environmental conditions with machine learning algorithms. As such, the numerical model is used as a proxy for the experimental structure to generate training data on which statistical model development can be performed; the test data acquired experimentally can subsequently be used to diagnose the structure. An extensive experimental benchmark study is carried out on a full-scale steel bridge where relevant structural damage is implemented. Supervised learning is performed, allowing for level I (existence), level II (location) and level III (type) damage detection. The feasibility of the framework is discussed with respect to its potential for detecting local and global structural damage and its applicability to similar bridges that are currently in service.

4.2 The hybrid SHM framework

4.2.1 Operational and environmental variability

Variability in the operational and environmental conditions is one of the main challenges in deploying an SHM system for bridges in operation. For bridges, the operational conditions mainly include live loads that are typically caused by traffic, while environmental conditions include wind loading, temperature effects and humidity.

The most influential source of variability in the modal properties is due to temperature effects. Several studies have reported the variation in the modal properties of bridges caused by temperature. In general, variations within 5–10% of the fundamental natural frequencies can be expected on a daily and seasonal basis [5], [28]–[31]. However, several studies in the literature have reported larger variations in the natural frequencies [32]–[36]. The bridges experiencing large

variations in the natural frequencies include certain concrete and composite steel-concrete highway and railway bridges located in cold climates. A step-like variation in the natural frequencies can be obtained for such bridges during a yearly season, particularly around or below the freezing point. Such changes in the natural frequencies are explained by a contribution to the global stiffness of the structure, generally generated by the asphalt layer in highway bridges and the ballast in certain types of railway bridges.

Commonly, changes in the lower modes of the structure are reported, typically the first 2–6 modes, and the general observation is that the natural frequencies decrease with increasing temperatures. With the variability in operational and environmental conditions presenting a challenge for deploying SHM systems for bridges, this effect and the subsequent influence on damage detection must be addressed in the hybrid SHM framework.

4.2.2 The hybrid SHM framework

The proposed hybrid SHM framework consists of several steps that are conducted with the aim of determining whether damage is present in the structure. The framework concept, shown in Figure 4.1 simulates all possible outcomes for the relevant damage states of the structure based on a calibrated numerical FE model, including simulations of the variations in the operational and environmental conditions, and uses the outcome of the simulations as an input to obtain a machine learning model. Experimental data are subsequently tested on the machine learning model to provide decision support or structural diagnosis of the structure, i.e., to determine whether damage is present in the structure. Herein, a damage state includes a relevant damage type at a specific location in the structure.

The hybrid SHM framework assumes the existence of an initial period for structural monitoring. The purpose of the structural monitoring step is twofold. First, structural monitoring provides data as an input for model updating to obtain a calibrated FE model. Such a calibrated FE model that accurately represents the structure is needed to produce meaningful data. Second, structural monitoring provides data to the machine learning model for subsequent structural diagnosis. Such data can be obtained from a global or a local sensor system, or both, on the structure. It is acknowledged that data enrichment, although not considered in this study, can be applied to improve the machine learning model. As such, the presented framework can be used as a dynamic learning process if the machine learning model is updated continuously with undamaged data, i.e., if the structural diagnosis results in true negative (TN) indications of damage. The presented framework is applicable to new and existing bridge structures.

In this study, the hybrid SHM framework is demonstrated through damage detection of a bridge. As such, the remainder of the paper is organized into three parts. In the first part, represented by the left side of the hybrid SHM framework flowchart, an extensive experimental benchmark study performed on a full-scale steel bridge to obtain acceleration time series from a global and local sensor setup is presented. Measurements are obtained before and after relevant structural damage is imposed on the bridge. Operational modal analysis (OMA) is performed

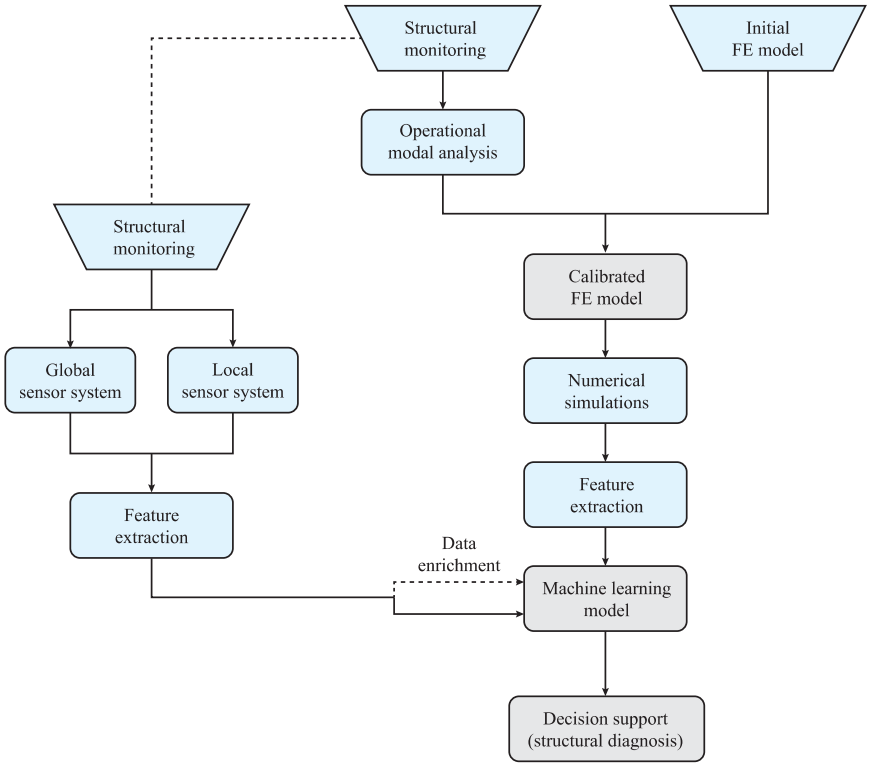

Figure 4.1: Flowchart of the hybrid SHM framework. The dashed lines indicate a possible connection.

as a part of the feature extraction process to obtain the modal parameters of the bridge. The data obtained from the experimental study provide samples for the test set in the machine learning model. The second part, represented by the right side of the hybrid SHM framework flowchart, describes the process for generating training data and obtaining the machine learning model. A numerical FE model is first established, and model updating is performed to obtain a calibrated FE model. Different damage types are imposed on all the relevant locations in the FE model, and numerical simulations that take variations in the environmental conditions into consideration are carried out to obtain data from the damage states. Importantly, numerical simulations of the baseline, or undamaged condition, are performed. Furthermore, the feature extraction process and the machine learning algorithm applied are described. In the final part, the results from the structural diagnosis are presented, and an evaluation of the hybrid SHM framework is provided.

Figure 4.2: The Hell Bridge Test Arena.

4.3 Experimental study

4.3.1 The Hell Bridge Test Arena benchmark study

The Hell Bridge Test Arena, shown in Figure 4.2, is a steel riveted truss bridge formerly in operation as a train bridge. The bridge is used as a full-scale damage detection test structure [37]. Figure 4.3 shows an overview of the bridge structural system, which is composed of the two bridge walls, bridge deck and lateral bracing. The bridge was used for an extensive experimental benchmark study carried out in 2020, where it was damaged in a number of damage scenarios while structural monitoring was performed. Table 4.1 summarizes the different structural state conditions, including the environmental conditions experienced during the benchmark study period.

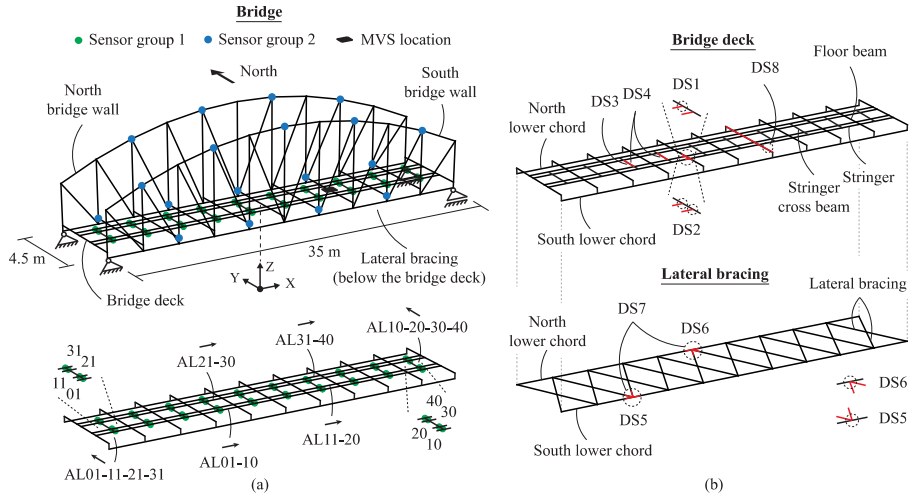

Figure 4.3: Overview of the Hell Bridge Test Arena. (a) Bridge structural system, sensor layout and location of the modal vibration shaker (MVS). (b) Damage states introduced to the bridge deck and lateral bracing.

Table 4.1: Overview and descriptions of the structural state conditions, including the environmental conditions, during the experimental benchmark study period.

Label	State condition	Category[1]	Type	Description	Weather	Temp. (°C)	Wind speed (m/s)
UDS	Un damaged	-	Baseline condition	-	Cloudy and rainy	10–11	1–2
DS1	Damaged	Local	Stringer-to-floor-beam connection	Single connection damaged	Cloudy	12	4–8
DS2	Damaged	Local	Stringer-to-floor-beam connection	Multiple connections damaged	Cloudy	10	4–8
DS3	Damaged	Local	Stringer cross beam	Main part of the single cross beam removed	Cloudy and rainy	10	1–4
DS4	Damaged	Local	Stringer cross beam	Main parts of multiple cross beams removed	Rainy	10	1–4
DS5	Damaged	Global	Lateral bracing connection	Single connection damaged	Cloudy	9	1–4
DS6	Damaged	Global	Lateral bracing connection	Single connection damaged	Cloudy	11	2–6
DS7	Damaged	Global	Lateral bracing connection	Multiple connections damaged	Cloudy	12	1–6
DS8	Damaged	Global	Connection between the floor beam and main load-carrying member	Single connection damaged	Sunny	15	2–6

[1] Local: damage to the secondary steel structure. Global: damage to the primary steel structure.

4.3.2 Experimental setup

Figure 4.3a shows an overview of the sensor setup used in the experimental benchmark study. An instrumentation system from National Instruments consisting of multiple cRIO-9036 controllers was used to acquire data from accelerometers in a local and global sensor setup involving sensor groups 1 and 2, respectively. Synchronous sampling was ensured by global positioning system (GPS) timing of

the individual controllers. Sensor group 1 (SG1) consisted of 40 single-axis accelerometers (Dytran 3055D3) for measuring the local response of the bridge deck in the vertical direction (global z-direction), whereas sensor group 2 (SG2) consisted of 18 triaxial accelerometers (Dytran 3583BT and 3233A) for measuring the global response of the bridge in both the lateral and vertical directions (global y and z-directions). Data were sampled at 400 Hz. The data were detrended, low-pass filtered and resampled to 100 Hz prior to analysis. The bridge was excited in the vertical direction using a modal vibration shaker (APS 420) located at approximately one-third of the bridge span to excite as many structural vibration modes as possible. The modal vibration shaker was operated in the sine sweep mode by applying a band-limited sinusoidal load in the range of 2–55 Hz with a logarithmic sweep speed of 1 Oct/min.

Figure 4.3b shows an overview of the type and location of the damage introduced in the bridge. Four different damage types were considered: stringer-to-floor-beam connections; stringer cross beams; lateral bracing connections; and connections between the floor beams and main load-carrying members. These are the most common and frequently reported damage types in the literature [1]: fatigue damage occurring in and below the bridge deck. Furthermore, these are the most severe but relevant damage types for the type of bridge considered in this study. The damage types are evaluated with respect to the likelihood of occurrence and summarized in Table 4.2. The undamaged state of the bridge was represented by the baseline condition, whereas the damaged states were represented by the different damage types with varying degrees of severity. To represent different degrees of severity, each damage type was introduced at one or more locations in the bridge. For each damage state, damage was introduced, measurements were performed, and the damage was then repaired. In this way, measurements were obtained both before and after introducing damage to the bridge.

Table 4.2: Evaluation of damage states based on [1].

Damage type	Abbreviation	Damage state(s)	Likelihood of occurrence
Stringer-to-floor-beam connection	DT1	DS1, DS2	Moderate
Stringer cross beam	DT2	DS3, DS4	Moderate
Lateral bracing connection	DT3	DS5, DS6, DS7	Low
Connection between the floor beam and main load-carrying member	DT4	DS8	High

Damage was introduced by replacing existing rivets with bolts. Moreover, the damage types were imposed by temporarily removing the bolts. Each damage state comprised highly progressed damage, representing large cracks or loose connections that open and close under dynamic loading, typically caused by traffic or large environmental loads. Consequently, the damage was considered by removing all bolts in each state condition. This damage progression leads to a redistribution of forces that would be demanding on the structure over time; however, it is not considered critical to the instant structural integrity due to the structural redundancy of the bridge. One test was performed for each state condition. For each test, time series data were generated from 75 sensor channels, i.e., 40 channels from sensor group 1 and 35 channels from sensor group 2. Note that one channel in the lateral direction was excluded from sensor group 2.

Of the four damage types considered in the experimental study, damage types 1 and 4, i.e., the stringer-to-floor-beam connections and the connections between the floor beams and main load-carrying members, are of major importance with respect to traffic loading and structural integrity. Furthermore, damage types 2 and 3, i.e., the stringer cross beams and lateral bracing connections, ensure the stability of the bridge against lateral and torsional loads, mainly during environmental loading, and are of minor importance with respect to traffic loading and immediate structural integrity. Therefore, damage types 1 and 4, shown in Figure 4.4, are considered in this study. Details of the damage types, including the underlying mechanisms, can be found in [1].

Operational and environmental variabilities impose difficulties on the damage detection process. The environmental conditions for the different structural state conditions are summarized in Table 4.1. Considerable variability in the weather occurred during the experimental study, with moderate variabilities in the temperature and wind speed range. These variabilities, which are highly representative of the climate where the bridge is located, can affect the structural response and mask changes caused by damage. Furthermore, such variabilities complicate the damage detection process and challenge the machine learning model, which is established based on numerical simulations only. No sources of variability were considered for the operational condition, which was limited to the operation of the modal vibration shaker.

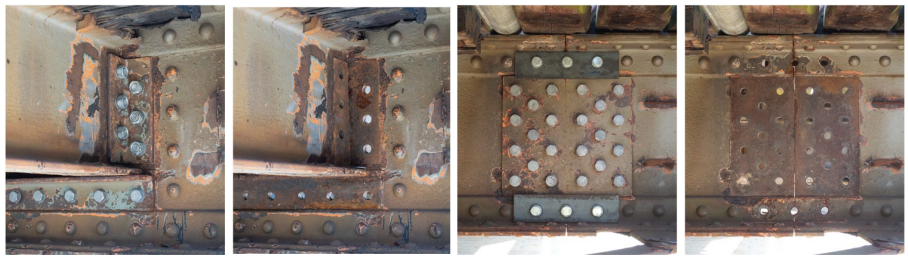

(a) (b)

Figure 4.4: The damage types imposed on the bridge before and after damage. (a) Damage type 1. (b) Damage type 4.

4.3.3 Operational modal analysis

OMA was performed to obtain the modal properties, such as the natural frequencies and mode shapes, of the bridge in the different damage states. Apart from the general aim of establishing as many modes as possible, there were two main challenges in modal identification: first, distinguishing all relevant modes between the different damage states; and second, correctly identifying closely spaced modes in frequency. To solve these challenges, three methods for output-only system identification were considered: frequency domain decomposition (FDD) [38], [39], data-driven stochastic subspace identification (data-SSI) [40], and covariance-driven stochastic subspace identification (cov-SSI) [41]. The cov-SSI was found to be the most appropriate method, particularly for distinguishing the relevant modes between the different damage states.

Data from SG1 and SG2 (75 channels) were used in the analyses. The results from the cov-SSI analyses are highly dependent on the input parameters and the selection of such parameters, including the number of blockrows, order and stabilization criteria. Satisfactory results were obtained by setting the number of blockrows equal to 200 and defining the range of order between 0–200 with 100 evenly spaced values and a maximum order of 200. Furthermore, for the selection of stable poles to include in the stabilization diagram, a frequency deviance of 1%, a damping deviance of 5% and a modal assurance criterion (MAC) threshold of 95% were used. Additionally, a stability level of 4 was used. For further details of the stabilization criteria, refer to Kvåle et al. [42], [43]. The cov-SSI parameters were set to be equal for all damage states.

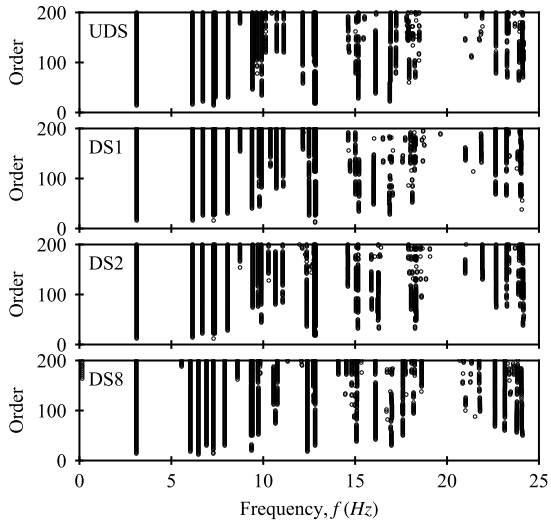

Figure 4.5: Stabilization plots for the cov-SSI analysis of the different damage states.

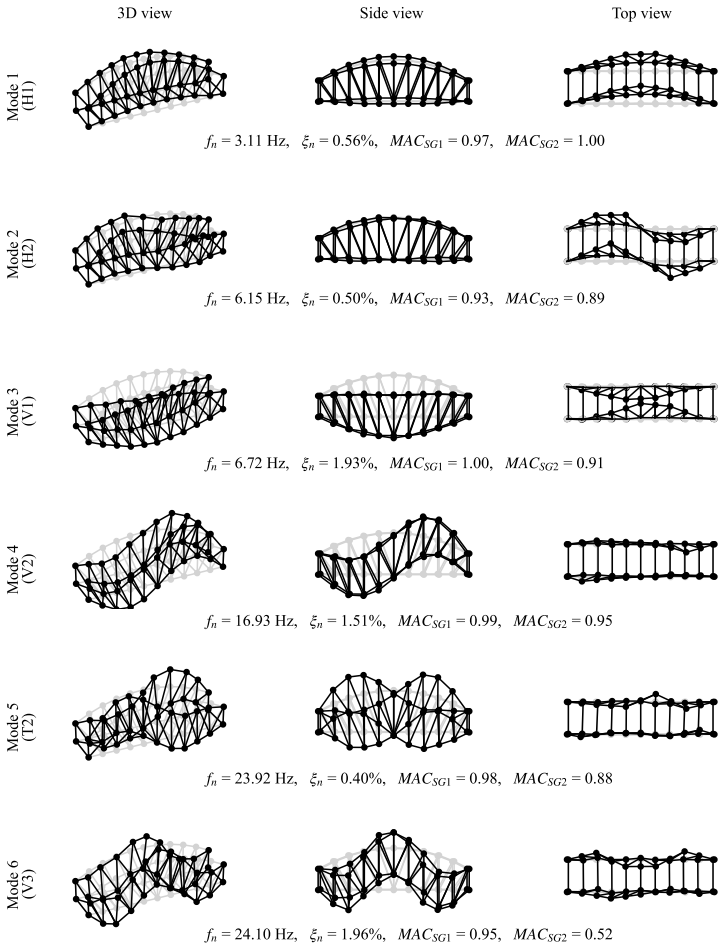

Figure 4.6: Mode shapes used in the hybrid SHM framework obtained from the cov-SSI analysis in the undamaged state. The following abbreviations are used: H (horizontal), V (vertical) and T (torsional). Linear interpolation of the mode shapes is performed for illustration purposes.

Damage categorized as global is expected to have a larger influence on the structural response than damage categorized as local. The stabilization plots from the different damage states in the 0–25 Hz frequency range are presented in Figure 4.5. The stabilization plot changes with different damage states, which is a challenge in the system identification process. This is observed particularly for DS8, where new modes appear due to the global damage imposed on the structural system. Hence, a manual evaluation was performed to ensure that the correct modes were established. With reference to the undamaged state, more than 40 physical modes up to a frequency of approximately 40 Hz were identified from the cov-SSI analysis. From these modes, the six most relevant modes within the 0–25

Hz frequency range were chosen to be used in the hybrid SHM framework. Figure 4.6 shows the mode shapes along with the natural frequencies, damping ratios and MAC values between the experimental and numerical mode shape vectors from the calibrated FE model for SG1 and SG2. The reasoning behind the choice of these modes is included in Section 4.4.1. The OMA can be considered as feature extraction to obtain the experimental test set, which is then input to the machine learning model.

4.4 Numerical model and simulations

4.4.1 Calibrated FE model

The purpose of model updating is to obtain a validated numerical FE model that is in good agreement with the measurements and a validated FE model being computationally efficient for numerical simulations. The initial FE model and the calibration of the FE model using an improved sensitivity-based finite element model updating procedure are described in a separate study by Svendsen et al. [44], [45]. A description of the FE model is included below for convenience.

The FE model is established using the FE software ABAQUS with site inspections and specifications from technical drawings as the basis. The primary structure of the bridge is included in the model, i.e., the vertical walls, the bridge deck, and the lateral bracing. The secondary structure is included in the modeling of the bridge deck to obtain an accurate structural representation for damage detection purposes. Other secondary structure and nonstructural items are represented by lumped point masses on the bridge deck to obtain a proper mass distribution. A beam element model representation is used, and the bridge is modeled as simply supported on one end (global translational x, y and z-direction constrained) and rolled boundary conditions on the opposite end (global translational x-direction partly constrained by spring elements and y and z-direction constrained). As such, the FE model is obtained with reduced complexity. Figure 4.7 shows the FE model of the bridge. The calibrated FE model is referred to as the reference model.

Three criteria are applied to select the modes for the hybrid SHM framework. First, the modes should represent global modes in both the horizontal and vertical directions. Second, the modes should represent a wide frequency range, be well identifiable from the output-only system identification (stable poles in the cov-SSI)

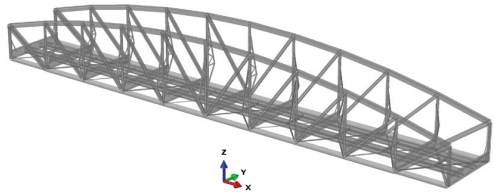

Figure 4.7: FE model.

Table 4.3: Comparison of the modal properties between the experimental results and the calibrated FE model.

Mode	Description	Frequency, f_n (Hz)		Abs. diff (%)	MAC	
		Experimental	Numerical		SG1	SG2
1	H1	3.11	3.25	4.37 %	0.97	1.00
2	H2	6.15	6.22	1.17 %	0.93	0.89
3	V1	6.72	6.62	1.47 %	1.00	0.91
4	V2	16.93	15.98	5.64 %	0.99	0.95
5	T2	23.92	24.64	3.01 %	0.98	0.88
6	V3	24.10	24.39	1.23 %	0.95	0.52

and be identifiable by considering ambient vibrations from wind. Third, the modes should be identifiable in the calibrated FE model based on changes made during all relevant numerical simulations. Based on this, six modes are chosen. The detailed results for the natural frequencies and MAC values from the experimental study and the calibrated FE model are summarized in Table 4.3. The average absolute frequency error is 2.81%, and the average MAC values of the local and global sensor setups are 0.97 and 0.86 for the considered modes, respectively.

4.4.2 Modeling of damage

The damage types are each represented using no connectivity between the elements in the numerical model at the specific damage locations. There are two main advantages of this damage representation: first, the complexity of the numerical model is minimized by avoiding spring elements or similar complex linear or nonlinear damage modeling; and second, this is an accurate and realistic representation of loose structural connections. A comparison of the results obtained from the numerical and experimental analyses of the damage states is performed to visualize the effect of introducing damage in the structure and verify the introduction of damage in the numerical model. Figure 4.8 shows the percentage change in the natural frequencies for all damage states from the undamaged state, as evaluated for all modes. Furthermore, Figure 4.9 and Figure 4.10 show the MAC values between the mode shape vectors of the undamaged state and the damage states for the local and global sensor setups.

Figure 4.8, Figure 4.9 and Figure 4.10 provide information on how the imposed damage changes the natural frequencies and mode shapes of the bridge compared to the baseline condition (undamaged state). It is observed that increasing the damage severity of DT1 (DS1 and DS2) induces increasing changes in both the natural frequencies and MAC values for the experimental and numerical analyses. Furthermore, the local damage, represented by DT1, generally influences the changes in the natural frequencies and MAC values less than the global damage, represented by DT4 (DS8). Consequently, it is concluded that (1) there is consistency in the results for the different damage states upon considering the experimental and numerical analyses separately, and (2) there is adequate

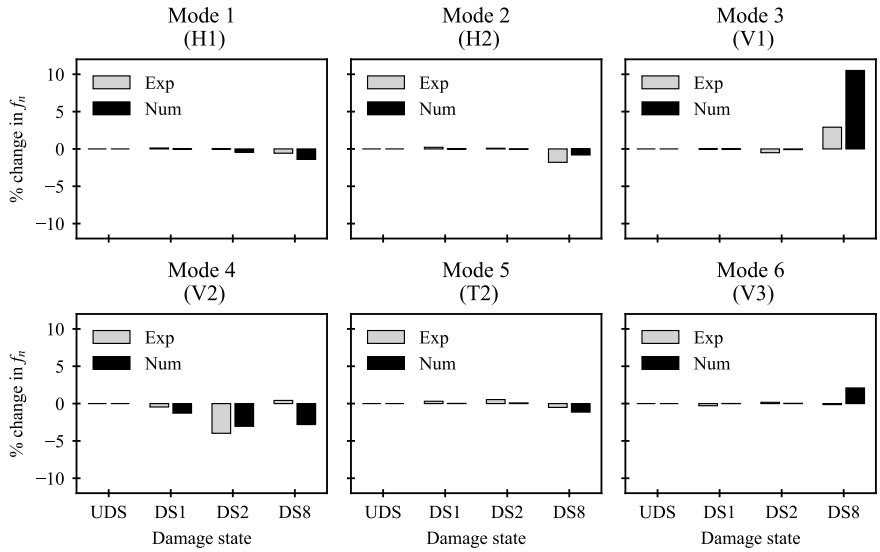

Figure 4.8: The percentage change of the natural frequencies for all damage states based on the undamaged state (UDS) for all modes, considering the experimental and numerical analyses.

correspondence in the change of the natural frequencies and MAC values between the experimental and numerical analyses. Furthermore, an important observation is that the most significant changes in the natural frequencies are generally within a range that can be expected due to variations in operational and environmental conditions.

4.4.3 Numerical simulations

Numerical simulations are performed that represent all relevant damage states of the structure based on the calibrated FE model, which includes likely variations in the environmental conditions. The purpose of the numerical simulations is to generate training data for the machine learning model. Consequently, the modal properties obtained from the numerical simulations are used as damage-sensitive features in the machine learning model. Two datasets are generated through numerical simulations using the calibrated FE model. The basic information in the datasets is summarized in Table 4.4. Each dataset contains the same total number of simulations; however, different assumptions regarding the variation in the environmental conditions for the damage types are introduced. As such, the datasets represent how long the damage is assumed in the structural system; dataset 1 assumes a shorter presence of damage in the structural system than dataset 2. The variation is targeted based on the natural frequencies of the bridge and is further described in Section 4.4.4 below.

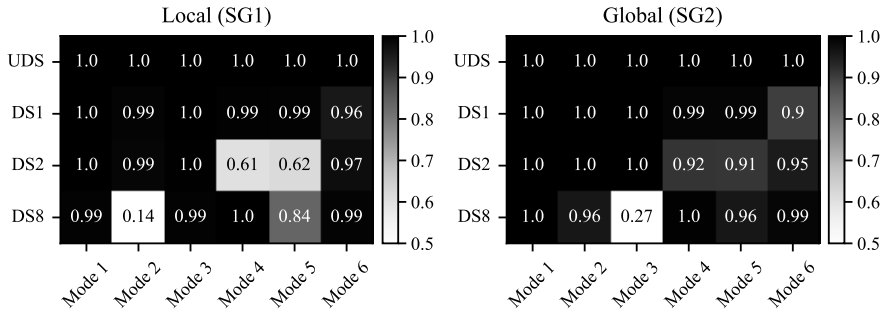

Figure 4.9: MAC values between the mode shape vectors of the undamaged state (UDS) and the damage states in the experimental study.

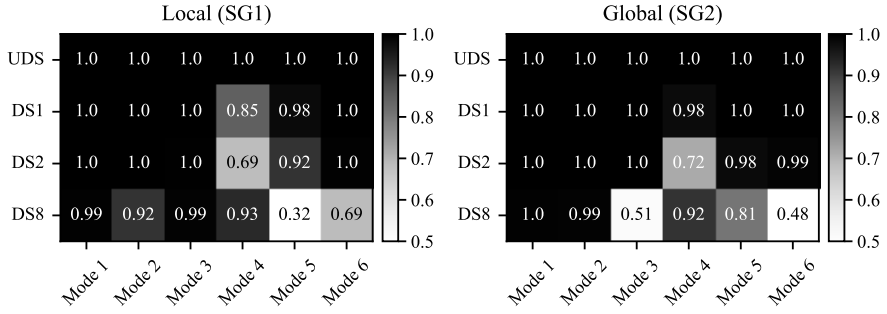

Figure 4.10: MAC values between the mode shape vectors of the undamaged state (UDS) and the damage states in the numerical study.

Table 4.4: Simulation information.

Damage type	Possible damage locations	Total no. of simulations	Simulation variation[1]	
			Dataset 1	Dataset 2
UDS	-	1000	±5%	±5%
DT1(1)	80	240	±0.5%	±2%
DT1(2)	40	240	±0.5%	±2%
DT4	22	264	±0.5%	±2%

[1] Simulated variation in the environmental conditions.

In the datasets, the variation in each damage type (class label) is based on (1) the number of simulated damage locations and (2) the simulated change in the environmental conditions. For each damage type, damage is successively introduced in all possible locations in the bridge. The stringer-to-floor-beam connections (DT1), which are introduced with damage in both single and multiple connections to represent increasing severity, are denoted as DT1(1) and DT1(2), respectively. Altogether, 1744 simulations are performed for each dataset. For each simulation, an eigenvalue analysis is performed, and the natural frequencies along

with the normalized mode shape values for each mode from the local (SG1) and global (SG2) sensor setups are extracted. A total of 250 modes are extracted for each simulation. To ensure the correct identification of modes for each simulation, a mode match index (MMI) is used

$$MMI = (1-\gamma)MAC_{r,s} - \gamma\frac{|f_r - f_s|}{f_r} \tag{4.1}$$

where γ is a value between 0 and 1 that provides the weighting for consideration between the MAC values and the natural frequencies, f. The subscripts r and s denote the modes obtained from the numerical reference model and the numerical model under consideration in the simulation run, respectively. The reliable identification of modes is obtained by setting $\gamma = 0.5$.

4.4.4 Environmental variation in the numerical simulations

Variability in the environmental conditions must be included to obtain realistic training data as an input to the machine learning model. Considering environmental conditions is particularly important for the baseline condition. The most influential source of variability in the modal properties is due to temperature effects. In general, changes in temperature affect the global material properties and system characteristics and have a considerable influence on the natural frequencies of a bridge structure.

Variation in the environmental conditions is simulated by varying the steel density parameter ρ of the numerical model because it has the most significant influence on the modal parameters. The parameter is changed within a specific range from the reference model to obtain the desired variation in natural frequencies for the undamaged and damaged states. A variation up to approximately 10% (±5%) targeted based on the natural frequencies is assumed in the baseline condition. Furthermore, variations of approximately 1% (±0.5%) and 4% (±2.0%) targeted based on the natural frequencies are assumed for datasets 1 and 2, respectively, for the different damage types. To obtain the total number of simulations for each damage type, evenly distributed parameter values within the specific ranges are generated and used as input for the numerical simulations.

Table 4.5 presents the maximum and minimum changes obtained in the natural frequencies for the relevant modes in the baseline condition, which is obtained by changing the ratio of the steel density parameter by ±10% of the reference value. The table shows that varying this parameter provides an almost uniform change in the natural frequencies for the relevant modes considered. As such, the simulations performed mainly represent the environmental change because no other variations in the operational and environmental conditions are included. Note that it is assumed that a step-like variation in natural frequencies, which is typically obtained around or below the freezing point, can be disregarded in the representation of environmental change. This assumption is considered valid because the structural and nonstructural components are not expected to significantly affect the stiffness of the bridge around or below the freezing point, particularly considering that the bridge has timber sleepers and hence no ballast.

Table 4.5: Minimum and maximum changes in natural frequencies from variation from the environmental conditions in the baseline condition.

Mode	Natural frequency (Hz)			Change in frequency from the reference model (%)	
	Ref. model (1.0ρ)	Lower (0.9ρ)	Upper (1.1ρ)	Lower (0.9ρ)	Upper (1.1ρ)
1	3.248	3.396	3.118	4.55 %	-4.01 %
2	6.217	6.534	5.942	5.09 %	-4.43 %
3	6.619	6.946	6.328	4.94 %	-4.38 %
4	15.976	16.569	15.442	3.71 %	-3.34 %
5	24.644	25.812	23.661	4.74 %	-3.99 %
6	24.394	25.279	23.546	3.63 %	-3.47 %

4.5 Feature extraction and machine learning

4.5.1 Feature extraction

In the context of SHM, machine learning is applied to associate the damage-sensitive features with the state of the structure to distinguish between the undamaged and damaged states. In this study, modal properties such as the natural frequencies and mode shapes, including mode shape derivatives, are used as damage-sensitive features in the machine learning model. The underlying assumption associated with the use of modal properties as damage-sensitive features is that the imposed damage will somehow change the stiffness, mass or energy dissipation characteristics of the structure.

Natural frequencies provide a high-level assessment of the structural dynamic characteristics, mainly allowing for level I (existence) damage detection. Mode shapes, including the mode shape derivatives, provide spatial information about the structural dynamic characteristics and allow for level I (existence) and level II (location) damage detection. Mode shape information is particularly useful for structures with regular geometry, such as bridges, that are equipped with an appropriate number of sensors.

The natural frequencies and mode shapes, including mode shape derivatives, are considered useful as damage-sensitive features in the hybrid SHM framework for three main reasons: first, the natural frequencies and mode shapes are straightforward to establish both experimentally and numerically; second, for a numerical model, the natural frequencies and mode shapes are obtained by solving the eigenvalue problem, which is computationally efficient and consequently suitable for a large number of simulations; and third, the possibility of level I (existence), level II (location) and level III (type) damage detection is enabled when combined with supervised learning.

4.5.2 Mode shape derivatives

The mode shape derivatives can be used to enable a high sensitivity to localized damage. The mode shape curvature κ is established using the central difference approximation to the second derivative of the mode shape vector $\boldsymbol{\varphi}$ as [46]

$$\kappa_i = \frac{\varphi_{i-1} - 2\varphi_i + \varphi_{i+1}}{h^2} \tag{4.2}$$

where h is the length between the equally spaced sensor locations i. The curvature at the ends is approximated using backward and forward difference approximations. The summed absolute mode shape curvature difference makes it possible to consider multiple modes and is defined as

$$\Delta\boldsymbol{\kappa} = \sum_{j=1}^{R} \left| \boldsymbol{\kappa}_{j_u} - \boldsymbol{\kappa}_{j_d} \right| \tag{4.3}$$

where R is the total number of considered modes. Furthermore, the subscripts u and d refer to the undamaged and damaged structures, respectively. The summed absolute mode shape curvature difference is normalized between 0 and 1 before being used as an input for the machine learning model to make the experimental and numerical results conform. The derivative process related to the mode shape curvature amplifies any discontinuities in the mode shapes caused by damage.

The following clarifications should be noted. First, the mode shape curvature, which is based on a beam formulation, is applied to the local sensor setup (SG1). The setup is divided into four parts in the longitudinal direction of the bridge to establish the full formulations for all sensors. The formulation for each part is applied separately and subsequently concatenated. Second, the FE model is used to represent the undamaged state of the bridge for the experimental (test) and numerical (training) data. This representation is equivalent to assuming that the SHM system can be installed at any time during the bridge lifetime. This approach is beneficial for existing bridges; however, it requires a precise FE model. Furthermore, since the undamaged state is represented in the calculations of the mode shape curvature, this method is used here only for predicting the damage states in the structural diagnosis of the structure. Consequently, in the structural diagnosis of the structure, the prediction of the undamaged state is excluded.

4.5.3 Machine learning

In supervised training, labeled data are available. Supervised learning is made possible through the numerical generation of training data with the relevant damage types included. Supervised learning allows for level I, II and III damage detection and is considered for group classification only. A training matrix $\mathbf{X} \in \mathbb{R}^{n \times p}$ with n samples and p features and a test matrix $\mathbf{Z} \in \mathbb{R}^{m \times p}$ with m samples are composed of data from both the undamaged and damaged conditions. The target variable $\mathbf{y} \in \mathbb{N}^{n \times 1}$ is a vector containing the class labels y. $\mathbf{x}_i \in \mathbb{R}^{1 \times p}$ and $\mathbf{z}_i \in \mathbb{R}^{1 \times p}$ refer to arbitrary samples with an index i from the training and test matrices, respectively, and have a corresponding class label y_i. The data obtained from the numerical simulations provide samples for the training set in the machine

learning model, whereas the data obtained from the experimental study provide samples for the test set.

In this study, the support vector machine (SVM) algorithm is applied [47]. The SVM algorithm is computationally efficient and capable of performing linear and nonlinear classification, making it highly suitable for SHM applications. The training data are divided into 80% for training and 20% for testing. A grid search with 5-fold cross-validation is performed on the training data to find the optimal hyperparameters and increase the ability of the SVM algorithm to generalize to unseen data. The regularization parameter C, the kernel functions, and the corresponding kernel coefficients γ are considered the most important hyperparameters of the SVM algorithm and are consequently used as input in the grid search. The grid search conducts an extensive search over the specified hyperparameters to obtain the best cross-validation score. Furthermore, the combination of hyperparameters that provides the best cross-validation score is chosen accordingly.

4.6 Results

4.6.1 General

The hybrid SHM framework for damage detection is evaluated using three different cases. The cases are used to consider natural frequencies, mode shapes and mode shape derivatives separately as damage-sensitive features. All sensor channels from each sensor group are taken into consideration. Furthermore, a total of 1744 numerical and 4 experimental observations are included. Hence, the training matrix $\mathbf{X}^{1744\times6}$ and test matrix $\mathbf{Z}^{4\times6}$ are used for the natural frequencies. For the mode shapes and mode shape derivatives, the training matrices $\mathbf{X}^{1744\times40}$ and $\mathbf{X}^{1744\times35}$ are used for the local (SG1) and global (SG2) sensor setups, respectively, with corresponding test matrices $\mathbf{Z}^{4\times40}$ and $\mathbf{Z}^{4\times35}$. The features are scaled to zero mean and unit variance to improve the performance of the SVM algorithm.

In the cases considering natural frequencies and mode shapes, the damage detection performances are evaluated in terms of level I and III damage detection. For the level I damage detection performance, the evaluation is performed in terms of Type I and Type II errors, which are referred to as false positive (FP) and false negative (FN) indications of damage, respectively. For the level III damage detection performance, the evaluation is performed in terms of the correct damage predictions for the different damage types. The damage detection performances are also evaluated in terms of level II damage detection in the case considering mode shape derivatives.

Additionally, the machine learning performances are included in the evaluation of the results. Machine learning performance can be a possible source of uncertainty in the results and is evaluated by means of the cross-validation score (CV score), the area under the curve (AUC) and the fraction of correct predictions (score). The AUC value refers to the area under the receiver operating characteristics (ROC) curve, which represents the relative trade-offs between true

positives (TPs), or the probability of detection, and FPs, or the probability of false alarms [48].

4.6.2 Case 1 – Natural frequencies

In the case considering natural frequencies, damage detection is investigated by considering datasets 1 and 2 with different ranges of environmental variability in the undamaged state (baseline). Figure 4.11 and Figure 4.12 show the results from the prediction of the experimental test set and the corresponding performances of the machine learning algorithm for datasets 1 and 2, respectively. The true label is denoted on the x-axis of the result matrices. The correct predictions are highlighted in the figures, whereas the Type I and Type II errors, including the total number of errors, are summarized in Table 4.6.

Three general observations are made from the results presented in Figure 4.11, Figure 4.12 and Table 4.6. First, the total number of Type I and Type II errors decreases with decreasing variability in the environmental conditions. Hence, it becomes more difficult to perform level I and level III damage detection with increasing variability in the environmental conditions. Second, it is observed from the results of dataset 1 that all the damage types are established. DT1 was detected with the lowest variability in the environmental conditions (±1%), DT4 was detected with a slightly higher variability (±2%), and UDS was detected for the remaining variability in the environmental conditions. Third, the machine learning performances are generally considered acceptable. However, the performances are lower for dataset 2 than dataset 1. As such, it becomes more difficult for the machine learning algorithm to make correct predictions when large changes in environmental conditions affect the damage states. However, the generally high machine learning performances indicate that the different damage states can be separated under variability in the environmental conditions. Overall, the results clearly show that changes in the environmental conditions mask damage, resulting in Type II errors. Consequently, using natural frequencies as damage-sensitive features in this study results in low damage detection capabilities for high variability in the environmental conditions.

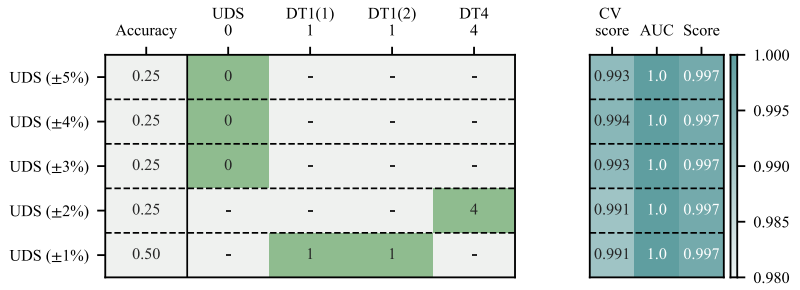

Figure 4.11: Prediction results including the performances of the machine learning algorithm for dataset 1 in the case considering natural frequencies.

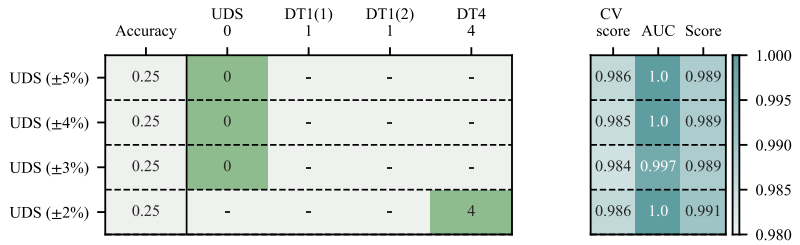

Figure 4.12: Prediction results including the performances of the machine learning algorithm for dataset 2 in the case considering natural frequencies. The UDS (±1%) is excluded due to the variation of ±2% for the different damage types in dataset 2.

Table 4.6: Damage detection results obtained by considering Type I and Type II errors for different ranges of environmental variability in the undamaged state (baseline) of datasets 1 and 2.

	Dataset 1			Dataset 2		
UDS simulation	Type I (FP)	Type II (FN)	Total	Type I (FP)	Type II (FN)	Total
UDS (±5%)	0	3	3	0	3	3
UDS (±4%)	0	3	3	0	3	3
UDS (±3%)	0	2	2	0	3	3
UDS (±2%)	1	0	1	1	0	1
UDS (±1%)	1	0	1	-	-	-

4.6.3 Case 2 – Mode shapes

To investigate the damage detection capabilities in the case considering mode shapes, analyses are performed separately for each mode. Figure 4.13 and Figure 4.14 show the results from the prediction of the experimental test set and the corresponding performances of the machine learning algorithm for the local (SG1) and global (SG2) sensor setups of datasets 1 and 2, respectively. Here, the damage prediction results obtained per mode are arranged horizontally, whereas those obtained per sample in the test set are arranged vertically. The Type I and Type II errors are summarized in Table 4.7, and the damage predictions for the different damage types are summarized in Table 4.8.

From the results obtained for Case 2, two important observations are made. First, all the damage types can be predicted. In general, although Type I errors are reported, there are few Type II errors that indicate strong level I damage detection capabilities. Furthermore, local damage represented by DT1 is best identified by the higher modes, whereas global damage represented by DT4 is best identified by the lower modes. Second, the local sensor setup (SG1) performs better than the global sensor setup (SG2). SG1 obtains better prediction results than SG2 in terms of the total number of correct damage type predictions and the ability to detect different damage types (including the undamaged state).

Table 4.7: Damage detection results obtained by considering Type I and Type II errors for datasets 1 and 2.

Mode	Dataset 1				Dataset 2			
	Local		Global		Local		Global	
	Type I (FP)	Type II (FN)	Type I (FP)	Type II (FN)	Type I (FP)	Type II (FN)	Type I (FP)	Type II (FN)
Mode 1	1	0	1	0	1	0	1	0
Mode 2	1	0	1	0	1	0	1	0
Mode 3	1	0	1	0	1	0	1	0
Mode 4	0	1	1	0	0	1	1	0
Mode 5	1	1	1	0	0	1	1	0
Mode 6	1	0	1	0	1	0	1	0

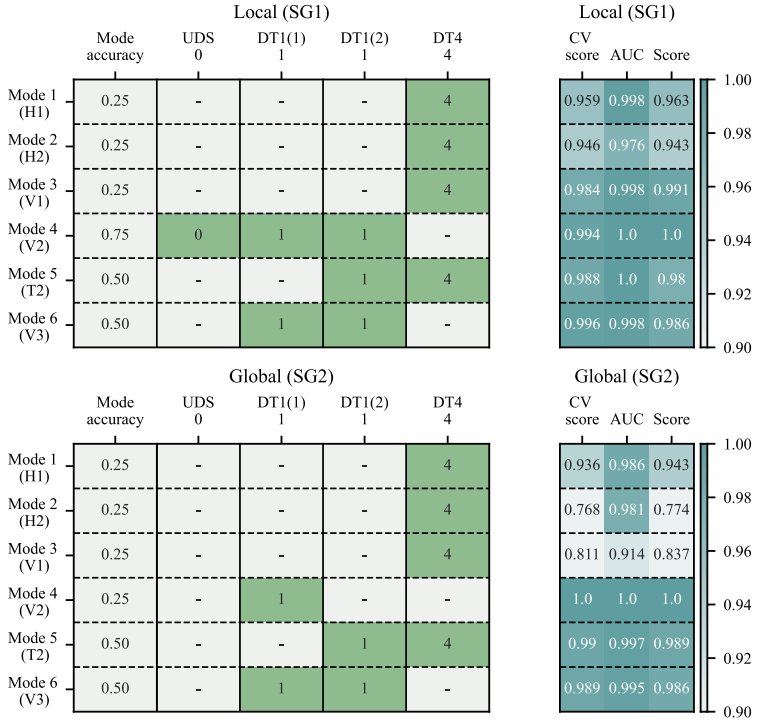

Figure 4.13: Prediction results including the performances of the machine learning algorithm for the local (SG1) and global (SG2) sensor setups with dataset 1 in the case considering mode shapes.

Furthermore, by comparing the results obtained for the different datasets, it is observed that SG1 is not affected by a change in the environmental conditions of the damage types. Conversely, SG2 obtains lower damage prediction results with increasing variability in the environmental conditions of the damage types.

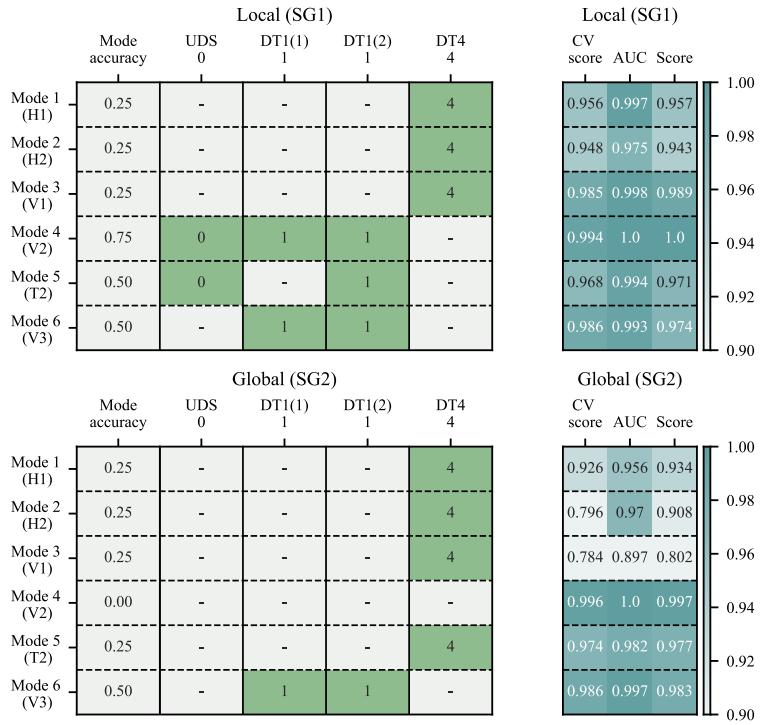

Figure 4.14: Prediction results including the performances of the machine learning algorithm for the local (SG1) and global (SG2) sensor setups with dataset 2 in the case considering mode shapes.

Table 4.8: Correct damage prediction results for the different damage types in datasets 1 and 2.

Dataset	Sensor group	UDS	DT1	DT4	Total
Dataset 1	Local (SG1)	1	5	4	10
	Global (SG2)	0	4	4	8
Dataset 2	Local (SG1)	2	5	3	10
	Global (SG2)	0	4	2	6

It should also be noted that the machine learning performances are generally better for the higher modes (modes 4–6) than the lower modes (modes 1–3), which might be a possible explanation for the generally low damage detection capability of the lower modes. Overall, from the results obtained, using mode shapes as damage-sensitive features provides strong damage detection capabilities, with the best performance obtained using the local sensor setup (SG1).

4.6.4 Case 3 – Mode shape derivatives

Based on the results obtained for Case 2, the damage detection capabilities are investigated by considering only the local sensor setup (SG1) in the case considering mode shape curvatures. Therefore, level I damage detection is assumed. Figure 4.15 and Figure 4.16 show the prediction of the experimental test set and the corresponding performances of the machine learning algorithm with datasets 1 and 2, respectively. Similar results are presented in Figure 4.17 and Figure 4.18 for three different configurations of summed absolute mode shape curvature difference. Since the undamaged state is represented in the mode shape curvature calculations, the prediction of the undamaged state is excluded. Consequently, the results presented consider only the damage types with imposed damage on the structure.

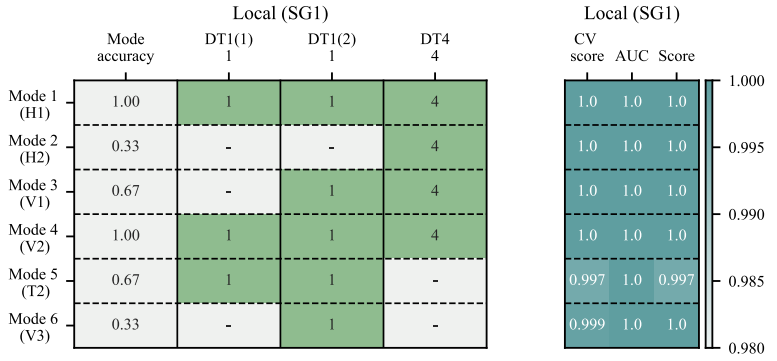

Figure 4.15: Prediction results including the performances of the machine learning algorithm for each mode in dataset 1 in the case considering mode shape curvatures.

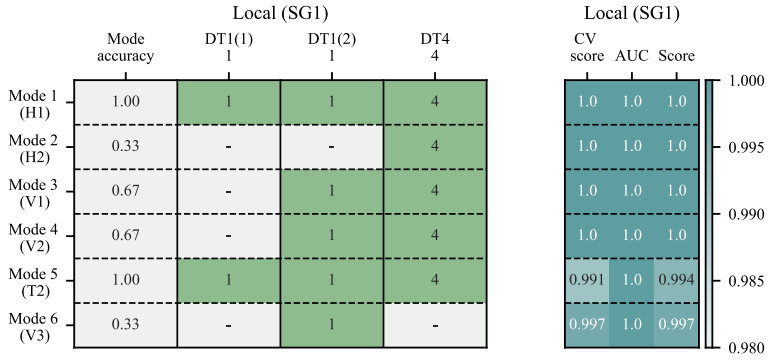

Figure 4.16: Prediction results including the performances of the machine learning algorithm for each mode in dataset 2 in the case considering mode shape curvatures.

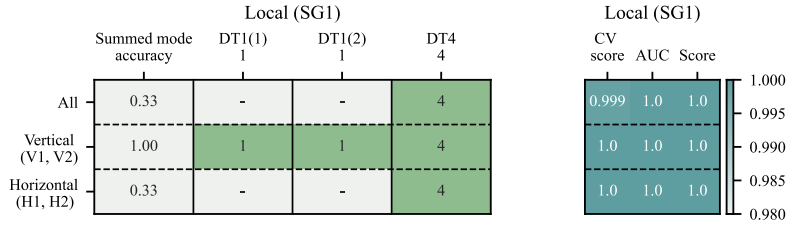

Figure 4.17: Prediction results including the performances of the machine learning algorithm for the configurations of summed modes in dataset 1 in the case considering mode shape curvatures.

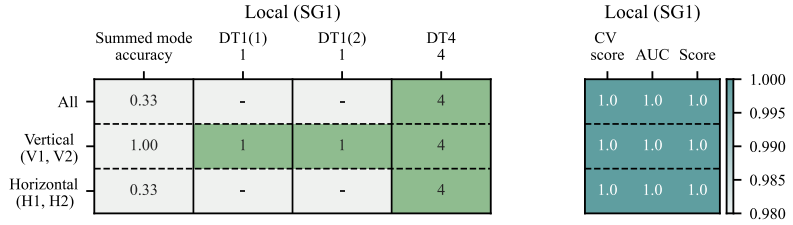

Figure 4.18: Prediction results including the performances of the machine learning algorithm for the configurations of summed modes in dataset 2 in the case considering mode shape curvatures.

From the results obtained in Figure 4.15 and Figure 4.16, it is observed that the damage prediction is strong. DT1 and DT4 are predicted well, with particular prediction improvements for the lower modes. Furthermore, modes 1 (H1), 4 (V2) and 5 (T2) predict all damage types correctly when considering both datasets. It is also observed that the mode shape curvatures are little affected by the difference in the datasets, and the machine learning performances are nearly optimal for all modes. The configurations of the summed absolute mode shape curvature difference provide an effective means of evaluating several modes together. From the results obtained in Figure 4.17 and Figure 4.18, it is clear that all damage types are correctly predicted in the vertical configuration when considering both datasets, whereas only DT4 is correctly predicted in the other configurations. Consequently, when the damage is not severe, as with DT1, inaccurate predictions are made if modes that are not significantly affected by damage are included in the calculations of the mode shape curvatures. It should also be noted that the machine learning performances are optimal.

To evaluate the performance in terms of level II damage detection, the experimental and numerical inputs to the machine learning model for the summed absolute mode shape curvature difference are compared in Figure 4.19 considering the vertical and horizontal configurations. The inputs are normalized between 0 and 1. The relevant peaks of the curvature related to the damage types are labeled with the corresponding sensor names. The experimental and numerical input conform for DT1 and DT4 in the vertical configuration and for DT4 in the horizontal configuration. These results correspond well with the results presented in Figure 4.17 and Figure 4.18.

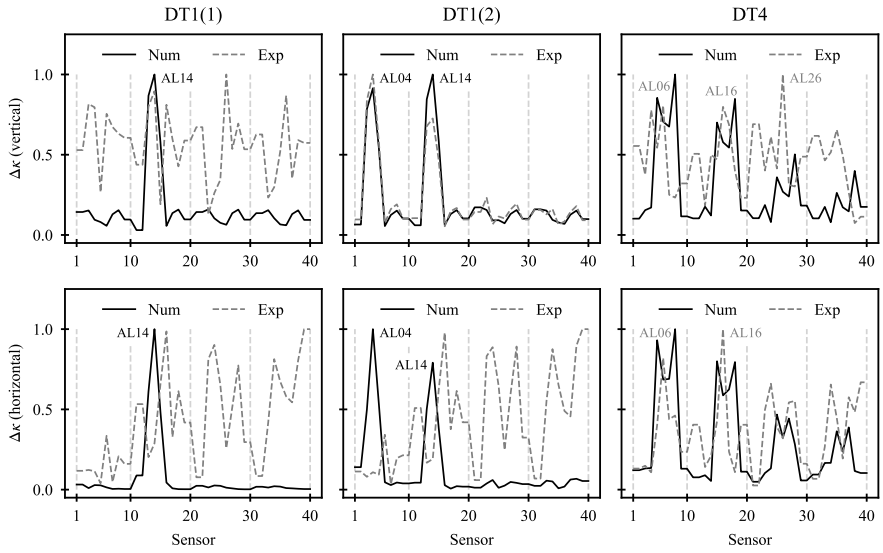

Figure 4.19: Comparison of the numerical and experimental input to the machine learning model considering the summed absolute mode shape curvature difference for the vertical and horizontal configurations.

Furthermore, and most importantly, the sensors representing the peaks are located nearest to the damaged areas of the bridge deck. Consequently, the damage types are successfully localized.

Two additional important observations are made. First, the experimental results are jagged and unclear compared to the numerical results. This observation is explained by the differentiation process, which amplifies high-frequency noise. Normalization is performed after the differentiation process, resulting in higher mean values of the experimental curvature than the numerical curvature. The experimental results are noisy, and the damage is less distinct from these results. On the other hand, the numerical results are less noisy and more distinct where the damage is represented for both configurations, clearly illustrating the difficulties in working with experimental data. Second, the machine learning model is able to recognize DT1(1) in the vertical configuration despite the noise in the data from the experimental study. This observation clearly demonstrates the superior abilities of the machine learning model in distinguishing damage.

4.7 Discussion

From the results obtained for the different cases investigated in the hybrid SHM framework, the following general observations are made:

- Relevant structural damage in steel bridges can be found under a simulated variation in the environmental conditions. All the damage types considered, including the undamaged state (baseline), can be established in this way. Moreover, level I (existence), level II (location) and level III (type) damage detection can be performed by separately evaluating

different cases of natural frequencies, mode shapes and mode shape derivatives.

- The case considering natural frequencies generally provides Type II errors or false negative indications of damage, whereas the case considering mode shapes generally provides Type I errors or false positive indications of damage. Furthermore, using natural frequencies provides low damage detection capabilities for high variability in environmental conditions. Consequently, using mode shapes is more reliable for detecting damage. Moreover, the cases considering mode shapes and mode shape derivatives increase the damage detection capabilities.
- The local sensor setup (SG1) performed better than the global setup (SG2) with respect to the damage detection of both local and global damage types. Using a local sensor setup that consists of a grid of sensors covering the part of the bridge where damage is most commonly experienced, i.e., the bridge deck, allows for increased damage detection capabilities. As such, the local sensor setup should be used for damage detection purposes, whereas the global sensor setup should be used for system identification and model updating purposes. The results clearly demonstrate the effect that a dense sensor setup has on the increased damage detection capabilities, particularly for performing level II damage detection. Consistent level II damage detection covering all possible damage locations of the imposed damage types cannot be performed without a systematic, and preferably dense, sensor network. A sparse sensor network, however, is not considered a limitation for applying the hybrid SHM framework.
- Datasets 1 and 2 consider low and high variations in the environmental conditions of the damage types compared to the baseline, respectively. The datasets thus represent how long damage is assumed to persist in the system: dataset 1 assumes that damage has been present for a short time period, while dataset 2 assumes that damage has been present for a long time period. From the cases considering mode shapes and mode shape derivatives, the local sensor setup (SG1) was not affected by the difference in the datasets. However, from the case of mode shapes, the global sensor setup (SG2) obtained lower damage detection capabilities with dataset 2.

The deviations between the numerical and experimental results, resulting in reduced classification results, are caused by uncertainties. There are several uncertainties related to the different parts of the hybrid SHM process. In particular, such uncertainties are related to (1) the representation of the FE model and numerical simulations, (2) the estimation of modal parameters using OMA and the corresponding system identification method(s), (3) the performance of the machine learning algorithm and (4) the statistical representation of the experimental data. Furthermore, for the representation of the FE model and numerical simulations, the uncertainties are related to simplifications in the numerical modeling, the model updating procedure, the modeling of damage and the representation of environmental variability in the numerical simulations. As such, this part of the hybrid SHM process is essential. Reducing the identified uncertainties in the

different parts of the hybrid SHM process can further enhance the damage detection process and enable improved classification results.

The advantage of using natural frequencies as damage-sensitive features is that they are straightforward to establish both numerically and experimentally. Furthermore, few sensors are required. However, natural frequencies are sensitive to changes in the operational and environmental conditions and insensitive to local structural damage (particularly associated with the global modes of the structure). Consequently, the low sensitivity of the frequency shifts to damage requires either a very precise numerical model, precise measurements, or significant levels of damage for them to be an effective damage indicator. These requirements were not fulfilled in this study. However, there are several advantages of using mode shapes and mode shape derivatives as damage-sensitive features. Mode shapes and mode shape derivatives are less affected by variation in the environmental conditions than natural frequencies, and they can perform level I, II and III damage detection. Although more effort and more sensors are needed to establish mode shapes and mode shape derivatives than natural frequencies, they provide increased damage detection capabilities, which is also demonstrated in this study.

From the hybrid SHM framework presented, experimental data can be applied by considering the OMA from ambient vibration or vibration from regular loading conditions. Traffic-induced vibration is not necessary but can be beneficial with respect to operational variability. Using OMA, or output-only system identification, requires only response measurements; this is clearly beneficial for large structures such as bridges, structures in service and structures with an SHM system that typically provide data based on undamaged conditions.

4.8 Conclusion

This paper presented a novel hybrid SHM framework for damage detection in bridges. The framework is based on the hybrid SHM approach and combines the use of a numerical model to generate data from different structural state conditions under varying environmental conditions with machine learning algorithms to obtain a machine learning model. Based on the machine learning model, experimental test data can be applied to provide decision support or diagnose the structure in a supervised learning approach. The supervised learning approach allows for level I, II and III damage detection.

The hybrid SHM framework was demonstrated through damage detection of a full-scale steel bridge. A machine learning model was established by simulating all possible outcomes of the relevant damage states for the structure using a calibrated FE model, including simulations of environmental conditions. An extensive experimental benchmark study of the bridge was performed to obtain data from a local and global sensor setup under different structural state conditions. The data obtained from the experimental study provided samples to the test set in the machine learning model. Three different cases of damage-sensitive features were evaluated. Based on the evaluation of the different cases, different levels of damage detection were performed. All the damage types considered were established. As such, by considering the uncertainties related to the hybrid SHM framework,

damage detection and structural diagnosis were successfully performed. In conclusion, the hybrid SHM framework is demonstrated to work.

The main limitation of the hybrid SHM framework is the need for a precise numerical model for successful classification. There is a trade-off between a calibrated numerical model in good agreement with measurements and a calibrated numerical model being computationally efficient for numerical simulations. Nevertheless, the hybrid SHM framework presented in this paper demonstrates that damage detection can be successfully performed using a numerical model with reduced complexity. Relevant structural damage can be found in steel bridges. Moreover, the framework is applicable to any bridge structure in which relevant structural damage can be simulated and experimental data obtained. Further investigation should be conducted to (1) reduce the identified uncertainties in the hybrid SHM framework for sharper classification, (2) incorporate data enrichment into machine learning and (3) implement more damage types and increase the statistical representation of the experimental data.

Acknowledgements

The Hell Bridge Test Arena is financially supported by Bane NOR and the Norwegian Railway Directorate.

References

[1] R. Haghani, M. Al-Emrani, and M. Heshmati, “Fatigue-Prone Details in Steel Bridges,” *Buildings*, vol. 2, no. 4, pp. 456–476, 2012, doi: 10.3390/buildings2040456.

[2] H. Sohn, “Effects of environmental and operational variability on structural health monitoring,” *Philos. Trans. R. Soc. A Math. Phys. Eng. Sci.*, vol. 365, no. 1851, pp. 539–560, 2007, doi: 10.1098/rsta.2006.1935.

[3] L. Sun, Z. Shang, Y. Xia, S. Bhowmick, and S. Nagarajaiah, “Review of Bridge Structural Health Monitoring Aided by Big Data and Artificial Intelligence: From Condition Assessment to Damage Detection,” *J. Struct. Eng.*, vol. 146, no. 5, p. 04020073, 2020, doi: 10.1061/(asce)st.1943-541x.0002535.

[4] M. Vagnoli, R. Remenyte-Prescott, and J. Andrews, “Railway bridge structural health monitoring and fault detection: State-of-the-art methods and future challenges,” *Struct. Heal. Monit.*, vol. 17, no. 4, pp. 971–1007, 2018, doi: 10.1177/1475921717721137.

[5] J. J. Moughty and J. R. Casas, “A state of the art review of modal-based damage detection in bridges: Development, challenges, and solutions,” *Appl. Sci.*, vol. 7, no. 5, 2017, doi: 10.3390/app7050510.

[6] C. R. Farrar and K. Worden, “An introduction to structural health monitoring,” *Philos. Trans. R. Soc. A Math. Phys. Eng. Sci.*, vol. 365, no. 1851, pp. 303–315, 2007, doi: 10.1098/rsta.2006.1928.

[7] C. R. Farrar and K. Worden, *Structural Health Monitoring: A Machine Learning Perspective*. Wiley, 2012.

[8] R. J. Barthorpe, “On Model- and Data-Based Approaches to Structural Health Monitoring,” The University of Sheffield, 2010.

[9] K. Worden and J. M. Dulieu-Barton, “An Overview of Intelligent Fault Detection in Systems and Structures,” *Struct. Heal. Monit.*, vol. 3, no. 1, pp. 85–98, Mar. 2004, doi: 10.1177/1475921704041866.

[10] A. Rytter, “Vibrational Based Inspection of Civil Engineering Structures,” University of Aalborg, Denmark, 1993.

[11] E. Reynders, A. Teughels, and G. De Roeck, “Finite element model updating and structural damage identification using OMAX data,” *Mech. Syst. Signal Process.*, vol. 24, no. 5, pp. 1306–1323, 2010, doi: 10.1016/j.ymssp.2010.03.014.

[12] E. Reynders, G. De Roeck, P. G. Bakir, and C. Sauvage, “Damage Identification on the Tilff Bridge by Vibration Monitoring Using Optical Fiber Strain Sensors,” *J. Eng. Mech.*, vol. 133, no. 2, pp. 185–193, Feb. 2007, doi: 10.1061/(ASCE)0733-9399(2007)133:2(185).

[13] A. Teughels and G. De Roeck, “Structural damage identification of the highway bridge Z24 by FE model updating,” *J. Sound Vib.*, vol. 278, no. 3, pp. 589–610, 2004, doi: 10.1016/j.jsv.2003.10.041.

[14] J. Maeck, B. Peeters, and G. De Roeck, “Damage identification on the Z24 bridge using vibration monitoring,” *Smart Mater. Struct.*, vol. 10, no. 3, pp. 512–517, 2001, doi: 10.1088/0964-1726/10/3/313.

[15] O. Huth, G. Feltrin, J. Maeck, N. Kilic, and M. Motavalli, “Damage Identification Using Modal Data: Experiences on a Prestressed Concrete Bridge,” *J. Struct. Eng.*, vol. 131, no. 12, pp. 1898–1910, 2005, doi: 10.1061/(asce)0733-9445(2005)131:12(1898).

[16] I. Behmanesh and B. Moaveni, “Probabilistic identification of simulated damage on the Dowling Hall footbridge through Bayesian finite element model updating,” *Struct. Control Heal. Monit.*, vol. 22, no. 3, pp. 463–483, Mar. 2015, doi: 10.1002/stc.1684.

[17] C. R. Farrar, S. W. Doebling, and D. A. Nix, “Vibration-based structural damage identification,” *Philos. Trans. R. Soc. A Math. Phys. Eng. Sci.*, vol. 359, no. 1778, pp. 131–149, Jan. 2001, doi: 10.1098/rsta.2000.0717.

[18] H. Sohn, K. Worden, and C. R. Farrar, “Statistical damage classification under changing environmental and operational conditions,” *J. Intell. Mater. Syst. Struct.*, vol. 13, no. 9, pp. 561–574, 2002, doi: 10.1106/104538902030904.

[19] H. Pan, M. Azimi, F. Yan, and Z. Lin, “Time-Frequency-Based Data-Driven Structural Diagnosis and Damage Detection for Cable-Stayed Bridges,” *J. Bridg. Eng.*, vol. 23, no. 6, p. 04018033, Jun. 2018, doi: 10.1061/(ASCE)BE.1943-5592.0001199.

[20] A. Santos, E. Figueiredo, M. F. M. Silva, C. S. Sales, and J. C. W. A. Costa, “Machine learning algorithms for damage detection: Kernel-based approaches,” *J. Sound Vib.*, vol. 363, pp. 584–599, 2016, doi: 10.1016/j.jsv.2015.11.008.

[21] E. Figueiredo, G. Park, C. R. Farrar, K. Worden, and J. Figueiras, “Machine learning algorithms for damage detection under operational and environmental variability,” *Struct. Heal. Monit.*, vol. 10, no. 6, pp. 559–572, 2011, doi: 10.1177/1475921710388971.

[22] F. Magalhães, A. Cunha, and E. Caetano, “Vibration based structural health monitoring of an arch bridge: From automated OMA to damage detection,” *Mech. Syst. Signal Process.*, vol. 28, pp. 212–228, Apr. 2012, doi: 10.1016/j.ymssp.2011.06.011.

[23] A. Santos, E. Figueiredo, M. Silva, R. Santos, C. Sales, and J. C. W. A. Costa, “Genetic-based EM algorithm to improve the robustness of Gaussian mixture models for damage detection in bridges,” *Struct. Control Heal. Monit.*, vol. 24, no. 3, pp. 1–9, 2017, doi: 10.1002/stc.1886.

[24] E. Reynders, G. Wursten, and G. De Roeck, “Output-only structural health monitoring in changing environmental conditions by means of nonlinear system identification,” *Struct. Heal. Monit.*, vol. 13, no. 1, pp. 82–93, 2014, doi: 10.1177/1475921713502836.

[25] E. Figueiredo and E. Cross, “Linear approaches to modeling nonlinearities in long-term monitoring of bridges,” *J. Civ. Struct. Heal. Monit.*, vol. 3, no. 3, pp. 187–194, 2013, doi: 10.1007/s13349-013-0038-3.

[26] M. Malekzadeh, G. Atia, and F. N. Catbas, “Performance-based structural health monitoring through an innovative hybrid data interpretation framework,” *J. Civ. Struct. Heal. Monit.*, vol. 5, no. 3, pp. 287–305, 2015, doi: 10.1007/s13349-015-0118-7.

[27] E. Figueiredo, I. Moldovan, A. Santos, P. Campos, and J. C. W. A. Costa, “Finite Element–Based Machine-Learning Approach to Detect Damage in Bridges under Operational and Environmental Variations,” *J. Bridg. Eng.*, vol. 24, no. 7, p. 04019061, Jul. 2019, doi: 10.1061/(ASCE)BE.1943-5592.0001432.

[28] E. J. Cross, K. Y. Koo, J. M. W. Brownjohn, and K. Worden, "Long-term monitoring and data analysis of the Tamar Bridge," *Mech. Syst. Signal Process.*, vol. 35, no. 1–2, pp. 16–34, 2013, doi: 10.1016/j.ymssp.2012.08.026.

[29] S. Soyoz and M. Q. Feng, "Long-Term Monitoring and Identification of Bridge Structural Parameters," *Comput. Civ. Infrastruct. Eng.*, vol. 24, no. 2, pp. 82–92, Feb. 2009, doi: 10.1111/j.1467-8667.2008.00572.x.

[30] J. M. Ko and Y. Q. Ni, "Technology developments in structural health monitoring of large-scale bridges," *Eng. Struct.*, vol. 27, no. 12, pp. 1715–1725, Oct. 2005, doi: 10.1016/j.engstruct.2005.02.021.

[31] C. R. Farrar, P. J. Cornwell, S. W. Doebling, and M. B. Prime, "Structural Health Monitoring Studies of the Alamosa Canyon and I-40 Bridges," 2000.

[32] I. Gonzales, M. Ülker-Kaustell, and R. Karoumi, "Seasonal effects on the stiffness properties of a ballasted railway bridge," *Eng. Struct.*, vol. 57, pp. 63–72, 2013, doi: 10.1016/j.engstruct.2013.09.010.

[33] V. Zabel, M. Brehm, and S. Nikulla, "The influence of temperature varying material parameters on the dynamic behavior of short span railway bridges," in *Proceedings of ISMA 2010 - International Conference on Noise and Vibration Engineering, including USD 2010*, 2010, pp. 1519–1529.

[34] J. T. Kim, J. H. Park, and B. J. Lee, "Vibration-based damage monitoring in model plate-girder bridges under uncertain temperature conditions," *Eng. Struct.*, vol. 29, no. 7, pp. 1354–1365, 2007, doi: 10.1016/j.engstruct.2006.07.024.

[35] B. Peeters, J. Maeck, and G. De Roeck, "Vibration-based damage detection in civil engineering: excitation sources and temperature effects," *Smart Mater. Struct.*, vol. 10, no. 3, pp. 518–527, Jun. 2001, doi: 10.1088/0964-1726/10/3/314.

[36] B. Peeters and G. De Roeck, "One-year monitoring of the Z24-Bridge: environmental effects versus damage events," *Earthq. Eng. Struct. Dyn.*, vol. 30, no. 2, pp. 149–171, Feb. 2001, doi: 10.1002/1096-9845(200102)30:2<149::AID-EQE1>3.0.CO;2-Z.

[37] B. T. Svendsen, G. T. Frøseth, and A. Rönnquist, "Damage Detection Applied to a Full-Scale Steel Bridge Using Temporal Moments," *Shock Vib.*, vol. 2020, pp. 1–16, Feb. 2020, doi: 10.1155/2020/3083752.

[38] R. Brincker, L. Zhang, and P. Andersen, "Modal Identification from Ambient Responses using Frequency Domain Decomposition," in *IMAC 18: Proceedings of the International Modal Analysis Conference (IMAC)*, 2000, pp. 625–630.

[39] R. Brincker, L. Zhang, and P. Andersen, “Modal identification of output-only systems using frequency domain decomposition,” *Smart Mater. Struct.*, vol. 10, no. 3, pp. 441–445, 2001, doi: 10.1088/0964-1726/10/3/303.

[40] P. Van Overschee and B. De Moor, *Subspace Identification for Linear Systems*. Boston, MA: Springer US, 1996. doi: 10.1007/978-1-4613-0465-4.

[41] L. Hermans and H. van der Auweraer, “Modal testing and analysis of structures under operational conditions: industrial applications,” *Mech. Syst. Signal Process.*, vol. 13, no. 2, pp. 193–216, 1999.

[42] K. A. Kvåle, O. Øiseth, and A. Rønnquist, “Operational modal analysis of an end-supported pontoon bridge,” *Eng. Struct.*, vol. 148, pp. 410–423, 2017, doi: 10.1016/j.engstruct.2017.06.069.

[43] K. A. Kvåle, “KOMA toolbox.” 2021. doi: 10.5281/zenodo.4727880.

[44] B. T. Svendsen, Ø. W. Petersen, G. T. Frøseth, and A. Rønnquist, “Improved finite element model updating of a full-scale steel bridge using sensitivity analysis,” *Struct. Infrastruct. Eng.*, pp. 1–17, Jul. 2021, doi: 10.1080/15732479.2021.1944227.

[45] B. T. Svendsen, “FE model updating in Python.” 2020. doi: http://doi.org/10.5281/zenodo.4243875.

[46] A. K. Pandey, M. Biswas, and M. M. Samman, “Damage detection from changes in curvature mode shapes,” *J. Sound Vib.*, vol. 145, no. 2, pp. 321–332, Mar. 1991, doi: 10.1016/0022-460X(91)90595-B.

[47] F. Pedregosa *et al.*, “Scikit-learn: Machine Learning in Python,” *J. Mach. Learn. Res.*, vol. 12, pp. 2825–2830, 2011.

[48] T. Fawcett, “ROC graphs: Notes and practical considerations for researchers,” Palo Alto, CA, 2004.

Part 4

The content of this part is submitted to an international peer-reviewed journal:

Svendsen, B. T., Frøseth, G. T., Øiseth, O., and Rønnquist, A. (2021). *A data-based structural health monitoring approach for damage detection in steel bridges using experimental data*. Journal of Civil Structural Health Monitoring, 1-15. https://doi.org/10.1007/s13349-021-00530-8.

Abstract

There is a need for reliable structural health monitoring (SHM) systems that can detect local and global structural damage in existing steel bridges. In this paper, a data-based SHM approach for damage detection in steel bridges is presented. An extensive experimental study is performed to obtain data from a real bridge under different structural state conditions, where damage is introduced based on a comprehensive investigation of common types of steel bridge damage reported in the literature. An analysis approach that includes a setup with two sensor groups for capturing both the local and global responses of the bridge is considered. From this, an unsupervised machine learning algorithm is applied and compared with four supervised machine learning algorithms. An evaluation of the damage types that can best be detected is performed by utilizing the supervised machine learning algorithms. It is demonstrated that relevant structural damage in steel bridges can be found and that unsupervised machine learning can perform almost as well as supervised machine learning. As such, the results obtained from this study provide a major contribution towards establishing a methodology for damage detection that can be employed in SHM systems on existing steel bridges.

Keywords: Structural health monitoring (SHM), damage detection, machine learning, statistical model development, receiver operating characteristics (ROC) curves, experimental study, bridge, fatigue.

Chapter 5

5 A data-based structural health monitoring approach for damage detection in steel bridges using experimental data

5.1 Introduction

For bridges, structural health monitoring (SHM) systems provide information regarding the state of the bridge condition, with the aim of increasing the economic and life-safety benefits through damage identification. Many highway and railway bridges in Europe and the US, which experience increasing demands with respect to traffic loads and intensity, are approaching or have exceeded their original design lives. A large part of these bridges are steel and composite steel-concrete bridges. Based on an overview and comprehensive investigation of the common damage types experienced by such bridges that are reported in the literature [1], it is found that most damages are caused by fatigue and most frequently occur in or below the bridge deck. With the large number of existing bridges in infrastructure, lifetime extension is the preferred option for ensuring continuous operation. Consequently, there is a need for reliable SHM systems that can detect both local and global structural damage in such bridges.

SHM is referred to as the process of implementing an automated and online strategy for damage detection in a structure [2], [3]. There are two main approaches in SHM: model-based and data-based [4], [5]. In the model-based approach, a numerical finite element model is continuously updated based on new measurement data to identify damage. The data-based approach, however, builds a statistical model based on experimental data only and generally relies on, but are not limited to, machine learning algorithms for damage identification. Additionally, a hybrid approach to SHM can be made that takes principles from both the model-based and data-based approaches into consideration. The analysis of the distributions of damage-sensitive features by machine learning algorithms, either supervised or unsupervised learning algorithms, is referred to as statistical model development [6]. Here, and in the context of SHM, supervised learning refers to the situation where data are available from both the undamaged and damaged conditions of the structure, whereas unsupervised learning refers to the situation where data are available only from the undamaged condition. For bridges in operation, data from both the undamaged and damaged conditions are rarely available, and consequently, unsupervised learning is often required. Furthermore, bridges are subjected to changes in operational and environmental conditions, which complicate the detection of structural damage. One of the fundamental challenges in SHM is the process of separating changes caused by operational and environmental conditions from changes caused by structural damage, referred to as data normalization [7]. However, prior to including data normalization, principal knowledge about the damage detection possibilities of existing steel bridges must

be established by considering relevant structural damage during stable operational and environmental conditions.

Applications of statistical model development have received increasing attention in the technical literature in recent years. In the absence of data from actual bridges, numerical models or test structures are commonly applied [8]–[11]. A significant contribution is the work performed by Figueiredo et al. [12], where damage detection under varying operational and environmental conditions is taken into consideration using the Los Alamos National Laboratory (LANL) test structure. Further work using the same test structure is performed by Santos et al. [13]. There are, however, inherent uncertainties in using a numerical model for damage detection, not only in the establishment of the numerical model itself but also in the modelling of structural damage. Similarly, damage introduced to laboratory test structures must be based on several assumptions and can, at best, be only a moderate representation of actual structural damage. Nevertheless, in the presence of data from actual bridges, important contributions to statistical model development related to damage detection studies on the Z24 prestressed concrete bridge [14] have been reported [15]–[18]. These studies mainly investigate the effects of operational and environmental conditions on damage detection using natural frequencies as damage-sensitive features. However, the relevant structural damage introduced to this bridge is mostly applicable to concrete bridges. Similar works with other bridge applications that are considered important contributions within this topic are found in [19], [20]. Except for [14], [21]–[26], few experimental studies have been reported in the literature where relevant structural damage is imposed on bridges. Furthermore, there are currently no studies in the literature where statistical model development is performed based on experimental studies on steel bridges.

This paper presents a data-based SHM approach for damage detection in steel bridges. The aim is to detect relevant structural damage based on the statistical model development of experimental data obtained from different structural state conditions. The Hell Bridge Test Arena, a steel riveted truss bridge formerly in operation as a train bridge and therefore representative of the many bridges still in service, is used as a full-scale damage detection test structure [27], [28]. An extensive experimental study is performed to obtain acceleration time series from the densely instrumented bridge under different structural state conditions during stable operational and environmental conditions. As such, relevant structural damage is implemented, the bridge is excited using a modal vibration shaker for simulating ambient vibration, and measurements are obtained from a setup containing two sensor groups to capture both the local and global responses of the bridge. The damage types chosen, including their locations, are based on the most common and frequently reported damage types in the literature: fatigue damage occurring in and below the bridge deck. The damage is considered highly progressed, representing loose connections and large cracks that open and close under dynamic loading. Autoregressive (AR) parameters are used as damage-sensitive features. The use of AR parameters has proven to be beneficial mainly because they are sensitive to the nonlinear behaviour of damage [29], which is a typical behaviour resulting from fatigue damage. Statistical model development is

performed by considering both supervised and unsupervised machine learning. Four supervised machine learning algorithms are applied to test the abilities of different machine learning algorithms to detect structural damage, learn the structure of the data and determine how well the different damage types can be classified. The Mahalanobis squared distance (MSD), shown to be a highly suitable data normalization approach in terms of strong classification performance and low computational effort [12], is implemented as an unsupervised machine learning algorithm by novelty detection. Finally, the performances of the machine learning algorithms are assessed via both receiver operating characteristics (ROC) curves and confusion matrices.

Two novel contributions to the field of SHM regarding its application to bridges are made in this paper. First, statistical model development provides insight into the performances of several supervised machine learning algorithms based on a unique dataset established from a real-world application and allows for a study on the detectability of different damage types. Although these results have limited practical significance since data from both undamaged and damaged conditions are rarely available for bridges in operation, such information is invaluable for the SHM process and in the design of SHM systems. Second, a comparison between supervised and unsupervised learning algorithms is made. The implication of this insight provides a major contribution towards establishing a methodology for damage detection that can be employed in SHM systems on existing steel bridges.

The outline of this paper is as follows. Section 5.2 provides a description of the experimental setup, including the damage introduced to the bridge and the operational and environmental conditions experienced during the measurements. Section 5.3 describes the feature extraction and the process of selecting the appropriate AR model order in addition to giving a brief overview of the supervised and unsupervised machine learning algorithms applied in this study. Section 5.4 presents the utilized analysis approach and the results obtained from the statistical models developed using the supervised and unsupervised machine learning algorithms. Finally, Sections 5.5 and 5.6 summarize the work, discuss the analysis results obtained and suggest further work.

5.2 Experimental study

5.2.1 Experimental setup

The Hell Bridge Test Arena, shown in Figure 5.1, is used as a full-scale damage detection test structure. The structural system of the bridge is composed of two bridge walls, the bridge deck and the lateral bracing. Figure 5.2 shows a schematic overview of the bridge.

An instrumentation system from National Instruments consisting of three cRIO-9036 controllers was used to acquire data from 58 accelerometers. The accelerometers were divided into a setup containing two sensor groups. Sensor group 1 consisted of 40 single-axis accelerometers (Dytran 3055D3) located below the bridge deck to measure the vertical response (global z-direction). Sensor group 2 consisted of 18 triaxial accelerometers (Dytran 3583BT and 3233A) located

Figure 5.1: The Hell Bridge Test Arena.

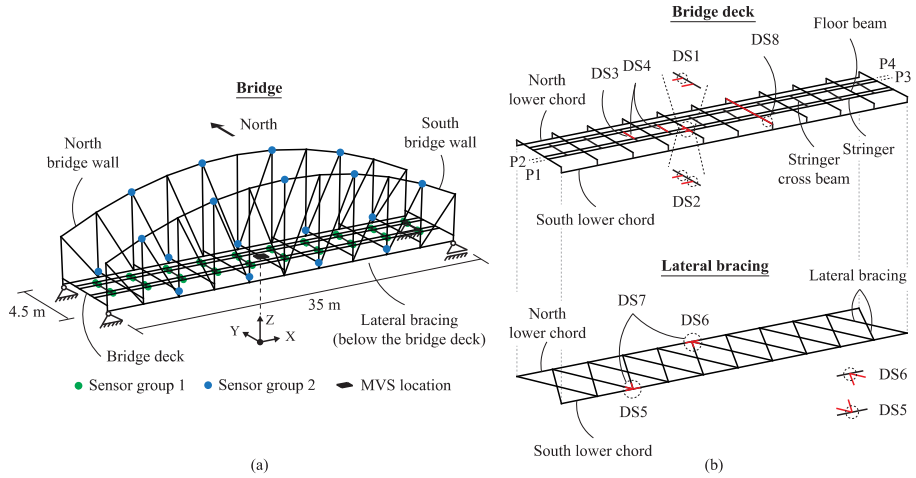

Figure 5.2: Overview of the Hell Bridge Test Arena. (a) Bridge layout, including the locations of the modal vibration shaker (MVS) and sensors. (b) Damage introduced to the bridge deck and lateral bracing.

above the bridge deck, i.e., on the bridge walls, to measure the lateral and vertical responses (global y and z-directions). Data were sampled at 400 Hz. The data were detrended, filtered and resampled to 100 Hz before they were used for analysis. The bridge was excited in the vertical direction using a modal vibration shaker (APS 420) located at the bridge midspan. A band-limited random white noise in the range of 1-100 Hz with a maximum peak-to-peak excitation amplitude (stroke) of 150 mm was applied to simulate ambient vibration. The location of the modal vibration shaker and the sensor positions on the bridge are shown in Figure 5.2(a).

Ten different structural state conditions were considered, as summarized in Table 5.1. The structural state conditions were categorized into two groups: undamaged and damaged states. In the first group, the reference structural state of the bridge was represented by the baseline condition. Two baseline conditions were established under similar environmental conditions. In the second group, the damage states of the bridge were represented by different damage types with varying degrees of severity. Altogether, eight different damage states were established by considering four different damage types: stringer-to-floor-beam connections; stringer cross beams; lateral bracing connections; and, connections between floor beams and main load-carrying members. The variation in the degree

of severity was considered by introducing each damage type at one or more locations in the bridge. The damage states were established consecutively in a sequence: damage was introduced, measurements were performed, and the damage was subsequently repaired. The damage types were chosen based on two considerations: first, these are the most common and frequently reported damage types in the literature [1]; and second, these are the most severe but relevant damage types for this type of bridge. An overview of the damage types introduced in the bridge, including their locations, is shown in Figure 5.2(b).

Table 5.1: Overview and descriptions of the structural state conditions.

Label	State condition	Categorization[1]	Type	Description
UDS1	Undamaged	-	Baseline condition	Before all damage state conditions
UDS2	Undamaged	-	Baseline condition	After all damage state conditions
DS1	Damaged	Local	Stringer-to-floor-beam connection	Single connection damaged
DS2	Damaged	Local	Stringer-to-floor-beam connection	Multiple connections damaged
DS3	Damaged	Local	Stringer cross beam	Main part of single cross beam removed
DS4	Damaged	Local	Stringer cross beam	Main parts of multiple cross beams removed
DS5	Damaged	Global	Lateral bracing connection	Single connection damaged
DS6	Damaged	Global	Lateral bracing connection	Single connection damaged
DS7	Damaged	Global	Lateral bracing connection	Multiple connections damaged
DS8	Damaged	Global	Connection between the floor beam and main load-carrying member	Single connection damaged

[1] Local: damage to the secondary steel structure. Global: damage to the primary steel structure.

Figure 5.3: The damage types imposed on the bridge. (a) Stringer-to-floor-beam connection. (b) Stringer cross beam. (c) Lateral bracing connection. (d) Connection between the floor beam and main load-carrying member.

The damage types, shown in Figure 5.3, were imposed by temporarily removing the bolts. All bolts were removed in each damage state condition. The damage types considered involved highly progressed damage, representing loose connections and large cracks that open and close under dynamic loading. As such, each damage represented a fully developed crack resulting from fatigue, leading to a total loss of functionality of the considered connection or beam. Such damage progression, which leads to a redistribution of forces, would be demanding on the structure over time but not critical to the immediate structural integrity due to the redundancy inherent in the design of the bridge. Details regarding the damage types, including the associated mechanism, can be found in [1].

80 tests were performed for each state condition, resulting in a total of 800 tests. For each test, time series data were generated over 10.24 sec, and data were obtained from a total of 75 sensor channels (40 channels from sensor group 1 and 35 channels from sensor group 2). Note that one channel in the lateral direction from sensor group 2 was excluded. Accelerometers were included in sensor groups 1 and 2 to capture the local and global responses of the bridge, respectively.

5.2.2 Operational and environmental conditions

Variability in the operational and environmental conditions imposes difficulties on the damage detection process. In general, operational conditions mainly include live loads, whereas environmental conditions include temperature effects, wind loading and humidity. During the measurements, no sources of variability were considered for the operational condition, which was limited to the operation of the modal vibration shaker only. The environmental conditions were logged during the measurements and summarized in Table 5.2.

The environmental conditions were stable during the measurement period, which gives confidence that any changes observed in the results are caused by the damage imposed in the different damage states. An increase in the temperature occurred during the testing of DS3 and DS4; however, this temperature change was found to have little impact on the damage detection process.

Table 5.2: Environmental conditions during the measurement period.

State	Temperature (°C)	Wind speed (m/s)	Weather
UDS1	10-11	1-2	Cloudy
UDS2	13	0-2	Partly cloudy and sunny
DS1	14	0-2	Partly cloudy and sunny
DS2	13	0	Partly cloudy and sunny
DS3	21	0-2	Sunny
DS4	22	0-2	Sunny
DS5	13	0-2	Partly cloudy and sunny
DS6	13	0-2	Partly cloudy and sunny
DS7	13	0-2	Partly cloudy and sunny
DS8	11	0-2	Partly cloudy and sunny

5.3 Feature extraction and machine learning algorithms

5.3.1 Feature extraction

In the context of SHM, machine learning is applied to associate the damage-sensitive features derived from measured data with a state of the structure; the basic problem is to distinguish between the undamaged and damaged states. In this study, an AR model is used to extract damage-sensitive features from time series data. For a specific time series, the AR(p) model of order p is given as [30]

$$y_t = \sum_{j=1}^{p} \phi_j y_{t-j} + \varepsilon_t \tag{5.1}$$

where y_t is the measured response signal, ϕ_j denotes the AR parameter(s) to be estimated and ε_t is the random error (residual) at the time index t. The use of AR parameters has proven useful for SHM applications regarding civil infrastructure mainly for three reasons [12], [29]: first, the parameters are sensitive to the nonlinear behaviour of damage, which is a typical behaviour resulting from fatigue damage; second, feature extraction depends only on the time series data obtained from the structural response; and third, the implementation is simple and straightforward.

To determine the appropriate order for a time series, two model selection criteria are commonly used: the Akaike information criterion (AIC) and the Bayesian model criterion (BIC). The AR model with the lowest AIC or BIC value gives the optimal order p.

5.3.2 AR model order selection

To find a common AR model order that can be applied to all time series, a model selection evaluation is performed. Analyses are performed for a selection of time series by considering the AIC and BIC values obtained by AR(p) models of increasing order p. The root mean square (RMS) values of the residuals are also considered as a heuristic approach, where the residuals are the differences between

the model's one-step-ahead predictions and the real values of the time series. The results are based on the average results of all sensor channels, which are obtained by performing analyses of 80 tests in the undamaged state condition (40 tests from UDS1 and UDS2, respectively). Analyses of the AR parameters are performed using the *statsmodels* module in Python [31].

Figure 5.4 shows the results obtained by considering the normalized AIC and BIC values in addition to the RMS values of the residuals. The optimal order, p, is determined by the lowest values or by the convergence point of the values for a varying order. It is observed that the curves generally follow each other well and that the curves decrease rapidly for the lowest model orders. Although the AR models of order 8 or higher prove to be close to optimal representations of the time series, a lower-order model is used in this study. The choice of AR model order is important, not only because the optimal order provides the best representation of the time series but because the AR parameters are used as inputs for the machine learning algorithms in a concatenated format, affecting the dimension of the feature space. A high AR model order increases the dimension of the feature space. Consequently, there is a trade-off between obtaining the optimal time series representation and reducing the uncertainty of dealing with high-dimensional data. Data with high dimensionality may lead to problems related to the curse of dimensionality [32]; as the feature space dimension increases, the number of training samples required to generalize a machine learning model also increases drastically. Although a lower-order model is arguably not the optimal representation, it can still provide a good representation of the time series for use with all state conditions, and it reduces the uncertainty associated with high-dimensional data for the considered analysis approach. Therefore, for each test of each state condition, AR(5) models are established for the time series obtained from all sensor channels. The features are used as inputs to the machine learning algorithms for supervised and unsupervised learning.

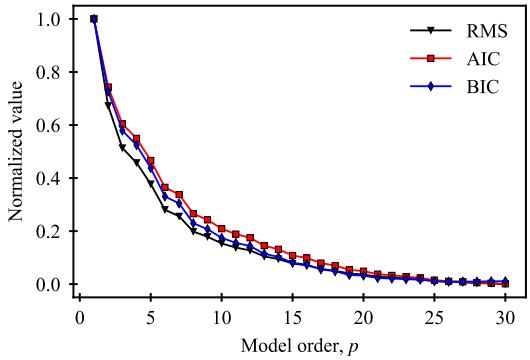

Figure 5.4: Average AIC, BIC and RMS values for AR(p) models of increasing order p from all sensor channels for a selection of time series from the undamaged state condition.

5.3.3 Supervised learning

For supervised learning, a training matrix $\mathbf{X} \in \mathbb{R}^{n \times k}$ with n samples and k features and a test matrix $\mathbf{Z} \in \mathbb{R}^{m \times k}$ with m samples are composed of data from both the undamaged and damaged conditions. The target variable $\mathbf{y} \in \mathbb{N}^{n \times 1}$ is a vector composed of the class labels y. $\mathbf{x}_i \in \mathbb{R}^{1 \times k}$ and $\mathbf{z}_i \in \mathbb{R}^{1 \times k}$ denote arbitrary samples with an index i from the training and test matrices, respectively, with a corresponding class label y_i. Note that k here is the total number of features to be included.

Supervised machine learning algorithms are considered for group classification only. The supervised machine learning algorithms are applied to test the abilities of different machine learning algorithms to detect structural damage, learn the underlying structure of the data and determine how well the different damage types can be classified. For this purpose, four common supervised machine learning algorithms are chosen: the k-nearest neighbours (kNN), the support vector machine (SVM), the random forests (RF) and the Gaussian naïve Bayes (NB) algorithms. Each algorithm yields different properties with respect to complexity, computational efficiency, and performance in terms of the size of the training data and dimensionality of the feature space. In the context of SHM, the presented algorithms have never before been applied in supervised learning for damage detection on actual bridges, and only a few applications have been reported with respect to numerical studies or experimental studies using test structures [33], [34]. The theoretical backgrounds of the presented algorithms can be found in [35], [36], and practical examples (including implementations) can be found in [37], [38].

5.3.4 Unsupervised learning

For unsupervised learning, a training matrix $\mathbf{X} \in \mathbb{R}^{n \times k}$ with n samples and k features is composed of data from the undamaged condition only, and a test matrix $\mathbf{Z} \in \mathbb{R}^{m \times k}$ with m samples is composed of data from both the undamaged and damaged conditions. Unsupervised learning by novelty detection is implemented to take into consideration that data from the structure are generally only available in the undamaged condition. Novelty detection occurs when only training data from the undamaged state condition, i.e., the normal condition, are used to establish if a new sample point should be considered as different (an outlier). Consequently, if there are significant deviations, the algorithm indicates novelty. For SHM applications, several unsupervised machine learning algorithms have been reported in the literature [8], [12], [13], [17], [18], [33]. However, the MSD is found to be a highly suitable data normalization approach in terms of strong classification performance and low computational effort [12].

The MSD is a normalized measure of the distance between a sample point and the mean of the sample distribution and is defined as

$$DI_i = \left(\mathbf{z}_i - \overline{\mathbf{x}}\right)\mathbf{C}^{-1}\left(\mathbf{z}_i - \overline{\mathbf{x}}\right)^T \tag{5.2}$$

where $\mathbf{z}_i \in \mathbb{R}^{1 \times k}$ is the new sample point and potential outlier, $\overline{\mathbf{x}} \in \mathbb{R}^{1 \times k}$ is the mean of the sample observations (sample centroid) and $\mathbf{C} \in \mathbb{R}^{k \times k}$ is the covariance

matrix. Both $\bar{\mathbf{x}}$ and $\mathbf{C}$ are obtained from the training matrix $\mathbf{X}$. The MSD is used as a damage index, which is denoted as DI.

To determine if a sample point is an inlier or outlier, a threshold value can be established using Monte Carlo simulations. The procedure of this method is adopted from [39] and summarized by the following steps for a 1% threshold:

1. A $(n \times k)$ matrix is constructed, where each element is a randomly generated number from a normal distribution with zero mean and unit standard deviation. The MSD for all n samples is calculated and the largest value is stored.
2. Step 1 is repeated for a minimum of 1000 trials. The array with all of the largest MSD values is structured in descending order.
3. The threshold value is established by considering the MSD values in the structured array in which 1% of the trials occur.

The threshold value is dependent on the numbers of observations and dimensions for the considered case.

5.4 Experimental analysis and results

5.4.1 Analysis approach

In the analysis approach used in this study, all sensor channels from each sensor group are taken into consideration simultaneously. The features are concatenated and applied as inputs for the machine learning algorithms. Hence, the setups for sensor groups 1 and 2 yield feature vectors with dimensions of 200 (40×5) and 175 (35×5), respectively. Statistical model development is performed based on the experimental study using both supervised and unsupervised learning for each setup separately.

5.4.2 Supervised learning

In supervised learning, labelled data are available. The supervised machine learning algorithms presented in Section 5.3.3 are implemented. The features are scaled to zero mean and unit variance for the algorithms, where relevant, to improve their performances.

The data are divided into 75% for training and 25% for testing. Consequently, the training matrix $\mathbf{X}$ has dimensions of 600×200 and 600×175 for sensor groups 1 and 2, respectively. The two baseline conditions (UDS1 and UDS2) are merged for the undamaged state condition (UDS) and include a total of 120 tests, whereas 60 tests are included for each damage state condition (DS1-DS8). Hence, a total of nine different class labels are included for evaluation. To find the optimal hyperparameters and increase the abilities of the machine learning algorithms to generalize to unseen data, a grid search with 5-fold cross validation is performed on the training data. The grid search conducts an exhaustive search over the specified hyperparameters to obtain the best cross-validation score. The hyperparameters of each algorithm, together with the final values obtained from the

grid search, are summarized in Table 5.3. The test matrix $\mathbf{Z}$ has dimensions of 200×200 and 200×175 for sensor groups 1 and 2, respectively. Since the undamaged state condition is merged, it includes a total of 40 tests, whereas 20 tests are included for each damage state condition. For evaluation purposes, each sample from the test data is classified into one of the nine classes, resulting in a multi-class classification approach.

To evaluate the performances of the machine learning algorithms, also referred to as classifiers, ROC curves are established. The ROC curves represent the relative trade-offs between true positives (TP), or the probability of detection, and false positives (FP), or the probability of a false alarm [40]. Figure 5.5 shows the averaged ROC curves, including the areas under the curves (AUCs), by considering all the classifiers for sensor groups 1 and 2. Each averaged ROC curve represents the micro-average of all classes, i.e., the contributions from all classes are aggregated to compute the average. To compare the classifiers, the ROC performances are reduced to scalar AUC values that represent the expected performances. Hence, a perfect classification is represented by the point (0, 1) with an AUC value of 1.0. Consequently, from the plots in Figure 5.5, it is concluded that all classifiers perform well; however, the SVM outperforms the other classifiers and obtains perfect classification results for both sensor groups.

Table 5.3: Specified hyperparameters for the supervised machine learning algorithms. The final values of the hyperparameters are provided in parentheses for sensor groups 1 and 2. Details of the hyperparameters are specified in [37], [38].

	Hyperparameters				
Algorithm	Parameter 1	Parameter 2	Parameter 3	Parameter 4	Parameter 5
SVM	Regularization strength (0.1, 0.01)	Kernel type (linear, linear)	Kernel coefficient (NA, NA)[1]	-	-
RF	Number of trees (200, 100)	Node impurity criterion (Entropy, Gini)	Maximum tree depth (10, 6)	Minimum leaf node samples (4, 4)	Maximum number of features for best split (14, 7)
NB[2]	-	-	-	-	-
kNN	Number of neighbours (1, 5)	Leaf size (1, 1)	Parameter for the Minkowski metrics (1, 1)	-	-

[1] The kernel coefficient is not applicable (NA) for the linear kernel.

[2] One parameter can be tuned in the NB algorithm; however, the default value was chosen.

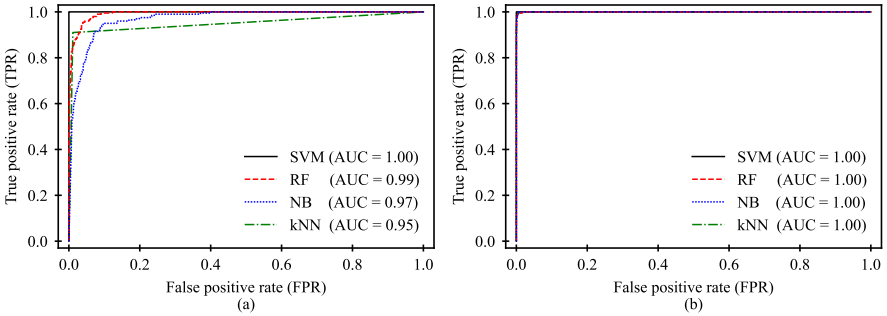

Figure 5.5: Averaged ROC curves for the machine learning algorithms. (a) Sensor group 1. (b) Sensor group 2.

To obtain a more detailed view of the results, normalized multi-class confusion matrices for each classifier are established and shown in Figure 5.6. By considering both sensor groups, it is clearly seen that the class labels are mostly incorrectly classified within each damage type, with a few exceptions. In particular, damage in the stringer cross beams, represented by the class labels DS3 and DS4, and damage in the lateral bracing connections, represented by DS5, DS6 and DS7, represent the majority of the incorrect predictions made. Accordingly, DS3 is incorrectly classified as DS4 or vice versa, and DS5 is incorrectly classified as DS6 or DS7, or vice versa. Interestingly, the stringer-to-floor-beam connection type of damage, represented by DS1 and DS2, and the connection between the floor beam and main load-carrying member type of damage, represented by DS8, are correctly classified by all classifiers. It is also seen that the naïve Bayes classifier performs worst for the stringer cross beam and lateral bracing connection types of damage relative to all classifiers, which is not very well reflected in the averaged ROC curves. There are two main explanations for the results obtained. First, damage in the stringer cross beams is categorized as local damage, and consequently, it is expected that introducing this type of damage generally has little influence on the structural response and thus makes it difficult to classify. Second, damage in the lateral bracing connections is categorized as global damage and is expected to have a global effect, rather than a local effect, on the structural response. Additionally, these two damage types influence the structural response mainly in the lateral direction of the bridge, which also explains the differences in the results obtained between sensor groups 1 and 2, since sensor group 1 only measures the response in the vertical direction.

An important part of the statistical model development process for supervised learning is to characterize the type of damage that can best be detected. Information regarding the damage types that are most difficult to detect when using the analysis approach considered is valuable information for bridge owners. In doing so, the true positive rate (TPR) (or recall) and positive predictive value (PPV) (or precision) are good measures. These measures are defined as

$$TPR = \frac{TP}{TP + FN} \tag{5.3}$$

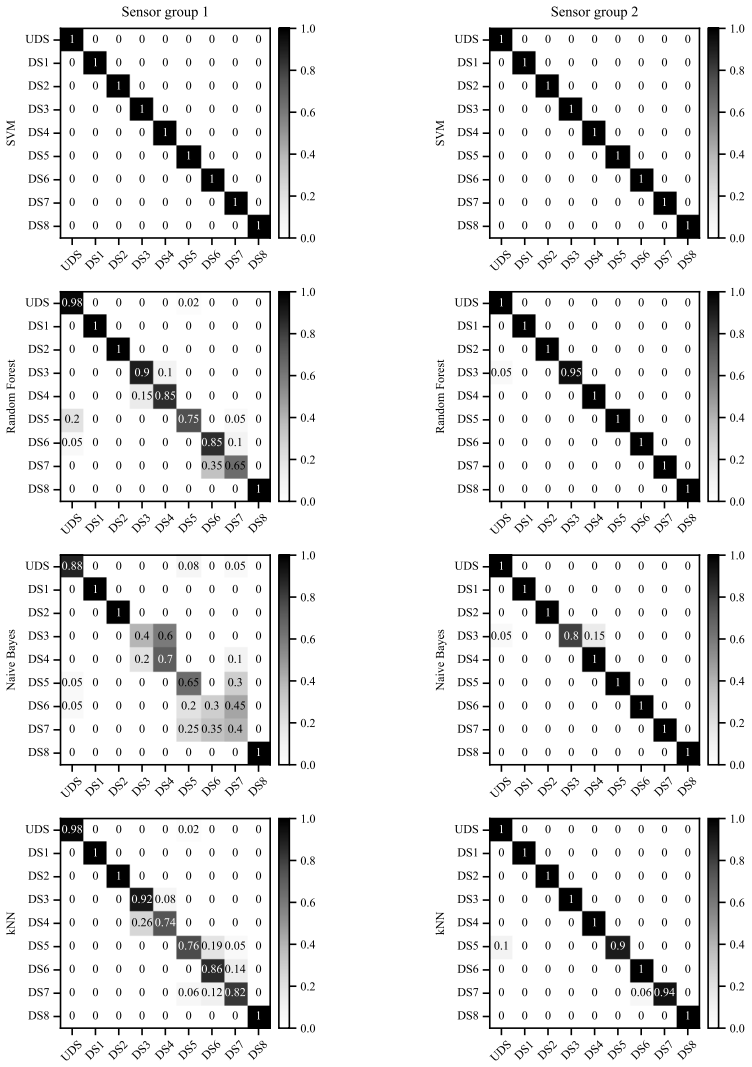

Figure 5.6: Normalized confusion matrices obtained from supervised learning by considering both sensor groups. For each confusion matrix, the predicted label is on the x-axis, and the true label is on the y-axis.

$$PPV = \frac{TP}{TP + FP} \tag{5.4}$$

where TP denotes the true positives, FN represents the false negatives and FP signifies the false positives for a specified class. The TPR measures the proportions of correctly identified positives, whereas PPV measures the proportions of positive results. Additionally, the $F1$ score is the harmonic mean of the recall and precision. Table 5.4 summarizes the mean values of the TPR, PPV and $F1$ scores of the four classifiers for all class labels.

Table 5.4: Mean values of the TPRs, PPVs and F1 scores of the four classifiers.

Class label	Sensor group 1			Sensor group 2		
	TPR	PPV	F1 score	TPR	PPV	F1 score
UDS	0.957	0.958	0.956	1.000	0.988	0.994
DS1	1.000	1.000	1.000	1.000	1.000	1.000
DS2	1.000	1.000	1.000	1.000	1.000	1.000
DS3	0.805	0.836	0.811	0.938	1.000	0.966
DS4	0.822	0.827	0.820	1.000	0.967	0.983
DS5	0.790	0.837	0.808	0.976	1.000	0.988
DS6	0.752	0.709	0.722	1.000	0.983	0.991
DS7	0.718	0.733	0.722	0.985	1.000	0.992
DS8	1.000	1.000	1.000	1.000	1.000	1.000

From the results obtained, and by specifically considering the TPR, it is concluded that, on average, damage in the stringer-to-floor-beam connections and the connection between the floor beam and main load-carrying member are classified best, followed by damage in the stringer cross beams and the lateral bracing connections. Furthermore, a higher degree of stringer cross beam damage (DS4) is classified better than a lower degree (DS3); however, a similar conclusion cannot be made about the damage in the lateral bracing connections, with no obvious explanation. Nevertheless, and most importantly, by using an appropriate classifier such as the SVM, all damages can be correctly classified. The results from the SVM, based on the grid search, were obtained using a linear kernel for both sensor groups, proving that the dataset is linearly separable.

5.4.3 Unsupervised learning

In unsupervised learning, no labelled data are available. The MSD algorithm presented in Section 5.3.4 is implemented as a novelty detection method.

To obtain a reasonable amount of data from the undamaged state condition, the training matrix $\mathbf{X}$ is based on the measured data with a level of noise added. Thus, to establish the training matrix, 80 tests from the undamaged state condition are used as basic training data, i.e., 40 tests from each of the two baseline conditions (UDS1 and UDS2). The basic training data are copied 20 times, and each copy is subsequently corrupted with white Gaussian noise. Noise is added with a signal-to-noise ratio (SNR) equal to 20 using the definition

$$SNR = \frac{\mu}{\sigma} \tag{5.5}$$

where μ is the mean of the absolute value of each individual feature considering all the samples in the basic training data and σ is the standard deviation (or RMS) of the noise. Notably, the statistics of each feature in the feature vector are taken into consideration during noise generation. The result is a suitable mean vector $\overline{\mathbf{x}}$ and covariance matrix $\mathbf{C}$ representing the undamaged state condition. Adding training data corrupted with noise improves and stabilizes the MSD algorithm and

is found to be a good solution in situations where adequate measured training data are not available [39]. Consequently, the training matrix $\mathbf{X}$ has dimensions of 1600×200 and 1600×175 for sensor groups 1 and 2, respectively. The test matrix $\mathbf{Z}$ is composed of the remaining data from the undamaged state condition (UDS), i.e., 80 tests from the two baseline conditions (UDS1 and UDS2), and 80 tests from each of the damage state conditions (DS1-DS8). Thus, the test matrix has dimensions of 720×200 and 720×175 for sensor groups 1 and 2, respectively. For evaluation purposes, each sample from the test data is classified as either undamaged or damaged, resulting in a binary classification approach.

Figure 5.7 shows the ROC curves for the MSD algorithm, including the AUC values, obtained by considering both sensor groups. From this figure, it is concluded that the algorithm performs well: good classification results are obtained for sensor group 1, and perfect classification results are obtained for sensor group 2. The performance of the classifier regarding the 1% threshold is shown in Figure 5.8, where the damage indices (DIs) from the state conditions are established for both sensor groups. Additionally, the state conditions of the respective test numbers are added for informative purposes at the top of the plots. In the binary classification approach, *FP* (false positive indications of damage) and *FN* (false negative indications of damage) are referred to as Type I and Type II errors, respectively. Type I errors are observed in all the tests based on the undamaged state condition (black markers) that are above the threshold, whereas Type II errors are observed in all the tests based on the damaged state condition (grey markers) that are below the threshold. For quantification purposes, these errors are summarized in Table 5.5 for both sensor groups with respect to the considered thresholds.

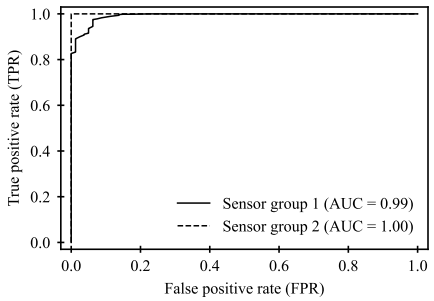

Figure 5.7: ROC curves yielded by the MSD algorithm by considering both sensor groups.

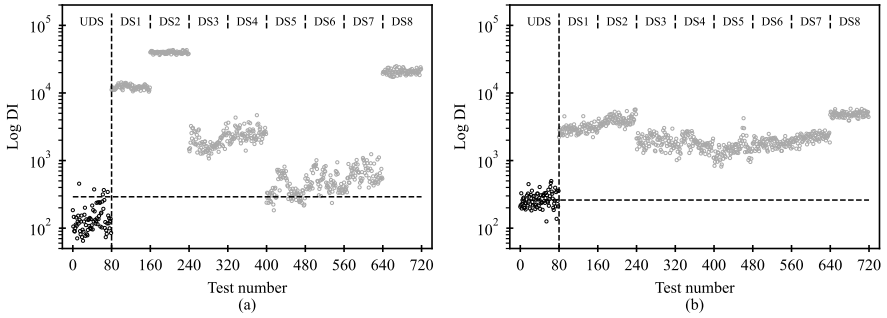

Figure 5.8: Damage indices (DIs) yielded by the MSD algorithm for the undamaged (black) and damaged (grey) state conditions with respect to the threshold value (dashed line) established from the Monte Carlo simulations. (a) Sensor group 1. (b) Sensor group 2.

Table 5.5: Type I and II errors for both sensor groups yielded by the MSD algorithm.

Setup	Error		
	Type I (FP)	Type II (FN)	Total
Sensor group 1	5 (6.3%)	26 (4.1%)	31 (4.3%)
Sensor group 2	39 (48.8%)	0 (0.0%)	39 (5.4%)

The results show that the setup for sensor group 1 yields the best performance with regard to avoiding false positive indications of damage (6.3%). The setup for sensor group 2 has a very low performance regarding false positive indications of damage (48.8%); however, it has an excellent performance when detecting damage (0.0%). Overall, the total misclassification rate obtained is lower for sensor group 1 (4.3%) than for sensor group 2 (5.4%). Nonetheless, these are good results for a novelty detection method. Additionally, an interesting observation in Figure 5.8(a) is the clear trend showing that larger degrees of severity for each damage type also provide generally larger damage indices: DS2 > DS1, DS4 > DS3 and DS7 > DS6 and DS5. Although this is not observed in Figure 5.8(b), it clearly shows that the MSD algorithm performs well, particularly for the sensor group 1 setup.

5.4.4 Sensitivity analysis

To investigate the effect of a dense sensor network on the classification results, a sensitivity analysis is performed in the unsupervised learning with a reduced number of sensors in sensor group 1. Two cases are considered. In case 1, the sensors located in positions P1 and P2 in the longitudinal direction of the bridge are included, shown in Figure 5.2, whereas the sensors in positions P3 and P4 are included in case 2. As such, only 20 sensors are included in each case, and the sensors located closest to the damage state conditions DS1, DS2 and DS8 are included in case 1. Figure 5.9 and Figure 5.10 show the ROC curves and performance of the classifier regarding the 1% threshold for both cases, respectively. The Type I and II errors are summarized in Table 5.6.

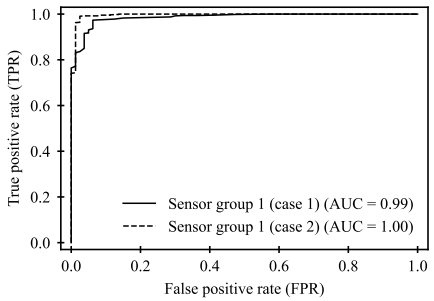

Figure 5.9: ROC curves yielded by the MSD algorithm by considering both cases in sensor group 1.

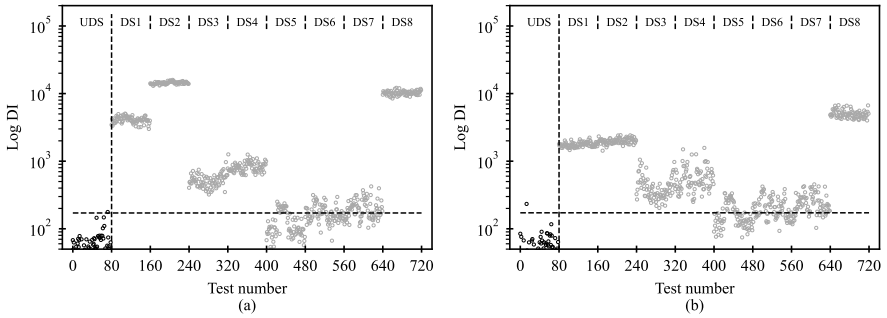

Figure 5.10: Damage indices (DIs) yielded by the MSD algorithm for the undamaged (black) and damaged (grey) state conditions with respect to the threshold value (dashed line) established from the Monte Carlo simulations. (a) Case 1 in sensor group 1. (b) Case 2 in sensor group 1.

Table 5.6: Type I and II errors for both cases in sensor group 1, including the original case, yielded by the MSD algorithm.

Case	Error		
	Type I (FP)	Type II (FN)	Total
Original	5 (6.3%)	26 (4.1%)	31 (4.3%)
Case 1	1 (1.3%)	141 (22.0%)	142 (19.7%)
Case 2	1 (1.3%)	101 (15.8%)	102 (14.2%)

From the results obtained, and through a comparison with the original case in sensor group 1 where all sensors are included, the effect of a dense sensor network can be clearly observed. Particularly, two important observations are made. First, although the performance regarding false negative indications of damage for case 1 (22.0%) is higher than that for case 2 (15.8%), case 1 shows more distinct results for damage state conditions DS1, DS2 and DS8 than case 2. These results indicate the positive effect of sensors being located near the damage locations. Second, the total misclassification rates of cases 1 (19.7%) and 2 (14.2%) are higher than that in the original case (4.3%). The low performance of both cases regarding outliers,

or false negative indications of damage, is more unfavourable than that of incorrectly diagnosing inliers, or false positive indications of damage. Hence, reducing the number of sensors drastically increase the false negative indications of damage, which clearly demonstrates the importance of a dense sensor network.

5.5 Summary and discussion

From the statistical model development in supervised learning, three major observations are made. First, relevant structural damage in steel bridges can, in fact, be found. More specifically, by considering the hierarchical structure of damage identification [3], [41], level I (existence) and level III (type) damage detection can be performed. Second, how well structural damage can be classified strongly depends on the machine learning algorithm being applied. The machine learning algorithms perform differently; however, the SVM achieves perfect classification results and outperforms the other algorithms, including those that can capture complex nonlinear behaviours. Third, a study on the detectability of the different damage types, based on the average performances of the classifiers, shows that damage to the lateral bracing connections is most often misclassified, followed by damage to the stringer cross beams. The other damage types are perfectly classified and represent the damage types that can best be detected. Such information is invaluable for the design of SHM systems with respect to instrumentation setup and sensor placement, and it provides insight into which damage types can generally be expected to be difficult to detect and those that are not for a similar analysis approach.

Data from both the undamaged and damaged conditions are generally not available for bridges in operation. Hence, unsupervised learning is required, where data from only the undamaged condition are available. Consequently, the results obtained from unsupervised learning are emphasized in this study. From the statistical model development, it is observed that the MSD algorithm performs well for the considered analysis approach with respect to minimizing the number of both false positive and false negative indications of damage. This algorithm has a high classification performance, is computationally efficient, and does not require any assumptions or tuning of parameters, although training data are added numerically to obtain improved performance. As such, the results obtained in this study, particularly by comparing supervised and unsupervised learning, are of major importance. Specifically, the unsupervised learning algorithm performs almost equally as well as the best supervised learning algorithms. This not only demonstrates that relevant structural damage in steel bridges can be classified using unsupervised learning but also shows that a methodology for damage detection can be employed on existing bridges.

In this study, variability in the operational and environmental conditions was not taken into consideration using data normalization. To include data normalization, a larger variability in the environmental conditions than that experienced during the measurements is needed for the baseline data that represent the undamaged state condition. As such, periodic measurements that take all seasonal variations into consideration should be a minimum requirement. This is

not included in the scope of this study, and future work should assess whether changes caused by damage can be separated from changes caused by any operational and environmental conditions. Such an assessment will reduce the uncertainty in the process of damage state assessment. Furthermore, it is acknowledged that for a future assessment based on long-term monitoring where data normalization is included, unsupervised learning methods such as the auto-associative neural network (AANN) and Gaussian mixture models (GMMs) should be considered, particularly in the presence of nonlinear effects caused by variability in the operational and environmental conditions [17].

There are several advantages of the analysis approach presented in this study. The approach is computationally efficient from a machine learning perspective because many sensors can be evaluated simultaneously. Consequently, both supervised and unsupervised learning (novelty detection) can easily be performed. Furthermore, the approach allows for level I (existence) and level III (type) damage detection (the latter is only for supervised learning) but limits the possibility of performing level II (location) damage detection in unsupervised learning due to the large number of sensors widely distributed over the structure. The importance of a large number of sensors in a dense sensor network is demonstrated through a sensitivity analysis. The dense sensor network ensures a low total misclassification rate and enhances the damage detection capabilities. The main disadvantage of the analysis approach, however, is the high dimension of the feature space, which limits the number of features that can be included per sensor channel. From a general perspective, this limitation can be solved by increasing the number of samples in the training data or by performing dimension reduction techniques. From the results obtained in this study, despite this limitation, damage detection can still be successively performed.

AR parameters were found to be excellent damage-sensitive features in this study, and an AR(5) model was considered adequate. A low-order model was primarily used to reduce the dimension of the feature space for the analysis approach considered but also because low variations in the environmental and operational conditions were experienced during the measurements. The AR(5) model was able to capture the underlying dynamics of the structure and to accurately discriminate the undamaged and damaged states when applied as inputs for the machine learning algorithms under both supervised and unsupervised learning. However, it is important to note that environmental and operational conditions can introduce changes in the structural response. Furthermore, such changes can mask changes in any responses related to damage when a low model order is used, as shown by Figueiredo et al. [29]. This awareness is needed when using low-order models. Increasing the model order can easily be done when appropriate training data are available.

As a final note, the dataset used in this study was a result of measurements obtained using a dense instrumentation setup that was widely distributed over the structure, to capture both the local and global structural responses. Additionally, different damage types and degrees of severity were considered, and the operational and environmental conditions were logged. Consequently, the dataset obtained is unique in the context of performing damage detection in steel bridges.

5.6 Conclusion

The primary motive of SHM is to design a system that minimizes false positive indications of damage for economic and reliability concerns and false negative indications of damage for life-safety issues. For bridges, such a system should primarily be considered in an unsupervised learning approach, where data from only the undamaged condition are available.

This paper presented a data-based SHM approach for damage detection in steel bridges. The results obtained from an extensive experimental study proved that relevant structural damage in steel bridges, which is typically caused by fatigue, can be established using unsupervised learning. As such, this study provides a major contribution towards establishing a methodology for damage detection that can be employed in SHM systems on existing steel bridges. Future work will assess data normalization, where changes caused by damage can be separated from changes caused by any operational and environmental conditions, to reduce the uncertainty in the resulting damage state assessment.

Acknowledgements

The Hell Bridge Test Arena is financially supported by Bane NOR and the Norwegian Railway Directorate.

References

[1] R. Haghani, M. Al-Emrani, and M. Heshmati, “Fatigue-Prone Details in Steel Bridges,” *Buildings*, vol. 2, no. 4, pp. 456–476, 2012, doi: 10.3390/buildings2040456.

[2] C. R. Farrar and K. Worden, “An introduction to structural health monitoring,” *Philos. Trans. R. Soc. A Math. Phys. Eng. Sci.*, vol. 365, no. 1851, pp. 303–315, 2007, doi: 10.1098/rsta.2006.1928.

[3] K. Worden and J. M. Dulieu-Barton, “An Overview of Intelligent Fault Detection in Systems and Structures,” *Struct. Heal. Monit.*, vol. 3, no. 1, pp. 85–98, Mar. 2004, doi: 10.1177/1475921704041866.

[4] C. R. Farrar and K. Worden, *Structural Health Monitoring: A Machine Learning Perspective*. Wiley, 2012.

[5] R. J. Barthorpe, “On Model- and Data-Based Approaches to Structural Health Monitoring,” The University of Sheffield, 2010.

[6] C. R. Farrar, S. W. Doebling, and D. A. Nix, “Vibration-based structural damage identification,” *Philos. Trans. R. Soc. A Math. Phys. Eng. Sci.*, vol. 359, no. 1778, pp. 131–149, Jan. 2001, doi: 10.1098/rsta.2000.0717.

[7] H. Sohn, K. Worden, and C. R. Farrar, “Statistical damage classification under changing environmental and operational conditions,” *J. Intell. Mater. Syst. Struct.*, vol. 13, no. 9, pp. 561–574, 2002, doi: 10.1106/104538902030904.

[8] A. C. Neves, I. González, J. Leander, and R. Karoumi, “Structural health monitoring of bridges: a model-free ANN-based approach to damage detection,” *J. Civ. Struct. Heal. Monit.*, vol. 7, no. 5, pp. 689–702, 2017, doi: 10.1007/s13349-017-0252-5.

[9] A. C. Neves, I. González, R. Karoumi, and J. Leander, “The influence of frequency content on the performance of artificial neural network–based damage detection systems tested on numerical and experimental bridge data,” *Struct. Heal. Monit.*, Jun. 2020, doi: 10.1177/1475921720924320.

[10] H. Pan, M. Azimi, F. Yan, and Z. Lin, “Time-Frequency-Based Data-Driven Structural Diagnosis and Damage Detection for Cable-Stayed Bridges,” *J. Bridg. Eng.*, vol. 23, no. 6, p. 04018033, Jun. 2018, doi: 10.1061/(ASCE)BE.1943-5592.0001199.

[11] M. Malekzadeh, G. Atia, and F. N. Catbas, “Performance-based structural health monitoring through an innovative hybrid data interpretation framework,” *J. Civ. Struct. Heal. Monit.*, vol. 5, no. 3, pp. 287–305, 2015, doi: 10.1007/s13349-015-0118-7.

[12] E. Figueiredo, G. Park, C. R. Farrar, K. Worden, and J. Figueiras, “Machine learning algorithms for damage detection under operational and environmental variability,” *Struct. Heal. Monit.*, vol. 10, no. 6, pp. 559–572, 2011, doi: 10.1177/1475921710388971.

[13] A. Santos, E. Figueiredo, M. F. M. Silva, C. S. Sales, and J. C. W. A. Costa, “Machine learning algorithms for damage detection: Kernel-based approaches,” *J. Sound Vib.*, vol. 363, pp. 584–599, 2016, doi: 10.1016/j.jsv.2015.11.008.

[14] G. De Roeck, “The state-of-the-art of damage detection by vibration monitoring: The SIMCES experience,” *J. Struct. Control*, vol. 10, no. 2, pp. 127–134, 2003, doi: 10.1002/stc.20.

[15] E. Reynders, G. Wursten, and G. De Roeck, “Output-only structural health monitoring in changing environmental conditions by means of nonlinear system identification,” *Struct. Heal. Monit.*, vol. 13, no. 1, pp. 82–93, 2014, doi: 10.1177/1475921713502836.

[16] E. Figueiredo, I. Moldovan, A. Santos, P. Campos, and J. C. W. A. Costa, “Finite Element–Based Machine-Learning Approach to Detect Damage in Bridges under Operational and Environmental Variations,” *J. Bridg. Eng.*, vol. 24, no. 7, p. 04019061, Jul. 2019, doi: 10.1061/(ASCE)BE.1943-5592.0001432.

[17] E. Figueiredo and E. Cross, “Linear approaches to modeling nonlinearities in long-term monitoring of bridges,” *J. Civ. Struct. Heal. Monit.*, vol. 3, no. 3, pp. 187–194, 2013, doi: 10.1007/s13349-013-0038-3.

[18] A. Santos, E. Figueiredo, M. Silva, R. Santos, C. Sales, and J. C. W. A. Costa, “Genetic-based EM algorithm to improve the robustness of Gaussian mixture models for damage detection in bridges,” *Struct. Control Heal. Monit.*, vol. 24, no. 3, pp. 1–9, 2017, doi: 10.1002/stc.1886.

[19] C. K. Oh, H. Sohn, and I.-H. Bae, “Statistical novelty detection within the Yeongjong suspension bridge under environmental and operational variations,” *Smart Mater. Struct.*, vol. 18, no. 12, p. 125022, Dec. 2009, doi: 10.1088/0964-1726/18/12/125022.

[20] F. Magalhães, A. Cunha, and E. Caetano, “Vibration based structural health monitoring of an arch bridge: From automated OMA to damage detection,” *Mech. Syst. Signal Process.*, vol. 28, pp. 212–228, Apr. 2012, doi: 10.1016/j.ymssp.2011.06.011.

[21] C. R. Farrar *et al.*, “Dynamic characterization and damage detection in the I-40 bridge over the Rio Grande,” 1994.

[22] M. Dilena and A. Morassi, “Dynamic testing of a damaged bridge,” *Mech. Syst. Signal Process.*, vol. 25, no. 5, pp. 1485–1507, 2011, doi: 10.1016/j.ymssp.2010.12.017.

[23] M. Döhler, F. Hille, L. Mevel, and W. Rücker, “Structural health monitoring with statistical methods during progressive damage test of S101 Bridge,” *Eng. Struct.*, vol. 69, pp. 183–193, 2014, doi: 10.1016/j.engstruct.2014.03.010.

[24] R. V. Farahani and D. Penumadu, “Damage identification of a full-scale five-girder bridge using time-series analysis of vibration data,” *Eng. Struct.*, vol. 115, pp. 129–139, 2016, doi: 10.1016/j.engstruct.2016.02.008.

[25] C. W. Kim, K. C. Chang, S. Kitauchi, and P. J. McGetrick, “A field experiment on a steel Gerber-truss bridge for damage detection utilizing vehicle-induced vibrations,” *Struct. Heal. Monit.*, vol. 15, no. 2, pp. 174–192, 2016, doi: 10.1177/1475921715627506.

[26] C.-W. Kim, F.-L. Zhang, K.-C. Chang, P. J. McGetrick, and Y. Goi, “Ambient and Vehicle-Induced Vibration Data of a Steel Truss Bridge Subject to Artificial Damage,” *J. Bridg. Eng.*, vol. 26, no. 7, pp. 1–9, 2021, doi: 10.1061/(asce)be.1943-5592.0001730.

[27] B. T. Svendsen, G. T. Frøseth, and A. Rönnquist, “Damage Detection Applied to a Full-Scale Steel Bridge Using Temporal Moments,” *Shock Vib.*, vol. 2020, pp. 1–16, Feb. 2020, doi: 10.1155/2020/3083752.

[28] B. T. Svendsen, Ø. W. Petersen, G. T. Frøseth, and A. Rønnquist, "Improved finite element model updating of a full-scale steel bridge using sensitivity analysis," *Struct. Infrastruct. Eng.*, pp. 1–17, Jul. 2021, doi: 10.1080/15732479.2021.1944227.

[29] E. Figueiredo, J. Figueiras, G. Park, C. R. Farrar, and K. Worden, "Influence of the autoregressive model order on damage detection," *Comput. Civ. Infrastruct. Eng.*, vol. 26, no. 3, pp. 225–238, 2011, doi: 10.1111/j.1467-8667.2010.00685.x.

[30] G. E. P. Box, G. M. Jenkins, G. C. Reinsel, and G. M. Ljung, *Time Series Analysis: Forecasting and Control (5th Edition)*. Wiley, 2015.

[31] S. Seabold and J. Perktold, "Statsmodels: Econometric and Statistical Modeling with Python," in *Proceedings of the 9th Python in Science Conference*, 2010, pp. 92–96. doi: 10.25080/Majora-92bf1922-011.

[32] R. E. Bellman, *Adaptive Control Processes*. Princeton University Press, 1961.

[33] L. Sun, Z. Shang, Y. Xia, S. Bhowmick, and S. Nagarajaiah, "Review of Bridge Structural Health Monitoring Aided by Big Data and Artificial Intelligence: From Condition Assessment to Damage Detection," *J. Struct. Eng.*, vol. 146, no. 5, p. 04020073, 2020, doi: 10.1061/(asce)st.1943-541x.0002535.

[34] M. Flah, I. Nunez, W. Ben Chaabene, and M. L. Nehdi, "Machine Learning Algorithms in Civil Structural Health Monitoring: A Systematic Review," *Arch. Comput. Methods Eng.*, Jul. 2020, doi: 10.1007/s11831-020-09471-9.

[35] K. Koutroumbas and S. Theodoridis, *Pattern Recognition*, 4th ed. Academic Press Inc, 2008.

[36] T. Hastie, R. Tibshirani, and J. Friedman, *The Elements of Statistical Learning*, 2nd ed. Springer, 2009.

[37] A. Géron, *Hands-On Machine Learning with Scikit-Learn, Keras, and TensorFlow*, 2nd ed. O'Reilly Media, Inc., 2019.

[38] F. Pedregosa *et al.*, "Scikit-learn: Machine Learning in Python," *J. Mach. Learn. Res.*, vol. 12, pp. 2825–2830, 2011.

[39] K. Worden, G. Manson, and N. R. J. Fieller, "Damage detection using outlier analysis," *J. Sound Vib.*, vol. 229, no. 3, pp. 647–667, 2000, doi: 10.1006/jsvi.1999.2514.

[40] T. Fawcett, "ROC graphs: Notes and practical considerations for researchers," Palo Alto, CA, 2004.

[41] A. Rytter, “Vibrational Based Inspection of Civil Engineering Structures,” University of Aalborg, Denmark, 1993.

DEPARTMENT OF STRUCTURAL ENGINEERING
NORWEGIAN UNIVERSITY OF SCIENCE AND TECHNOLOGY

N–7491 TRONDHEIM, NORWAY
Telephone: +47 73 59 47 00

"Reliability Analysis of Structural Systems using Nonlinear Finite Element Methods",
C. A. Holm, 1990:23, ISBN 82-7119-178-0.

"Uniform Stratified Flow Interaction with a Submerged Horizontal Cylinder",
Ø. Arntsen, 1990:32, ISBN 82-7119-188-8.

"Large Displacement Analysis of Flexible and Rigid Systems Considering Displacement-Dependent Loads and Nonlinear Constraints",
K. M. Mathisen, 1990:33, ISBN 82-7119-189-6.

"Solid Mechanics and Material Models including Large Deformations",
E. Levold, 1990:56, ISBN 82-7119-214-0, ISSN 0802-3271.

"Inelastic Deformation Capacity of Flexurally-Loaded Aluminium Alloy Structures",
T. Welo, 1990:62, ISBN 82-7119-220-5, ISSN 0802-3271.

"Visualization of Results from Mechanical Engineering Analysis",
K. Aamnes, 1990:63, ISBN 82-7119-221-3, ISSN 0802-3271.

"Object-Oriented Product Modeling for Structural Design",
S. I. Dale, 1991:6, ISBN 82-7119-258-2, ISSN 0802-3271.

"Parallel Techniques for Solving Finite Element Problems on Transputer Networks",
T. H. Hansen, 1991:19, ISBN 82-7119-273-6, ISSN 0802-3271.

"Statistical Description and Estimation of Ocean Drift Ice Environments",
R. Korsnes, 1991:24, ISBN 82-7119-278-7, ISSN 0802-3271.

“Properties of concrete related to fatigue damage: with emphasis on high strength concrete”,
G. Petkovic, 1991:35, ISBN 82-7119-290-6, ISSN 0802-3271.

"Turbidity Current Modelling",
B. Brørs, 1991:38, ISBN 82-7119-293-0, ISSN 0802-3271.

"Zero-Slump Concrete: Rheology, Degree of Compaction and Strength. Effects of Fillers as Part Cement-Replacement",
C. Sørensen, 1992:8, ISBN 82-7119-357-0, ISSN 0802-3271.

"Nonlinear Analysis of Reinforced Concrete Structures Exposed to Transient Loading",
K. V. Høiseth, 1992:15, ISBN 82-7119-364-3, ISSN 0802-3271.

"Finite Element Formulations and Solution Algorithms for Buckling and Collapse Analysis of Thin Shells",
R. O. Bjærum, 1992:30, ISBN 82-7119-380-5, ISSN 0802-3271.

"Response Statistics of Nonlinear Dynamic Systems",
J. M. Johnsen, 1992:42, ISBN 82-7119-393-7, ISSN 0802-3271.

"Digital Models in Engineering. A Study on why and how engineers build and operate digital models for decisison support",
J. Høyte, 1992:75, ISBN 82-7119-429-1, ISSN 0802-3271.

"Sparse Solution of Finite Element Equations",
A. C. Damhaug, 1992:76, ISBN 82-7119-430-5, ISSN 0802-3271.

"Some Aspects of Floating Ice Related to Sea Surface Operations in the Barents Sea",
S. Løset, 1992:95, ISBN 82-7119-452-6, ISSN 0802-3271.

"Modelling of Cyclic Plasticity with Application to Steel and Aluminium Structures",
O. S. Hopperstad, 1993:7, ISBN 82-7119-461-5, ISSN 0802-3271.

"The Free Formulation: Linear Theory and Extensions with Applications to Tetrahedral Elements with Rotational Freedoms",
G. Skeie, 1993:17, ISBN 82-7119-472-0, ISSN 0802-3271.

"Høyfast betongs motstand mot piggdekkslitasje. Analyse av resultater fra prøving i Veisliter'n",
T. Tveter, 1993:62, ISBN 82-7119-522-0, ISSN 0802-3271.

"A Nonlinear Finite Element Based on Free Formulation Theory for Analysis of Sandwich Structures",
O. Aamlid, 1993:72, ISBN 82-7119-534-4, ISSN 0802-3271.

"The Effect of Curing Temperature and Silica Fume on Chloride Migration and Pore Structure of High Strength Concrete",
C. J. Hauck, 1993:90, ISBN 82-7119-553-0, ISSN 0802-3271.

"Failure of Concrete under Compressive Strain Gradients",
G. Markeset, 1993:110, ISBN 82-7119-575-1, ISSN 0802-3271.

"An experimental study of internal tidal amphidromes in Vestfjorden",
J. H. Nilsen, 1994:39, ISBN 82-7119-640-5, ISSN 0802-3271.

"Structural analysis of oil wells with emphasis on conductor design",
H. Larsen, 1994:46, ISBN 82-7119-648-0, ISSN 0802-3271.

"Adaptive methods for non-linear finite element analysis of shell structures",
K. M. Okstad, 1994:66, ISBN 82-7119-670-7, ISSN 0802-3271.

"On constitutive modelling in nonlinear analysis of concrete structures",
O. Fyrileiv, 1994:115, ISBN 82-7119-725-8, ISSN 0802-3271.

"Fluctuating wind load and response of a line-like engineering structure with emphasis on motion-induced wind forces",
J. Bogunovic Jakobsen, 1995:62, ISBN 82-7119-809-2, ISSN 0802-3271.

"An experimental study of beam-columns subjected to combined torsion, bending and axial actions",
A. Aalberg, 1995:66, ISBN 82-7119-813-0, ISSN 0802-3271.

"Scaling and cracking in unsealed freeze/thaw testing of Portland cement and silica fume concretes",
S. Jacobsen, 1995:101, ISBN 82-7119-851-3, ISSN 0802-3271.

"Damping of water waves by submerged vegetation. A case study of laminaria hyperborea",
A. M. Dubi, 1995:108, ISBN 82-7119-859-9, ISSN 0802-3271.

"The dynamics of a slope current in the Barents Sea",
Sheng Li, 1995:109, ISBN 82-7119-860-2, ISSN 0802-3271.

"Modellering av delmaterialenes betydning for betongens konsistens",
Ernst Mørtsell, 1996:12, ISBN 82-7119-894-7, ISSN 0802-3271.

"Bending of thin-walled aluminium extrusions",
Birgit Søvik Opheim, 1996:60, ISBN 82-7119-947-1, ISSN 0802-3271.

"Material modelling of aluminium for crashworthiness analysis",
Torodd Berstad, 1996:89, ISBN 82-7119-980-3, ISSN 0802-3271.

"Estimation of structural parameters from response measurements on submerged floating tunnels",
Rolf Magne Larssen, 1996:119, ISBN 82-471-0014-2, ISSN 0802-3271.

“Numerical modelling of plain and reinforced concrete by damage mechanics”,
Mario A. Polanco-Loria, 1997:20, ISBN 82-471-0049-5, ISSN 0802-3271.

“Nonlinear random vibrations - numerical analysis by path integration methods”,
Vibeke Moe, 1997:26, ISBN 82-471-0056-8, ISSN 0802-3271.

“Numerical prediction of vortex-induced vibration by the finite element method”,
Joar Martin Dalheim, 1997:63, ISBN 82-471-0096-7, ISSN 0802-3271.

“Time domain calculations of buffeting response for wind sensitive structures”,
Ketil Aas-Jakobsen, 1997:148, ISBN 82-471-0189-0, ISSN 0802-3271.

"A numerical study of flow about fixed and flexibly mounted circular cylinders",
Trond Stokka Meling, 1998:48, ISBN 82-471-0244-7, ISSN 0802-3271.

“Estimation of chloride penetration into concrete bridges in coastal areas”,
Per Egil Steen, 1998:89, ISBN 82-471-0290-0, ISSN 0802-3271.

“Stress-resultant material models for reinforced concrete plates and shells”,
Jan Arve Øverli, 1998:95, ISBN 82-471-0297-8, ISSN 0802-3271.

“Chloride binding in concrete. Effect of surrounding environment and concrete composition”,
Claus Kenneth Larsen, 1998:101, ISBN 82-471-0337-0, ISSN 0802-3271.

“Rotational capacity of aluminium alloy beams”,
Lars A. Moen, 1999:1, ISBN 82-471-0365-6, ISSN 0802-3271.

“Stretch Bending of Aluminium Extrusions”,
Arild H. Clausen, 1999:29, ISBN 82-471-0396-6, ISSN 0802-3271.

“Aluminium and Steel Beams under Concentrated Loading”,
Tore Tryland, 1999:30, ISBN 82-471-0397-4, ISSN 0802-3271.

"Engineering Models of Elastoplasticity and Fracture for Aluminium Alloys",
Odd-Geir Lademo, 1999:39, ISBN 82-471-0406-7, ISSN 0802-3271.

"Kapasitet og duktilitet av dybelforbindelser i trekonstruksjoner",
Jan Siem, 1999:46, ISBN 82-471-0414-8, ISSN 0802-3271.

“Etablering av distribuert ingeniørarbeid; Teknologiske og organisatoriske erfaringer fra en norsk ingeniørbedrift”,
Lars Line, 1999:52, ISBN 82-471-0420-2, ISSN 0802-3271.

“Estimation of Earthquake-Induced Response”,
Símon Ólafsson, 1999:73, ISBN 82-471-0443-1, ISSN 0802-3271.

“Coastal Concrete Bridges: Moisture State, Chloride Permeability and Aging Effects”
Ragnhild Holen Relling, 1999:74, ISBN 82-471-0445-8, ISSN 0802-3271.

”Capacity Assessment of Titanium Pipes Subjected to Bending and External Pressure”,
Arve Bjørset, 1999:100, ISBN 82-471-0473-3, ISSN 0802-3271.

“Validation of Numerical Collapse Behaviour of Thin-Walled Corrugated Panels”,
Håvar Ilstad, 1999:101, ISBN 82-471-0474-1, ISSN 0802-3271.

“Strength and Ductility of Welded Structures in Aluminium Alloys”,
Miroslaw Matusiak, 1999:113, ISBN 82-471-0487-3, ISSN 0802-3271.

“Thermal Dilation and Autogenous Deformation as Driving Forces to Self-Induced Stresses in High Performance Concrete”,
Øyvind Bjøntegaard, 1999:121, ISBN 82-7984-002-8, ISSN 0802-3271.

“Some Aspects of Ski Base Sliding Friction and Ski Base Structure”,
Dag Anders Moldestad, 1999:137, ISBN 82-7984-019-2, ISSN 0802-3271.

"Electrode reactions and corrosion resistance for steel in mortar and concrete",
Roy Antonsen, 2000:10, ISBN 82-7984-030-3, ISSN 0802-3271.

"Hydro-Physical Conditions in Kelp Forests and the Effect on Wave Damping and Dune Erosion. A case study on Laminaria Hyperborea",
Stig Magnar Løvås, 2000:28, ISBN 82-7984-050-8, ISSN 0802-3271.

"Random Vibration and the Path Integral Method",
Christian Skaug, 2000:39, ISBN 82-7984-061-3, ISSN 0802-3271.

"Buckling and geometrical nonlinear beam-type analyses of timber structures",
Trond Even Eggen, 2000:56, ISBN 82-7984-081-8, ISSN 0802-3271.

”Structural Crashworthiness of Aluminium Foam-Based Components”,
Arve Grønsund Hanssen, 2000:76, ISBN 82-7984-102-4, ISSN 0809-103X.

“Measurements and simulations of the consolidation in first-year sea ice ridges, and some aspects of mechanical behaviour”,
Knut V. Høyland, 2000:94, ISBN 82-7984-121-0, ISSN 0809-103X.

”Kinematics in Regular and Irregular Waves based on a Lagrangian Formulation”,
Svein Helge Gjøsund, 2000-86, ISBN 82-7984-112-1, ISSN 0809-103X.

”Self-Induced Cracking Problems in Hardening Concrete Structures”,
Daniela Bosnjak, 2000-121, ISBN 82-7984-151-2, ISSN 0809-103X.

"Ballistic Penetration and Perforation of Steel Plates",
Tore Børvik, 2000:124, ISBN 82-7984-154-7, ISSN 0809-103X.

"Freeze-Thaw resistance of Concrete. Effect of: Curing Conditions, Moisture Exchange and Materials",
Terje Finnerup Rønning, 2001:14, ISBN 82-7984-165-2, ISSN 0809-103X

"Structural behaviour of post tensioned concrete structures. Flat slab. Slabs on ground",
Steinar Trygstad, 2001:52, ISBN 82-471-5314-9, ISSN 0809-103X.

"Slipforming of Vertical Concrete Structures. Friction between concrete and slipform panel",
Kjell Tore Fosså, 2001:61, ISBN 82-471-5325-4, ISSN 0809-103X.

"Some numerical methods for the simulation of laminar and turbulent incompressible flows",
Jens Holmen, 2002:6, ISBN 82-471-5396-3, ISSN 0809-103X.

“Improved Fatigue Performance of Threaded Drillstring Connections by Cold Rolling”,
Steinar Kristoffersen, 2002:11, ISBN: 82-421-5402-1, ISSN 0809-103X.

"Deformations in Concrete Cantilever Bridges: Observations and Theoretical Modelling",
Peter F. Takâcs, 2002:23, ISBN 82-471-5415-3, ISSN 0809-103X.

"Stiffened aluminium plates subjected to impact loading",
Hilde Giæver Hildrum, 2002:69, ISBN 82-471-5467-6, ISSN 0809-103X.

"Full- and model scale study of wind effects on a medium-rise building in a built up area",
Jónas Thór Snæbjørnsson, 2002:95, ISBN82-471-5495-1, ISSN 0809-103X.

“Evaluation of Concepts for Loading of Hydrocarbons in Ice-infested water”,
Arnor Jensen, 2002:114, ISBN 82-417-5506-0, ISSN 0809-103X.

”Numerical and Physical Modelling of Oil Spreading in Broken Ice”,
Janne K. Økland Gjøsteen, 2002:130, ISBN 82-471-5523-0, ISSN 0809-103X.

”Diagnosis and protection of corroding steel in concrete”,
Franz Pruckner, 20002:140, ISBN 82-471-5555-4, ISSN 0809-103X.

“Tensile and Compressive Creep of Young Concrete: Testing and Modelling”,
Dawood Atrushi, 2003:17, ISBN 82-471-5565-6, ISSN 0809-103X.

"Rheology of Particle Suspensions. Fresh Concrete, Mortar and Cement Paste with Various Types of Lignosulfonates",
Jon Elvar Wallevik, 2003:18, ISBN 82-471-5566-4, ISSN 0809-103X.

"Oblique Loading of Aluminium Crash Components",
Aase Reyes, 2003:15, ISBN 82-471-5562-1, ISSN 0809-103X.

"Utilization of Ethiopian Natural Pozzolans",
Surafel Ketema Desta, 2003:26, ISSN 82-471-5574-5, ISSN:0809-103X.

"Behaviour and strength prediction of reinforced concrete structures with discontinuity regions",
Helge Brå, 2004:11, ISBN 82-471-6222-9, ISSN 1503-8181.

"High-strength steel plates subjected to projectile impact. An experimental and numerical study",
Sumita Dey, 2004:38, ISBN 82-471-6282-2 (printed version), ISBN 82-471-6281-4 (electronic version), ISSN 1503-8181.

"Alkali-reactive and inert fillers in concrete. Rheology of fresh mixtures and expansive reactions."
Bård M. Pedersen, 2004:92, ISBN 82-471-6401-9 (printed version), ISBN 82-471-6400-0 (electronic version), ISSN 1503-8181.

"On the Shear Capacity of Steel Girders with Large Web Openings".
Nils Christian Hagen, 2005:9 ISBN 82-471-6878-2 (printed version), ISBN 82-471-6877-4 (electronic version), ISSN 1503-8181.

"Behaviour of aluminium extrusions subjected to axial loading".
Østen Jensen, 2005:7, ISBN 82-471-6873-1 (printed version), ISBN 82-471-6872-3 (electronic version), ISSN 1503-8181.

"Thermal Aspects of corrosion of Steel in Concrete".
Jan-Magnus Østvik, 2005:5, ISBN 82-471-6869-3 (printed version), ISBN 82-471-6868 (electronic version), ISSN 1503-8181.

"Mechanical and adaptive behaviour of bone in relation to hip replacement." A study of bone remodelling and bone grafting.
Sébastien Muller, 2005:34, ISBN 82-471-6933-9 (printed version), ISBN 82-471-6932-0 (electronic version), ISSN 1503-8181.

"Analysis of geometrical nonlinearities with applications to timber structures".
Lars Wollebæk, 2005:74, ISBN 82-471-7050-5 (printed version), ISBN 82-471-7019-1 (electronic version), ISSN 1503-8181.

“Pedestrian induced lateral vibrations of slender footbridges”,
Anders Rönnquist, 2005:102, ISBN 82-471-7082-5 (printed version), ISBN 82-471-7081-7 (electronic version), ISSN 1503-8181.

“Initial Strength Development of Fly Ash and Limestone Blended Cements at Various Temperatures Predicted by Ultrasonic Pulse Velocity”,
Tom Ivar Fredvik, 2005:112, ISBN 82-471-7105-8 (printed version), ISBN 82-471-7103-1 (electronic version), ISSN 1503-8181.

“Behaviour and modelling of thin-walled cast components”,
Cato Dørum, 2005:128, ISBN 82-471-7140-6 (printed version), ISBN 82-471-7139-2 (electronic version), ISSN 1503-8181.

“Behaviour and modelling of selfpiercing riveted connections”,
Raffaele Porcaro, 2005:165, ISBN 82-471-7219-4 (printed version), ISBN 82-471-7218-6 (electronic version), ISSN 1503-8181.

”Behaviour and Modelling og Aluminium Plates subjected to Compressive Load”,
Lars Rønning, 2005:154, ISBN 82-471-7169-1 (printed version), ISBN 82-471-7195-3 (electronic version), ISSN 1503-8181.

”Bumper beam-longitudinal system subjected to offset impact loading”,
Satyanarayana Kokkula, 2005:193, ISBN 82-471-7280-1 (printed version), ISBN 82-471-7279-8 (electronic version), ISSN 1503-8181.

“Control of Chloride Penetration into Concrete Structures at Early Age”,
Guofei Liu, 2006:46, ISBN 82-471-7838-9 (printed version), ISBN 82-471-7837-0 (electronic version), ISSN 1503-8181.

“Modelling of Welded Thin-Walled Aluminium Structures”,
Ting Wang, 2006:78, ISBN 82-471-7907-5 (printed version), ISBN 82-471-7906-7 (electronic version), ISSN 1503-8181.

”Time-variant reliability of dynamic systems by importance sampling and probabilistic analysis of ice loads”,
Anna Ivanova Olsen, 2006:139, ISBN 82-471-8041-3 (printed version), ISBN 82-471-8040-5 (electronic version), ISSN 1503-8181.

“Fatigue life prediction of an aluminium alloy automotive component using finite element analysis of surface topography”.
Sigmund Kyrre Ås, 2006:25, ISBN 82-471-7791-9 (printed version), ISBN 82-471-7791-9 (electronic version), ISSN 1503-8181.

”Constitutive models of elastoplasticity and fracture for aluminium alloys under strain path change”,
Dasharatha Achani, 2006:76, ISBN 82-471-7903-2 (printed version), ISBN 82-471-7902-4 (electronic version), ISSN 1503-8181.

“Simulations of 2D dynamic brittle fracture by the Element-free Galerkin method and linear fracture mechanics”,
Tommy Karlsson, 2006:125, ISBN 82-471-8011-1 (printed version), ISBN 82-471-8010-3 (electronic version), ISSN 1503-8181.

“Penetration and Perforation of Granite Targets by Hard Projectiles”,
Chong Chiang Seah, 2006:188, ISBN 82-471-8150-9 (printed version), ISBN 82-471-8149-5 (electronic version), ISSN 1503-8181.

“Deformations, strain capacity and cracking of concrete in plastic and early hardening phases”,
Tor Arne Hammer, 2007:234, ISBN 978-82-471-5191-4 (printed version), ISBN 978-82-471-5207-2 (electronic version), ISSN 1503-8181.

“Crashworthiness of dual-phase high-strength steel: Material and Component behaviour”,
Venkatapathi Tarigopula, 2007:230, ISBN 82-471-5076-4 (printed version), ISBN 82-471-5093-1 (electronic version), ISSN 1503-8181.

“Fibre reinforcement in load carrying concrete structures”,
Åse Lyslo Døssland, 2008:50, ISBN 978-82-471-6910-0 (printed version), ISBN 978-82-471-6924-7 (electronic version), ISSN 1503-8181.

“Low-velocity penetration of aluminium plates”,
Frode Grytten, 2008:46, ISBN 978-82-471-6826-4 (printed version), ISBN 978-82-471-6843-1 (electronic version), ISSN 1503-8181.

“Robustness studies of structures subjected to large deformations”,
Ørjan Fyllingen, 2008:24, ISBN 978-82-471-6339-9 (printed version), ISBN 978-82-471-6342-9 (electronic version), ISSN 1503-8181.

“Constitutive modelling of morsellised bone”,
Knut Birger Lunde, 2008:92, ISBN 978-82-471-7829-4 (printed version), ISBN 978-82-471-7832-4 (electronic version), ISSN 1503-8181.

“Experimental Investigations of Wind Loading on a Suspension Bridge Girder”,
Bjørn Isaksen, 2008:131, ISBN 978-82-471-8656-5 (printed version), ISBN 978-82-471-8673-2 (electronic version), ISSN 1503-8181.

"Cracking Risk of Concrete Structures in The Hardening Phase",
Guomin Ji, 2008:198, ISBN 978-82-471-1079-9 (printed version), ISBN 978-82-471-1080-5 (electronic version), ISSN 1503-8181.

"Modelling and numerical analysis of the porcine and human mitral apparatus",
Victorien Emile Prot, 2008:249, ISBN 978-82-471-1192-5 (printed version), ISBN 978-82-471-1193-2 (electronic version), ISSN 1503-8181.

"Strength analysis of net structures",
Heidi Moe, 2009:48, ISBN 978-82-471-1468-1 (printed version), ISBN 978-82-471-1469-8 (electronic version), ISSN1503-8181.

"Numerical analysis of ductile fracture in surface cracked shells",
Espen Berg, 2009:80, ISBN 978-82-471-1537-4 (printed version), ISBN 978-82-471-1538-1 (electronic version), ISSN 1503-8181.

"Subject specific finite element analysis of bone – for evaluation of the healing of a leg lengthening and evaluation of femoral stem design",
Sune Hansborg Pettersen, 2009:99, ISBN 978-82-471-1579-4 (printed version), ISBN 978-82-471-1580-0 (electronic version), ISSN 1503-8181.

"Evaluation of fracture parameters for notched multi-layered structures",
Lingyun Shang, 2009:137, ISBN 978-82-471-1662-3 (printed version), ISBN 978-82-471-1663-0 (electronic version), ISSN 1503-8181.

"Modelling of Dynamic Material Behaviour and Fracture of Aluminium Alloys for Structural Applications"
Yan Chen, 2009:69, ISBN 978-82-471-1515-2 (printed version), ISBN 978-82 471-1516-9 (electronic version), ISSN 1503-8181.

"Nanomechanics of polymer and composite particles"
Jianying He 2009:213, ISBN 978-82-471-1828-3 (printed version), ISBN 978-82-471-1829-0 (electronic version), ISSN 1503-8181.

"Mechanical properties of clear wood from Norway spruce"
Kristian Berbom Dahl 2009:250, ISBN 978-82-471-1911-2 (printed version) ISBN 978-82-471-1912-9 (electronic version), ISSN 1503-8181.

"Modeling of the degradation of TiB_2 mechanical properties by residual stresses and liquid Al penetration along grain boundaries"
Micol Pezzotta 2009:254, ISBN 978-82-471-1923-5 (printed version) ISBN 978-82-471-1924-2 (electronic version) ISSN 1503-8181.

"Effect of welding residual stress on fracture"
Xiabo Ren 2010:77, ISBN 978-82-471-2115-3 (printed version) ISBN 978-82-471-2116-0 (electronic version), ISSN 1503-8181.

"Pan-based carbon fiber as anode material in cathodic protection system for concrete structures"
Mahdi Chini 2010:122, ISBN 978-82-471-2210-5 (printed version) ISBN 978-82-471-2213-6 (electronic version), ISSN 1503-8181.

"Structural Behaviour of deteriorated and retrofitted concrete structures"
Irina Vasililjeva Sæther 2010:171, ISBN 978-82-471-2315-7 (printed version) ISBN 978-82-471-2316-4 (electronic version) ISSN 1503-8181.

"Prediction of local snow loads on roofs"
Vivian Meløysund 2010:247, ISBN 978-82-471-2490-1 (printed version) ISBN 978-82-471-2491-8 (electronic version) ISSN 1503-8181.

"Behaviour and modelling of polymers for crash applications"
Virgile Delhaye 2010:251, ISBN 978-82-471-2501-4 (printed version) ISBN 978-82-471-2502-1 (electronic version) ISSN 1503-8181.

"Blended cement with reducted CO_2 emission – Utilizing the Fly Ash-Limestone Synergy",
Klaartje De Weerdt 2011:32, ISBN 978-82-471-2584-7 (printed version) ISBN 978-82-471-2584-4 (electronic version) ISSN 1503-8181.

"Chloride induced reinforcement corrosion in concrete" Concept of critical chloride content – methods and mechanisms.
Ueli Angst 2011:113, ISBN 978-82-471-2769-9 (printed version) ISBN 978-82-471-2763-6 (electronic version) ISSN 1503-8181.

"A thermo-electric-Mechanical study of the carbon anode and contact interface for Energy savings in the production of aluminium".
Dag Herman Andersen 2011:157, ISBN 978-82-471-2859-6 (printed version) ISBN 978-82-471-2860-2 (electronic version) ISSN 1503-8181.

"Structural Capacity of Anchorage Ties in Masonry Veneer Walls Subjected to Earthquake". The implications of Eurocode 8 and Eurocode 6 on a typical Norwegain veneer wall.
Ahmed Mohamed Yousry Hamed 2011:181, ISBN 978-82-471-2911-1 (printed version) ISBN 978-82-471-2912-8 (electronic ver.) ISSN 1503-8181.

"Work-hardening behaviour in age-hardenable Al-Zn-Mg(-Cu) alloys".
Ida Westermann , 2011:247, ISBN 978-82-471-3056-8 (printed ver.) ISBN 978-82-471-3057-5 (electronic ver.) ISSN 1503-8181.

"Behaviour and modelling of selfpiercing riveted connections using aluminium rivets".
Nguyen-Hieu Hoang, 2011:266, ISBN 978-82-471-3097-1 (printed ver.) ISBN 978-82-471-3099-5 (electronic ver.) ISSN 1503-8181.

“Fibre reinforced concrete”.
Sindre Sandbakk, 2011:297, ISBN 978-82-471-3167-1 (printed ver.) ISBN 978-82-471-3168-8 (electronic ver) ISSN 1503:8181.

“Dynamic behaviour of cablesupported bridges subjected to strong natural wind”.
Ole Andre Øiseth, 2011:315, ISBN 978-82-471-3209-8 (printed ver.) ISBN 978-82-471-3210-4 (electronic ver.) ISSN 1503-8181.

“Constitutive modeling of solargrade silicon materials”
Julien Cochard, 2011:307, ISBN 978-82-471-3189-3 (printed ver). ISBN 978-82-471-3190-9 (electronic ver.) ISSN 1503-8181.

“Constitutive behavior and fracture of shape memory alloys”
Jim Stian Olsen, 2012:57, ISBN 978-82-471-3382-8 (printed ver.) ISBN 978-82-471-3383-5 (electronic ver.) ISSN 1503-8181.

“Field measurements in mechanical testing using close-range photogrammetry and digital image analysis”
Egil Fagerholt, 2012:95, ISBN 978-82-471-3466-5 (printed ver.) ISBN 978-82-471-3467-2 (electronic ver.) ISSN 1503-8181.

“Towards a better under standing of the ultimate behaviour of lightweight aggregate concrete in compression and bending”,
Håvard Nedrelid, 2012:123, ISBN 978-82-471-3527-3 (printed ver.) ISBN 978-82-471-3528-0 (electronic ver.) ISSN 1503-8181.

“Numerical simulations of blood flow in the left side of the heart”
Sigrid Kaarstad Dahl, 2012:135, ISBN 978-82-471-3553-2 (printed ver.) ISBN 978-82-471-3555-6 (electronic ver.) ISSN 1503-8181.

“Moisture induced stresses in glulam”
Vanessa Angst-Nicollier, 2012:139, ISBN 978-82-471-3562-4 (printed ver.) ISBN 978-82-471-3563-1 (electronic ver.) ISSN 1503-8181.

“Biomechanical aspects of distraction osteogensis”
Valentina La Russa, 2012:250, ISBN 978-82-471-3807-6 (printed ver.) ISBN 978-82-471-3808-3 (electronic ver.) ISSN 1503-8181.

“Ductile fracture in dual-phase steel. Theoretical, experimental and numerical study”
Gaute Gruben, 2012:257, ISBN 978-82-471-3822-9 (printed ver.) ISBN 978-82-471-3823-6 (electronic ver.) ISSN 1503-8181.

“Damping in Timber Structures”
Nathalie Labonnote, 2012:263, ISBN 978-82-471-3836-6 (printed ver.) ISBN 978-82-471-3837-3 (electronic ver.) ISSN 1503-8181.

“Biomechanical modeling of fetal veins: The umbilical vein and ductus venosus bifurcation”
Paul Roger Leinan, 2012:299, ISBN 978-82-471-3915-8 (printed ver.) ISBN 978-82-471-3916-5 (electronic ver.) ISSN 1503-8181.

“Large-Deformation behaviour of thermoplastics at various stress states”
Anne Serine Ognedal, 2012:298, ISBN 978-82-471-3913-4 (printed ver.) ISBN 978-82-471-3914-1 (electronic ver.) ISSN 1503-8181.

“Hardening accelerator for fly ash blended cement”
Kien Dinh Hoang, 2012:366, ISBN 978-82-471-4063-5 (printed ver.) ISBN 978-82-471-4064-2 (electronic ver.) ISSN 1503-8181.

“From molecular structure to mechanical properties”
Jianyang Wu, 2013:186, ISBN 978-82-471-4485-5 (printed ver.) ISBN 978-82-471-4486-2 (electronic ver.) ISSN 1503-8181.

“Experimental and numerical study of hybrid concrete structures”
Linn Grepstad Nes, 2013:259, ISBN 978-82-471-4644-6 (printed ver.) ISBN 978-82-471-4645-3 (electronic ver.) ISSN 1503-8181.

“Mechanics of ultra-thin multi crystalline silicon wafers”
Saber Saffar, 2013:199, ISBN 978-82-471-4511-1 (printed ver.) ISBN 978-82-471-4513-5 (electronic ver). ISSN 1503-8181.

“Through process modelling of welded aluminium structures”
Anizahyati Alisibramulisi, 2013:325, ISBN 978-82-471-4788-7 (printed ver.) ISBN 978-82-471-4789-4 (electronic ver.) ISSN 1503-8181.

“Combined blast and fragment loading on steel plates”
Knut Gaarder Rakvåg, 2013:361, ISBN978-82-471-4872-3 (printed ver.) ISBN 978-82-4873-0 (electronic ver.). ISSN 1503-8181.

“Characterization and modelling of the anisotropic behaviour of high-strength aluminium alloy”
Marion Fourmeau, 2014:37, ISBN 978-82-326-0008-3 (printed ver.) ISBN 978-82-326-0009-0 (electronic ver.) ISSN 1503-8181.

“Behaviour of threated steel fasteners at elevated deformation rates”
Henning Fransplass, 2014:65, ISBN 978-82-326-0054-0 (printed ver.) ISBN 978-82-326-0055-7 (electronic ver.) ISSN 1503-8181.

“Sedimentation and Bleeding”
Ya Peng, 2014:89, ISBN 978-82-326-0102-8 (printed ver.) ISBN 978-82-326-0103-5 (electric ver.) ISSN 1503-8181.

“Impact against X65 offshore pipelines”
Martin Kristoffersen, 2014:362, ISBN 978-82-326-0636-8 (printed ver.) ISBN 978-82-326-0637-5 (electronic ver.) ISSN 1503-8181.

“Formability of aluminium alloy subjected to prestrain by rolling”
Dmitry Vysochinskiy, 2014:363,, ISBN 978-82-326-0638-2 (printed ver.) ISBN 978-82-326-0639-9 (electronic ver.) ISSN 1503-8181.

“Experimental and numerical study of Yielding, Work-Hardening and anisotropy in textured AA6xxx alloys using crystal plasticity models”
Mikhail Khadyko, 2015:28, ISBN 978-82-326-0724-2 (printed ver.) ISBN 978-82-326-0725-9 (electronic ver.) ISSN 1503-8181.

“Behaviour and Modelling of AA6xxx Aluminium Alloys Under a Wide Range of Temperatures and Strain Rates”
Vincent Vilamosa, 2015:63, ISBN 978-82-326-0786-0 (printed ver.) ISBN 978-82-326-0787-7 (electronic ver.) ISSN 1503-8181.

“A Probabilistic Approach in Failure Modelling of Aluminium High Pressure Die-Castings”
Octavian Knoll, 2015:137, ISBN 978-82-326-0930-7 (printed ver.) ISBN 978-82-326-0931-4 (electronic ver.) ISSN 1503-8181.

“Ice Abrasion on Marine Concrete Structures”
Egil Møen, 2015:189, ISBN 978-82-326-1034-1 (printed ver.) ISBN 978-82-326-1035-8 (electronic ver.) ISSN 1503-8181.

“Fibre Orientation in Steel-Fibre-Reinforced Concrete”
Giedrius Zirgulis, 2015:229, ISBN 978-82-326-1114-0 (printed ver.) ISBN 978-82-326-1115-7 (electronic ver.) ISSN 1503-8181.

“Effect of spatial variation and possible interference of localised corrosion on the residual capacity of a reinforced concrete beam”
Mohammad Mahdi Kioumarsi, 2015:282, ISBN 978-82-326-1220-8 (printed ver.) ISBN 978-82-1221-5 (electronic ver.) ISSN 1503-8181.

“The role of concrete resistivity in chloride-induced macro-cell corrosion”
Karla Horbostel, 2015:324, ISBN 978-82-326-1304-5 (printed ver.) ISBN 978-82-326-1305-2 (electonic ver.) ISSN 1503-8181.

“Flowable fibre-reinforced concrete for structural applications”
Elena Vidal Sarmiento, 2015-335, ISBN 978-82-326-1324-3 (printed ver.) ISBN 978-82-326-1325-0 (electronic ver.) ISSN 1503-8181.

“Development of chushed sand for concrete production with microproportioning”
Rolands Cepuritis, 2016:19, ISBN 978-82-326-1382-3 (printed ver.) ISBN 978-82-326-1383-0 (electronic ver.) ISSN 1503-8181.

“Withdrawal properties of threaded rods embedded in glued-laminated timer elements”
Haris Stamatopoulos, 2016:48, ISBN 978-82-326-1436-3 (printed ver.) ISBN 978-82-326-1437-0 (electronic ver.) ISSN 1503-8181.

“An Experimental and numerical study of thermoplastics at large deformation”
Marius Andersen, 2016:191, ISBN 978-82-326-1720-3 (printed ver.) ISBN 978-82-326-1721-0 (electronic ver.) ISSN 1503-8181.

“Modeling and Simulation of Ballistic Impact”
Jens Kristian Holmen, 2016:240, ISBN 978-82-326-1818-7 (printed ver). ISBN 978-82-326-1819-4 (electronic ver.) ISSN 1503-8181.

“Early age crack assessment of concrete structures”
Anja B. Estensen Klausen, 2016:256, ISBN 978-82-326-1850-7 (printed ver). ISBN 978-82-326-1851-4 (electronic ver.) ISSN 1503-8181.

“Uncertainty quantification and sensitivity analysis for cardiovascular models”
Vinzenz Gregor Eck, 2016:234, ISBN 978-82-326-1806-4 (printed ver.) ISBN 978-82-326-1807-1 (electronic ver.) ISSN 1503-8181.

“Dynamic behaviour of existing and new railway catenary systems under Norwegain conditions”
Petter Røe Nåvik, 2016:298, ISBN 978-82-326-1935-1 (printed ver.) ISBN 978-82-326-1934-4 (electronic ver.) ISSN 1503-8181.

“Mechanical behaviour of particle-filled elastomers at various temperatures”
Arne Ilseng, 2016-295, ISBN978-82-326-1928-3 (printed ver.) ISBN 978-82-326-1929-0 (electronic ver.) ISSN 1503-8181.

“Nanotechnology for Anti-Icing Application”
Zhiwei He, 2016:348, ISBN 978-82-326-2038-8 (printed ver.) ISBN 978-82-326-2019-5 (electronic ver.) ISSN 1503-8181.

“Conduction Mechanisms in Conductive Adhesives with Metal-Coated Polyer Spheres”
Sigurd Rolland Pettersen, 2016:349, ISBN 978-326-2040-1 (printed ver,) ISBN 978-82-326-2041-8 (electronic ver.) ISSN 1503-8181.

“The interaction between calcium lignosulfonate and cement”
Alessia Colombo, 2017:20, ISBN 978-82-326-2122-4 (printed ver.) ISBN 978-82-326-2123-1 (electronic ver.) ISSN 1503-8181.

“Behaviour and Modelling of Flexible Structures Subjected to Blast Loading”
Vegard Aune, 2017:101, ISBN 978-82-326-2274-0 (printed ver.) ISBN 978-82-326-2275-7 (electronic ver.) ISSN 1503-8181.

“Behaviour of steel connections under quasi-static and impact loading”
Erik Løhre Grimsmo, 2017:159, ISBN 978-82-326-2390-7 (printed ver.) ISBN 978-82-326-2391-4 (electronic ver.) ISSN 1503-8181.

“An experimental and numerical study of cortical bone at he macro and Nano-scale”
Masoud Ramenzanzadehkoldeh,, 2017:208, ISBN 978-82-326-2488-1 (printed ver.) ISBN 978-82-326-2489-8 (electronic ver.) ISSN 1503-8181.

“Optoelectrical Properties of a Novel Organic Semiconductor: 6,13-Dichloropentacene”
Mao Wang, 2017:130, ISBN 978-82-326-2332-7 (printed ver.) ISBN 978-82-326-2333-4) (electronic ver.) ISSN 1503-8181.

“Core-shell structured microgels and their behavior at oil and water interface”
Yi Gong, 2017:182, ISBN 978-82-326-2436-2 (printed. ver.) ISBN 978-82-326-2437-9 (electronic ver.) ISSN 1503-8181.

“Aspects of design of reinforced concrete structures using nonliear finite element analyses”
Morten Engen, 2017:149, ISBN 978-82-326-2370-9 (printed ver.) ISBN 978-82-326-2371-6 (electronic ver.) ISSN 1503-8181.

“Numerical studies on ductile failure of aluminium alloys”
Lars Edvard Dæhli, 2017:284, ISBN 978-82-326-2636-6 (printed ver.) ISBN 978-82-326-2637-3 (electronic ver.) ISSN 1503-8181.

“Modelling and Assessment of Hydrogen Embrittlement in Steels and Nickel Alloys”
Haiyang Yu, 2017:278, ISBN 978-82-326-2624-3 (printed. ver.) ISBN 978-82-326-2625-0 (electronic ver.) ISSN 1503-8181.

“Network arch timber bridges with light timber deck on transverse crossbeams”
Anna Weronika Ostrycharczyk, 2017:318, ISBN 978-82-326-2704-2 (printed ver.) ISBN 978-82-326-2705-9 (electronic ver.) ISSN 1503-8181.

“Splicing of Large Glued Laminated Timber Elements by Use of Long Threated Rods”
Martin Cepelka, 2017:320, ISBN 978-82-326-2708-0 (printed ver.) ISBN 978-82-326-2709-7 (electronic ver.) ISSN 1503-8181.

“Thermomechanical behaviour of semi-crystalline polymers: experiments, modelling and simulation”
Joakim Johnsen, 2017-317, ISBN 978-82-326-2702-8 (printed ver.) ISBN 978-82-326-2703-5 (electronic ver.) ISSN 1503-8181.

“Small-Scale Plasiticity under Hydrogen Environment”
Kai Zhao, 2017:356, ISBN 978-82-326-2782-0 (printed ver.) ISBN 978-82-326-2783-7 (electronic er.) ISSN 1503-8181.

“Risk and Reliability Based Calibration of Structural Design Codes”
Michele Baravalle, 2017:342, ISBN 978-82-326-2752-3 (printed ver,) ISBN 978-82-326-2753-0 (electronic ver.) ISSN 1503-8181.

“Dynamic behaviour of floating bridges exposed to wave excitation”
Knut Andreas Kvåle, 2017:365, ISBN 978-82-326-2800-1 (printed ver.) ISBN 978-82-326-2801-8 (electronic ver.) ISSN 1503-8181.

“Dolomite calcined clay composite cement – hydration and durability”
Alisa Lydia Machner, 2018:39, ISBN 978-82-326-2872-8 (printed ver.). ISBN 978-82-326-2873-5 (electronic ver.) ISSN 1503-8181.

“Modelling of the self-excited forces for bridge decks subjected to random motions: an experimental study”
Bartosz Siedziako, 2018:52, ISBN 978-82-326-2896-4 (printed ver.). ISBN 978-82-326-2897-1 (electronic ver.) ISSN 1503-8181.

“A probabilistic-based methodology for evaluation of timber facade constructions”
Klodian Gradeci, 2018:69, ISBN 978-82-326-2928-2 (printed ver.) ISBN 978-82-326-2929-9 (electronic ver.) ISSN 1503-8181.

“Behaviour and modelling of flow-drill screw connections”
Johan Kolstø Sønstabø, 2018:73, ISBN 978-82-326-2936-7 (printed ver.) ISBN 978-82-326-2937-4 (electronic ver.) ISSN 1503-8181.

“Full-scale investigation of the effects of wind turbulence characteristics on dynamic behavior of long-span cable-supported bridges in complex terrain”
Aksel Fenerci, 2018 100, ISBN 9978-82-326-2990-9 (printed ver.) ISBN 978-82-326-2991-6 (electronic ver.) ISSN 1503-8181.

“Modeling and simulation of the soft palate for improved understanding of the obstructive sleep apnea syndrome”
Hongliang Liu, 2018:101, ISBN 978-82-326-2992-3 (printed ver.) ISBN 978-82-326-2993-0 (electronic ver.) ISSN 1503-8181.

“Long-term extreme response analysis of cable-supported bridges with floating pylons subjected to wind and wave loads”.
Yuwang Xu, 2018:229, ISBN 978-82-326-3248-0 (printed ver.) ISBN 978-82-326-3249-7 (electronic ver.) ISSN 1503-8181.

“Reinforcement corrosion in carbonated fly ash concrete”
Andres Belda Revert, 2018:230, ISBN 978-82-326-3250-3 (printed ver.) ISBN 978-82-326-3251-0 (electronic ver.) ISSN 1503-8181.

“Direct finite element method for nonliear earthquake analysis of concrete dams including dam-water-foundation rock interaction”
Arnkjell Løkke, 2018:252, ISBN 978-82-326-3294-7 (printed ver.) ISBN 978-82-326-3295-4 (electronic ver.) ISSN 1503-8181.

“Electromechanical characterization of metal-coated polymer spheres for conductive adhesives”
Molly Strimbeck Bazilchuk, 2018:295, ISBN 978-82-326-3380-7 (printed. ver.) ISBN 978-82-326-3381-4 (electrical ver.) ISSN 1503-8181.

“Determining the tensile properties of Artic materials and modelling their effects on fracture”
Shengwen Tu, 2018:269, ISBN 978-82-326-3328-9 (printed ver.) ISBN 978-82-326-3329-6 (electronic ver.) ISSN 1503-8181.

“Atomistic Insigth into Tranportation of Nanofluid in Ultra-confined Channel”
Xiao Wang, 2018:334, ISBN978-82-326-3456-9 (printed ver.) ISBN 978-82-326-3457-6 (electronic ver.) ISSN 1503-8181.

“An experimental and numerical study of the mechanical behaviour of short glass-fibre reinforced thermoplastics”.
Jens Petter Henrik Holmstrøm, 2019:79, ISBN 978-82-326-3760-7 (printed ver.) ISBN 978-82-326-3761-4 (electronic ver.) ISSN 1503-8181.

“Uncertainty quantification and sensitivity analysis informed modeling of physical systems”
Jacob Sturdy, 2019:115, ISBN 978-82-326-3828-4 (printed ver.) ISBN 978-82-326-3829-1 (electric ver.) ISSN 1503-8181.

“Load model of historic traffic for fatigue life estimation of Norwegian railway bridges”
Gunnstein T. Frøseth, 2019:73, ISBN 978-82-326-3748-5 (printed ver.) ISBN 978-82-326-3749-2 (electronic ver.) ISSN 1503-8181.

“Force identification and response estimation in floating and suspension bridges using measured dynamic response”
Øyvind Wiig Petersen, 2019:88, ISBN 978-82-326-3778-2 (printed ver.) ISBN 978-82-326-377-9 (electronic ver.) ISSN 1503-8181.

“Consistent crack width calculation methods for reinforced concrete elements subjected to 1D and 2D stress states”
Reignard Tan, 2019:147, ISBN 978-82-326-3892-5 (printed ver.) ISBN 978-82-326-3893-2 (electronic ver.) ISSN 1503-8181.

“Nonlinear static and dynamic isogeometric analysis of slender spatial and beam type structures”
Siv Bente Raknes, 2019:181, ISBN 978-82-326-3958-8 (printed ver.) ISBN 978-82-326-3959-5 (electronic ver.) ISSN 1503-8181.

“Experimental study of concrete-ice abrasion and concrete surface topography modification”
Guzel Shamsutdinova, 2019:182, ISBN978-82-326-3960-1 (printed ver.) ISBN 978-82-326-3961-8 (electronic ver.) ISSN 1503-8181.

“Wind forces on bridge decks using state-of-the art FSI methods”
Tore Andreas Helgedagsrud, 2019:180, ISBN 978-82-326-3956-4 (printed ver.) ISBN 978-82-326-3957-1 (electronic ver.) ISSN 1503-8181.

“Numerical Study on Ductile-to-Brittle Transition of Steel and its Behavior under Residual Stresses”
Yang Li, 2019:227, ISBN 978-82-326-4050-8 (printed ver.) ISBN 978-82-326-4015-5 (electronic ver.) ISSN 1503-8181.

“Micromechanical modelling of ductile fracture in aluminium alloys”
Bjørn Håkon Frodal, 2019:253, ISBN 978-82-326-4102-4 (printed ver.) ISBN 978-82-326-4103-1 (electronic ver.) ISSN 1503-8181.

“Monolithic and laminated glass under extreme loading: Experiments, modelling and simulations”
Karoline Osnes, 2019:304, ISBN 978-82-326-4204-5 (printed ver.) ISBN 978-82-326-4205-2 (electronic ver.) ISSN 1503-8181.

“Plastic flow and fracture of isotropic and anisotropic 6000-series aluminium alloys: Experiments and numerical simulations “
Susanne Thomesen, 2019:312, ISBN 978-82-326-4220-5 (printed ver.), ISBN 978-82-326-4221-2 (electriniv ver.) ISSN 1503-8181

“Stress-laminated timber decks in bridges”
Francesco Mirko Massaro, 2019:346, ISBN 978-82-326-4288-5 (printed ver.), ISBN 978-82-326-4289-2 (electronic ver.) ISSN 1503-8181

“Connections between steel and aluminium using adhesive bonding combined with self-piercing riveting: Testing, modelling and analysis”
Matthias Reil, 2019:319, ISBN 978-82-326-4234-2 (printed ver.), ISBN 978-82-326-4235-9 (electronic ver.) ISSN 1503-8181

“Designing Polymeric Icephobic Materials”
Yizhi Zhuo, 2019:345, ISBN 978-82-326-4286-1 (printed ver.), ISBN 978-82-326-4287-8 (electronic ver.) ISSN 1503-8181

“Fundamental Mechanisms of Ice Adhesion”
Rønneberg, Sigrid 2020:87, ISBN 978-82-326-4527-8 (printed version) ISBN 978-82- 326-4524-5 (electronic version) ISSN 1503-8181

“Mechanical modeling of the polymeric coating on a subsea pipeline”
Vestrum, Ole 2020:105, ISBN 978-82-326-4562-6 (printed version) ISBN 978-82- 4563-3 (electronic version ISSN 1503-8181

“Conceptual form-finding in structural engineering”
Marcin Luczkowski 2020:232, ISBN 978-82-326-4812-2 (printed version) ISBN 978-82-326-4813-9 (electronic version) ISSN 1503-8181

“Self-assembled superstructures of magnetic nanoparticles: advanced nanofabrication and enhanced mechanical properties”
Verner Håkonsen 2020:271, ISBN 978-82-326-4890-0 (printed version) ISBN 978-82- 326-4891-7 (electronic version) ISSN 1503-8181

“Micromechanical modelling of fracture in ductile alloys with applications to high-strength steel”
Sondre Bergo 2020:313, ISBN 978-82-326-4974-7 (printed version) ISBN 978-82-326- 4975-4 (electronic version) ISSN 1503-8181

“Fracture in wood of Norway spruce - Experimental and numerical study”
Katarzyna Ostapska 2020:314, ISBN 978-82-326-4976-1 (printed version) ISBN 978- 82-326-4977-8 (electronic version) ISSN 1503-8181

“Dynamic anti-icing surfaces (DAIS)”
Feng Wang 2020:330 ISBN 978-82-326-5006-4 (printed version) ISBN 978-82-326-5007-1 (electronic version) ISSN 1503-8181

“«Multiaxial Fatigue analysis of offshore mooring chains, considering the effects of residual stresses and corrosion pits»
Ershad P. Zarandi 2020:337 ISBN 978-82-326-5020-0 (printed version) ISBN 978-82-326-5021-7 (electronic version) ISSN 1503-8181

“Production and documentation of frost durable high-volume fly ash concrete: air entrainment, cracking and scaling in performance testing”
Andrei Shpak 2020:366 ISBN 978-82-326-5078-1 (printed version) ISBN 978-82-326-5079-8 (electronic version) ISSN 1503-8181

“Physics-based and data-driven reduced-order blood flow models: Applications to coronary artery disease diagnostics”
Fredrik Eikeland Fossan 2020:362 ISBN 978-82-326-5070-5 (printed version) ISBN 978-82-326-5071-2 (electronic version) ISSN 1503-8181

“Multi-scale modelling and simulation of ductile failure in aluminium structures”
Henrik Granum 2020:374 ISBN 978-82-326-5094-1 (printed version) ISBN 978-82-326-5095-8 (electronic version) ISSN 1503-8181

“Testing and modelling of multi-material joints”
Jon Fredrick Berntsen 2020:368 ISBN 978-82-326-5082-8 (printed version) ISBN 978-82-326-5083-5 ISSN 1503-8181

“Heuristic models for wear prediction and dynamic-based condition monitoring techniques in pantograph-catenary interaction”
Stefano Derosa 2020:381 ISBN 978-82-326-5108-5 (printed version) ISBN 978-82-326-5109-2 (electronic version) ISSN 1503-8181

“Experimental and numerical study of dilation in mineral filled PVC”
Sindre Nordmark Olufsen 2020:388 ISBN 978-82-326-5122-1 (printed version) ISBN 978-82-326-5123-8 (electronic version) ISSN 1503-8181

“Residual stresses and dimensional deviation in metal additive manufacturing: prediction and mitigation methods”
Li Sun 2020:411 ISBN 978-82-471-9600-7 (printed version) ISBN 978-82-471-9581-9 (electronic version) ISSN 1503-8181 (printed version) ISSN 2703-8084 (online version)

“Moment-resisting timber frames with semi-rigid connections”
Aivars Vilguts 2021:88 ISBN 978-82-326-6987 (printed version) ISBN 978-82-326-5737-7 (electronic version) ISSN 2703-8084 (online version)

“Thermal transport in metal-polymer systems”
Susanne Sandell 2021:63 ISBN 978-82-326-5304-1 (printed version) ISBN 978-82-326-6278-4 (electronic version) ISSN 2703-8084 (online version)

“Competitive timber floors”
Sveinung Ørjan Nesheim 2021:134 ISBN 978-82-326-6481-8 (printed version) ISBN 978-82-326-5399-7 (electronic version) ISSN 2703-8084

“Thermodynamics of Nanoscale Films and Fluid Volumes”
Bjørn Andre Strøm 2021:166 ISBN 978-82-326-6778-9 (printed version) ISBN 978-82-326-5900-5 (electronic version) ISSN 2703-8084 (online version)

“Characterization and modeling of the mechanical behavior of polymer foam”
Daniel Thor Morton 2021:173 ISBN 978-82-326-6245-6 (printed version) ISBN 978-82-326-5699-8 (electronic version) ISSN 2703-8084 (online version)

“Atomistic Insights to Interfacial Dynamics”
Yuequn Fu 2021:233 ISBN 978-82-326-5530-4 (printed version) ISBN 978-82-326-6894-6 (electronic version) ISSN 2703-8084 (online version)

“Mechanisms and enhancement of CO2 condensation heat transfer”
Ingrid Snustad 2021:236 ISBN 978-82-326-5606-6 ISBN 978-82-236-6715-4 (electronic version) ISSN 2703-8084

“Experimental study of reinforced concrete slabs subjected to fire exposure and blast loading”
Assis Arano Barenys 2021:239 ISBN 978-82-326-5289-1 ISBN 978-82-326-5876-3 (electronic version) ISSN 2703-8084 (online version)

“Long-term extreme buffeting response investigations for long-span bridges considering uncertain turbulence parameters based on field measurements”
Tor Martin Lystad 2021:216 ISBN 978-82-326-5797-1 (printed version) ISBN 978-82-326-6154-1 (electronic version) ISSN 2703-8084 (online version)

“Development and Application of a Vision-Based System for Structural Monitoring of Railway Catenary System”
Tengjiao Jiang 2021:280 ISBN 978-82-326-6866-3 (printed ver.) ISBN 978-82-326-5778-0 (electronic ver.) ISSN 1503-8181 (online ver.)

ISBN 978-82-326-6327-9 (printed ver.)
ISBN 978-82-326-5895-4 (electronic ver.)
ISSN 1503-8181 (printed ver.)
ISSN 2703-8084 (online ver.)

NTNU
Norwegian University of
Science and Technology